

THE MOLECULAR BIOLOGY AND REGULATION OF PLASTID DIVISION

**Thesis submitted for the degree of
Doctor of Philosophy
At the University of Leicester**

**by
Cassie Patricia Aldridge BSc
Department of Biology
University of Leicester**

October 2006

UMI Number: U225124

All rights reserved

INFORMATION TO ALL USERS

The quality of this reproduction is dependent upon the quality of the copy submitted.

In the unlikely event that the author did not send a complete manuscript and there are missing pages, these will be noted. Also, if material had to be removed, a note will indicate the deletion.



UMI U225124

Published by ProQuest LLC 2013. Copyright in the Dissertation held by the Author.
Microform Edition © ProQuest LLC.

All rights reserved. This work is protected against
unauthorized copying under Title 17, United States Code.



ProQuest LLC
789 East Eisenhower Parkway
P.O. Box 1346
Ann Arbor, MI 48106-1346

The Molecular Biology and Regulation of Plastid Division, Cassie Patricia Aldridge

Plastid division is a complex process essential for the maintenance and accumulation of plastids in plant cells. Plastids are not formed *de novo* but arise by binary fission from pre-existing plastids in a process that involves both prokaryotic- and eukaryotic-derived proteins. The prokaryotic-derived Min proteins mediate plastid division site selection by controlling the formation of the Z-ring, the initial event of plastid division. The Z-ring is formed by the polymerisation of the FtsZ proteins into a contractile ring at the future division site and acts as a scaffold for the assembly of the rest of the division machinery. This study aims to elucidate AtMinD1 function in *Arabidopsis thaliana* and demonstrates that AtMinD1 has Ca²⁺-dependent ATPase activity that is stimulated by AtMinE1. Site directed mutagenesis was used to create an active site mutant of AtMinD1, analysis of this mutant revealed loss of interaction with AtMinE1 and mislocalisation. The interaction of the stromal plastid division components was also investigated. Colocalisation and bimolecular fluorescence complementation assays revealed that AtFtsZ1-1 and AtFtsZ2-1 are capable of forming both homopolymeric and heteropolymeric filaments, AtMinD1 and AtMinE1 interact both with themselves and each other and ARC6 interacts specifically with AtFtsZ2-1. Many of the components involved in plastid division have yet to be identified. To identify novel plastid division components, yeast two-hybrid screening and co-immunoprecipitation were used to hunt for novel interacting partners of FtsZ proteins. Although much work has been dedicated to unravelling the machinery of plastid division, very little is known about the regulation of plastid division. DNA microarrays were used to investigate changes in nuclear gene expression upon chloroplast division inhibition. Quantitative PCR experiments demonstrate that the expression of *AtFtsZ1-1*, *AtFtsZ2-1*, *AtMinD1* and *AtMinE1* is light regulated and yeast one-hybrid screening was used to hunt for transcriptional activators/enhancers of *AtMinD1* and *AtMinE1*.

Acknowledgements

I would like to thank my supervisor Simon Møller for his support, encouragement and enthusiasm during the last three years. I would also like to thank the rest of the research group, Trudie Allen, Sally Adams and especially Jodi Maple and Xiang-Ming Xu whose help and knowledge have been invaluable throughout my PhD. I would like to thank Lisa Doyle, Sally Adams, Trudie Allen and Jodi Maple for inspirational discussions in various drinking establishments. I would also like to thank Garry Whitelam and his group for their support and use of equipment and the BBSRC for funding this project. Finally, I would like to thank my family and friends for all their support particularly my wonderful boyfriend Adam Conway for financial support.

Abbreviations used in this study

AD: Activation Domain

BD: DNA-Binding Domain

BiFC: Bimolecular Fluorescence Complementation

CFP: Cyan Fluorescent Protein

EMS: Ethyl Methane Sulfonate

FRET: Fluorescence Resonance Energy Transfer

H: Histidine

L: Leucine

NI: No Induction of AtMinD1

PD ring: Plastid-dividing ring

Pi: Inorganic Phosphate

PI: Prolonged Induction of AtMinD1

QPCR: Quantative PCR

SD: Synthetic Drop-out supplement

SDS-PAGE: Sodium Dodecyl Sulfate PolyAcrylamide Gel Electrophoresis

T: Tryptophan

TI: Temporal induction of AtMinD1

TLC: Thin Layer Chromatography

YFP: Yellow Fluorescent Protein

Contents.

1. Introduction	1
1.1. General introduction	1
1.2. Basic morphology of plastid division	1
1.3. Bacterial cell division versus plastid division	5
1.3.1. <i>FtsZ</i>	7
1.3.2. <i>MinD</i>	10
1.3.3. <i>MinE</i>	13
1.4. <i>accumulation and replication of chloroplasts (arc) mutants</i>	14
1.4.1. <i>Physiology of arc mutants</i>	15
1.4.2. <i>Hierarchy of arc mutants</i>	18
1.4.3. <i>ARC3</i>	21
1.4.4. <i>ARC5</i>	22
1.4.5. <i>ARC6</i>	25
1.4.6. <i>ARC11</i>	26
1.5. Novel plastid division proteins	27
1.5.1. <i>Alb4</i>	27
1.5.2. <i>GIANT CHLOROPLAST 1</i>	28
1.5.3. <i>AtCDT1</i>	30
1.5.4. <i>MscS-like (MSL) proteins</i>	31
1.5.5. <i>FZL</i>	32
1.6. Conclusions	33
2. Materials and Methods	35
2.1. Plant growth	35
2.1.1. <i>Plant growth media.</i>	35

2.1.2. <i>In vitro</i> culture	35
2.1.3. Soil culture	35
2.1.4. Plant transformation	36
2.2. Bacterial work	37
2.2.1. Growth and storage of bacteria	37
2.2.2. <i>E. coli</i> transformation	38
2.2.3. Transformation of <i>Agrobacterium tumefaciens</i>	38
2.3. Molecular biology	39
2.3.1. Nucleic acid preparation	39
2.3.1.1. Plant DNA extraction	39
2.3.1.2. Plant RNA extraction	40
2.3.1.3. Plasmid preparation from bacterial overnights	40
2.3.1.4. DNA extraction from agarose gels	40
2.3.1.5. Quantification of DNA and RNA	40
2.3.2. Enzymatic manipulation of nucleic acids	40
2.3.2.1. Endonuclease restriction of nucleic acids	40
2.3.2.2. Dephosphorylation of 5' ends	41
2.3.2.3. DNA ligations	41
2.3.2.4. PCR	42
2.3.2.5. RT-PCR	42
2.3.2.6. Quantitative PCR (QPCR)	43
2.3.2.7. DNA sequencing	43
2.3.3. Protein Preparation	44
2.3.3.1. Protein extraction from <i>Arabidopsis</i>	44
2.3.3.2. Protein extraction from <i>E. coli</i> BL21(DE3)pLysS	44
2.3.3.3. Purification of His-tagged proteins	45
2.3.3.4. Purification of GST-tagged proteins	45
2.3.3.5. Co-immunoprecipitation	46

2.3.3.6. <i>Protein quantification</i>	46
2.3.4. <i>ATPase assays</i>	47
2.3.5. <i>Electrophoresis and related techniques</i>	47
2.3.5.1. <i>Agarose gels</i>	47
2.3.5.2. <i>SDS-PAGE</i>	48
2.3.5.3. <i>Coomassie staining of polyacrylamide gels</i>	49
2.3.5.4. <i>Western blotting</i>	49
2.4. Yeast work	50
2.4.1. <i>Growth and storage of yeast</i>	50
2.4.2. <i>Small scale transformation of yeast</i>	51
2.4.3. <i>Yeast mating</i>	51
2.4.4. <i>Yeast one-hybrid library construction and screening</i>	52
2.4.5. <i>Plasmid rescue from yeast</i>	53
2.4.6. <i>Quantitative assessment of protein-protein interactions in yeast</i>	53
2.4.7. <i>Colony lift filter assays</i>	54
2.5. Localisation Studies	54
2.5.1. <i>Particle bombardment of tobacco</i>	54
2.5.2. <i>Co-localisation of fusion proteins in living chloroplasts</i>	55
2.5.3. <i>Bimolecular Fluorescence Complementation assays.</i>	55
2.6. Microscopy	56
2.6.1. <i>Light microscopy sample preparation</i>	56
2.6.2. <i>Fluorescence microscopy</i>	56
2.6.3. <i>Image acquisition</i>	56

3. The plastid division protein AtMinD1 is a Ca²⁺-ATPase stimulated by AtMinE1 **58**

3.1. Introduction	58
--------------------------	-----------

3.2 Results	61
3.2.1. <i>AtMinD1</i> is a Ca^{2+} -dependent ATPase	61
3.2.2. <i>AtMinE1</i> stimulates the ATPase activity of <i>AtMinD1</i>	62
3.2.3. <i>AtMinD1(K72A)</i> exhibits mis-localisation inside chloroplasts	68
3.2.4. <i>AtMinD1(K72A)</i> can dimerise	70
3.2.5 <i>AtMinD1(K72A)</i> is unable to interact with <i>AtMinE1</i>	71
3.3. Discussion	74
3.3.1. <i>AtMinD1</i> is an ATPase	74
3.3.2. <i>EcMinD</i> and <i>AtMinD1</i> exhibit functional differences	74
3.3.3. <i>AtMinD1</i> ATPase activity is required for correct localization	76
3.3.4. Conclusion	77

4. Interaction analysis of stromal plastid division proteins 79

4.1. Introduction	79
4.2. Results	82
4.2.1. Co-localisation of <i>Arabidopsis</i> Min proteins	82
4.2.2. <i>AtMinD1</i> and <i>AtMinE1</i> interact	83
4.2.3. Interaction of <i>Arabidopsis</i> FtsZ proteins	83
4.2.4. FtsZ proteins co-localise outside of a normal ring structure	85
4.2.5. ARC6 co-localises with the Z-ring	88
4.2.6. ARC6 interacts specifically with <i>AtFtsZ2</i>	88
4.3. Discussion	92
4.3.1. <i>Arabidopsis</i> Min proteins interact	92
4.3.2. <i>Arabidopsis</i> FtsZ proteins co-localise	93
4.3.3. ARC6 co-localises with FtsZ proteins	94
4.3.4. Conclusions	95

5. Searching for novel chloroplast division components using protein-protein interaction approaches.	97
5.1. Introduction	97
5.2. Results	99
5.2.1. Selection of baits for yeast two-hybrid screen	99
5.2.2. Generation of baits for yeast two-hybrid screen	100
5.2.3. Testing baits for autoactivation	102
5.2.4. Screening the cDNA library	103
5.2.5. Selection of positive clones	105
5.2.6. Testing unique clones for re-interaction	110
5.2.7. DNA sequencing and analysis of unique clones.	110
5.2.8. Analysis of candidate clones	116
5.2.9. Testing for interaction between F2-21 and GC1	122
5.2.10. Using Co-immunoprecipitation to hunt for novel chloroplast division components	122
5.3. Discussion	128
5.3.1. Selection of candidate clones	128
5.3.2. Analysis of F2-44	129
5.3.3. Analysis of F2-10	131
5.3.4. Analysis of F2-21	133
5.3.5. Using co-immunoprecipitation to hunt for novel chloroplast division components	134
5.3.6. Conclusion	136
6. Regulation of gene expression and plastid division	138
6.1 Introduction	138
6.2. Results.	142
6.2.1. Light regulation of FtsZ1-1, FtsZ2-1, AtMinD1 and AtMinE1.	142

6.2.2. DNA Microarray analysis	145
6.2.2.1. Selection of genes for further analysis	153
6.2.2.2. Analysis of selected genes	154
6.2.3. Analysis of the promoter regions of the min genes	155
6.2.3.1. Constructing Yeast one-hybrid baits	167
6.2.3.2. Testing baits for leaky HIS3 expression	168
6.2.3.3. Library construction	168
6.2.3.4. Analysis of Library Clones	176
6.2.3.5. Analysis of candidates using E1 as bait.	181
6.2.3.6. Analysis of candidates using E2 as bait.	182
6.3. Discussion	186
6.3.1. Expression of Arabidopsis ftsZ and min genes is light regulated	186
6.3.2. Affect of chloroplast division inhibition on nuclear gene expression	188
6.3.3. Analysis of the promoter regions of AtMinD1 and AtMinE1	190
6.3.4. Yeast one-hybrid screening	191
7. Discussion	193
7.1 Characterisation of AtMinD1 and the Min system.	193
7.2. Future directions in the characterisation of the min system	196
7.3. Assembly of the stromal plastid division machinery	197
7.4. Future directions in assembly of chloroplast division components	200
7.5. Hunting for novel chloroplast division components	201
7.6. Future directions in the hunt for novel plastid division components	202
7.7. Regulation of chloroplast division	203
7.8. Future directions for investigation of the regulation of plastid division.	205
7.9. Numerous chloroplasts versus giant chloroplasts	206
7.10. Concluding remarks	207

References **208**

Appendix 1. Vectors used in this study **231**

A1. pET-14b	231
A2. pGADT7	232
A3. pGADT7-Rec2	233
A4. pGBKT7	234
A5. pHIS2	235
A6. pGEX-6P	236
A7. pPCR-Script	237
A8. PER-10	238
A9. pTA-211	239
A10. pWEN15	240
A11. pWEN18	241

Appendix 2. Publications resulting from this study **242**

Appendix 3. Plasmids used in this study **243**

Addenda consisting of one CD-ROM

DNA Microarray Data:

- B1. Control vs Temporal induction of AtMinD1**
- B2. Control vs Prolonged induction of AtMinD1**
- B3. Temporal vs Prolonged induction of AtMinD1**

1. Introduction

1.1. General introduction

Plastids are essential plant organelles. They develop from small, colourless, undifferentiated proplastids in dividing meristematic cells which subsequently differentiate into several plastid types depending on the developmental stage and cell type during cell differentiation. Different plastid types are defined by virtue of their storage components and internal structure and include chloroplasts, leucoplasts, amyloplasts, etioplasts, elaioplasts and chromoplasts. Although most attention has been directed towards chloroplasts because of their photosynthetic capability, plastids are involved in many vital plant processes such as lipid, hormone, amino acid and phytochrome chromophore biosynthesis as well as nitrate and sulphur assimilation (Galili, 1995; Ohlrogge and Browse, 1995). It is generally accepted that plastids originated from endosymbiotic cyanobacteria (Margulis, 1970; Gray, 1999; McFadden, 2001) and like bacteria, new plastids arise through the binary fission of pre-existing plastids, no *de novo* synthesis of plastids occurs. Because of this plastid division is important not only for the maintenance of plastid populations in dividing plant cells but also for accumulation of large numbers of chloroplasts in photosynthetic cells in order to maximize photosynthesis. Dividing chloroplasts were observed in the late 1960s; however it is only during the last decade that the molecular events underlying plastid division have begun to be unravelled. Not only have a number of new protein components of the division machinery been identified but insight into biochemical activities and inter-protein relationships has shed light on the intricate complexity of plastid division in higher plants.

1.2. Basic morphology of plastid division

Chloroplast division was first documented in 1969 when dumbbell-shaped chloroplasts were observed in spinach followed by a subsequent increase in chloroplast number per cell (Possingham and Saurer, 1969), subsequent observations of dumbbell-shaped chloroplasts in other plant species, such as tobacco and sesame established that chloroplasts replicate by constriction division (Boasson *et al.*, 1972; Platt-Aloia and Thompson, 1977). From morphological analysis, the process of chloroplast division can be separated into four distinct stages (Possingham and Lawrence, 1983, Leech *et al.*, 1981): (i) Plastid elongation, (ii) Plastid constriction and dumbbell formation, (iii) Further constriction, isthmus

formation and thylakoid membrane separation, and (iv) Isthmus breakage, plastid separation and envelope resealing.

Initial insight into ultrastructural changes during plastid division came from electron microscopy studies that identified fuzzy plaques of electron-dense material covering or displacing the constricting isthmus of dividing chloroplasts (Leech *et al.*, 1981). Later studies using the red alga *Cyanidium caldarium*, a unicellular organism containing a single chloroplast, revealed this fuzzy plaque to be an electron-dense ring-like structure located on the cytosolic face of the membrane encircling the constricting isthmus. This structure was termed the plastid-dividing ring or PD ring (Mita *et al.*, 1986). Subsequently, in *Avena sativa*, the PD-ring structure was resolved and found to consist of two rings; an inner PD ring on the stromal face of the inner envelope and an outer PD ring on the cytosolic face of the outer envelope (Hashimoto, 1986). These two PD rings have now been detected in numerous plant and algal species and are thought to represent a universal feature of dividing chloroplasts in all plant cells. Interestingly, a third PD ring was identified in the intermembrane space of single chloroplasts found in the unicellular red alga *Cyanidioschyzon merolae* (Miyagishima *et al.*, 1998a). Although this third PD ring has only been observed in *C. merolae* it is highly possible that it is ubiquitous throughout plant species. How the PD rings operate together to bring about chloroplast division has begun to be unravelled. *C. merolae* is a useful organism in which to study the behaviour of the PD rings because plastid division can be synchronised through a 12 hour light/12 hour dark regimen (Suzuki *et al.*, 1994) and in *C. merolae* the PD rings can be observed clearly from the start of plastid division. Transmission electron microscope studies utilizing synchronised cultures of *C. merolae* revealed that the timing of assembly and the behaviour of each PD ring during chloroplast division is different (Miyagishima *et al.*, 1998b; Miyagishima *et al.*, 1999; Miyagishima *et al.*, 2001b). The inner PD ring forms first followed by the middle and outer PD rings, however, all of the rings form before any visual constriction at the division site. During constriction, the inner and middle PD rings remain a constant thickness but decrease in overall volume. This volume decrease is in proportion with constriction suggesting a steady loss of components from these two rings as constriction proceeds. In contrast, the outer PD ring widens and thickens during constriction indicating no loss of components and eventually becomes a wide, thick, and rigid structure (Miyagishima *et al.*, 1999). Late in constriction the middle and inner PD rings disassemble completely and disappear before the daughter plastids are severed whilst the outer PD ring remains attached until after completion of division and disassembles just after

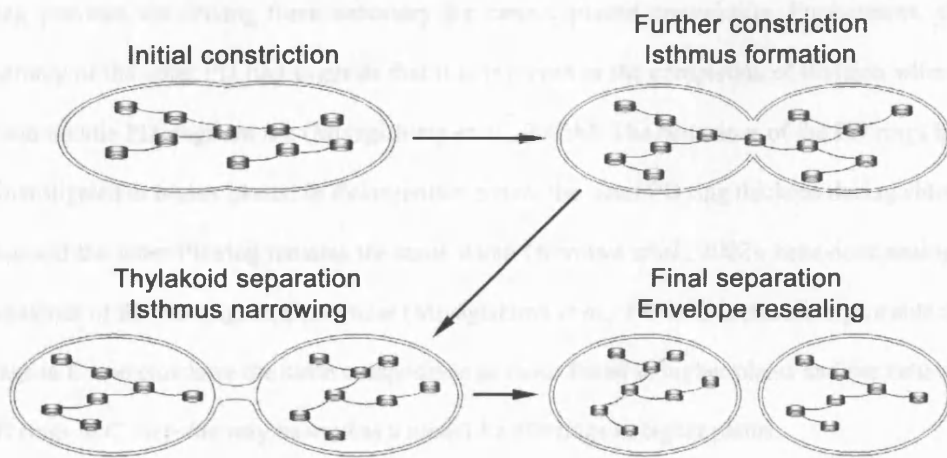


Fig. 1. 1 Schematic overview of the morphological changes that take place during plastid division in higher plants. Plastid division is initiated by slight elongation and constriction, followed by further constriction and isthmus formation. Later stages of constriction involve isthmus narrowing and the separation of the thylakoid membranes. Finally the isthmus breaks, the envelopes reseal followed by the complete separation of the two daughter plastids. Figure taken from Aldridge *et al.*, 2005.

division (Miyagishima *et al.*, 2001b). The distinct behaviour of the rings implies that PD ring protein composition is different. The thickening of the outer PD ring during constriction suggests that the outer PD ring provides the driving force necessary for central plastid constriction. Furthermore, the late disassembly of the outer PD ring suggests that it is involved in the completion of division whereas the inner and middle PD rings are not (Miyagishima *et al.*, 2001b). The behaviour of the PD rings has also been investigated in higher plants. In *Pelargonium zonale* the outer PD ring thickens during chloroplast division and the inner PD ring remains the same width (Kuroiwa *et al.*, 2002), behaviour analogous to the behaviour of the PD rings in *C. merolae* (Miyagishima *et al.*, 1999). It is therefore probable that the PD rings in *C. merolae* have the same composition as those found in higher plants and the behaviour of the PD rings in *C. merolae* may be used as a model for PD rings in higher plants.

As proteins involved in plastid division have been identified suggestions for the composition of the PD rings have been proposed. The isolation and cloning of *arc5*, one of 12 *accumulation and replication of chloroplast* mutants identified in a screen of ethyl methane sulphonate mutagenised *Arabidopsis* seeds, has revealed that *ARC5* encodes a dynamin-like protein that localises into a ring-like structure at the division site on the cytosolic face of the chloroplast envelope (Gao *et al.*, 2003). Because of the localisation of *ARC5* it was suggested that filaments of *ARC5* form the outer PD ring. The outer PD ring has been shown in *C. merolae* to consist of a bundle of unidentified 5 nm filaments that coil around the constriction site (Miyagishima *et al.*, 2001a). Some dynamin strands have an approximate diameter of 6 nm (Klockow *et al.*, 2002) adding credibility to the proposal that *ARC5* is the main constituent of the outer PD ring. However, further analysis to investigate the protein composition of the PD rings identified a 56 kDa protein as a candidate for the main component of the 5 nm bundles (Miyagishima *et al.*, 2001a), at 87 kDa *ARC5* is larger than expected.

Because of their cyanobacterial origins, it was speculated relatively early that plastid division might share common features with bacterial cell division. A key player in bacterial cell division is *FtsZ*, a structural homologue of tubulin (Löwe and Amos, 1998). Polymerisation of *FtsZ* into a contractile Z-ring initiates bacterial cell division (Bi and Lutkenhaus, 1991; Lutkenhaus and Addinall, 1997). Three *FtsZ* homologues have been identified in *Arabidopsis* (Osteryoung and Vierling, 1995). All three *FtsZ* proteins have been found to co-localise into a Z-ring within the stroma at the division site in *Arabidopsis* and tobacco (Vitha *et al.*, 2001; Fujiwara and Yoshida, 2001; McAndrew *et al.*, 2001; Maple *et al.*, 2005). Because of the stromal Z-ring localisation it was first thought that *FtsZ*

might have been the main component of the inner PD ring. Further analyses have shown that the Z-ring is distinct from components of the inner PD ring and actually forms a ring on the stromal side of the inner PD ring (Miyagishima *et al.*, 2001b). Analysis of Z-ring formation in *C. merolae* revealed that it forms 3-4 hours before the formation of the PD rings (Kuroiwa *et al.*, 2002) suggesting that the Z-ring determines the site of division after which there is recruitment and assembly of the PD rings (Kuroiwa *et al.*, 2002). It has been postulated that the Z-ring based system evolved from a cyanobacterial endosymbiont whereas the PD ring system has probably been recruited from the eukaryotic host (Miyagishima *et al.*, 2001b).

Although most research has centred on the ultrastructural changes that take place during chloroplast division some information exists, although limited, regarding proplastid division. Proplastids are small, undifferentiated, colourless plastids found in dividing meristematic cells from which all plastids in differentiated cells originate. Meristematic cells contain between 10 and 20 proplastids (Juniper and Clowes, 1965; Lyndon and Robertson, 1976) and these differentiate into a variety of plastid types as cell differentiation proceeds (Cran and Possingham, 1972). In order to maintain appropriate proplastid segregation during cell division, proplastids must divide prior to cytokinesis. Indeed, dumbbell-shaped proplastids containing central constrictions have been observed indicative of proplastid division (Chaly and Possingham, 1981; Whatley, 1983). In addition and in contrast to wild-type, the *Arabidopsis* chloroplast division mutant *arc6* (see later sections) has only two enlarged proplastids present in apical meristematic cells demonstrating that proplastid division is under cellular regulation. In meristematic cells proplastid division keeps pace with cell division but as cells differentiate the number of plastids per cell increases suggesting that the release of plastid division constraints is an early event during plant cell differentiation (Lyndon and Robertson, 1976). This further suggests that the regulation of proplastid division is different from that of division of differentiated plastids although to-date limited evidence exists.

1.3. Bacterial cell division versus plastid division

Because of the bacterial ancestry of plastids, it was hypothesised that plastid division may share many features with bacterial cell division. The availability of whole bacterial genome sequences combined with the advantage of a well defined bacterial system, has made it an invaluable tool to investigate the molecular mechanism of plastid division.

Cell division in bacteria is carried out by a complex macromolecular machinery, often called the divisome. The divisome consists of at least ten proteins that bring about septation of the bacterial cell to form two equal and identical daughter cells (Ma *et al.*, 1996; Lutkenhaus and Addinall, 1997; Wang *et al.*, 1997; Yu and Margolin, 1997; Din *et al.*, 1998; Chen *et al.*, 1999; Weiss *et al.*, 1999; Ma and Margolin, 1999). FtsZ is arguably the most crucial component of the divisome and is conserved in virtually all eubacteria, archaea and organelles of many eukaryotes (Margolin, 2000). FtsZ is a structural homologue of tubulin (Nogales *et al.*, 1998) and undergoes GTP-dependant polymerisation to form a contractile ring, the Z-ring, at the future division site. Formation of the Z-ring is generally accepted to be the key event in the initiation of cell division and the Z-ring is believed to act as a scaffold for assembly of the remaining proteins involved in division of the bacterial cell. After formation of the Z-ring the other proteins that make up the divisome (FtsA, FtsB, FtsI, FtsK, FtsL, FtsN, FtsQ, FtsW, FtsZ and ZipA, see Table 1) localise to the divisome according to a defined and linear hierarchy of dependence. Once the divisome is assembled septation of the bacterial cell takes place.

Prior to cell division it is critical for the cell to establish the site at which division should take place. Equal division of the bacterial cell requires strict fidelity of Z-ring placement at mid-cell. To achieve this, in *E. coli*, two different mechanisms are recognised to restrict Z-ring formation to the mid-cell point. The first is nucleoid occlusion; this as yet poorly-defined mechanism prevents septation over nucleoids which would result in fragmentation of the genome and probable demise of the cell. To date only two proteins have been identified to be involved in nucleoid occlusion; Noc in *Bacillus subtilis* (Wu and Errington, 2004) and SlmA in *E. coli* (Bernhardt and de Boer, 2005). How these proteins operate to prevent Z-ring formation is yet to be elucidated. The second, more well defined mechanism is the min system which requires the components of the *minB* operon. Mutations within the *minB* operon lead to the formation of minicells (de Boer *et al.*, 1990; Labie *et al.*, 1990) as septation of the bacterial cell frequently occurs near the cell poles instead of mid-cell. The *minB* operon encodes three proteins; MinC, MinD and MinE that act in concert to limit the placement of the Z-ring to mid-cell. MinC acts as an antagonist to FtsZ polymerisation preventing formation of a stable Z-ring (Hu *et al.*, 1999), however, MinC lacks site specificity so it will inhibit FtsZ polymerisation anywhere in the cell (de Boer *et al.*, 1992). Topological specificity is conferred on MinC by the coordinated action of MinD and MinE (Hu and Lutkenhaus, 1999). So far only homologues of FtsZ, MinD and MinE have been identified in *Arabidopsis*.

1.3.1. FtsZ

Quantitative Western blotting in *E. coli* revealed there to be ~15,000 molecules of FtsZ per cell (Lu *et al.*, 1998), enough to span the circumference of the cell several times suggesting that the Z-ring is composed of multiple strands of FtsZ polymers. Studies have shown that the Z-ring is a highly dynamic structure that undergoes rapid assembly and disassembly. At any one time only 30% of the FtsZ protein within the cell is contained within the Z-ring (Stricker *et al.*, 2002) and there is a constant exchange between the FtsZ monomers contained within the Z-ring and the pool of FtsZ protein in the cytoplasm (Stricker *et al.*, 2002). Observations of FtsZ structures in *E. coli* and *B. subtilis* suggest that between formation of a functional medial Z-ring, spiral-like intermediates exist suggesting that FtsZ not only forms the Z ring but also is part of a highly dynamic, potentially helical cytoskeleton in bacterial cells (Theander and Margolin, 2004; Ben-Yehuda and Losick, 2002).

The Z-ring plays an essential role in constriction of the cell membrane as well as in coordination of the whole process of division. Although the method of Z-ring constriction remains elusive several models have been proposed. Of these, the model with the most evidential support is that constriction is brought about by FtsZ filaments losing subunits through depolymerisation of the Z-ring. Observations that support this hypothesis are that overexpression of FtsZ prevents cell division; this would be explained if loss of FtsZ monomers is required for constriction, and also the overall highly dynamic structure of the Z-ring lends support to the proposal of a constriction model based on depolymerisation. In this model, protofilament pieces might be removed from the ring more quickly than they are replaced, re-annealing of the remaining filaments could only occur when they move closer together, and this might lead to a circumferential constriction that could power cell division.

A homologue of *E. coli* FtsZ was identified in *Arabidopsis* through homology searches (Osteryoung and Vierling, 1995). *Arabidopsis* FtsZ shares over 40% amino acid identity to many bacterial FtsZ proteins but is more closely related to those from cyanobacteria compared to other prokaryotes sharing 50% protein similarity to the cyanobacterial FtsZ (Osteryoung and Vierling, 1995). After the identification of the first FtsZ homolog in *Arabidopsis* a further two homologues were revealed. In contrast to bacteria that encode a single *FtsZ* gene it became apparent that there were two distinct families of FtsZ proteins in *Arabidopsis* and other plant species (Osteryoung *et al.*, 1998; Osteryoung and McAndrew, 2001; Stokes and Osteryoung, 2003). These two families of FtsZ proteins have been termed FtsZ1 and FtsZ2 and it was originally thought that they arose by a duplication event

Table 1. 1 Proteins required for cell division in *E. coli*.

Class	Protein	Function	Reference	Arabidopsis homologue
Division site selection	MinC	FtsZ inhibitor	Hu <i>et al.</i> , 1999	-
	MinD	MinC activating protein	Zhou and Lutkenhaus, 2004	Colletti <i>et al.</i> , 2000
	MinE	Topological specificity	de Boer <i>et al.</i> , 1989	Maple <i>et al.</i> , 2002
Z-ring associated	FtsZ	Forms Z-ring scaffold	Dai and Lutkenhaus, 1991	Osteryoung and Vierling 1995
	FtsA	Stabilisation of Z-ring. recruits downstream components	Addinall and Lutkenhaus, 1996	-
	ZipA	Stabilises Z-ring at the membrane recruits downstream components	Hale and de Boer, 1997	-
	ZapA	Promotes Z-ring formation	Gueiros-Filho and Losick, 2002	-
**"Late" division proteins	FtsEX	Unknown function	Schmidt <i>et al.</i> , 2004	-
	FtsK (K)	Chromosome segregation	Begg <i>et al.</i> , 1995	-
	FtsQ (Q)	Unknown function	Chen <i>et al.</i> , 1999	-
	FtsL (L)	Unknown function	Ghigo and Beckwith, 2000	-
	FtsB (B)	Unknown function	Buddelmeijer <i>et al.</i> , 2002	-
	FtsW (W)	Unknown function, SEDS family	Pastoret <i>et al.</i> , 2004	-
	FtsI (I)	Division specific transpeptidase	Weiss <i>et al.</i> , 1999	-
	AmiC	Amidase required for cell separation	Bernhardt and de Boer, 2003	-
	FtsN (N)	Unknown function, contains murein binding domain	Dai and Lutkenhaus, 1996	-

* Late division proteins refers to proteins that require binding of FtsA and ZipA to the divisome complex before they are able to bind the divisome complex.

from a single *FtsZ* gene present in the cyanobacterial ancestor of chloroplasts (Osteryoung and McAndrew, 2001). Recent phylogenetic analysis indicates that the divergence of the two *FtsZ* families occurred between the divergence of red and green algae signifying the duplication of the *FtsZ* gene may have happened in the cyanobacterial progenitor of chloroplasts (Stokes and Osteryoung, 2003). *FtsZ* proteins from the two families are distinguished by conserved differences in amino acid sequences. Plant *FtsZ* proteins share most of the structural features common to the bacterial proteins and all *FtsZ* proteins can be divided into two structural domains (Osawa and Erikson, 2005), a highly conserved N-terminal domain which is sufficient for polymerisation (Wang *et al.*, 1997), and a more variable C-terminal domain. One of the most important features of the N-terminal domain is the Rossmann fold, a motif frequently found in nucleotide-binding proteins (Löwe and Amos, 1998). The Rossmann fold, essential for GTP-hydrolysis, harbours the GTP-binding tubulin signature motif GGGTG(T/S)G (de Boer *et al.*, 1992; RayChadhuri and Park, 1992) and contains additional residues that contact the guanine nucleotide (Wang *et al.*, 1997; Löwe and Amos, 1999; Osteryoung and McAndrew, 2001). The C-terminal domain of *FtsZ* is more variable among different organisms. Important features present in the C-terminal domain include highly conserved “synergy” residues believed to regulate GTP-hydrolysis and loop structures that are possibly involved in calcium binding (Löwe and Amos, 1998). Interestingly, calcium binding has been shown not to be essential for *FtsZ* assembly at least in *E. coli* (Mukherjee and Lutkenhaus, 1999). Also present in the C-terminal domain is the core domain that is required in *E. coli* *FtsZ* for direct interactions with ZipA and FtsA (Ma *et al.*, 1996; Wang *et al.*, 1997; Din *et al.*, 1998; Liu *et al.*, 1999; Hale *et al.*, 2000; Mosyak *et al.*, 2000; Yan *et al.*, 2000). ZipA is thought to function by anchoring *FtsZ* to the membrane and supporting Z-ring structure whilst FtsA is thought to stabilise *FtsZ* proto-filaments preventing depolymerisation of the Z-ring. In *Mycobacterium*, which has no FtsA or ZipA, this peptide binds FtsW (Datta *et al.*, 2002). The core domain is conserved in the plant *FtsZ2* proteins but not in *FtsZ1* proteins and it is possible that FtsA- and ZipA-like proteins interact specifically with *FtsZ2* and not *FtsZ1*. However, no homologues of FtsA or ZipA have as yet been identified in *Arabidopsis* or in other plant species.

FtsZ was first demonstrated to be an essential chloroplast division component in the moss *Physcomitrella patens* where a knockout of the *FtsZ* homologue caused the inhibition of chloroplast division resulting in cells containing only one large chloroplast (Strepp *et al.*, 1998). The same phenotype is observed in *Arabidopsis* where reduced expression of *FtsZ* from either family causes

inhibition of chloroplast division (Osteryoung *et al.*, 1998). This demonstrates that both FtsZ1 and FtsZ2 are essential for chloroplast division and overexpression studies furthermore revealed that the correct stoichiometric amount is paramount for correct division to occur. Levels of FtsZ1 elevated as little as three-fold are enough to cause the inhibition of chloroplast division (Stokes *et al.*, 2000). Similarly in *P. patens* overexpression of FtsZ2 causes plastid division inhibition in a dose-dependant manner (Kießling *et al.*, 2000). This dose dependency is also witnessed in *E. coli*; a slight increase in the level of FtsZ actually increases cell division whereas a high level of FtsZ inhibits cell division producing long filamentous cells (Ward and Lutkenhaus, 1985). In *Arabidopsis*, FtsZ proteins from both families were found to form a ring structure at the plastid midpoint suggesting that both families have a role as part of the Z-ring (Vitha *et al.*, 2001; Fujiwara and Yoshida, 2001; McAndrew *et al.*, 2001). Recent studies have begun to show functional differences between FtsZ proteins from the two families. *Nicotiana tabacum* FtsZ1 is localised only in the stroma, whereas FtsZ2 although predominantly present in the stroma is also found associated with the envelope membranes (El-Kafafi *et al.*, 2005). FtsZ proteins lack a clear membrane-spanning sequence and in *E. coli* ZipA is thought to anchor FtsZ to the membrane. ZipA interacts with FtsZ through the core domain of FtsZ (Hale *et al.*, 2000; Haney *et al.*, 2001) which is present in FtsZ2 family proteins but absent in FtsZ1 proteins. Although a homologue of ZipA has not been reported in higher plants, it seems possible that a fraction of FtsZ2 proteins through interaction with a ZipA-like protein is tightly associated with the membrane. In addition El-Kafafi *et al.*, 2005 have shown that in *in vitro* experiments tobacco FtsZ1 but not FtsZ2 is able to polymerise. This is surprising since proteins from both the FtsZ families have very similar N-terminal domains and in *E. coli* FtsZ the N-terminal domain is sufficient for polymerisation (Wang *et al.*, 1997).

1.3.2. MinD

Accurate placement of the division septum requires the Min proteins. In *E. coli* the Min system consists of three proteins MinC, MinD and MinE that act in concert to limit Z-ring placement to midcell. MinC acts as an inhibitor to FtsZ polymerisation preventing formation of a stable Z-ring (Hu *et al.*, 1999), *E. coli* MinD is a peripheral membrane protein (de Boer *et al.*, 1989) that associates with the *E. coli* cytoplasmic membrane via a short C-terminal amphipathic helix termed the membrane targeting sequence (MTS) (Hu and Lutkenhaus 2003; Szeto *et al.*, 2003). MinD belongs to a large family of

ATPases that contain a deviant WalkerA motif involved in the binding and hydrolysis of ATP (de Boer *et al.*, 1991). MinD membrane association requires binding of ATP (Hu *et al.*, 2002; Lackner *et al.*, 2003) and association with the membrane increases the strength of interaction between MinD molecules by 25-fold (Taghbalout *et al.*, 2006). It has been suggested that upon binding the membrane MinD undergoes a conformational change that promotes the self assembly of MinD molecules to produce membrane-associated MinD polymeric protofilaments at the cell pole (Suefuji *et al.*, 2002; Lackner *et al.*, 2003; Taghbalout *et al.*, 2006). MinD interacts with both MinC and MinE (Huang *et al.*, 1996; Suefuji *et al.*, 2002; Ma *et al.*, 2003; Ma *et al.*, 2004) and has two main functions; to activate the Z-ring inhibitor MinC (Zhou and Lutkenhaus, 2004) and to localise MinC and MinE to the membrane (Raskin and de Boer 1999). Interaction with MinE stimulates the ATPase activity of membrane-bound MinD (Hu and Lutkenhaus, 2001) and causes diassociation of MinD from the membrane (Hu and Lutkenhaus, 2001) and oscillation to the opposite cell pole.

The Min system has been extensively studied in *E. coli* and the Min oscillation cycle can be divided into the following pathway of events: ATP-bound MinD interacts with MinC and activates MinC-mediated division inhibition (de Boer *et al.*, 1991; Zhou and Lutkenhaus, 2004). MinD also recruits MinC to the membrane where together they form a stable inhibition complex at the polar zone of the cell (Huang *et al.*, 1996; Huang *et al.*, 2003). At the membrane MinD is able to polymerise (Suefuji *et al.*, 2002; Lackner *et al.*, 2003; Taghbalout *et al.*, 2006), creating a polar zone of the MinD/C inhibitor. MinE imparts topological specificity to this inhibition complex through its interactions with MinD. MinE binds to the MinD/C complex stimulating the ATPase activity of MinD (Hu and Lutkenhaus, 2001), causing dissociation of MinD from the membrane (Suefuji *et al.*, 2002) and oscillation to the opposite cell pole where MinD again forms a stable complex with MinC until again being released by MinE. In this way MinE acts as a topological specificity factor constantly redistributing MinD and MinC so that all three components repeatedly oscillate from one cell pole to the other in a ~40 second cycle (Fu *et al.*, 2001; Huang *et al.*, 2003). This oscillation means that the time-averaged concentration of MinC and MinD is lowest at midcell allowing Z-ring formation to occur here. Recent evidence indicates that MinD travels along a spiral-like path and it has been suggested that the polymerisation of MinD into a helical filament underlies the dynamic behaviour exhibited by MinD (Shih *et al.*, 2003).

The possibility that a min-based system may operate in the division site-selection in plastid division was initially indicated by the identification of homologues of MinD and MinE in the plastid genome of the unicellular chlorophyte *Chlorella vulgaris* (Wakasugi *et al.*, 1997). This was followed by the identification of a MinD homologue in the nuclear genome of *Arabidopsis* (Colletti *et al.*, 2000), rice and Marigold (Moehs *et al.*, 2001). *Arabidopsis* MinD was identified through homology searches using the protein sequence of *C. vulgaris* MinD as the query input. The *Arabidopsis* homologue, referred to as AtMinD1, shares 65% amino acid similarity to MinD from *C. vulgaris* and greater than 40% amino acid identity with other bacterial MinD proteins (Colletti *et al.*, 2000). The *AtMinD1* gene encodes a protein of 326 amino acids which includes an N-terminal chloroplast targeting transit peptide (Colletti *et al.*, 2000).

The importance of AtMinD1 in plastid division in *Arabidopsis* was established by the phenotypes observed when *AtMinD1* expression is altered. Reduced levels of *AtMinD1* gives rise to chloroplast size heterogeneity within individual cells and chloroplasts are consistently fewer in number and larger in size compared to wild-type cells (Colletti *et al.*, 2000). The heterogeneity in chloroplast size is reminiscent of the asymmetric division and subsequent minicell formation in *E. coli* when MinD is inactivated, suggesting functional conservation between the *Arabidopsis* AtMinD1 and the *E. coli* MinD. Increased levels of *AtMinD1* leads to a dramatic reduction in the number of chloroplasts per cell demonstrating that overexpression of *AtMinD1* partially inhibits chloroplast division (Colletti *et al.*, 2000; Kanamaru *et al.*, 2000). The few chloroplasts present are greatly enlarged resembling the filamentation phenotype observed in *E. coli* when MinD is expressed at high levels (de Boer *et al.*, 1989). AtMinD1 mode of action also seems to be conserved amongst different plant species; AtMinD1 overexpression in transgenic tobacco plants results in inhibition of chloroplast division (Dinkins *et al.*, 2001).

AtMinD1-GFP fusion protein experiments reveal a distinct interplastidic localisation of AtMinD1 often forming one or two discrete spots at polar zones of chloroplast (Maple *et al.*, 2002, Fujiwara *et al.*, 2004) (Fig. 2.). The localisation pattern is similar to that observed in *rodA* spherical *E. coli* cells (Corbin *et al.*, 2002) and it is expected that AtMinD1 exhibits dynamic behaviour analogous to *E. coli* MinD although this has not yet been observed. AtMinD1 is always observed in close proximity to the envelope region suggesting that like *E. coli* MinD, it is a membrane-associated protein

(Maple *et al.*, 2002). AtMinD1 also dimerises and it is likely that it is capable of polymerization (Fujiwara *et al.*, 2004; Aldridge and Møller, 2005; Maple *et al.*, 2005).

1.3.3. MinE

In *E. coli*, MinE confers topological specificity on the MinC/D inhibitor complex by suppressing the action of the division inhibitor at mid-cell but not at the cell poles (de Boer *et al.*, 1989). In the absence of MinE, MinC/D localises uniformly to the membrane and prevents Z-ring formation throughout the cell resulting in filamentous cells (Hu and Lutkenhaus, 1999; Raskin and de Boer, 1999). MinE has two functions; to suppress the MinC/D inhibitor and to confer topological specificity on MinC/D. The dual functions of MinE are mediated by two separate domains of the MinE protein; an N-terminal anti MinCD domain (AMD) and a C-terminal topological specificity domain (TSD) (Pichoff *et al.*, 1995; Zhao *et al.*, 1995; Hu and Lutkenhaus, 2001). MinE controls the oscillation of MinC/D through interaction of MinE with MinD whereby MinE stimulates MinD ATPase activity (Hu and Lutkenhaus, 2001; Suefuji *et al.*, 2002) causing disassembly and disassociation of MinD from the membrane (Hu *et al.*, 2002; Suefuji *et al.*, 2002) and oscillation to the opposite pole of the cell.

The bulk of MinE accumulates in a ring-like structure at the medial edge of the MinD polar zone (Raskin and de Boer, 1997). MinE is also present at the periphery of the cell between the cell pole and the MinE ring resembling the localisation of MinD (Raskin and de Boer, 1997). The MinE ring is not static but is a dynamic structure that undergoes a repetitive cycle of migration, dissolution and reformation; the MinE-ring moves from a mid-cell position to a pole of the cell where it dissipates followed by the formation of a new ring at mid-cell which then moves to the opposite cell pole (Hale *et al.*, 2001; Fu *et al.*, 2001). Formation of the MinE ring requires MinD (Raskin and de Boer, 1997; Fu *et al.*, 2001) in the absence of MinD; MinE is evenly distributed throughout the cytoplasm (Raskin and de Boer, 1997; Fu *et al.*, 2001) Conversely MinE is required for the formation of MinD polar zones (Raskin and de Boer, 1999; Hu and Lutkenhaus, 2001).

MinE interacts weakly with MinD (Huang *et al.*, 1996; Ma *et al.*, 2003). MinC and MinE bind to overlapping sites on the MinD surface and MinE binding interferes with the interaction between MinC and MinD (Ma *et al.*, 2003) and can promote the release of MinC from a MinC/D phospholipid complex (Lackner *et al.*, 2003). Interaction with MinD is mediated through the α -helical region of the MinE AMD and involves the formation of a coiled-coil structure (Ma *et al.*, 2003). The interaction

between MinE and MinD stimulates the ATPase activity of MinD; MinD Lysine 11 within the Walker A region (P-loop) competes with MinE for residues within MinD α -helix 7 (Ma *et al.*, 2004). MinE-mediated disruption of the non-covalent interaction between lysine 11 and α -helix 7 changes the lysine 11 side-chain orientation and the P-loop conformation and this transmits an activation signal to the neighbouring catalytic domain or to the bound ATP bringing about ATP hydrolysis (Ma *et al.*, 2004).

AtMinE1 was identified in *Arabidopsis* based on its similarity to prokaryotic and chloroplast-encoded MinE proteins (Itoh *et al.*, 2001; Maple *et al.*, 2002; Reddy *et al.*, 2002). The role of AtMinE1 in chloroplast division was demonstrated in *Arabidopsis* and tobacco plants with elevated levels of AtMinE1 (Itoh *et al.*, 2001; Maple *et al.*, 2002; Reddy *et al.*, 2002). In these plants mesophyll cells contained a reduced number of enlarged chloroplasts which showed striking size heterogeneity within single cells. Analysis of the chloroplast division phenotype in hypocotyls of seedlings overexpressing AtMinE1 showed the presence of chloroplasts with misplaced constriction sites towards one pole of the plastid giving rise to a 'minicell' phenotype similar to that of *E. coli* overexpressing MinE (Maple *et al.*, 2002) Although sequence homology is less well conserved between MinE proteins compared to MinD proteins, overexpression of AtMinE1 in *E. coli* can induce the minicelling phenotype observed when endogenous MinE is overexpressed in *E. coli* (Maple *et al.*, 2002).

Sequence alignments of AtMinE1 with the *E. coli* minE sequence suggests that the *Arabidopsis* protein harbours an N-terminal AMD domain, however the C-terminal TSD domain region is less conserved. TSD domains from various species show limited similarity, suggesting evolutionary divergence of TSD function, possibly to integrate the MinE protein into the division machineries of different species. AtMinE1 has a distinct intraplastidic localisation pattern, localising as a single spot or as two spots in close proximity towards one end of the chloroplast and co-localises and interacts with AtMinD1 (Maple *et al.*, 2005) (Fig. 2.), this suggests that these two proteins act in concert in a way analogous to the Min complex in bacteria. Indeed, AtMinE1 has been observed to exhibit dynamic behaviour in *E. coli* reminiscent of the endogenous *E. coli* MinE end-to-end oscillatory patterns (Maple *et al.*, 2002).

1.4. accumulation and replication of chloroplasts (arc) mutants

Although the ultrastructural events that occur during chloroplast division have been studied since the late 1960s, it wasn't until the early 1990s that work began to investigate the nature of the molecular

control of plastid division. To identify the genes controlling the different phases of chloroplast division a collection of mutants defective in plastid division was generated. A genetic screen was developed based on the visual identification of *Arabidopsis* ethyl methane sulphonate (EMS) mutagenized, and later T-DNA-mutagenized, seedlings with altered numbers and sizes of chloroplasts in mesophyll cells (Pyke and Leech, 1991). The resulting collection of *arc* (accumulation and replication of chloroplasts) mutants define at least twelve loci with greatly reduced (-95%) or greatly increased (+50%) chloroplast numbers per mesophyll cell. They define loci which are important in both the process of plastid division and in control of plastid population size within a cell during development. The distinctive phenotypes exhibited by the *arc* mutants suggest that they encode genes with several unique roles in the plastid division process and hence represent a rich resource of new plastid division genes.

1.4.1. Physiology of *arc* mutants

arc6 has the most extreme chloroplast mutant phenotype with only 1-3 chloroplasts per mesophyll cell, the chloroplasts of *arc6* are 20-fold larger than wild-type chloroplasts (Pyke *et al.*, 1994). Although the number and size of the *arc6* chloroplasts are dramatically different from wild-type chloroplasts, the *arc6* mutation does not appear to have a significant effect on the ability of the chloroplasts to function normally since the growth of *arc6* plants is not severely affected compared to wild-type in controlled growth conditions (Pyke *et al.*, 1994). In agreement with this, ultrastructure analysis has revealed that although *arc6* chloroplasts are very elongated, the arrangement and distribution of the thylakoid membranes are not drastically different compared to wild-type (Pyke *et al.*, 1994). *arc6* has a global effect on plastid development; proplastids in both shoot and root meristems are reduced in number and all differentiated plastid types within the plant appear to be affected, including mesophyll and epidermal cell chloroplasts, root plastids, guard cell plastids and petal chromoplasts (Pyke *et al.*, 1994; Robertson *et al.*, 1995; Pyke and Page, 1998). Shoot apical meristems cells contain only two proplastids and these proplastids are highly variable in size but on average two-fold larger than wild-type proplastids (Robertson *et al.*, 1995). *arc6* proplastids in meristematic cells must be capable of limited division since no cells in *arc6* meristems or leaf mesophyll cells lack plastids and segregation of plastids in new cells still occurs and although the mechanism behind this is unclear. The controlled segregation of plastids is apparently less stringent in stomatal development since ~30% of stomata lack plastids in one or both guard cells (Robertson *et al.*, 1995). This phenotype appears to be due to

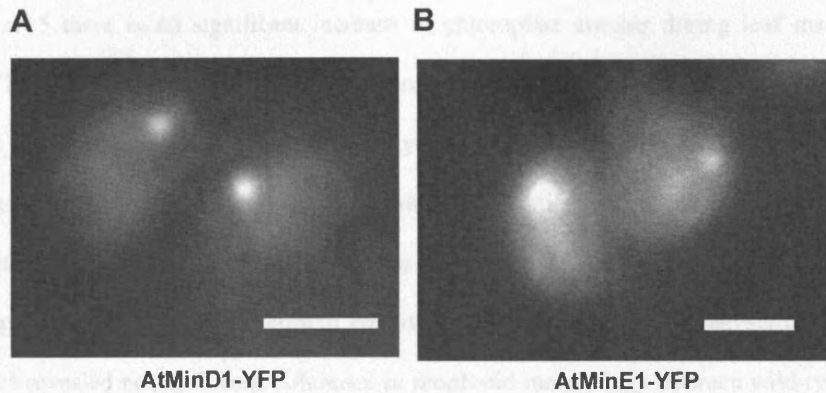


Fig. 1. 2 The distinct intraplasmic localisation of AtMinD1 and AtMinE1. (A) AtMinD1 localises usually as one spot at one end of the chloroplast or often as two spots at opposite ends of the chloroplast. (B) AtMinE1 localises as either one spot at one end of the chloroplast or as two spot in close proximity at one end of the chloroplast.

perturbations in proplastid populations leading to plastids segregating abnormally during stomatal development. *arc12* is not allelic to *arc6* but shows a similar phenotype (Pyke 1999; Yamamoto *et al.*, 2002).

In *arc5* there is no significant increase in chloroplast number during leaf mesophyll cell expansion. There are only 13 chloroplasts per mesophyll cell (Pyke and Leech, 1994), which reflects the complement of proplastids partitioned into the young post-mitotic cells suggesting that the *arc5* mutation does not affect proplastid development but functions at a later stage in chloroplast development. However, recent studies have shown that the *arc5* mesophyll cells can contain between 3-15 chloroplasts depending on the growth conditions (Gao *et al.*, 2003). Analysis of meristematic tissue of *arc5* revealed no significant difference in proplastid morphology between wild-type and *arc5* and epidermal and vascular plastids in *arc5* appear normal confirming that *ARC5* acts specifically in chloroplast development in leaf mesophyll cells (Robertson *et al.*, 1996). Mature *arc5* chloroplasts in fully expanded mesophyll cells are 6-fold larger than wild-type chloroplasts (Pyke and Leech, 1994) and all of the *arc5* chloroplasts are dumbbell shaped, exhibiting a central constriction suggesting that the *arc5* mutation prevents the completion of constriction during chloroplast division (Pyke and Leech, 1994; Robertson *et al.*, 1996). *arc3* plants contain ~18 chloroplasts per mesophyll cell, and like *arc5*, *arc3* chloroplast numbers do not significantly increase during cell development (Pyke and Leech, 1992). Like *arc5*, some cells of *arc3* have been observed to contain as few as three chloroplasts in addition to cells frequently containing a heterogeneous chloroplast population as observed in *arc11* and *arc10* (Maple *et al.*, In press).

In *arc1* and *arc7* there is an increased rate of chloroplast accumulation during cell expansion compared to wild-type, producing an increase in chloroplast number per cell (Pyke and Leech, 1992). The increased number of chloroplasts per cell plan area is associated with a reduction in chloroplast size compared to wild-type (Pyke and Leech, 1992).

arc11 and *arc10* have a heterogeneous population of chloroplasts; they vary greatly in size and are frequently larger than wild-type (Marrison *et al.*, 1999). The heterogeneous size of *arc11* chloroplasts has arisen through asymmetric division of the chloroplasts and the chloroplasts are often highly elongated and exhibit multiple constriction events (Marrison *et al.*, 1999; Fujiwara *et al.*, 2004).

In all of the *arc* mutants, modified patterns in chloroplast accumulation are compensated for by differences in chloroplast size (Pyke and Leech, 1992). In those *arc* mutants with a reduction in

chloroplast number the chloroplasts are substantially larger than wild-type chloroplasts and in *arc* mutants with more chloroplasts per cell the chloroplasts are smaller than wild-type (Pyke and Leech, 1992; Pyke *et al.*, 1994).

1.4.2. Hierarchy of *arc* mutants

Studies using double mutants of the *arc* loci have been performed to establish the hierarchy and possible epistatic relationships of the *ARC* genes (Pyke and Leech, 1994; Marrison *et al.*, 1999).

In double mutants with *arc1*, novel chloroplast phenotypes are observed (Marrison *et al.*, 1999). In double mutants of *arc5/arc1* and *arc3/arc1* chloroplast number per mesophyll cell is greater when *arc5* and *arc3* mutations are expressed in the *arc1* background than when expressed alone (Pyke and Leech, 1994). In both double mutants the relationship between number of chloroplasts per mesophyll cell and mesophyll cell size is intermediate between that of the two parental *arc* mutants; *arc5/arc1* has ~49 chloroplasts and *arc3/arc1* has ~26 chloroplasts compared to *arc5* (13), *arc3* (18) and *arc1* (108) (Pyke and Leech, 1994; Marrison *et al.*, 1999). The *arc1/arc6* double mutant contains on average 9 chloroplasts per cell, less than *arc1* (108) but more than *arc6* (2) (Marrison *et al.*, 1999). In the *arc1/arc11* double mutant the chloroplast phenotype is also an intermediate of the parental *arc* mutants, there are on average more chloroplasts in the *arc1/arc11* double mutant (79) but the *arc1/arc11* double mutant exhibits the variable chloroplast size indicative of the *arc11* mutation (Marrison *et al.*, 1999) These phenotype suggest that the *ARC1* gene acts independently of the *ARC6*, *ARC11*, *ARC3* and *ARC5* genes during chloroplast division.

In double mutants of *arc11*, *arc3* and *arc5* with *arc6* each contained 1-2 chloroplasts per mesophyll cell, identical size distribution and appearance to *arc6* chloroplasts (Marrison *et al.*, 1999) indicating that *ARC6* gene action is upstream of *ARC11*, *ARC3* and *ARC5* gene action.

The *arc3/arc11* double mutant is similar but not identical to *arc11*. The *arc3/arc11* double mutant resembles *arc3* in the proportion of large chloroplasts with cell plan areas between 400 and 600 μm^2 but resembles *arc11* chloroplasts in number (27) and size range (Marrison *et al.*, 1999) suggesting that *ARC11* is partially epistatic to *ARC3* (Marrison *et al.*, 1999). The *arc5/arc11* double mutant has on average 12 chloroplasts indicating that like *arc5* no chloroplast divisions have been completed (Marrison *et al.*, 1999). Not all of the chloroplasts in the *arc5/arc11* double mutant have the characteristic dumb-bell shape found in *arc5* chloroplasts and the appearance of the *arc5/arc11* double

Table 1. 2 A summary of 11 *Arabidopsis arc* mutants indicating their phenotype, chloroplast size and chloroplast number. Table taken from Aldridge *et al.*, 2005.

Geno-type	Eco-type	Chloroplast size (μm^2)	Chloroplast number/cell	Chloroplasts/1 nm^2 mesophyll cell plan area	Notes	Reference
WT	Ler	50	120	25	Spherical	Pyke and Leech, 1992
WT	Ws	50	80-90	20-23	Spherical	Pyke <i>et al.</i> , 1994; Rutherford, 1996
WT	Col	50	100	23	Spherical	Osteryoung <i>et al.</i> , 1998
<i>arc1</i>	Ler	25	108	32	Increased number of smaller chloroplasts	Pyke and Leech, 1992; Marrison <i>et al.</i> , 1999
<i>arc2</i>	Ler	110	40	9	Fewer chloroplasts/cell than WT	Pyke and Leech, 1992
<i>arc3</i>	Ler	200-300	18	4-5	Heterogeneous chloroplast size	Pyke and Leech, 1992; Pyke and Leech, 1994; Marrison <i>et al.</i> , 1999
<i>arc5</i>	Ler	300-900	3-15	1-4	Dumbbell shaped chloroplasts	Pyke and Leech, 1994; Robertson <i>et al.</i> , 1996; Marrison <i>et al.</i> , 1999; Gao <i>et al.</i> , 2003
<i>arc6</i>	Ws	1000	2	0.5	One or two large chloroplasts	Pyke <i>et al.</i> , 1994; Robertson <i>et al.</i> , 1995; Vitha <i>et al.</i> , 2003
<i>arc7</i>	Ws	40	80	26	Pale first leaves	Rutherford, 1996; Pyke, 1999
<i>arc8</i>	Ws	110	45	10	Moderately enlarged chloroplasts	Rutherford, 1996
<i>arc9</i>	Ws	140	34	12	Moderately enlarged chloroplasts	Rutherford, 1996
<i>arc10</i>	Ws	170	38	6	Highly variable in size	Rutherford, 1996; Pyke, 1999
<i>arc11</i>	Ler	110	30	7	Heterogeneous chloroplast size	Marrison <i>et al.</i> , 1999; Colletti <i>et al.</i> , 2000; Fujiwara <i>et al.</i> , 2004
<i>arc12</i>	Col	ND	1-2	ND	Similar to <i>arc6</i>	Pyke, 1999; Yamamoto <i>et al.</i> , 2002

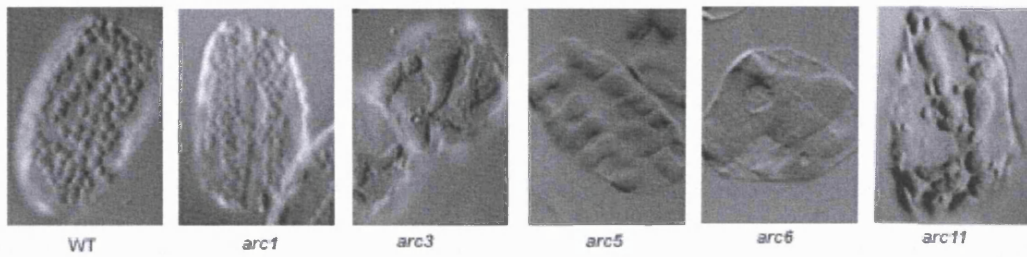


Fig. 1. 3. Isolated leaf mesophyll cells from fully expanded leaves of wild-type *Arabidopsis thaliana* (Ler) and *arc* mutants viewed with Nomarski differential interference contrast optics. Wild-type (WT), *arc6*, *arc3*, *arc6* and *arc11*. adapted from Marrison *et al*, 1999. Scale bar = 25 μ m.

mutant is consistent with *ARC5* acting downstream of *ARC11* during chloroplast division (Marrison *et al.*, 1999). *arc3* and *arc5* have very similar chloroplast numbers in fully expanded leaves making analysis of the double mutant difficult. However in young expanding leaves the *arc3/arc5* double mutant has a chloroplast phenotype more characteristic of *arc3* at this stage (Marrison *et al.*, 1999) and in addition the *arc3/arc5* double mutant has no dumb-bell shaped chloroplasts characteristic of *arc5* (Marrison *et al.*, 1999). The chloroplast phenotype suggests that *ARC3* and *ARC5* function in the same pathway and *ARC3* acts upstream of *ARC5* (Marrison *et al.*, 1999).

1.4.3. *ARC3*

It is thought that *ARC3* plays an important role in the initiation of chloroplast division, since the number of chloroplasts in *arc3* mesophyll cells is the same as the final proplastid number indicating that no chloroplast division occurs (Pyke and Leech 1992, 1994; Marrison *et al.*, 1999). Sequence alignments of *ARC3* reveal that it is a chimera of the prokaryotic gene, *FtsZ*, and a eukaryotic gene, phosphatidylinositol-4-phosphate 5-kinase (PIP5K). The N-terminal *FtsZ*-homologous region of *ARC3* does not have a complete GTP-binding and hydrolysis motifs highly conserved among bacteria and archaea, suggesting that the *FtsZ* domain of *ARC3* may have a different function to *AtFtsZ1-1* and *AtFtsZ2-1*. The C-terminal PIP5K-homologous region of *ARC3* has no catalytic domain of PIP5K and no kinase activity has been detected in biochemical assays (Shimida *et al.*, 2004) but this region does contain MORN (membrane occupation and recognition nexus) repeat motifs. In animal cells, MORN repeat motifs in junctophilin proteins, which are components of the junctional complexes present between the plasma membrane and the endoplasmic reticulum, are necessary for binding to the plasma membrane (Takeshima *et al.*, 2000). Therefore it has been proposed that the MORN repeats in *ARC3* mediate attachment of *ARC3* to the chloroplast envelope (Shimida *et al.*, 2004). A further middle domain of *ARC3* is also identified which shares no homology to other proteins (Maple *et al.*, In press). Sequence analysis revealed that in *arc3-1* a single base-pair mutation at nucleotide position 2001 results in the conversion of tryptophan at position 667 of *ARC3* to a stop codon (Shimida *et al.*, 2004).

ARC3 is located in a ring-like structure at the site of chloroplast division during the early and middle stages of the process (Shimida *et al.*, 2004; Maple *et al.*, In press) and *ARC3* has also been shown to form short filaments and discrete foci within chloroplasts (Maple *et al.*, In press). It was originally reported that *ARC3*, like *ARC5*, was located on the cytosolic surface of the outer envelope

membrane (Shimida *et al.*, 2004) however, recent *in vitro* chloroplast import and protease protection assays have demonstrated that ARC3 is a stromal plastid protein (Maple *et al.*, In press). The stromal localisation of ARC3 was confirmed through fusion of the predicted transit peptide of ARC3 to YFP, ARC3₁₋₆₇-YFP localises exclusively to chloroplasts confirming that ARC3 is a stromal plastid protein (Maple *et al.*, In press). ARC3 interacts with other stromal division proteins and these interactions are mediated through different domains of ARC3; the middle domain of ARC3 (ARC3₃₆₂₋₅₈₀) is sufficient for interaction with AtMinD1, AtMinE1 and ARC3. The N-terminal FtsZ-like domain of ARC3 (ARC3₁₋₃₆₁) interacts strongly with AtFtsZ1-1 and AtFtsZ1-1 also interacts less strongly with ARC3₃₆₂₋₅₈₀. The C-terminal MORN repeats (ARC3₅₈₁₋₇₄₁) are not required for any ARC3 interactions (Maple *et al.*, In press). Localisation analysis of different domains of ARC3 revealed that ARC3₁₋₅₉₈-YFP (FtsZ-like domain and middle domain) localises mostly to ring-like structures and less often to discrete foci and TP.ARC3₃₆₂₋₇₄₁-YFP (middle domain and MORN repeats) localised exclusively to discrete spots in close proximity to the chloroplast (Maple *et al.*, In press). Subsequent co-localisation analysis reveals that ARC3-YFP co-expressed with AtFtsZ1-CFP display tightly co-localised rings whilst ARC3-YFP and AtMinD1-CFP are observed to tightly co-localise as one or two spots (Maple *et al.*, In press).

ARC3 overexpression leads to chloroplast division arrest and in *arc3*, which contains a truncated version of ARC3, cells with a heterogeneous chloroplast population are frequently observed (Maple *et al.*, In press). Detailed analysis of *arc3* chloroplast found frequent division site misplacement (Maple *et al.*, In press) indicating that like AtMinD1 and AtMinE1, ARC3 is involved in division site placement. Because of the dual interaction with AtFtsZ1-1 and AtMinD1 and the involvement of ARC3 in correct division site placement it has been speculated that ARC3 fulfils a MinC-like function during chloroplast division (Maple *et al.*, In press).

1.4.4. ARC5

The *arc5* locus was mapped to chromosome III (Marrison *et al.*, 1999). Fine mapping and a novel antisense strategy subsequently led to the identification of a candidate gene for ARC5 from a BAC clone (MMB12) showing a G-to-A substitution, changing a tryptophan to a stop codon (Gao *et al.*, 2003). ARC5 is a 777 amino acid protein related to a group of dynamin-like proteins unique to plants (Gao *et al.*, 2003). ARC5 has one homologue (At1g53140) in a duplicated region of the *Arabidopsis* genome whose function might overlap with that of ARC5 although cannot prevent the mutant

chloroplast division phenotype exhibited in *arc5* mesophyll cells (Gao *et al.*, 2003). ARC5 contains three motifs found in other dynamin-like proteins: an N-terminal GTPase domain, a pleckstrin (PH) domain, shown in some proteins to mediate membrane association, and a C-terminal GTPase effector domain thought to interact directly with the GTPase domain and mediate self-assembly (Danino and Hinshaw, 2001; Gao *et al.*, 2003).

Analysis of an *arc1/arc5* double mutant revealed that *arc5* chloroplasts are capable of limited division (Marrison *et al.*, 1999). In *arc5* the premature stop codon could result in the production of a truncated protein consisting of just the GTPase domain, which may maintain partial activity. It is possible that in *arc5* the presence of the truncated protein and/or the ARC5 homologue is sufficient to maintain division of a small number of proplastids in the meristem, but that increased levels of ARC5 (and the homologue) are required for the proliferation of large populations of chloroplasts in expanding mesophyll cells.

ARC5-GFP localises to a ring-like structure on the cytosolic surface of the outer chloroplast envelope membrane at the site of chloroplast constriction (Gao *et al.*, 2003). The ARC5-GFP ring is speckled in appearance suggesting a discontinuous localisation of ARC5-GFP (Gao *et al.*, 2003). The cytosolic location of ARC5 and the lack of obvious counterparts in prokaryotes suggests that ARC5 evolved from a dynamin-related protein present in the eukaryotic ancestor of plants (Gao *et al.*, 2003). Because of the localisation of ARC5 it has been suggested that filaments of ARC5 form the outer PD ring. In *C. merolae*, the outer PD ring consists of a bundle of 5 nm filaments (Miyagishima *et al.*, 2001a). Some dynamin strands have an approximate diameter of 6 nm (Klockow *et al.*, 2002) suggesting that ARC5 could be the main constituent of the outer PD ring. However at 87 kDa ARC5 is larger than the 56 kDa protein proposed to be the likely candidate for the main component of the 5 nm bundles (Miyagishima *et al.*, 2001a). The function of ARC5 during chloroplast division is yet to be established, dynamin and its relatives have been shown to participate in a wide range of organellar fission and fusion events in eukaryotes (Danino and Hinshaw, 2001; Hinshaw, 2000) and some evidence supports proposals that dynamin acts as a force generating 'constrictase' at the neck of budding vesicles during endocytosis (Sweitzer and Hinshaw 1998). Therefore it is possible that ARC5 provides the force for constriction of the division septa during chloroplast division. ARC5 is not required for Z-ring formation as Z-rings can be observed in the *arc5* mutant (Gao *et al.*, 2003).

Phylogenetic analysis has shown that ARC5 is distantly related to dynamin-like proteins shown to play a role in mitochondrial division in higher plants (ADL2b; Arimura and Tsutsumi, 2002), yeast (Dnm1p; Bleazard *et al.*, 1999), mammals (Drp1; Smirnova *et al.*, 2001) and red algae (CmDnm1; Nishida *et al.*, 2003). Several of these proteins (ADL2b, CmDnm1 and Dnm1p) have been shown to localise to mitochondrial constriction sites and ARC5 appears to represent a new class of dynamin-like proteins unique to chloroplast division in *Arabidopsis*.

Screening of 10,000 EMS plants by microscopic observation of mesophyll cell chloroplasts identified two mutant lines where chloroplasts were frequently constricted and larger than those in wild-type plants, a phenotype similar to *arc5* (Miyagishima *et al.*, 2006). These two mutant lines were found to be allelic and were termed *pdv-1*. Map-based cloning determined that *PDV1* corresponded to At5g53280 (Miyagishima *et al.*, 2006). A BLAST search of the *Arabidopsis* genome revealed a homologue of PVD1 termed PVD2. Microscopic analysis of T-DNA insertions of PVD2 revealed that chloroplasts in mesophyll cells were frequently constricted and larger than those of wild-type plants, suggesting that PVD2 has function similar to but not redundant with that of PVD1 (Miyagishima *et al.*, 2006). A *pdv1 pdv2* double mutant contains only one to two centrally constricted chloroplasts per cell indicating that PVD1 and PVD2 have partially overlapping functions that are required at the late stage of plastid division (Miyagishima *et al.*, 2006). PDV1-GFP localises as a discontinuous ring structure at the plastid division site (Miyagishima *et al.*, 2006) in a similar pattern to the localisation of ARC5 (Gao *et al.*, 2003). ARC5 localises normally as a discontinuous ring at the chloroplast division site in the *pdv1* and *pdv2* single mutants but not in the *pdv1 pdv2* double mutant (Miyagishima *et al.*, 2006). This result demonstrates that PDV1 and PVD2 are required for the localisation of ARC5 at the division site but that PDV1 or PVD2 alone is sufficient for ARC5 localisation. FtsZ localises normally to the Z-ring in *arc5* and in the *pdv1 pdv2* double mutant (Vitha *et al.*, 2001; Miyagishima *et al.*, 2006). This data suggests a hierarchical localisation of FtsZ, PDV1 and PVD2 and ARC5 at the division site, in this order (Miyagishima *et al.*, 2006). Fractionation and *in vitro* chloroplast import experiments revealed that PDV1 is an integral outer envelope membrane protein leading to the suggestion that PDV1 and PVD2 may mediate the coordination of the Z-ring and the cytosolic ARC5 ring (Miyagishima *et al.*, 2006). Mutational analysis of PDV1 revealed that the conserved C-terminal Gly residue found both PDV1 and PVD2 mediates recognition of the division site (Miyagishima *et al.*, 2006) indicating that PDV1 could convey topological information from the putative C-terminal intermembrane space region

to the N-terminal cytosolic region by recognising the division site. The function of PDV1 and PVD2 remains to be elucidated; they may operate solely to recruit ARC5 or other cytosolic division components to the division site.

1.4.5. *ARC6*

ARC6 is a homologue of the cyanobacterial cell division gene *ftn2* (Koksharova and Wolk, 2002). In cyanobacteria, mutations of *ftn2* display a filamentous morphology with cells up to 100-fold longer than wild-type cells. Electron microscopy reveals that sites of cell division in *ftn2* mutants are much less frequent compared to wild-type (Koksharova and Wolk, 2002). Sequencing of the *ARC6* gene in the *arc6-1* mutant revealed that nucleotide 1141 of the open reading frame is mutated, resulting in a premature stop codon that truncates the encoded protein from 801 to 324 amino acids (Vitha *et al.*, 2003).

ARC6 homologues have been identified in all available fully sequenced cyanobacterial genomes and also in rice, fern, moss and green alga but not in non-cyanobacterial prokaryotes, indicating that *ARC6* is a descendent of the cyanobacterial *Ftn2* gene (Vitha *et al.*, 2003). All *ARC6*-like proteins contain a conserved N-terminal region which contains a putative J-domain characteristic of DNAJ cochaperones (Vitha *et al.*, 2003). DnaJ proteins are believed to deliver polypeptide substrates to Hsp70 chaperones for processing. The J-domain stimulates Hsp70 ATPase activity necessary for stable binding of Hsp70 to its protein substrates (reviewed in Walter and Buchner, 2002). In *E. coli*, HscA (an Hsp70 family protein) is involved in FtsZ-ring formation, through a chaperon-like interaction with FtsZ (Uehara *et al.*, 2001). It is attractive to speculate that *ARC6* may play an analogous role in *Arabidopsis*, acting as an plastid division-specific Hsp70 cochaperone.

A putative transmembrane region was identified in *ARC6* and *in vitro* chloroplast import and protease protection assays suggest that *ARC6* spans the inner chloroplast envelope membrane with the N-terminus, including the J-domain extending into the chloroplast stroma (Vitha *et al.*, 2003). *ARC6*-GFP localises to a ring at the centre of the chloroplasts detectable in both unconstricted and deeply constricted chloroplasts (Vitha *et al.*, 2003) suggesting that *ARC6* functions throughout chloroplast division.

FtsZ filament morphology was examined in the *arc6* mutant background; *arc6* chloroplasts contain numerous short, disorganised FtsZ filaments and lack the intact Z-ring typical of wild-type

chloroplasts (Vitha *et al.*, 2003) suggesting a role for ARC6 in Z-ring assembly or maintenance. Overexpression of ARC6 causes inhibition of chloroplast division. FtsZ filaments in plants overexpressing ARC6 are long and numerous and occasionally form spirals or rings around the enlarged chloroplasts (Vitha *et al.*, 2003) suggesting an ARC6-mediated excessive FtsZ polymerisation and/or stabilisation. In *E. coli*, FtsA and ZipA are believed to be involved in stabilisation and anchoring the Z-ring. In *E. coli* mutants lacking both FtsA and ZipA, division is blocked and FtsZ forms arcs and dots instead of rings (Pichoff *et al.*, 2002). Although no homologues of these bacterial proteins have been identified in the *Arabidopsis* genome, ARC6 may prove to play a function analogous to FtsA and ZipA, anchoring and/or stabilising the FtsZ ring at the plastid division site. Interestingly, in the *arc6* mutant FtsZ1 and FtsZ2 levels are consistently lower than wild-type (Vitha *et al.*, 2003) however, overexpression of ARC6 does not affect FtsZ protein levels (Vitha *et al.*, 2003) The lower levels of FtsZ1 and FtsZ2 in *arc6* suggest that ARC6 is involved in FtsZ regulation however it is unclear how FtsZ levels are altered in *arc6*.

1.4.6. ARC11

arc11 contains a decreased number of mostly elongated and expanded chloroplasts with irregular shapes as compared to wild-type (Fujiwara *et al.*, 2004). Microscopic analysis of *arc11* chloroplasts reveals multiple constrictions placed randomly, but in parallel along the long axis of the chloroplasts (Fujiwara *et al.*, 2004). The asymmetrical placement of constriction sites results in a heterogeneous population of chloroplasts in terms of size and shape including the appearance of spherical mini chloroplasts (Fujiwara *et al.*, 2004), a phenotype reminiscent of *E. coli min* mutants (Bi and Lutkenhaus, 1993). Sequence analysis of AtMinD1 in *arc11* reveals a single cytosine to guanine substitution in AtMinD1 at position 296 within α -helix 11 at the C-terminus of AtMinD1 (AtMinD1(A296G)) (Fujiwara *et al.*, 2004). Expression of wild-type AtMinD1 in *arc11* complements the mutant chloroplast division phenotype confirming that *arc11* is a loss-of-function mutant of AtMinD1 (Fujiwara *et al.*, 2004). Surprisingly, overexpression of AtMinD1(A296G) causes chloroplast division inhibition (Fujiwara *et al.*, 2004) as observed for overexpression of wild-type AtMinD1 (Colletti *et al.*, 2000; Kanamaru *et al.*, 2000) demonstrating that AtMinD1(A296G) has retained its division inhibition activity but has lost the ability to control appropriate placement of the division apparatus (Fujiwara *et al.*, 2004). AtMinD1(A296G)-YFP fusion protein localises to large and distorted

fluorescent aggregates and/or multiple fluorescent spots (Fujiwara *et al.*, 2004) in contrast to wild-type AtMinD1 which localises to one or two discrete spots at polar regions in chloroplasts (Maple *et al.*, 2002). AtMinD1 has been shown to form homodimers using both the yeast two-hybrid system and Fluorescence Resonance Energy Transfer (FRET) assays in living plant cells. This dimerisation capacity is abolished by the single point mutation in AtMinD1(A269G) (Fujiwara *et al.*, 2004) suggesting that the C-terminal domain is involved in dimerisation. The loss of dimerisation capacity of AtMinD1(A269G) probably explains the mis-localisation of AtMinD1(A269G) and ultimately leads to aberrant division site placement observed in *arc11* chloroplasts.

1.5. Novel plastid division proteins

Recently a number of non-*arc* related plastid division proteins have been identified which do not seem to form part of the classical Min protein-mediated division pathway in *Arabidopsis*. The identification and characterisation of these proteins has clearly strengthened the idea that plastid division in higher plants represents a complex interplay between prokaryotic- and eukaryotic-derived protein components.

1.5.1. Alb4

Alb4 was originally identified as the C-terminal domain of ARTEMIS (*Arabidopsis thaliana* envelope membrane integrase) which was identified in a search for proteins involved in chloroplast biogenesis (Fulgosi *et al.*, 2002). Subsequently it was established that the gene originally described as ARTEMIS actually contained two open reading frames, the upstream located open reading frame is predicted to encode a hypothetical 65 kDa protein with unknown function and the second open reading frame encodes Alb4 a protein belonging to the Alb3/OxaI/YidC family of integral membrane proteins (Gerdes *et al.*, 2006). Alb3, OxaI and YidC belong to an evolutionary conserved protein family mediating protein insertion into the thylakoid membrane of chloroplasts, the inner membrane of mitochondria and inner membrane of bacteria, respectively.

Alb4 is localised to the thylakoid membrane in a similar distribution to Alb3 (Gerdes *et al.*, 2006). Alb3 (*albino3*) is involved in the insertion of light-harvesting antenna proteins into the thylakoid membrane (Moore *et al.*, 2000) and an *alb3* null mutant of *Arabidopsis* shows a drastic albinotic phenotype with pigment deficiency and arrested chloroplast development (Sundberg *et al.*, 1997).

Reduction of Alb4 affects the shape of chloroplasts; chloroplasts of a T-DNA insertion line and RNAi lines of Alb3 are larger and more spherical in appearance compared to chloroplasts of wild-type plants (Gerdes *et al.*, 2006). The thylakoids of T-DNA insertion lines and RNAi lines of *alb3* are less well organised and not so appressed which may be due to the enlarged chloroplasts (Gerdes *et al.*, 2006).

When ARTEMIS was originally identified, transposon insertion *Arabidopsis* plants with greatly reduced levels of the ARTEMIS protein were shown to have extended, duplicated or triplicated, undividing chloroplasts. Despite the failure of the envelope membranes to complete constriction, the thylakoid membranes of these plants were visibly constricted at the centre of the chloroplasts and apparently portioned between the two halves of the organelle (Fulgosi *et al.*, 2002). The phenotype of chloroplasts in plants with reduced levels of Alb3 are not as severe as those reported for ARTEMIS (Gerdes *et al.*, 2006) and therefore reduction of Alb3 cannot account for the mutant chloroplast division phenotype previously described. Reanalysis of the ARTEMIS gene shows that the transposon insertion occurs in the region of the At1g24490 gene which was previously identified as the encoding the N-terminal portion of ARTEMIS (Gerdes *et al.*, 2006). The exact localisation and function of the At1g24490 gene product has not yet been resolved but it will be interesting to see if it encodes a protein involved in plastid division.

1.5.2. GIANT CHLOROPLAST 1

GIANT CHLOROPLAST 1 (GC1) (also called AtSulA) was originally identified based on its similarity to putative cell division inhibitor SulA proteins in *Anabaena* sp. PCC 7120 (all2390) and *Synechocystis* sp. PCC 6803 (slr1223), although no function had been reported for the cyanobacterial proteins (Maple *et al.*, 2004; Raynaud *et al.*, 2004). The *Synechocystis* homologue of GC1 is crucial for cell survival as for *Synechocystis* slr1223 deletion mutants homoploids could not be identified (Raynaud *et al.*, 2004). Microscopic analysis of heteroploid clones revealed that up to 40% initiated but failed to complete cell division, resulting in cloverleaf-like structures, demonstrating that slr1223 is required for correct cell division in *Synechocystis* (Raynaud *et al.*, 2004). A role for GC1 in chloroplast division was initially demonstrated through analysis of transgenic *Arabidopsis* plants with greatly reduced (-95%) levels of *GCI* transcript (Maple *et al.*, 2004). It was found that GC1-deficiency by co-suppression results in mesophyll cells harbouring 1-2 giant chloroplasts. Interestingly, antisense

transgenic lines with as much as a 70% reduction in *GCI* transcript levels showed wild-type chloroplast division profiles, indicating that transcript levels must be severely reduced to effect chloroplast division (Maple *et al.*, 2004). In striking contrast, *GCI* overexpression has no effect on chloroplast division in mesophyll cells suggesting *GCI* acts as a positive plastid division factor (Maple *et al.*, 2004). More recently it has been reported that overexpression of a *GCI*-YFP fusion protein in *Arabidopsis* transgenic plants can also lead to a chloroplast division defect, with lines harbouring a range of chloroplast numbers per cell (60% with 80 chloroplasts (wild-type-like); 11% with 40-60, 24% with 10-40 and 2% with 1 chloroplast per cell) (Raynaud *et al.*, 2004). Interestingly, in this study overexpression did not alter plastid division in the same way in all plants from the same line, or indeed in all cells or in all plastids. Also, a root plastid division phenotype was observed indicating that *GCI* mode of action might not be limited to photosynthetic tissues where it is primarily expressed. The observed differences in phenotypes amongst different lines and within lines are intriguing and may reflect differences in protein abundance and stability in different cell types. Clearly further functional analysis of *GCI* during plastid division is required to resolve these discrepancies.

GCI is plastid-localised and within chloroplasts *GCI* localises uniformly to the stromal side of the entire chloroplast envelope (Maple *et al.*, 2004). Membrane association of *GCI* is mediated through a C-terminal amphipathic helix of *GCI* (Maple *et al.*, 2004). *GCI* can dimerise but does not interact with AtFtsZ1-1, AtFtsZ2-1, AtMinD1 or AtMinE1 (Maple *et al.*, 2004) suggesting that *GCI* is probably not directly involved in the FtsZ-mediated plastid division pathway in *Arabidopsis*. At the secondary structure level *GCI* has high (80-90%) structural similarity to nucleotide-sugar epimerases (Maple *et al.*, 2004). Epimerases control and change the stereochemistry of carbohydrate-hydroxyl substitutions, often modifying protein activity or surface recognition (Baker *et al.*, 1998), however, to date no data exists to support *GCI* as having epimerase activity and *GCI* mode of action within plastid division remains to be resolved.

GCI shows homology to the bacterial cell division inhibitor SulA, In *E. coli*, transcription of *SulA* is induced by the SOS response (Huisman *et al.*, 1984) and SulA inhibits FtsZ polymerisation, delaying cell division until DNA damage is repaired (Justice *et al.*, 2000). Because of the homology of *GCI* to SulA this raises the possibility that an analogous SOS response pathway could exist in plants. Indeed it has been demonstrated that overexpression of *GCI* can rescue the plastid division defect observed in plants overexpressing AtFtsZ1-1 or AtFtsZ2-1. However, in *E. coli*, SulA operates to

inhibit cell division through direct interaction with FtsZ and no interaction can be detected between GC1 and FtsZ1-1 or FtsZ2-1 (Maple *et al.*, 2004; Raynaud *et al.*, 2004).

1.5.3. *AtCDT1*

AtCDT1a and *AtCDT1b* are prereplication factors crucial for cell proliferation and genome stability (Castellano *et al.*, 2004). In *Saccharomyces cerevisiae*, CDT1 is only synthesised in G1 phase of the cell division cycle (Tanaka and Diffley, 2002). Together with CDC6, CDT1 binds to the Origin Recognition Complex (ORC), which is already bound to the origin of replication. The resultant complex is called the Pre-Replication Complex. The formation of this complex allows a heterohexameric protein complex of proteins MCM2-7 to bind to the origin and this entire hexamer acts as a helicase unwinding the double-stranded DNA to enable replication of the genome (Tanaka and Diffley, 2002; Nishitani and Lygerou, 2002).

Simultaneous down regulation of *AtCDT1a* and *AtCDT1b* through RNAi results in severe developmental defects for the plant as a whole; plants have reduced stature and leaves that are pale, crumpled and smaller than those of wild-type (Raynaud *et al.*, 2005). Microscopic analysis of these plants reveals that cells in the *AtCDT1*-RNAi plants have a two-fold reduction in average cell area and it has been suggested that cell division is also inhibited in *AtCDT1*-RNAi plants due to an impairment in DNA replication which is sufficient to increase the required time to complete a cell cycle (Raynaud *et al.*, 2005). *AtCDT1*-RNAi plants display severe plastid division defects; 50% of cells contain few but enlarged chloroplasts, in most of these abnormal cells the chloroplast number is reduced to 3-4 chloroplasts per cell (Raynaud *et al.*, 2005). The pale colour of the leaves of *AtCDT1*-RNAi plants is accounted for by a 30-50% reduction in the amount of chlorophyll a and chlorophyll b.

AtCDT1 silencing increases endoreplication (Raynaud *et al.*, 2005). DAPI staining of the cells exhibiting plastid division defects suggested a correlation between the size of the nucleus (and thus endoreduplication level) and the severity of the plastid division defect, indicating that DNA replication and chloroplast biogenesis are simultaneously altered in the *AtCDT1*-RNAi plants (Raynaud *et al.*, 2005).

AtCDT1a-GFP accumulates both in the nuclei and in plastids (Raynaud *et al.*, 2005) and *AtCDT1a* interacts with ARC6 in the yeast two-hybrid system and in BiFC assays in BY-2 protoplasts. The dual localisation of *AtCDT1a*-GFP to the nucleus and plastids and the reduction in cell division and plastid

division in AtCDT1-RNAi plants has led to speculation that AtCDT1 could co-ordinate cell and plastid division.

1.5.4. MscS-like (MSL) proteins

MscS (mechanosensitive channel of small conductance) proteins are found in most bacterial and archaeal genomes, in fission yeast and in plants (Pivetti *et al.*, 2003). In *E. coli* MscS channels are directly responsive to membrane tension and opening of these channels results in a flux of ions across the membrane. In bacteria, mechosensitive ion channels are believed to serve as osmotic safety valves protecting the bacteria from rupture during hypo-osmotic shock (Levina *et al.*, 1999). *Arabidopsis* contains ten MscS-like (MSL) genes (Pivetti *et al.*, 2003). One of these, MSL3 is capable of restoring hypo-osmotic-shock survival to an *E. coli* strain lacking the three mechosensitive ion channels MscS, MscL and MscK (Haswell and Meyerowitz, 2006). Indicating that MSL3 functions as mechosensitive ion channels. MSL2 has a very similar structure to MSL3 composing of an N-terminal chloroplast transit peptide, five transmembrane helices and a C-terminal cytoplasmic domain (Haswell and Meyerowitz, 2006).

msl2-1/msl3-1 double mutants have variegated leaves and exhibit disruptions in cell arrangement and morphology as well as overall leaf shape (Haswell and Meyerowitz, 2006). Chloroplasts enlarged to various extents are observed in mesophyll cells of *msl2-1/msl3-1* leaves, these enlarged chloroplasts show no ultrastructural changes compared to wild-type chloroplasts (Haswell and Meyerowitz, 2006). Enlargement of plastids is also observed in leaf epidermis cells and root cells of *msl2-1/msl3-1* (Haswell and Meyerowitz, 2006).

As predicted by the presence of a transit peptide MSL2-GFP and MSL3-GFP are both plastid localised, within the chloroplasts MSL2-GFP and MSL3-GFP localise to one or two distinct spots at one or both ends of the chloroplast and are associated with the chloroplast envelope (Haswell and Meyerowitz, 2006). Colocalisation studies with AtMinE1 reveal that MSL2-GFP and MSL3-GFP appear to co-localise with AtMinE1 (Haswell and Meyerowitz, 2006) however it is not clear what the relationship is between these proteins, perhaps it is simply that both the Min and MSL proteins are localising to the poles of the chloroplast as defined by some as yet unidentified mechanism.

Although a function in chloroplast division is yet to be defined it has been proposed that MSL2 and MSL3 are required to relieve the pressure produced by the constriction of dividing chloroplasts (Haswell

and Meyerowitz, 2006) and a role for plastid envelope tension in controlling plastid division and morphology has been suggested (Pyke, 2006). Chloroplasts in mesophyll cells are densely packed and studies of the *arc* mutants that contain chloroplasts of various sizes has revealed a compensatory mechanism between chloroplast number per cell and chloroplast size whereby the total cell plan area occupied by chloroplast remains unperturbed by a reduced or increased number of chloroplasts (Pyke and Leech, 1994; Marrison *et al.*, 1999). However whether there is a role for membrane tension in the regulation of chloroplast division requires further investigation.

1.5.5. FZL

FZL is a FZO-like protein identified in *Arabidopsis* through homology to *Drosophila* FZO (Gao *et al.*, 2006). FZO is a dynamin-related membrane-remodelling protein that mediates fusion between mitochondrial outer membranes in animals and fungi. FZL encodes a protein of 912 amino acids including a putative GTPase domain and two transmembrane domains similar to FZO proteins (Gao *et al.*, 2006). FZL also contains a chloroplast transit peptide and FZL localises to the chloroplast in a punctuate pattern most evident at the chloroplast periphery but also throughout the chloroplast (Gao *et al.*, 2006). Protease protection and fractionation assays reveal that FZL is targeted to the stromal side of the chloroplast envelope and also to the thlakoid membranes (Gao *et al.*, 2006).

T-DNA insertion mutants of *fzl* display pale leaves and fewer but enlarged chloroplasts that are heterogeneous in size (Gao *et al.*, 2006). Ultrastructural analysis of the chloroplasts of the T-DNA insertion mutants of *fzl* reveal that the morphology of the thylakoid is greatly affected in the *fzl* mutants; grana lamellae are less uniform in length and stacked in a staggered fashion leading to a disorganised thylakoid array (Gao *et al.*, 2006). The phenotypes of the chloroplasts in the *fzl* mutants indicate a role for FZL in regulating thylakoid organisation and chloroplast morphology however overexpression of functional FZL-GFP does not cause chloroplast division defects. In contrast to the chloroplast phenotype, mitochondrial morphology and ultrastructure is unaffected in the *flz* mutants demonstrating that FZL does not influence mitochondrial morphology like FZO proteins in animals and fungi (Gao *et al.*, 2006).

Mutational studies of the putative GTPase domain of FZL suggests that GTP binding and/or hydrolysis is required for both FZL function and also for the punctuate pattern of localisation of FZL (Gao *et al.*, 2006). The possible role of FZL in chloroplast division is yet to be clarified and it is likely

that the perturbed chloroplast morphology observed in the *fz1* mutants results from a change in membrane morphology and dynamics rather than a defect in chloroplast division.

1.6. Conclusions

Since the realisation, approximately thirty years ago, that plastids divide inside plant cells our understanding of the plastid division process in higher plants has increased considerably particularly during the last decade. Through a combination of two main approaches; using bacterial cell division as a paradigm and through the cloning of several *arc* mutants we are now in a position to start constructing meaningful working models of the plastid division process. Several important key points emerge when combining findings to date. First, it is clear that plants have retained crucial prokaryote-derived plastid division proteins such as FtsZ, MinD and MinE (Osteryoung and Vierling, 1995; Colletti *et al.*, 2000; Maple *et al.*, 2002) and that these show distinct intraplastidic localisation patterns (McAndrew *et al.*, 2001; Maple *et al.*, 2002; Fujiwara *et al.*, 2004). Second, through the characterisation of several ARC proteins it is evident that plastid division is controlled by a complex interplay between prokaryote- and eukaryote-derived protein components (Gao *et al.*, 2003; Shimida *et al.*, 2004). Third, subcellular localisation studies have demonstrated that plastid division is not only controlled by proteins residing in the plastid stroma but also by cytoplasmic proteins (Gao *et al.*, 2003; Shimida *et al.*, 2004).

The aim of this study is to further our general understanding of the molecular mechanism of chloroplast division in *Arabidopsis*. The main objectives of this study are to:

1. To begin to appreciate how the individual protein components function as part of the division machinery through the molecular and biochemical analysis of AtMinD1.
2. To begin to dissect the molecular mechanism of the chloroplast division machinery through the analysis of all potential protein-protein interactions between stromal chloroplast division components.
3. To try to identify new components of the chloroplast division machinery through use of yeast two-hybrid screens and co-immunoprecipitation
4. To investigate the regulation of chloroplast division.

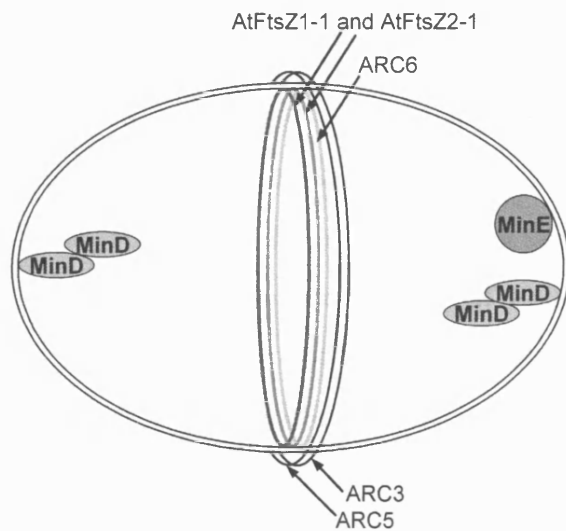


Fig. 1. 4. A working model of plastid division in higher plants showing the identified protein components to date, their localization patterns and protein–protein interaction properties. MinD forms homodimers and localizes to one or two spots at either side of chloroplasts in proximity to the inner envelope membrane. Similarly, MinE localizes most often to one spot at one side of chloroplasts. GC1 localizes to the stromal side of the inner envelope membrane and forms dimers but is unable to interact with MinD, MinE, FtsZ1-1 or FtsZ2-1. FtsZ forms a Z ring at the centre of chloroplasts as does ARC6, while ARC5 and ARC3 localizes to ring-like structures on the cytosolic surface of the outer envelope membrane. Figure adapted from Aldridge *et al.*, 2005.

2. Materials and Methods

2.1. Plant growth

Arabidopsis thaliana cv. Columbia or *Arabidopsis thaliana* cv. Landsberg and *Nicotiana tabacum* cv. Samsun were used for all experiments unless otherwise stated.

2.1.1. Plant growth media.

Lehle medium, for *in vitro* growth of *Arabidopsis* seedlings, was prepared by mixing 5 ml 1 M KNO₃, 2.5 ml 1 M KH₂PO₄, 2 ml 1 M MgSO₄, 2.5 ml Sequestrene (2.5 g FeSO₄.7H₂O and 3.3 g Na₂EDTA in 400 ml sdH₂O was brought to the boil and allowed to cool on a magnetic stirrer for ~30 minutes before adjusting the final volume to 450 ml) and 1 ml micronutrients (70 mM H₃BO₃, 14 mM MnCl₂, 0.5 mM CuSO₄, 1 mM ZnSO₄, 0.2 mM NaMoO₄, 0.1 mM CaCl₂) in a final volume of 1 l. Bio Agar (biogene.com) was added at 0.6% before autoclaving and the media stored at room temperature. Appropriate antibiotics were added at the following concentrations: kanamycin 40 µg.ml⁻¹, hygromycin 20 µg.ml⁻¹.

2.1.2. In vitro culture

All *Arabidopsis* seeds to be germinated *in vitro* were surface-sterilised by first shaking in a 10% bleach (Super bleach steriliser, Coventry chemicals ltd) solution for ~20 minutes followed by washing six times in sdH₂O. Sterilised seeds were dried on filter paper in a laminar flow hood and sown on Lehle medium (Section 2.1.1). Seeds were stratified for two days at 4°C in the dark before being transferred to a growth room and grown at 21°C under continuous light at a light intensity of ~80 µmol s⁻¹ m⁻². When the plants were required to set seed, or if adult plants were required for analysis, seedlings were transferred to soil as described in Section 2.1.3. after 14-18 days.

2.1.3. Soil culture

Arabidopsis plants were grown in Levingtons F2 Seed and Modular Compost, silver sand and vermiculite (medium 2.0-5.0mm, Sinclair). *Arabidopsis* plants were grown in 24 compartment trays. Each tray contained a ratio of 6:1:2 of compost: vermiculite: sand. Plants were grown under long-day conditions at 20°C in a controlled temperature greenhouse. The light intensity was typically 150-200 µmol.m⁻².sec⁻¹. Plants that were germinated *in vitro* on Lehle medium were transferred to water-

saturated soil 14-18 days after germination and kept covered with a propagator lid for two-four days following transfer. For *Arabidopsis* plants grown for *Agrobacterium* transformation (Section 2.2.3.), seeds were sown directly onto soil. Pots were covered with a foil propagator lid and placed at 4°C for two-four days before being transferred to the greenhouse. The foil covered propagator lid was then replaced with a standard propagator lid until the seedlings were fully germinated. All plants were watered from the base.

Arabidopsis seeds were harvested by breaking dry siliques over a piece of paper and then sifting the seed through mesh to remove dry plant material.

Tobacco seeds were germinated on soil in the same way as for *Arabidopsis* seeds but were grown in a controlled temperature greenhouse at 32°C under long-day conditions and the light intensity was typically 100-150 $\mu\text{mol.m}^{-2}.\text{sec}^{-1}$.

2.1.4. Plant transformation

Transgenic *Arabidopsis* were generated using *Agrobacterium*-mediated transformation protocol based on the floral dip method (Clough and Bent, 1998). 81 cm² pots were sown with ~10 plants per pot and grown in a temperature controlled greenhouse at 20°C. The primary inflorescences were normally cut when they reached ~5 cm to promote the generation of secondary inflorescences. The plants were used for transformation when the secondary inflorescences reached no more than 10 cm in height and had a few open flowers.

Constructs for transformation into *Arabidopsis* were transformed into *Agrobacterium* strain ABI (Section 2.2.3). For each construct a starter culture was initiated by inoculating 5 ml of LB (Section 2.2.1) supplemented with 50 $\mu\text{g.ml}^{-1}$ kanamycin and 50 $\mu\text{g.ml}^{-1}$ spectinomycin, with one fresh *Agrobacterium* colony, this starter culture was incubated at 28°C for 24 hours in a shaking incubator. 4 ml saturated starting culture was used to inoculate 1 litre of LB split between 2 conical flasks containing the same antibiotics as the starting culture. Cultures were again incubated at 28°C in a shaking incubator and grown until OD₆₀₀ = 1.8-2.0 (~16 hours after inoculation). The cultures were centrifuged at 4000 rpm for 15 minutes in a GSA rotor (Sorvall) at room temperature. The pellet was resuspended in 1 litre of dipping media (0.5 % w/v sucrose and 10 mM MgCl₂) and 0.05 % Silwet L-77 added immediately prior to dipping. The suspended culture is split between 500 ml shallow jars and the *Arabidopsis* inflorescences immersed for 15 minutes by dipping the *Arabidopsis* plants upside down

and submerging them in the jars. The excess liquid was gently shaken from the plants and the plants were laid down on their side and loosely covered with cling film to provide a humid environment. 24 hours after dipping the film was removed and the plants were grown under standard conditions until the siliques were dry and the seed ready for harvesting. The seed was bulk harvested and the first generation was screened for transformants. Screening for T₁ seeds was performed on Lehle medium containing 40 µg.ml⁻¹ kanamycin or 20 µg.ml⁻¹ hygromycin depending on the construct used. Kanamycin or hygromycin resistant seedlings were selected ~10 days after germination and transferred to fresh Lehle plates before being transplanted to soil.

2.2. Bacterial work

2.2.1. Growth and storage of bacteria

The bacterial strains used in this study are listed in Table 1. All *E. coli* strains were cultured in liquid LB media (10 g NaCl, 10 g Tryptone and 5 g Yeast extract were combined in a final volume to 1 l, autoclaved and stored at room temperature) in a shaking incubator at 250 rpm, or on LB-agar plates (1.5 % agar was added to LB media before autoclaving). All *E. coli* cultures were grown at 37 °C. *Agrobacterium* strain ABI was also grown in LB or on LB-agar but in incubators set at 28°C. When appropriate, antibiotics were added at the following concentrations: 50 µg.ml⁻¹ ampicilin; 34 µg.ml⁻¹ chloromphenical; 50 µg.ml⁻¹ kanamycin; 50 µg.ml⁻¹ spectinomycin. For blue-white selection X-gal was added to the LB-agar plates at a final concentration of 0.5 mg.ml⁻¹.

For short term storage (up to 3 months) cells were streaked onto LB-agar plates and stored at 4°C. For long term storage bacterial glycerol stocks were produced by mixing 500 µl of an overnight culture with 500 µl of sterile 50 % glycerol in a cryogenic tube. The glycerol stock was then snap frozen in liquid nitrogen and stored at -80°C for up to three years.

Table 1. Bacterial strains used in this study

	Genotype	Source/reference
<i>E. coli</i> DH5α	<i>endA1 hsdR17</i> (r _k ⁻ m _k ⁻), <i>supE44</i> , <i>thi1</i> , <i>recA1</i> , <i>gyrA</i> (Nal ^r), <i>relA1</i> , Δ(<i>lacZYA-argF</i>)U169, Φ80 <i>lacZ</i> Δ <i>M15</i>	Novagen
<i>E. coli</i> BL21(DE3)pLysS	<i>F ompT hsdS_B</i> (r _B ⁻ m _B ⁻) <i>gal dcm</i> (DE3) <i>pLysE</i> (Cam ^R)	Novagen

<i>A. tumefaciens</i> ABI	Contains the disarmed pTiC58 plasmid pMP90RK	Monsanto
------------------------------	--	----------

2.2.2. *E. coli* transformation

Transformation competent *E. Coli* DH5 α and BL21(DE3)pLysS were made using the following procedure: DH5 α or BL21(DE3)pLysS from glycerol were streaked onto a fresh LB-agar plate. A single colony from the plate was used to inoculate 5 ml of LB medium and was incubated at 37°C overnight in a shaking incubator. 1ml of the saturated overnight culture was used to inoculate 100 ml LB medium in a 250 ml conical flask, this culture was incubated until OD₆₀₀ = 0.5 (2-3 hours). The culture was transferred to chilled centrifuge tubes and centrifuged for 5 minutes at 3600 rpm at 4°C in a SS-34 rotor (Sorvall). After centrifugation the supernatant was discarded and the pellet resuspended in 40 ml of chilled MgCl₂ (0.1 M). The culture was centrifuged for 10 minutes at 3600 rpm at 4°C and the pellet resuspended in 40 ml chilled CaCl₂ (0.1 M) and incubated on ice for 30 minutes. The culture was again centrifuged for 10 minutes at 3600 rpm at 4 °C and the pellet resuspended in 4 ml MOPS glycerol (100 mM MOPS-NaOH, 50 mM CaCl₂, 20 % w/v glycerol; autoclaved and stored at 4°C). The chemically competent cells were dispensed into 100 μ l aliquots in 1.5 ml centrifuge tubes, snap frozen in liquid nitrogen and stored at -80°C.

To transform *E. coli*, aliquots of chemically competent cells in 1.5 ml centrifuge tubes were thawed on ice for ~5 minutes. 5 μ l of plasmid DNA was added to the cells and mixed by gentle pipetting. The cells were incubated on ice for ~15 minutes before being subjected to heat shock at 42°C for 90 seconds in a water bath followed by incubation on ice for 3 minutes. 200 μ l of LB medium was added to each transformation and the cells are allowed to recover at 37°C with shaking. 100 μ l of each transformation was spread onto an LB-agar plate containing appropriate antibiotics and X-gal and incubated at 37°C overnight.

2.2.3. Transformation of *Agrobacterium tumefaciens*

Competent *Agrobacterium* was prepared using the freeze-thaw method (An *et al.*, 1988). A starter culture was initiated by inoculating 5 ml of LB supplemented with 50 μ g.ml⁻¹ kanamycin with one fresh *Agrobacterium* colony. The following day 2 ml of the starter culture was used to inoculate 50 ml LB in a 250 ml conical flask and grown to an OD₆₀₀ of 0.5-1.0. The cells were then chilled on ice for

~10 min before harvesting at 3,000 rpm for 5 min at 4°C in a SS-34 rotor (Sorvall). The supernatant was discarded and the cells gently resuspended in 1 ml chilled 20 mM CaCl₂ solution. The cells were dispensed into 100 µl aliquots in 1.5 ml prechilled centrifuge tubes, snap frozen in liquid nitrogen and stored at -80°C.

For each transformation an aliquot of competent cells was put on ice and ~1 µg of plasmid DNA immediately added. The cells were then thawed by incubating the tube in a 37°C water bath for 5 min, mixing gently half way through. Subsequently 1 ml of LB media was added and the cells incubated at 28°C with gentle shaking (100 rpm) for ~4 hours. 150 µl of the cell was then spread on an LB-agar plate containing the appropriate antibiotic and incubated at 28°C for 2-3 days.

2.3. Molecular biology

DNA was stored at -20°C and RNA was stored at -80°C. Unless otherwise stated all room temperature centrifugation steps were carried out in an Eppendorf Centrifuge 5415 D, using a F45-24-11 fixed angle rotor, at maximum speed (16,110 x g; 13,200 rpm). All centrifugation steps carried out at 4°C were carried out in an Eppendorf Centrifuge 5417, using f-45-30-11 fixed angle rotor, maximum speed (25,000 x g; 16,400 rpm). Large volumes of bacterial cultures were centrifuged in a Sorvall refrigerated RC-6 centrifuge.

2.3.1. Nucleic acid preparation

2.3.1.1. Plant DNA extraction

The method used for DNA extraction from *Arabidopsis* is adapted from Edwards *et al.*, (1991). One leaf per plant was harvested and snap frozen in liquid nitrogen. 500 µl extraction buffer was added (200 mM Tris (pH 7.5), 250 mM NaCl, 25 mM EDTA (pH 8.0), 0.5 % (w/v) SDS) and the leaf ground using a pellet pestle (Sigma) and vortexed briefly to dispense large clumps. Samples were centrifuged for 5 minutes at 4°C. 400 µl of supernatant was mixed with 400 µl of isopropanol. Samples were incubated at -80°C for 30 minutes followed by centrifugation for 6 minutes at 4°C. The supernatant was removed and the pellet was rinsed with 70% ethanol and allowed to dry at room temperature for 20 minutes. The pellets were resuspended in 50 µl of sdH₂O. The samples were then centrifuged briefly and the supernatant removed to a fresh 1.5 ml centrifuge tube. 1-2 µl of sample was routinely used in PCR.

2.3.1.2. *Plant RNA extraction*

Plant RNA extractions were carried out using the GenElute™ Mammalian Total RNA Miniprep Kit in accordance with the manufacturer's instructions.

2.3.1.3. *Plasmid preparation from bacterial overnights*

Plasmid DNA was prepared from *E. coli* cultures using the GeneElute™ Plasmid Miniprep Kit (Sigma) or the QIAprep Spin Miniprep kit (Qiagen) in accordance with the manufacturer's instructions.

2.3.1.4. *DNA extraction from agarose gels*

DNA fragments were resolved by agarose gel electrophoresis (Section 2.3.5.1.) and visualised on a Benchtop trans-illuminator (Syngene). The desired band was excised from the gel using a sharp razor blade and excess agarose removed. The DNA was extracted from the gel slice by using the QIAquick Gel Extraction Kit (Qiagen) in accordance with the manufacturer's instructions.

2.3.1.5. *Quantification of DNA and RNA*

The concentration of double-stranded DNA (dsDNA) and RNA solutions was determined by measuring the absorbance at 260 nm (OD_{260}) in a spectrophotometer. An aliquot of the stock samples was diluted 1:200 in sdH_2O and the spectrophotometer calibrated using sdH_2O in a quartz cuvette. Measurements were made for each sample at OD_{260} and OD_{280} . The ratio OD_{260}/OD_{280} was used to estimate the purity of nucleic acid, since proteins absorb at 280 nm. A ratio between 1.8-2.0 meant that the level of contaminants was at an acceptable level. Concentrations of dsDNA and RNA were calculated using the equations:

$$1 \text{ OD unit } 260 \text{ nm} = 50 \text{ } \mu\text{g/ml dsDNA}$$

$$1 \text{ OD unit } 260 \text{ nm} = 40 \text{ } \mu\text{g/ml RNA.}$$

2.3.2. *Enzymatic manipulation of nucleic acids*

2.3.2.1. *Endonuclease restriction of nucleic acids*

For restriction enzyme digests between 0.5-1 μg plasmid DNA or ~200 ng PCR product was used. Restriction enzymes and buffers were obtained from New England Biolabs and the recommended

buffer used at 1x concentration in the reaction. At least 1 unit of restriction enzyme was used per microgram of DNA. Reactions were typically 10 µl total volume and digests were incubated at the appropriate temperature for \geq one hour. To stop the reaction the digests were incubated at 65°C or 80°C for 20 minutes, as per the manufacturer's instructions. To perform double digests with enzymes that do not have compatible buffers or to subsequently modify the DNA with shrimp alkaline phosphatase or ligase, after digestion a small quantity of the reaction (typically 2 µl) was analysed on an agarose gel and the remaining DNA was ethanol precipitated and then the subsequent treatment performed.

2.3.2.2. *Dephosphorylation of 5' ends*

Shrimp Alkaline Phosphatase (SAP) (Roche) was used to catalyse the dephosphorylation of 5' phosphates from linearised plasmid DNA. Approximately 50 ng of vector DNA was included in a reaction with 0.9 µl of 10x Dephosphorylation Buffer (supplied by Roche) and 1U SAP and the reaction mixture made up a final volume of 9 µl with sdH₂O. The reactions were incubated at 37°C for 10 minutes followed by inactivation of SAP through incubation at 65°C for 15 minutes and the linearised plasmid DNA used directly in ligations.

2.3.2.3. *DNA ligations*

Ligations were performed using T4 DNA ligase (Invitrogen). T4 DNA ligase catalyses the joining of two strands of DNA between the 5' phosphate and the 3' hydroxyl groups of adjacent nucleotides. PCR products were ligated into pPCR-Script (Stratagene) using a modified protocol with the PRC-Script Cam Cloning Kit (Stratagene). Blunt ended PCR products were purified using the StrataPrep® PCR Purification Kit (Stratagene) or SureClean solution (Bioline) as per the manufacturer's instructions. For ligations into the PCR-Script Cloning vector the following reaction was prepared: 1 µl PCR-Script Cam SK(+) cloning vector, 1 µl of PCR-Script 10x reaction buffer, 0.5 µl of 10mM rATP, 2-4 µl of blunt-ended PCR product, 0.5 µl *SrfI* restriction enzyme (5 U.µl⁻¹) and 0.5 µl of T4 DNA ligase (4 U.µl⁻¹) (Stratagene), the reaction volume was made up to a final volume of 10 µl with sdH₂O. The insert : vector ratio was typically 50:1. The ligation reactions were incubated at 16°C for ~16 hours followed by inactivation at 65°C for 10 minutes. All other ligations were carried out by combining 50 ng of linearised, dephosphorylated vector, 4 µl of 5x ligase buffer (supplied by Invitrogen), 0.5 µl T4 DNA

ligase (5 U. μl^{-1}) and 2–6 μl of insert DNA fragment in a final volume of 20 μl . The insert : vector ratio was typically 3:1 and all ligations were incubated at 16°C overnight followed by transformation into chemically competent *E. coli* (Section 2.2.2).

2.3.2.4. PCR

The Polymerase Chain Reaction (PCR) was used to screen bacterial colonies for the presence of plasmids, screen *Arabidopsis* insertion lines, analyse yeast one-hybrid library vectors, site-directed mutagenesis and gene construction.

For all general analytical PCR, YB-TAQ (Yorkshire Biosciences Ltd) was used. For all applications a reaction volume of 20 μl was used. The reaction mixture consisted of: 2 μl 10X reaction buffer (supplied by York Biosciences Ltd), 0.5 μl of dNTPs (10 mM each) (Yorkshire Biosciences Ltd), 0.4 μl MgCl_2 (50mM), 0.2 μl YB-TAQ (5 U. μl^{-1}), 0.5 μl of each primer (50 μl stock) and 1 μl of template DNA. For colony PCR the reaction volume was made up to 20 μl with sdH_2O and a small amount of bacterial colony added to the PCR reaction by touching a toothpick against a colony and then dipping the toothpick in the PCR tube. For cloning applications a ACCUZYME (Bioline) a high fidelity proof reading polymerase was used following the manufactures instructions. 1 ng plasmid DNA or 1 μl first strand cDNA (Section 2.3.2.5.) was used as a template in these reactions.

The thermal cycling program used for PCR amplification was preceded by as denaturing step of 95°C for 5 minutes followed by 35 cycles (analytical) or 20 cycles (cDNA amplification for cloning) of: (i) denaturation for 30 seconds at 95°C; ii) primer annealing for 30 seconds between 50-65°C; iii) elongation at 72°C for 0.5-2 min depending on the size of the expected product (60 seconds per kb). The cycling program was followed by 72°C for 5 min to promote completion of partial extension products and annealing of single-stranded complementary products and the PCR reaction was held at 4°C until analysis.

2.3.2.5. RT-PCR

RT-PCR was used to clone cDNAs and also to analyse transcript levels. RNA extracted through the method outlined in section 2.3.1.2. was treated with Deoxyribonuclease I (DNase I) (Sigma) to remove any contaminating DNA. The entire elution solution from RNA extraction (50 μl) was treated by adding 5 μl of 10x reaction buffer (supplied by Sigma) and 5 μl of DNase I followed by incubation for

15 minutes at room temperature. After 15 minutes DNase I was inactivated by the addition of 5 μl of stop solution (supplied by Sigma) and heating for 10 minutes at 70°C. RNA was quantified following the procedure in section 2.3.1.5. First strand cDNA synthesis was carried out using Moloney Murine Leukaemia Virus Reverse Transcriptase (M-MLV RT) (Promega). For each sample 2 μg of RNA was used. 2 μg RNA and 2 μl oligo dT primer (0.5 μg μl^{-1}) in a total volume of 15 μl sdH_2O was incubated at 70°C for 5 minutes to melt secondary structures within the template. Samples were cooled immediately on ice. To the annealed primer template solution the following components were added in the order shown: 5 μl M-MLV 5x Reaction buffer (supplied by Promega), 1.25 μl dNTPs (10 mM each) 1 μl M-MLV RT (200 U) and sdH_2O to a final volume of 25 μl . The reaction mixture was incubated at 42 °C for 60 minutes before the enzyme was inactivated at 70°C for 15 minutes. 1 μl of first-strand cDNA synthesis reaction was used as a template in each 20 μl PCR reaction.

2.3.2.6. *Quantitative PCR (QPCR)*

QPCR is a sensitive assay to quantify the initial amount of starting template (the amount of transcript) in a sample. QPCR monitors the PCR amplification product accumulation during each PCR cycle. For each sample a 20 μl reaction was set up: 10 μl Sigma SYBR® Green JumpStart™ Taq ReadyMix™, 1 μl of each 5 mM primers, 2 μl of first strand cDNA, made up to the final volume with sdH_2O . Reactions were set up using a robot (Corbett Research CAS1200) and QPCR was performed using a MJ Research Chromo 4™ QPCR machine using the program: Incubation at 94°C for 2 minutes followed by a cycle of 94°C for 30 seconds, 63°C for 30 seconds, 72°C for 30 seconds for 40 cycles. At the end of each cycle the plate is read measuring an increase in fluorescence. After the completion of the cycling program a melting curve from 75°C to 90°C with a read every 0.2°C is performed to check for the production of more than one PCR product. Data was analysed using Opticon Monitor software.

2.3.2.7. *DNA sequencing*

DNA sequencing was carried out by John Innes Centre Genome Laboratory (John Innes Centre, Norwich). 20 μl of plasmid (100-200 ng/ μl) in sdH_2O was sent for sequencing. The sequencing results were viewed using EditSeq (DNA Star) and Chromas (Technelysium) and assembled using SeqMan (DNA Star).

2.3.3. Protein Preparation

2.3.3.1. Protein extraction from *Arabidopsis*

Leaf tissue/seedlings of 0.4g were ground to a fine powder in liquid nitrogen and mixed with 1 ml ice-cold LE buffer (50 mM lithium phosphate (pH 8.0), 120 mM β -mercaptoethanol, 1 mM sodium monoiodoacetate, 1 mM phenylmethylsulphonylfluoride and 5% glycerol). The mixture was thawed and 20% (w/v) lithium dodecylsulphate (LIDS) added to a final concentration of 0.5%. Proteins were solubilised and denatured by incubating for 1 minute at 100°C and cell debris removed by centrifugation for 15 minutes at maximum speed. The supernatant was transferred to a fresh tube for subsequent analysis.

2.3.3.2. Protein extraction from *E. coli* BL21(DE3)pLysS

All protein expression in *E. coli* was carried out in the BL21(DE3)pLysS strain. Protein expression was always carried out in cultures from freshly transformed BL21 cells. A fresh colony of BL21 transformed with the appropriate expression construct was used to inoculate a 25 ml culture of LB media containing the appropriate antibiotic. Cultures were incubated at 37°C with shaking until they reached $OD_{600} = 0.5$. Protein expression was induced by the addition of 1.5 mM isopropyl β -D-thiogalactopyranoside (IPTG) and the culture was incubated for a further 2 hours. A small sample of the culture (1-5 ml) was removed and used to check for protein expression by SDS-PAGE (section 2.3.5.2.). The cells in the sample were harvested through centrifugation and resuspended in loading buffer (section 2.3.5.2.) before analysis by SDS-PAGE and coomassie staining (section 2.3.5.3.) or Western blotting (section 2.3.5.4.). The rest of the bacteria were harvested by centrifugation for 5 minutes at 3600 rpm in a SS-34 rotor (Sorvall). Protein was extracted from the bacteria by resuspending the pellet in either 5 ml of Denaturing Equilibration/Wash buffer (50 mM Sodium Phosphate, 6 M Guanidine-HCl and 300 mM NaCl (pH 7.0)) for His-tagged proteins or 5 ml Extraction buffer (140 mM NaCl, 10 mM Na_2HPO_4 , 1.8 mM KH_2PO_4 (pH 7.5)) for GST tagged proteins. The samples were agitated at 4 °C for 60 minutes and the cells disintegrated through 2 x 10 second bursts on a sonicator (Soniprep 150 MSE) using an amplitude of 14 microns. The samples were centrifuged at 12000 g for 20 minutes at 4°C in a SS-34 rotor (Sorvall) to pellet any insoluble material and the clarified sample transferred to a clean tube for subsequent protein purification.

2.3.3.3. Purification of His-tagged proteins

For His-tagged proteins (AtMinD1, AtMinD1(K72A) and EcMinE) TALON Metal Affinity Resin (Clontech) was used to purify the protein. The resin contains immobilised Co^{2+} ions. Histidine binds the Co^{2+} ions by sharing electron density of the imidazole nitrogen with the electron deficient orbitals of the Co^{2+} ions thus the His-tagged proteins are selectively bound to the resin.

The resin was prepared in accordance with the manufacturer's instructions. The clarified sample from section 2.3.3.2 was added to the resin and the sample was gently shaken at room temperature for 20 minutes to allow the His-tagged protein to bind to the resin. The sample was transferred to a 2 ml Disposable Gravity Column (Clontech) and the resin allowed to settle out of suspension. The end cap was removed and the sample was drained out of the column and collected. The sample was subsequently passed through the column twice more ensuring not to disturb the resin. The resin was washed three times by passing 5 ml Denaturing Equilibration/Wash buffer (Section 2.3.3.2) through the column. His-tagged protein was eluted from the resin by the addition of 3 ml Elution buffer (45 mM Sodium Phosphate, 5.4 M Guanidine-HCl, 270 mM NaCl and 150 mM Imidazole). Eluted protein was collected in 500 μl fractions. SDS-PAGE (Section 2.3.5.2.) followed by Coomassie staining (Section 2.3.5.3.) was used to establish the purity of the protein and which fractions contained the most protein. Following purification, proteins were refolded by dialysis against sodium phosphate buffers (50 mM sodium phosphate, 50 mM NaCl, 0.1 M EDTA, 1.5 mM dithiothreitol, 10% glycerol (pH 7.2)) containing 8 M-0 M urea.

2.3.3.4. Purification of GST-tagged proteins

Glutathione-Uniflow resin (Clontech) was used to purify glutathione S-transferase (GST) and GST-tagged AtMinE1. The resin was prepared and packed onto the column as described in the manufacturer's instructions. The clarified sample from section 2.3.3.2. was added to the column and the resin was resuspended. The resin was allowed to settle out of suspension and the sample was drained out of the column. The resin was washed three times with Extraction buffer (Section 2.3.3.2.) and the protein eluted from the resin by applying 4 ml Elution buffer (10 mM Glutathione in 50 mM Tris-HCl (pH 8.0)) to the column. The eluted protein was collected in 500 μl fractions and the purity of the protein verified by SDS-PAGE (Section 2.3.5.4.) followed by coomassie staining (Section 2.3.5.3).

2.3.3.5. *Co-immunoprecipitation*

FtsZ2-1-YFP was used as bait in co-immunoprecipitation assays. Expression of FtsZ2-1-YFP was induced by spraying in 20 day-old seedlings with 30 μ M dexamethasone. ~12 seedlings were harvested and tissue ground to a fine powder in liquid nitrogen. 2ml of extraction buffer (50 mM Tris (pH 7.5), 100 mM NaCl, 0.1% Triton x-100, 1 mM dithiothreitol and Complete Mini EDTA-free protease inhibitor cocktail tablet (Roche) (1 tablet for 10 ml extraction buffer)) was added to the ground seedlings and allowed to thaw. The sample was centrifuged at 10,000 g at 4°C for 5 minutes to get cleared lysates. The lysates were pre-cleaned with 100 μ l Protein G-sepharose® (Sigma) incubated at 4°C with agitation for 1 hour. The Protein G-sepharose was removed by centrifugation at 5,000 g at 4°C for 5 minutes, the supernatant was removed to a clean tube and 10 μ l Full-Length A.v. Polyclonal Living Colours Antibody (Clontech) (1:200 dilution) was added to precipitate FtsZ2-1-YFP. The sample was incubated at 4°C with agitation for 3 hours to allow complete precipitation of FtsZ2-1-YFP. 75 μ l Protein G-sepharose was added to precipitate the FtsZ2-1-YFP/antibody complex and the sample incubated for a further 3 hours. The sample was washed with extraction buffer 4 times. During each wash the sepharose beads were pelleted by centrifugation at 1,500 g for 4 minutes and resuspended in new wash buffer. After washing the beads were pelleted and the proteins released from the sepharose beads by boiling for 5 minutes in SDS gel loading buffer (section 2.3.5.2) and analysed by SDS-PAGE and Western blotting (section 2.3.5.4).

2.3.3.6. *Protein quantification*

The Bradford assay was used to quantify protein solutions. Bradford assay solutions were purchased from Bio-Rad (Bio-Rad protein assay). Concentrated solution (Bio-Rad) was diluted 1 in 5 with sdH₂O. 1ml of diluted reagent was mixed with 10 μ l of sample, incubated for two minutes and the absorbance measured at 595nm. The absorbance of protein standards containing between 0-2mg of Bovine Serum albumin (BSA) were also measured and the standard plotted on a graph of protein concentration against absorbance. The gradient of the graph of standards was used to calculate the concentration of the sample from the sample absorbance.

2.3.4. ATPase assays

For all assays, the reaction mixture contained 100 mM Tris-Cl (pH 7.4), 50 mM NaCl, 0.1 mM EDTA, 1.5 mM dithiothreitol, 10% glycerol, and 5 mM CaCl₂, except for the cation effects assays where 5 mM CaCl₂ was replaced with either 5 mM MgCl₂, KCl or MnCl₂. In experiments testing the effects of the AtMinD1(K72A) mutation, different cation effects and pH dependence, 10 μM [γ -³²P]ATP (specific activity 10 mCi/mmol) and 0.1 μM AtMinD1 or AtMinD1(K72A) were used and reactions (20 μl) were incubated for 1 h at 35°C and stopped with 1 μl of 1 M formic acid. In the time course assays for the double reciprocal plot 10-80 μM [γ -³²P]ATP and 0.1 μM AtMinD1 were used, reactions incubated at 35°C and stopped at the specified time. To analyse the effect of AtMinE1 and EcMinE on AtMinD1 ATP hydrolysis, 0.1 μM AtMinE1, 0.1 μM EcMinE and 0.1 μM AtMinD1 were used, reactions incubated at 35°C and stopped after 10 minutes. In all assays a no enzyme control was used to assess the background. Samples were spotted onto PEI-cellulose (POLYGRAM CEL 300 PEI, MACHEREYNAGEL) TLC plates, developed using 0.5 M LiCl and 0.5 M formic acid and radioactive nucleotides were visualized by autoradiography using x-ray film (Kodak). For quantification purposes plates were scanned using a phosphorimager (Cyclone Storage Phosphor System, Packard).

2.3.5. Electrophoresis and related techniques

2.3.5.1. Agarose gels

Agarose gel electrophoresis was used to separate and analyse DNA. Unless otherwise stated all gels were made at 1% using electrophoresis grade agarose (Melford) in 1x TAE (50 x TAE stock solution was prepared by mixing 242 g Tris base, 57.1 ml glacial acetic acid and 100 ml 0.5 M EDTA, pH 8.0 in a final volume of 1 l. From this a 1 x TAE working solution was made). Agarose gels were cast by melting the agarose in 1 x TAE. This solution was allowed to cool to ~50°C and 1 μl.ml⁻¹ EtBR (50 μg ml⁻¹) added before pouring the solution into a gel tray to harden. Loading buffer (6 x = 0.25% bromophenol blue, 0.25% Xylene cyanol Ff, 40% (w/v) sucrose in sdH₂O) was added to each DNA sample to a final concentration of 1x before loading. Molecular markers were used to determine the sizes of the DNA fragments: 2.5 μl of HyperLadder I (Bioline) was loaded per lane, giving a total of 360 ng of DNA. DNA was examined using a Benchtop transilluminator (Syngene) and photographed using a BioDoc-It system (UVP).

2.3.5.2. SDS-PAGE

SDS-PAGE was used to separate and analyse proteins. For all SDS-PAGE a 10% resolving gel and a 4% stacking gel was used. To prepare the resolving gel 3.3 ml of a 30% Acrylamide/Bis solution (37.5:1 Acrylamide : N,N'-Methylene-bis-acrylamide) (Bio-Rad) was combined with 2.5 ml 1.5 M Tris (pH 8.8), 50 μ l 20% (w/v) SDS and 4.0 ml sdH₂O. 10 μ l of TEMED (Bio-Rad) and 100 μ l of 10% ammonium persulfate was added whilst swirling the mixture. The mini-PROTEAN II system (Bio-Rad) was used to carry out electrophoresis. The glass plates were assembled according to the manufacturer's instructions and the resolving gel was pipetted into the gap between the glass plates leaving ~2.5 cm to the top of the smaller plate for the stacking gel. A layer of 70% isopropanol was laid over the resolving gel to flatten out the top of the gel and the gel was left to set for ~15 minutes. After the gel had set the gel apparatus was tipped upside down to pour off the isopropanol overlay and the top of the gel was washed with sdH₂O to remove any unpolymerised acrylamide. To prepare the stacking gel, 0.33 ml Acrylamide/Bis solution was combined with 0.63 ml of 0.5 M Tris (pH 6.8), 12.5 μ l of 20% (w/v) SDS, 1.5 ml sdH₂O, 2.5 μ l TEMED and 25 μ l of 10% ammonium persulfate. The stacking gel was poured directly on top of the resolving gel. Immediately the combs were inserted into the stacking solution and more stacking solution was applied between the teeth of the combs. The stacking gel was left to set for ~15 minutes and then combs removed and the wells were washed with sdH₂O. The gel was loaded into the electrophoresis apparatus and Tris-glycine electrophoresis buffer (25 mM Tris, 250 mM glycine (pH 8.3), 0.1% (w/v) SDS) was added to the top and bottom reservoirs.

Protein samples were prepared in the appropriate volume of 1x SDS gel loading buffer (50 mM Tris (pH 6.8), 100 mM dithiothreitol, 2% SDS, 0.1% bromophenol blue, 10% glycerol). For bacterial cell pellets the pellet was resuspended directly in 1x SDS gel loading buffer. For purified protein samples and for protein extracted from *Arabidopsis* a 4x SDS gel loading buffer was used diluted 4x by the protein sample. The protein samples in the loading buffer were incubated for 5 minutes in a boiling water bath to denature the proteins and immediately transferred to ice for 2 minutes. The protein samples were centrifuged for 2 minutes at maximum speed before being loaded onto the gel. 5 μ l of Molecular weight markers were also loaded into a lane of the gel to estimate the size of protein bands (Broad Range Protein Molecular Weight Markers (Promega)). The gels were run at typically 15V/cm until the bromophenol blue reached the bottom of the resolving gel.

After electrophoresis the gels were washed in de-ionised water and either used for Western blotting (section 2.3.5.4) or stained with coomassie (section 2.3.5.3).

2.3.5.3. *Coomassie staining of polyacrylamide gels*

To stain the proteins in polyacrylamide gels, coomassie staining was used. After electrophoresis gels were washed in deionised water and transferred to a plastic tray. Stain buffer (45% sdH₂O, 45% methanol, 10% acetic acid and 0.2% Brilliant Blue) was poured over the gel until the gel was completely submerged. The gel was then shaken gently on an orbital shaker SO1 (Stuart Scientific) at ~150 rpm for 20 minutes. The stain buffer was discarded and replaced with destain buffer (65% sdH₂O, 25% methanol, 10% acetic acid) and gently shaken until protein bands appeared. The destain buffer was replaced several times until no more coomassie stain could be removed from the gel.

2.3.5.4. *Western blotting*

Western blotting was used to verify the presence of FtsZ2-1-YFP in the co-immunoprecipitation experiments and AtMinD1, AtMinD1(K72A), EcMinE in overexpressing *E. coli*. Western blotting involves the transfer of proteins from a gel to a solid support. The solid support used for Western blotting was PROTRAN® Nitrocellulose Transfer Membrane (Whatman® Schleicher & Schuell). Three pieces of Whatman filter paper and a piece of nitrocellulose membrane were cut to the same size at the gel. The three pieces of Whatman filter paper were soaked in one of three buffers: cathode buffer (25 mM Tris (pH 9.4), 40 mM 6-Aminocaproic acid and 20% methanol), anode I (0.3 M Tris (pH 10.4) and 10% methanol) and anode II (25 mM Tris (pH 10.4) and 10% methanol). The nitrocellulose membrane was soaked in de-ionised water. A transfer tower was set up within an electrotransfer unit (made in house) and consisted of the cathode filter paper followed by the gel, nitrocellulose membrane, anode II filter paper and then the anode I filter paper. An electric current of 0.15 Amps was passed through the electrotransfer unit for 25 minutes to transfer the proteins from the gel to the nitrocellulose membrane. After blotting, the nitrocellulose membrane was stained with Ponceau S (0.1% (w/v) Ponceau S in 5% acetic acid) and the molecular marker bands were marked on the membrane. The membrane was blocked for 1 hour in TBS (20 mM Tris-HCl, (pH 7.4), 0.15 M NaCl) with 5% MARVEL and then washed three times in TBS. The membrane was incubated with the primary antibody at a 1:1000 dilution in TBS (Mouse anti-His (Invitrogen) for His-tagged AtMinD1, AtMinD1(K72A) and EcMinE

or Full-Length A.v. Polyclonal Antibody Living Colours Antibody (Clontech) for FtsZ2-2-YFP) followed by washing and incubation with the secondary antibody (anti-rabbit conjugated to HRP for FtsZ2-2-YFP or anti-mouse conjugated to alkaline phosphatase for His-tagged proteins). The blots were washed a further 3 times in TBS and the HRP or alkaline phosphatase were detected using BM Chemiluminescence Western Blotting Substrate (POD) (Roche) for HRP and SIGMA FAST™ BCIP/NPT (Sigma) for alkaline phosphatase, in accordance with the manufacturers' instructions.

2.4. Yeast work

2.4.1. Growth and storage of yeast

Yeast strains used in this study are listed in Table 2. The yeast strains were grown at 28-30°C in YPDA or SD (synthetic dextrose minimal medium) as appropriate. YPDA was made by adding 20 g difco peptone and 10 g yeast extract to 945 ml H₂O. The media was autoclaved and cooled to 55°C before the addition of 15 ml 0.2% adenine hemisulphate solution (final concentration 0.003% in addition to the trace amount of adenine present in YPD) and 2% dextrose (50 ml of a sterile 40% stock solution). SD media (a combination of a Minimal SD Base and a Dropout Supplement) is a synthetic, minimal medium lacking one or more specific nutrients. The specific nutrients omitted depend upon the selection medium desired, for example yeast cloning vectors carry nutritional markers to allow for selection of yeast transformants. For 1 l of 10x dropout supplement the following were combined minus the appropriate nutrients: 200 mg L-adenine hemisulphate, 200 mg L-arginine HCl, 200 mg L-histidine HCL monohydrate, 300 mg L-isoleucine, 1000 mg L-leucine, 300 mg L-lysine HCl, 200 mg L-methionine, 500 mg L-phenylalanine, 2000 mg L-threonine, 200 mg L-tryptophan, 300 mg L-tyrosine, 200 mg L-uracil and 1500 mg L-valine. The 10x stock was autoclaved and stored at 4°C. SD minimal medium was made by adding 6.7 g Yeast Nitrogen base without amino acids to 850 ml sdH₂O. The media was autoclaved and cooled to 55°C before the addition of 2% dextrose (50 ml of a sterile 40% stock solution) and 100 ml of the appropriate 10 x Dropout solution. For solid YPDA or SD media 1.5% (w/v) agar was added prior to autoclaving and the additional supplements added when the media had cooled to ~55°C before pouring plates.

Yeast grown on solid media were kept for up to 4 months by sealing the plate with parafilm and storing at 4°C. For long term storage yeast glycerol stocks were produced by pelleting 1.5 ml of freshly

grown yeast culture and resuspending the pellet in YPDA/20% glycerol in a cryogenic tube. The glycerol stock was then snap frozen in liquid nitrogen and stored at -80°C for up to three years.

Table 2. Yeast strains used in this study

Strain	Genotype	Source
HF7c	<i>MATa, ura3-52, his3-200, lys2-801, ade2-101, trp1-901, leu2-3, 112, gal4-542, gal80-538, LYS2 :: GAL1_{UAS}-GAL1_{TATA}-HIS3, URA3 :: GAL4^{17-mers(x3)}-CYC1_{TATA}-lacZ</i>	Clontech
AH109	<i>MATa, trp1-901, leu2-3, 112, ura3-52, his3-200, gal4Δ, gal80Δ, LYS2 :: GAL1_{UAS}-GAL1_{TATA}-HIS3, MEL1 GAL2_{UAS}-GAL2_{TATA}-ADE2, URA3::MEL1_{UAS}-MEL1_{TATA}-lacZ</i>	Clontech
Y187	<i>MATa, ura3-52, his3-200, ade 2-1010, trp 1-901, leu 2-3, 112, gal4Δ, met-, gal80Δ, URA3 :: GAL1_{UAS}-GAL1_{TATA}-lacZ, MEL1</i>	Clontech

2.4.2. Small scale transformation of yeast

A single yeast colony was used to inoculate 10 ml YPDA and incubated over-night at 30°C with shaking at 250 rpm until the culture reached saturation. For each transformation 1 ml cells was harvested in a 1.5 ml centrifuge tube by pulse centrifugation for 8 seconds at maximum speed. The supernatant was decanted and the cells were left in 50-100 µl of liquid. 2 µl of 10 mg/ml carrier DNA was added and the cells resuspended with a pipette tip. Plasmid DNA ~1 µg was added and the cells briefly vortexed. 0.5 ml of PLATE mixture was added (40 % PEG 4000 (w/v), 100 mM lithium acetate, 10 mM Tris-Cl (pH 7.5) and 1 mM EDTA) and briefly vortexed. 20 µl of 1.0 M dithiothreitol was added and the cells were again vortexed briefly. The cells were incubated at room temperature overnight (~16 hours) and subjected to heat shock by incubation at 42°C for 10 minutes. 100 µl of cells were withdrawn from the bottom of the tube and plated on SD media supplemented with the appropriate amino acids. Plates were incubated for 2-4 days at 30°C until colonies appeared.

2.4.3. Yeast mating

Yeast two-hybrid library screening was performed by yeast mating. Interacting clones were selected by virtue of their ability to grow on medium lacking His. A single, fresh Y187 [bait] yeast colony was used to inoculate 10 ml of SD/-Trp medium and grown overnight at 30°C at 250 rpm until the OD₆₀₀ = 0.8. A 1 ml aliquot of the AH109 [library] strain was thawed at room temperature. In a flat-bottomed 100 ml flask 9 mls of YPDA+ 50 µg/ml kanamycin was inoculated with 1 ml of the Y187 [bait]

overnight culture and 100 µl of AH109 [library]. The mating was incubated at 30°C with gentle shaking (40-50 rpm) for 22 hours, after which time an aliquot was examined using standard light microscopy to confirm the presence of diploids. The mating was then allowed to continue for four more hours. The mating mixture was spread onto 30 150 mm plates containing SD-LTH; 300 µl of mating mixture per plate and incubated at 30°C for 3-8 days until colonies became visible.

To determine the mating efficiency and the viability of diploids (number of clones screened), 100 µl of a 1:1,000, 1:100 and 1:10 dilution of the mating mixture was spread onto 90 mm plates containing SD/-Leu, SD/-Trp or SD/-Leu/-Trp. These plates were then incubated at 30°C until colonies appeared (usually after 2-3 days), and the number of colony forming units (cfu) counted. This data was used to calculate the number of viable cfu growing on each type of SD medium:

$$\frac{\text{cfu} \times 1000 \text{ } \mu\text{l/ml}}{\text{Vol. plated } (\mu\text{l}) \times \text{dilution factor}} = \# \text{ viable cfu/ml}$$

cfu/ml on SD/-Leu = viability of the AH109 [library] strain

cfu/ml on SD/-Trp = viability of the Y187 [bait] strain

cfu/ml on SD/-Leu/-Trp = viability of the diploids

To calculate the mating efficiency:

$$\frac{\# \text{ cfu/ml of diploids}}{\# \text{ cfu/ml of limiting partner}} \times 100 = \% \text{ Diploid}$$

2.4.4. Yeast one-hybrid library construction and screening

Library construction and screening was carried out using the BD Matchmaker™ One-hybrid Library Construction and Screening Kit following the guidelines provided by the manufacturer. To screen for interacting proteins 6 ml of screening mixture was plated onto 40, 15 cm round plates containing SD-LTH + optimal 3-AT for each screen.

To determine the transformation efficiency and to calculate the number of clones screened, 100 µl of a 1:1,000, 1:100 and 1:10 dilution of the mating mixture was spread onto 90 mm plates containing SD/-Leu, SD/-Trp or SD/-Leu/-Trp. These plates were then incubated at 30°C until colonies appeared (usually after 2-3 days), and the number of cfu counted.

The number of transformants per 3 µg of the library cloning vector pGADT7-Rec2 was calculated using the following equation:

$$\frac{\text{cfu on SD-Leu} \times \text{dilution factor}}{\text{volume plated (ml)}} \times 6 = \text{number of transformants per 3 } \mu\text{g of pGADT7-Rec2}$$

The number of clones screened was calculated using the following equation:

$$\frac{\text{cfu on SD-Trp} \times \text{dilution factor}}{\text{volume plated (ml)}} \times 6 = \text{number of clones screened}$$

2.4.5. Plasmid rescue from yeast

1.5 ml of yeast grown overnight in SD/-Trp/-Leu/-His were harvested by pulse spinning for 10 seconds in a micro-centrifuge. The cells were then resuspended in 100 µl of STET buffer (8% sucrose, 50 mM EDTA, 50 mM Tris-CL, pH 8.0, and 5% Triton X-100), the same volume of glass beads (0.45 µm) was added and the cells vortexed for 5 min. A second 100 µl of STET buffer was then added, the cells vortexed briefly and boiled for 3 minutes. After cooling briefly on ice the tube was centrifuged for 10 min at 4°C. 100 µl of the supernatant was transferred to a fresh tube containing 100 µl of 7.5 M ammonium acetate, incubated at -80°C for at least 20 min and then centrifuged for 10 min at 4°C at 13,000 g. 100 µl of supernatant was then added to 400 µl pre-cooled ethanol and centrifuged for 10 min at 13,000 g. The DNA pellet was dried and resuspended in 10 µl of sterile water. 5 µl of this solution was used to transform 50 µl of chemically competent DH5α *E. coli* cells using standard techniques. The cells were plated on LB-agar containing ampicillin (50 µg.ml⁻¹) to select for the pGADT7 library vector and incubated in a 37°C incubator overnight.

2.4.6. Quantitative assessment of protein-protein interactions in yeast

Quantative data for protein-protein interactions in yeast was obtained by growing 3 day old HF7c cells double transformants, transformed with the pGBK7T and pGADT7 plasmids encoding the proteins of interest for which an interaction was to be assessed, in liquid SD -LT media in a shaking incubator at 30°C until they reached a OD₆₀₀ of 1.0. 5 µl of cells were spotted onto SD -LT and SD-LTH media

plates. The plates were incubated for 4 days at 30°C. For quantification each yeast spot was suspended in 1 ml of liquid SD media and the OD₆₀₀ of the suspension recorded. The ratio of growth on SD/-TL and SD/-HLT was calculated for six individual pairs of spots and the average and standard deviation of these ratios calculated.

2.4.7. Colony lift filter assays

LacZ was used as a second reporter gene for analysis of positive clones identified in the yeast two-hybrid screens. The level of LacZ was estimated using colony lift filter assays. Yeast colonies were replica plated onto a fresh 100 mm plates containing SD-HTL and grown at 30 °C for 3 days. A piece of nitrocellulose filter paper cut to the same size as the petri dish was laid over the streaked yeast and gently pressed down onto the surface of the plate so that some of the yeast was attached to the filter paper. Using a pair of tweezers, the nitrocellulose filter was removed from the yeast plate and the filter was subjected to three freeze/thaw cycles by dipping the filter into liquid nitrogen and then allowing it to thaw, to lyse the yeast cells on the filter. A separate piece of Whatman filter paper was prepared: 2 ml of Z buffer/X-gal solution (60 mM Na₂HPO₄, 40 mM NaH₂PO₄.H₂O, 10 mM KCl, 1 mM MgSO₄.7H₂O, 39 mM 2-mercaptoethanol, 1 mg/ml X-gal pH 7.0) was added to a clean 100-mm plate and layer a 75-mm Whatman #1 filter was laid over the top to soak up the liquid. The thawed nitrocellulose filter paper was laid on top of the soaked Whatman filter paper yeast-side down and the assembly was incubated at 30 °C for up to 2 hours and checked periodically for the appearance of blue colonies.

2.5. Localisation Studies

2.5.1. Particle bombardment of tobacco

Particle bombardment (biolistic transformation) was used for the direct gene transfer into the leaf tissue of tobacco to transiently express YFP and CFP fusion proteins in tobacco leaves. This technique involves accelerating DNA-coated gold particles (the microcarriers) directly into intact tissues. To prepare the micro carriers for particle bombardment 60 mg of 1.0 µm gold microcarriers (BIO-RAD Laboratories) were suspended in 1 ml of 70% ethanol by vortexing for 5 minutes and then left to settle for 15 minutes. The gold particles were harvested by pulse centrifugation for 5 seconds, the ethanol was

removed and the particles washed 3 times with sdH₂O. The gold particles were again harvested and resuspended in 1 ml of 50% glycerol and stored at -20 °C.

To coat the DNA onto the gold micro carriers the glycerol stock was vortexed for 5 minutes and 20 µl of gold microcarriers were transferred to a clean tube. While vortexing 12 µl of plasmid DNA (10 µg/µl), 10 µl of 5 M CaCl₂ and 8 µl of 0.1M spermidine (free-base) were added to the gold followed by vortexing for 2 minutes. The mixture was incubated on ice for 30 minutes and then the microcarriers were pelleted by pulse centrifugation for 2 sec at maximum speed. The supernatant was carefully removed without disturbing the pellet and the pellet washed by adding 100 µl 70% ethanol and inverting the tube gently ten times. This wash step was repeated with 100 µl ethanol. The DNA coated micro carriers were thoroughly resuspended in 20 µl of ethanol by pipetting and 6 µl was spread over the centre of the macrocarrier (BIO-RAD Laboratories). Particle bombardment was carried out using a PDS-1000/HeTM Helium biolistic particle delivery system (BIORAD Laboratories), which is powered by a burst of helium gas to accelerate the microcarriers into the sample. All transformations were performed using 1100 psi rupture discs (BIO-RAD Laboratories) under 25 in Hg vacuum. Tobacco leaves were placed on Lehle medium. For each transformation the sample was bombarded with microcarriers twice and stored in the dark at room temperature for 24-48 hours before image acquisition.

2.5.2. Co-localisation of fusion proteins in living chloroplasts

For co-localisation studies fusions of proteins of interest were generated to YFP and CFP in the pWEN15 and pWEN18 vectors respectively (Kost *et al.*, 1998). The vectors were then co-bombarded into tobacco leaves. Samples were analysed after 24-48 hours and cells co-expressing the two plasmids analysed. Images were captured using exposure times suited to the intensity of each fluorophore, which were typically between 100-500 mseconds for YFP and 300-1000 mseconds for CFP. Images were individually contrast enhanced in Openlab (Improvision) and merged in Adobe Photoshop version 7.0 by overlaying the CFP image onto the YFP image and reducing the opacity of the CFP image to 50%.

2.5.3. Bimolecular Fluorescence Complementation assays.

The Bimolecular Fluorescence Complementation (BiFC) assay is based on the formation of a fluorescent complex when two non-fluorescent fragments of a fluorescent protein are brought together

by an interaction between proteins fused to the fragments (Hu *et al.*, 2002). The BiFC approach enables determination of the subcellular sites of protein interactions under conditions that correspond closely to the normal physiological environment.

A BiFC system for use in higher plants was generated by placing the N-terminal residues (1-154) and C-terminal residues (155-238) of the YFP protein under the control of the 35S promoter (Chapter 4). Vectors containing cDNA fusions to YFP₁₋₁₅₄ or YFP₁₅₅₋₂₃₈ were co-expressed in tobacco leaf cells by particle bombardment (Section 2.5.1.). Samples were analysed after 48 hours. In order to determine whether any fluorescence observed reflected a specific protein interaction, negative controls were carried out. Each cDNA fusion to YFP₁₋₁₅₄ or YFP₁₅₅₋₂₃₈ was expressed alone or in combination with a suitable “control” protein with which no interaction was predicted. All particle bombardments were carried out in triplicate for each sample.

2.6. Microscopy

All microscopy was carried out on a Nikon TE-2000U inverted fluorescence microscope equipped with 40x, 60x, and 100x oil immersion objectives (Nikon).

2.6.1. Light microscopy sample preparation

Tissue from *Arabidopsis* plants was prepared for light microscopy using the method of Pyke *et al.*, (1991). Whole seedlings or leaf samples were fixed in 3.5% glutaraldehyde for one hour and then softened in 0.1 M EDTA, pH 9.0 at 65°C for two hours. The samples were refrigerated overnight and chopped finely with a clean, sharp scalpel blade before viewing.

2.6.2. Fluorescence microscopy

Plant samples expressing YFP or CFP fusion proteins were generated using either particle bombardment (Section 2.5.1) or through the production of stably transformed transgenic *Arabidopsis* (Section 2.1.4). All plant samples were then prepared for analysis in the same way: a small amount of tissue (~1 cm²) was placed on a microscope slide with sdH₂O, covered with a 20x40 mm coverslip and firm pressure applied to remove air bubbles.

2.6.3. Image acquisition

Samples were viewed using Nomarski Differential Interference Contrast (DIC) microscopy. Colour images were captured on a Nikon D100 digital camera and processed in Adobe Photoshop version 7.0. using only those functions that apply to all pixels. Greyscale images were captured using a Hamamatsu Orca ER 1394 cooled CCD camera and image analysis was performed using Openlab software (Improvision). Fluorescence image acquisition was performed on a Nikon TE-2000U inverted fluorescence microscope equipped with an Exfo X-cite 120 fluorescence illumination system (Exfo) and filters for YFP (exciter HQ500/20, emitter S535/30), CFP (exciter S436/10, emitter S470/30) and chlorophyll autofluorescence (exciter HQ630/30, emitter HQ680/40) (Chroma Technologies, USA). All fluorescent images were captured using a Hamamatsu Orca ER 1394 cooled CCD camera. Standard image acquisition and analysis was performed using Openlab (Improvision). For analysis of *Arabidopsis* mesophyll cells for Chapter 6 Section 6.2.2.2. Unfixed samples of 21 day rosette leaves were analysed using the chlorophyll autofluorescence filter set. Volocity II (Improvision) was used to capture 0.5 μm Z-sections through the sample and to generate the extended focus image.

3. The plastid division protein AtMinD1 is a Ca²⁺-ATPase stimulated by AtMinE1

3.1. Introduction

Many of the proteins involved in plastid division are derived from bacterial components conserved from the cyanobacterial origins of higher plant chloroplasts (Osteryoung and Vierling, 1995; Colletti *et al.*, 2000; Itoh *et al.*, 2001; Maple *et al.*, 2002,). The best studied component of plastid division is FtsZ an ancient tubulin-like protein which polymerises to form a Z-ring to where other components of the division machinery are recruited (Bi and Lutkenhaus, 1991; Lutkenhaus and Addinall, 1997). The Z-ring is localised to the plastid midpoint (Vitha *et al.*, 2001; Fujiwara and Yoshida, 2001; McAndrew *et al.*, 2001) and correct Z-ring positioning is mediated by the coordinated action of the prokaryotic-derived Min proteins. The *E. coli minB* operon encodes MinC, MinD and MinE that together limit Z-ring placement to midcell (de Boer *et al.*, 1989; Bi and Lutkenhaus, 1993; Pichoff and Lutkenhaus, 2001). MinC is an antagonist of FtsZ polymerisation (Bi and Lutkenhaus, 1993; Pichoff and Lutkenhaus, 2001) and the topological distribution of MinC is controlled by the ATPase MinD and the topological specificity factor MinE (Hu and Lutkenhaus, 1999; Fu *et al.*, 2001; Raskin and de Boer, 1999). ATP-bound MinD recruits MinC to the membrane where the MinD/MinC complex forms a stable inhibition structure at the polar zone of the cell (Szeto *et al.*, 2002; Hu and Lutkenhaus, 2003; Zhou and Lutkenhaus, 2004). Topological specificity is conferred on this complex through the interaction of MinE with membrane-bound MinD whereby MinE stimulates MinD ATPase activity causing MinD to disassociate from the membrane and oscillation to the opposite pole of the cell (Hu and Lutkenhaus, 2001; Hale *et al.*, 2001; Hu *et al.*, 2002). The dynamic behaviour exhibited by MinD ensures that the lowest concentration of the MinD/MinC inhibitor complex occurs at midcell resulting in FtsZ polymerisation at the midpoint and appropriate placement of cell division (Meinhardt and de Boer, 2001).

AtMinD1 and AtMinE1 were identified in *Arabidopsis* based on their homology to MinD and MinE proteins from other organisms (Colletti *et al.*, 2000; Itoh *et al.*, 2001; Maple *et al.*, 2002). However, extensive homology searches have failed to identify a MinC homolog in plants, although abnormally large chloroplasts have been observed in tobacco overexpressing *E. coli* MinC (Tavva *et*

al., 2005). The importance of AtMinD1 in chloroplast division came from studies demonstrating that antisense repression of *AtMinD1* leads to Z-ring misplacement and asymmetric plastid division giving rise to chloroplast size heterogeneity within cells (Colletti *et al.*, 2000). Furthermore, overexpression of AtMinD1 leads to plastid division inhibition resulting in plant cells containing fewer but larger chloroplasts (Colletti *et al.*, 2000; Dinkins *et al.*, 2001). These phenotypes are reminiscent of minicelling and filamenting *E. coli* deficient in or overexpressing MinD (de Boer *et al.*, 1989), suggesting functional conservation between *E. coli* MinD and AtMinD1. In agreement with this, the polar localisation of *E. coli* MinD reflects the distinct intraplastidic localisation pattern of AtMinD1 which localises to either a single spot or as two spots at opposite poles of chloroplasts in close proximity to the chloroplast envelope (Maple *et al.*, 2002; Fujiwara *et al.*, 2004).

AtMinD1 encodes a protein of 326 amino acids which includes an N-terminal chloroplast-targeting transit peptide. Based on amino acid similarity AtMinD1 belongs to the ParA ATPase protein family containing a Walker A motif involved in the binding and hydrolysis of ATP. Like many ParA proteins, AtMinD1 can dimerise (Fujiwara *et al.*, 2004). Studies on the *accumulation and replication of chloroplasts 11 (arc11)* mutant have demonstrated that the asymmetric plastid division observed in *arc11* is due to a A296G missense mutation in AtMinD1 that leads to loss of dimerization and inappropriate intraplastidic localisation (Fujiwara *et al.*, 2004). This suggests that AtMinD1 dimerisation and correct intraplastidic localisation is in part important for correct Z-ring placement during *Arabidopsis* plastid division.

In *E. coli*, MinD is a weak ATPase (de Boer *et al.*, 1991) which is stimulated by MinE through a mechanism that involves a conformational change in the nucleotide binding site of MinD (Hu and Lutkenhaus, 2001; Ma *et al.*, 2004). Stimulation of *E. coli* MinD by MinE leads to a ten-fold increase in ATP hydrolysis but only in the presence of phospholipids (de Boer *et al.*, 1991), suggesting that membrane binding is required for MinE to activate MinD ATPase activity although interaction between MinD and MinE does not require MinD to be membrane associated (Taghbalout *et al.*, 2006). Because ATP hydrolysis leads to the release of MinD from the membrane (Hu *et al.*, 2002) and oscillation to the opposite pole of the bacterial cell, the ATPase activity of MinD is vital for the dynamic behaviour of the protein.

Due to the vital role that ATPase activity plays in *E. coli* MinD function, experiments were undertaken to investigate whether AtMinD1 also has ATPase activity. This study also attempts to

elucidate the function of AtMinD1 ATPase activity in order to explore the mechanism by which AtMinD1 brings about accurate placement of plastid division. Using site directed mutagenesis an active site AtMinD1(K72A) mutant is created and used to investigate how AtMinD1 ATPase activity functions in AtMinD1 localisation and interaction with AtMinE1.

3.2 Results

3.2.1. *AtMinD1* is a Ca^{2+} -dependent ATPase

Although *AtMinD1* and *MinD* from *E. coli* only show ~ 40% identity at the amino acid level both proteins contain identical Walker A motifs (Fig. 1A). To test whether, like *E. coli MinD*, *AtMinD1* is an ATPase a 981 bp full-length *AtMinD1* cDNA was PCR amplified using primers MIND/5 (5'-ATCATATGGCGGTCTGAGATTGTTC-3'; *Nde1* is underlined) and MIND/7 (5'-ATGGATCCTTAGCCGCCAAAGAAAGAGAAGAAGCC-3'; *BamH1* is underlined) and cloned into pPCR-Script (Stratagene) to generate pPCR-Script/*AtMinD1*. The full length *AtMinD1* cDNA was subsequently subcloned into the *Nde1* and *BamH1* sites of pET14b (Novagen) and expressed as a (His)₆-*AtMinD1* fusion protein in *E. coli* strain BL21 (DE3)pLysS. *AtMinD1* protein was insoluble therefore (His)₆-*AtMinD1* was purified by Co²⁺ affinity chromatography purification under denaturing conditions. (His)₆-*AtMinD1* was extracted from *E. coli* using the procedure outlined in Section 2.3.3.1. *AtMinD1* was purified from the cell lysate using TALON metal affinity resin (Clontech) and refolded through dialysis using buffers containing decreasing amounts of urea (Section 2.3.3.2). The first dialysis buffer contained 8M urea and in subsequent buffers the concentration of urea was reduced in 0.5M steps. A solution containing *AtMinD1* enclosed within a porous membrane was moved from one buffer to the next every 12 hours until the buffer no longer contained urea. Typical yields of *AtMinD1* ranged from 100-200 pmol *AtMinD1* per extraction. The purity of the refolded *AtMinD1* protein was verified by SDS-PAGE (Fig. 3.1B). To test for ATPase activity, 0.1μM purified *AtMinD1* protein was incubated with radiolabelled [γ -³²P]ATP at pH 7.4 in the presence of 5 mM CaCl₂ and analysed by TLC for the release of radiolabelled inorganic phosphate (Pi). Autoradiography showed that there was clear *AtMinD1*-induced ATP hydrolysis as compared to a no enzyme control demonstrating that *AtMinD1* is an ATPase (Fig. 3.1C). To ensure that the measured ATPase activity was due to *AtMinD1* and not a contaminating *E. coli* ATPase an active site *AtMinD1* mutant was generated by substituting the conserved Walker A lysine (K) for alanine (A) creating *AtMinD1*(K72A). To generate *AtMinD1*(K72A) two oligonucleotide primers, MIND/20 (5'-TTGCGGTGGTTGTCGTCCGCTCCAACACCGCCTTTTC-3') and MIND/21 (5'-CGGAAAAGCGGTGTTGGAGCGACGACAACCACCGC-3') were designed spanning the *AtMinD1* Walker A motif containing point mutations (underlined) changing the active site lysine (K) at position 72 to alanine (A). PCR amplification, using pPCR-Script/*AtMinD1* as a template and the primer pairs

MIND/5 - MIND/20 and MIND/21 - MIND/7 generated two AtMinD1 overlapping fragments which were joined together by Splicing by Overlap Extension using the flanking primers MIND/5 and MIND/7 to generate AtMinD1(K72A). The 981-bp full-length AtMinD1(K72A) cDNA was ligated into pPCR-Script to generate pPCR-Script/AtMinD1(K72A) and then subcloned into pET14b. AtMinD1(K72A) was expressed as a (His)₆ fusion protein in *E. coli*, purified and refolded as for wild-type AtMinD1 and the purity analysed by SDS-PAGE (Fig. 3.1B). 0.1 μM AtMinD1(K72A) was then incubated with [γ -³²P]ATP in the presence of 5 mM CaCl₂ and analysed by TLC. Autoradiography revealed no significant Pi release above the no enzyme control reaction (Fig. 3.1C) confirming that the K72A mutation inactivates AtMinD1 ATPase activity and that AtMinD1 ATP hydrolysis is mediated through the Walker A domain.

To more fully characterize the catalytic activity of AtMinD1 key kinetic parameters of AtMinD1-mediated ATP hydrolysis were determined. Using input [γ -³²P]ATP concentrations from 10-80 μM the release of radiolabelled Pi was quantified as a function of time in separate time course assays (Fig. 3.2A). From the initial reaction rates a reciprocal plot was produced and a K_m of 500 μM ATP and a V_{max} of 0.2 pmol ATP s⁻¹ were calculated (Fig. 3.2B). These values indicate that AtMinD1 is a weak ATPase. The extent of ATP hydrolysis as a function of protein concentration was calculated by measuring radiolabelled Pi release in response to increasing amounts of AtMinD1 after 60 minutes incubation at 35^oC (Fig. 3.3A). As seen from Fig. 3.3A the extent of ATP hydrolysis was proportional to the amount of input AtMinD1 and in the linear range of enzyme dependence 7 pmol of ATP was hydrolysed per pmol AtMinD1 which translates to a turnover number of ~ 2 fmol s⁻¹. Because divalent cations are known to influence the activity of ATPases (Berger and Girault, 2001) we investigated whether different cations had an effect on the ATPase activity of AtMinD1. 5mM CaCl₂ was replaced with either 5mM MgCl₂, KCl, or MnCl₂. Surprisingly, addition of Mg²⁺ had no significant effect on the activity of AtMinD1 (Fig. 3.3B) which is in contrast to the Mg²⁺-dependent ATPase activity of *E. coli* MinD (de Boer *et al.*, 1991). Similarly, K⁺ and Mn²⁺ did not significantly stimulate the ATPase activity of AtMinD1 (Fig. 3.3B). However, the addition of Ca²⁺ ions had a dramatic effect on AtMinD1 ATPase activity leading to a ~5-fold increase in ATP hydrolysis compared to reactions containing Mg²⁺ (Fig. 3.3B). Further kinetic analysis showed that maximum ATP hydrolysis occurs between pH 7.5-8 (Fig. 3.3C). Combined these data demonstrate that AtMinD1 is a Ca²⁺-dependent ATPase.

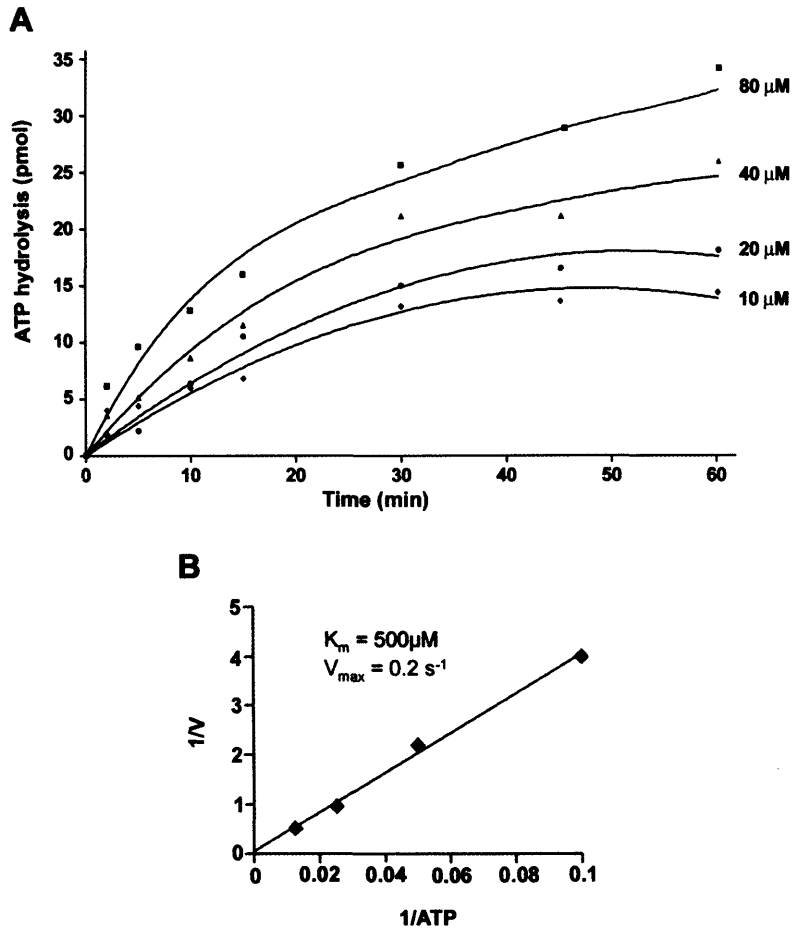


Fig. 3. 2. Time course analysis of AtMinD1 ATP hydrolysis. (A) 10, 20, 40, and 80 μM [$\gamma^{32}\text{P}$] ATP was added to reaction mixtures containing 0.1 μM of purified AtMinD1 and allowed to proceed for 60 minutes. The extent of radiolabelled Pi release was measured using TLC and quantified using a phosphorimager. (B) Steady-state kinetics of AtMinD1 ATP hydrolysis. A double reciprocal plot of Pi formation versus concentration of ATP used to calculate the K_m and V_{max} of AtMinD1.

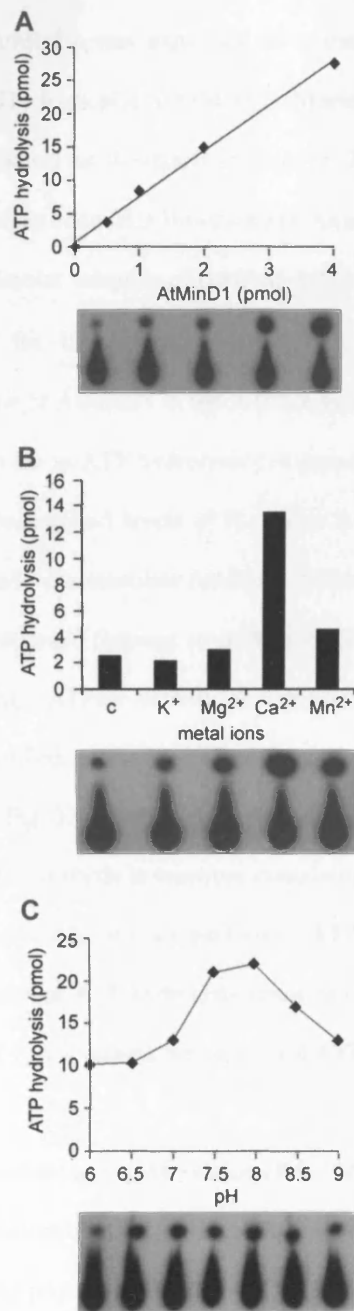


Fig. 3. 3. Characterisation of AtMinD1 ATP hydrolysis. (A) Increasing amount of AtMinD1 leads to a linear increase in ATP hydrolysis. (B) Cation dependence of AtMinD1 ATPase activity. (C) The effect of altering pH on the ATPase activity of AtMinD1.

3.2.2. *AtMinE1 stimulates the ATPase activity of AtMinD1*

In *E. coli* the ATPase activity of MinD is stimulated by MinE (Hu and Lutkenhaus, 2001) and because of the low basal ATPase activity of AtMinD1 we analysed whether AtMinE1 can stimulate AtMinD1-mediated ATP hydrolysis. AtMinE1 was expressed as a translational fusion to the C-terminus of glutathione S-transferase (GST) from pGEX/AtMinE1 (Maple *et al.*, 2002) in *E. coli* BL21 (DE3). Protein expression was performed as described in Section 2.3.3.2 and the soluble AtMinE1-GST fraction purified using glutathione resin (BD Biosciences). As a control GST was purified from pGEX-6P (Pharmacia Biotech). Equimolar amounts of purified AtMinE1-GST and AtMinD1 were incubated with CaCl₂ and [γ -³²P]ATP for 10 minutes followed by autoradiography and quantification by phosphoimaging. The inclusion of AtMinE1 in the ATPase assay had a marked effect on radiolabelled Pi release with a ~3-fold increase in ATP hydrolysis compared to reactions containing only AtMinD1 and taking into account the background levels of Pi release in assays only containing AtMinE1 (Fig. 3.4) demonstrating that AtMinE1 can stimulate AtMinD1 ATPase activity.

To ensure that the observed increase in ATP hydrolysis upon addition of AtMinE1 was not due to either inherent AtMinE1 ATPase activity or a contaminating *E. coli* ATPase we performed ATPase assays using only purified AtMinE1-GST. Although AtMinE1-GST assays did result in low background ATP hydrolysis (Fig. 3.4), probably due to contaminating *E. coli* protein(s), it is clear that the measured increase in ATP hydrolysis in reactions containing both AtMinD1 and AtMinE1 is due to AtMinD1 activity. To further verify this we performed ATPase assays with AtMinD1(K72A) and AtMinE1 which resulted in similar ATP hydrolysis levels as observed for AtMinE1-GST alone. As a control for the AtMinE1-GST fusion protein we performed ATPases using purified GST which resulted in no Pi release (Fig. 3.4).

To investigate the evolutionary conservation of the AtMinE1-stimulated AtMinD1 activity, *E. coli* MinE (EcMinE) was substituted AtMinE1 in ATPase assays. The 267 bp full-length *E. coli minE* gene was PCR amplified using primers EcE/3 (5'-ATCATATGGCATTACTCGATTTCTT-3' *Nde*I is underlined) and EcE/4 (5'-ATGGATCCCTTATTTTCAGCTCTTCTGCTTCC-3' *Bam*HI is underlined) and ligated into pET14b to generate pET14b/EcMinE and transformed into BL21 (DE3)pLysS. Protein expression was performed as described in Section 2.3.3.2. EcMinE was soluble and purified under native conditions using TALON metal affinity resin (BD Biosciences) following the user manual and the purity verified by SDS-PAGE. Although it has been previously demonstrated that AtMinE1 can

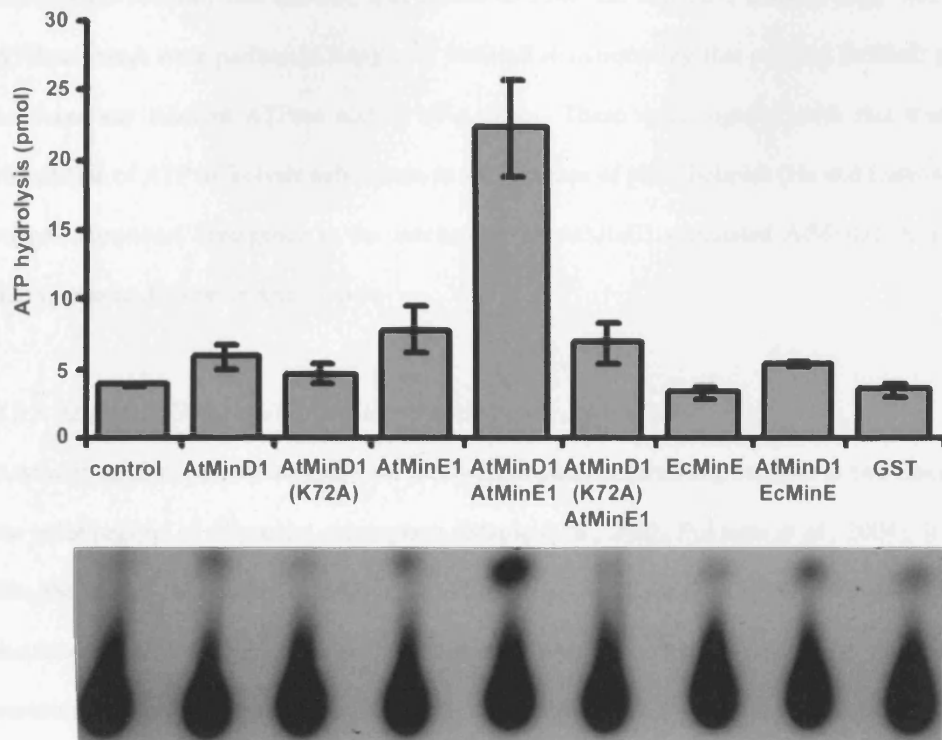
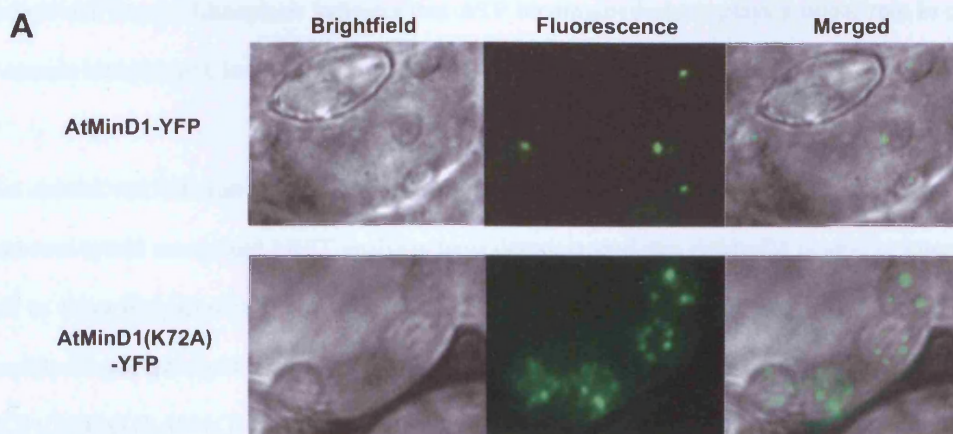


Fig. 3. 4. The effect of AtMinE1 on AtMinD1 activity. AtMinE1 and *E. coli* MinE (EcMinE) were added to AtMinD1 ATPase assays in equimolar amounts (1 pmol). The activity of AtMinD1 was analysed visually through autoradiography and quantified using a phosphorimager. Addition of AtMinE1 led to a 3-fold increase in the ATPase activity of AtMinD1. EcMinE was however unable to stimulate the AtMinD1 activity. GST is provided as a control to the GST-tagged AtMinE1.

function as a topological specificity factor during *E. coli* cell division (Maple *et al.*, 2002) repeated experiments revealed that EcMinE was unable to stimulate AtMinD1 activity (Fig. 3.4). As before, ATPase assays were performed using only EcMinE demonstrating that purified EcMinE protein does not have any inherent ATPase activity (Fig. 3.4). These data, together with fact that in *E. coli* stimulation of ATP hydrolysis only occurs in the presence of phospholipids (Hu and Lutkenhaus, 2001) suggest functional divergence in the mechanism of AtMinE1-stimulated AtMinD1 ATP hydrolysis during plastid division in *Arabidopsis*.

3.2.3. *AtMinD1(K72A)* exhibits mis-localisation inside chloroplasts

AtMinD1 exhibits distinct intraplastidic localisation patterns localising into one or two discrete spots at the polar regions of ellipsoidal chloroplasts (Maple *et al.*, 2002; Fujiwara *et al.*, 2004). In contrast to this, the A296G mutation in AtMinD1/ARC11 results in mis-localisation in the form of either large and distorted fluorescent aggregates and/or multiple speckles (Fujiwara *et al.*, 2004). To test whether a mutation within the nucleotide binding motif of AtMinD1 affects its localisation, translational fusions of AtMinD1 and AtMinD1(K72A) to YFP were created and transiently expressed in tobacco leaves by particle bombardment (Kost *et al.*, 1998). Full-length *AtMinD1* and *AtMinD1(K72A)* cDNAs were PCR-amplified using primers MIND/1 (5'-TACTCGAGATGGCGTCTCTGAGATTGTTC-3' *Xho*I is underlined) and MIND/6 (5'-ATGGTACCGCCGCCAAAGAAAGAGAAGAAGCC-3' *Kpn*I is underlined), removing the termination codon and cloned into pWEN18 as N-terminal fusions to YFP to generate pWEN18/AtMinD1 and pWEN18/AtMinD1(K72A). pWEN18/AtMinD1 and pWEN18/AtMinD1(K72A) were transiently expressed in tobacco leaves by particle bombardment (Section 2.5.1) and expression of AtMinD-YFP and AtMinD(K72A)-YFP was visualised by fluorescence microscopy. The number of speckles per chloroplast and the number of chloroplasts of several bombardments were recorded. As expected, the majority of AtMinD1-YFP (75%) localised into one or two discrete spots (Fig. 3.5A) (Maple *et al.*, 2002; Fujiwara *et al.*, 2004). In contrast, AtMinD1(K72A)-YFP forms multiple speckles with often up to six or more fluorescent speckles within chloroplast (Fig. 3.5). Unlike the previously described mis-localisation of AtMinD1(A296G) (Fujiwara *et al.*, 2004), protein aggregation is rarely observed in chloroplasts expressing AtMinD1(K72A)-YFP (Fig. 3.5). Furthermore, the AtMinD1(K72A)-YFP fusion protein frequently forms more speckles per chloroplast than reported for AtMinD1(A296G)-GFP suggesting that the cause of mis-localisation is



B

Protein	Number of cells	Number of speckles per chloroplast							Number of chloroplasts
		0	1	2	3	4	5	>6	
AtMinD1	38	3 1.9%	49 31.4%	68 43.6%	13 8.3%	19 12.2%	2 1.3%	2 1.3%	205
AtMinD1 (K72A)	40	0 0%	2 0.9%	16 7.8%	28 13.7%	25 12.2%	28 13.7%	106 51.7%	156

Fig. 3. 5. Intraplasmidic localisation patterns of AtMinD1 and AtMinD1(K72A) YFP fusion proteins in living chloroplasts. (A) AtMinD1 forms one or two spots within the chloroplasts whilst AtMinD1(K72A) forms multiple speckles. (B) Quantitative data from a typical analysis of a single particle bombardment of a tobacco leaf shows significant difference in the number of spots per chloroplast between AtMinD1 and AtMinD1(K72A). Only chloroplasts in which the number of spots/speckles could be accurately counted are included and analysis for each bombardment used a range of cells. Scale bars = 5µm.

different for AtMinD1(K72A)-YFP and AtMinD1(A296G)-GFP. The multiple speckling of AtMinD1(K72A) in chloroplasts indicates that ATP binding/hydrolysis plays a major role in ensuring the correct intraplasmidic localisation of AtMinD1.

3.2.4. *AtMinD1(K72A)* can dimerise

Yeast two-hybrid assays and FRET analyses have demonstrated that AtMinD1 is able to interact with itself to form homodimers (Fujiwara *et al.*, 2004). In line with this *E. coli* MinD undergoes self assembly on phospholipid vesicles to form filamentous polymeric structures (Hu *et al.*, 2002). Both ARC11/AtMinD1(A296G) and AtMinD1(K72A) exhibit mis-localisation in *Arabidopsis* plastids and it has been previously shown that the ARC11/AtMinD1(A296G) mis-localisation is probably due to loss of dimerisation (Fujiwara *et al.*, 2004). To investigate whether the observed mis-localisation of AtMinD1(K72A) was due to loss of dimerisation, yeast two-hybrid interaction studies were performed using restoration of histidine auxotrophy as a marker for interaction. Full-length *AtMinD1* and *AtMinD1(K72A)* were PCR amplified using primers MIND/5 and MIND/7 and subsequently cloned into pGADT7 (MATCHMAKER Two-Hybrid System, version 3, Clontech Laboratories) as fusions to the C-terminus of the GAL4 activation domain (AD-AtMinD1 and AD-AtMinD1(K72A)) and also ligated into pGBKT7 (MATCHMAKER Two-Hybrid System, version 3, Clontech Laboratories) as fusion to the C-terminus of the GAL4 DNA-binding domain (BD-AtMinD1 and BD-AtMinD1(K72A)). The resulting constructs were expressed in HF7c cells which can only grow in the absence of His upon positive protein-protein interactions. In agreement with previous observations (Fujiwara *et al.*, 2004) His auxotrophy was found to be restored in cells co-expressing AD-AtMinD1 and BD-AtMinD1 (Figure 6A). Similarly, HF7c cells co-expressing AD-AtMinD1(K72A) and BD-AtMinD1 or AD-AtMinD1 and BD-AtMinD1(K72A) (Fig. 3.6A) showed restoration of His auxotrophy revealing that the AtMinD1 K72A mutation does not affect AtMinD1 dimerisation. As a negative control AD-ARC11/AtMinD1(A296G) (Fujiwara *et al.*, 2004) and BD-AtMinD1 and AD-AtMinD1 and BD-ARC11/AtMinD1(A296G) (Fujiwara *et al.*, 2004) (Fig. 3.6A) were co-expressed in HF7c cells which, as expected, showed no growth without His. To ensure that the interactions detected were not due to autoactivation, each construct was co-expressed with the empty vector controls and showed no restoration of His auxotrophy.

To verify AtMinD1(K72A) can dimerise inside living chloroplasts, bimolecular fluorescence complementation (BiFC) assays were carried out. For BiFC, YFP is split into two fragments. Non-fluorescent N-terminal (NY) and C-terminal (CY) YFP fragments are fused to proteins of interest. If interaction occurs between these proteins, YFP is reconstituted and a fluorescent signal is observed. To perform BiFC assays YFP was split into two halves as previously described (Hu *et al.*, 2002). The N-terminal half (NY) consists of amino acids 1–154 of YFP and the C-terminal half (CY) consists of amino acids 155–238. A (Gly₁₀) linker sequence was incorporated at the N-terminus of the two YFP halves and the subsequent fragments were cloned into the pWEN18 vector generating pWEN-NY and pWEN-CY (Maple *et al.*, 2005). Full length AtMinD1(K72A) cDNA was PCR-amplified using primers MIND/1 and MIND/6 and cloned into pWEN-NY as a fusion to the N-terminal fragment of YFP (containing amino acids 1-154 of YFP). The resulting construct pWEN-NY/AtMIND1(K72A) was co-bombarded into tobacco along with pWEN-CY/AtMIND1 (Maple *et al.*, 2005) (containing amino acids 155-238 of YFP). As previously observed (Maple *et al.*, 2005), tobacco co-bombarded with pWEN-NY/AtMinD1 and pWEN-CY/AtMinD1 showed clear fluorescence (Fig. 3.6B). Tobacco co-bombarded with pWEN-NY/AtMinD1(K72A) and pWEN-CY/AtMinD1 also showed clear fluorescence (Fig. 6B) demonstrating that AtMinD1(K72A) is able to dimerise *in planta* and confirming that AtMinD1(K72A) mis-localisation is not due to loss of dimerisation as is observed for ARC11/AtMinD1 (A296G). Tobacco cells bombarded with single vectors (negative controls) showed no fluorescence, as expected.

3.2.5 AtMinD1(K72A) is unable to interact with AtMinE1

The MinE binding site in *E. coli* MinD is in close proximity to the ATP binding site on α -helix 7 (Ma *et al.*, 2004) and lysine 11 within the Walker A motif (equivalent to AtMinD1 lysine 67) interacts with residues within α -helix 7 competing with MinE (Ma *et al.*, 2004). This suggests that the *E. coli* MinD Walker A motif is involved in mediating MinD-MinE interaction (Ma *et al.*, 2004). To test whether the K72A mutation in AtMinD1 affects interaction with AtMinE1; AD-AtMinE1 and BD-AtMinE1 fusion proteins (Maple *et al.*, 2005) were co-expressed with BD-AtMinD1(K72A) and AD- AtMinD1(K72A) respectively in HF7c cells. In contrast to yeast cells co-expressing AD-AtMinE1 and BD-AtMinD1 or AD-AtMinD1 and BD-AtMinE1 (Figure 3.6A) showing growth on His-free media, HF7c cells co-expressing AD-AtMinE1 and BD-AtMinD1(K72A) or AD-AtMinD1(K72A) and BD-AtMinE1

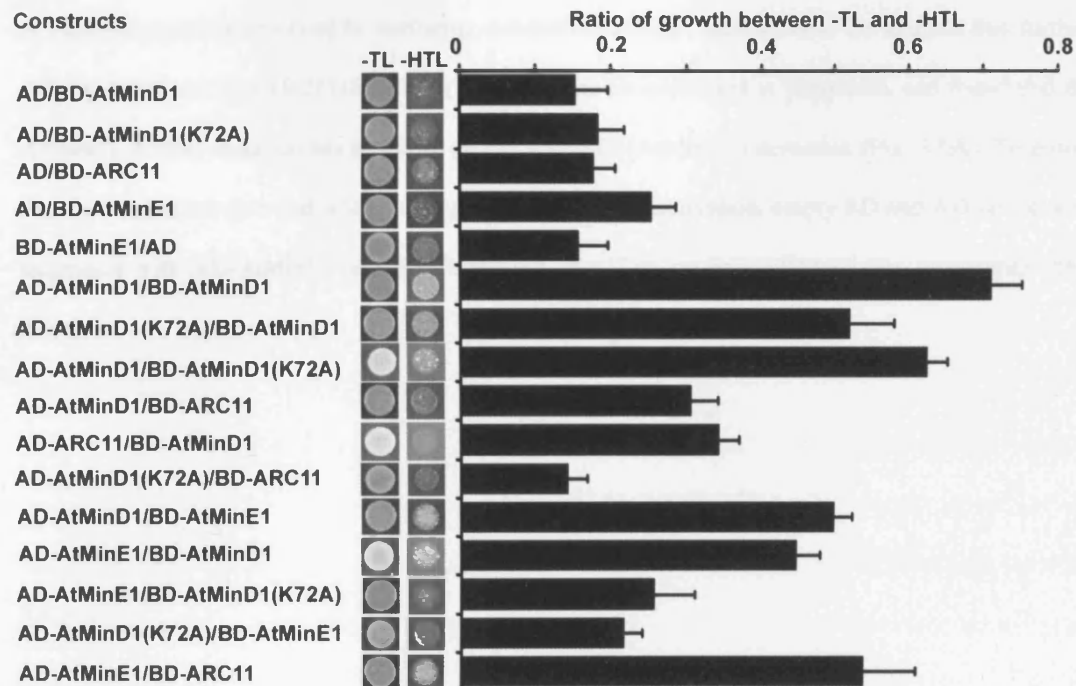
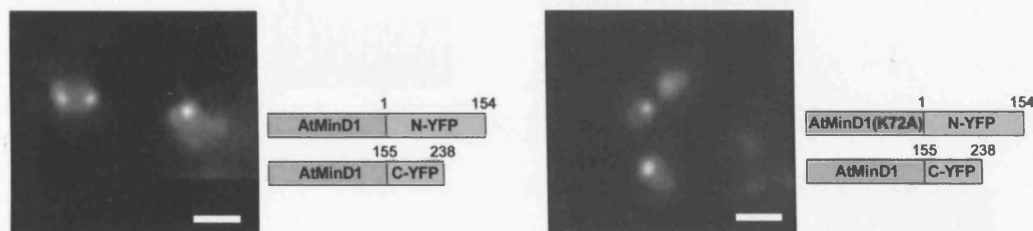
A**B**

Fig. 3. 6. Interactions of AtMinD1(K72A). (A) Yeast two-hybrid analysis of AtMinD1(K72A), AtMinD1 and AtMinE1 interactions. HF7c yeast cells were co-transformed with different vector combinations. Co-transformed HF7c colonies were grown overnight and spotted onto plates containing SD – Tryptophan and Leucine (SD-TL) and plates containing SD – Tryptophan, Leucine, and Histidine (SD-HTL). Interaction was determined by restoration of Histidine (H) auxotrophy and quantitative analysis based on the ratio of growth between growth on SD-TL and SD-HTL gives relative strength of interaction. (B) Bimolecular fluorescence complementation in living chloroplasts showing that both AtMinD1 and AtMinD1(K72A) can dimerize. Scale bar, 5µm.

showed no restoration of His auxotrophy (Fig. 3.6A) demonstrating that the K72A mutation in AtMinD1 abolishes AtMinD1 interaction with AtMinE1. This result suggests that the AtMinD1 Walker A motif is probably involved in mediating AtMinD1/AtMinE1 interactions. To analyse this further, AD-AtMinE1 and BD-ARC11/AtMinD1(A296G) were co-expressed in yeast cells and found that the AtMinD1 A296G mutation has no effect on the AtMinD1/AtMinE1 interaction (Fig. 3.6A). To ensure that the interactions detected were not due to AtMinE1 autoactivation, empty BD and AD vector were expressed with AD-AtMinE1 and BD-AtMinE1, revealing no restoration of His auxotrophy (Fig. 3.6A).

3.3. Discussion

The importance of AtMinD1 in plastid division has come from studies demonstrating that a disequilibrium of AtMinD1 levels in transgenic plants results in Z-ring misplacement and inappropriate plastid division (Colletti *et al.*, 2000; Dinkins *et al.*, 2001). Although little is known how AtMinD1 ensures correct Z-ring placement, through the cloning of the disrupted locus in *arc11*, it has been reported that AtMinD1 dimerisation is important for correct interplastidic localisation and central Z-ring positioning during plastid division (Fujiwara *et al.*, 2004).

3.3.1. *AtMinD1 is an ATPase*

AtMinD1 ATP hydrolysis is mediated through the Walker A domain (Fig. 3.1) as a K72A mutation within this motif leads to a complete loss of ATPase activity (Fig. 3.1C). The high K_m and low V_{max} values show that AtMinD1 is a weak ATPase, like its bacterial homolog (de Boer *et al.*, 1991) and the MinD-related protein ParA (Bouet and Funnell, 1999). The weak activity exhibited by AtMinD1 may be due to electrostatic properties of the ATP binding site. In the F_1 ATPase (Abrahams *et al.*, 1994) and in hydrolases (Coleman *et al.*, 1994) basic amino acids near the ATP γ -phosphate are responsible for stabilization of the transition state negative charge (Hayashi *et al.*, 2001) and both *E. coli* MinD and AtMinD1 lack these basic amino acids possibly explaining the weak ATP turnover. The low basal activity may however be an important feature of AtMinD1 mode of action as in *E. coli*, MinD membrane dissociation only occurs after ATPase activity stimulation by MinE and this plays an essential role in the MinCDE oscillatory cycle (Hu and Lutkenhaus, 2001; Hu *et al.*, 20002). Correspondingly ATP binding promotes MinD membrane binding (Hu and Lutkenhaus., 2002). Although AtMinD1 and AtMinE1 oscillatory behaviour has not been reported it is probable, based on the evolutionary conservation of the division machinery, that a similar mechanism occurs during plastid division.

3.3.2. *EcMinD and AtMinD1 exhibit functional differences*

Although *E. coli* MinD and AtMinD1 show a high degree of similarity at the amino acid level this study has found significant differences in the functioning of the two proteins, Firstly a difference in cation dependence of ATPase activity between Ca^{2+} -dependant AtMinD1 and Mg^{2+} -dependant *E. coli* MinD implies an important functional difference, probably signifying evolutionary adaptation as many

plant processes are regulated by calcium. Indeed studies have suggested a regulatory role for plastidic Ca^{2+} fluxes (Sai and Johnson, 2002) therefore it is possible plastidic Ca^{2+} levels regulate AtMinD1 activity during plastid division. However, the level of Ca^{2+} used in this study is above the physiological Ca^{2+} levels present in the chloroplasts (Sai and Johnson, 2002). Therefore it would be interesting to investigate whether physiological levels of Ca^{2+} , particularly during Ca^{2+} fluxes, would differentially affect the ATPase activity of AtMinD1. Secondly, while it has been demonstrated that AtMinE1 stimulates the activity of AtMinD1, as occurs between MinE and MinD in the *E. coli* system (Hu and Lutkenhaus, 2001), stimulation by AtMinE1 can occur independently of membrane binding (Fig 3.4) in contrast to the phospholipid-dependent MinE stimulation of *E. coli* MinD (de Boer *et al.*, 1991). This suggests functional divergence in the mechanism of AtMinE1-stimulated AtMinD1 ATP hydrolysis during plastid division in *Arabidopsis* compared to *E. coli* division. In *E. coli*, a 10-fold increase in MinD ATPase activity is observed when incubated with MinE and phospholipid vesicles (Hu and Lutkenhaus, 2001). AtMinE1 stimulates AtMinD1 ATPase activity in the absence of chloroplast envelope membranes, however only a 3-fold increase in ATPase activity is observed (Fig. 3.4). It is unlikely that the reduced fold change is due to insufficient AtMinE1 to achieve maximal ATPase activity as the ratio of AtMinD1:AtMinE1 used in the assays was 1:1 which is the same ratio used in experiments in *E. coli* that produced the 10-fold increase in ATPase activity (Hu and Lutkenhaus, 2001). In *E. coli*, maximal ATPase stimulation occurs at a 1:1 ratio of MinD:MinE (Suefuji *et al.*, 2002) and this is above the reported 1:0.7 ratio of MinD:MinE molecules in *E. coli* cells (Shih *et al.*, 2002). Therefore it seems likely that increased ATPase stimulation would be observed if AtMinD1 were bound to chloroplast membranes. Although AtMinD1 membrane binding has not been demonstrated, the localisation of AtMinD1 to the periphery of the chloroplast suggest that like *E. coli* MinD, AtMinD1 is a peripheral membrane protein (Hu and Lutkenhaus, 2001; Hu *et al.*, 2002; Fujiwara *et al.*, 2004). *E. coli* MinD membrane localisation is mediated by a C-terminal motif termed the Membrane-Targeting Sequence (MTS) (Szeto *et al.*, 2002; Hu and Lutkenhaus, 2003). The MTS is conserved across MinD proteins from eubacteria, archaea and chloroplasts (Szeto *et al.*, 2002) therefore it is probable that AtMinD1 does bind the chloroplast envelope. Although homology between MinD proteins across different species is high much more variation is found between MinE proteins. Purified MinE from *E. coli* is unable to stimulate AtMinD1 ATPase activity *in vitro* (Fig. 3.4) further indicating

that at least in part the mechanism of AtMinE1-stimulated AtMinD1 activity is different from that in prokaryotes.

3.3.3. *AtMinD1* ATPase activity is required for correct localisation

In *E. coli*, the active site MinD(K16Q) mutant exhibits mis-localisation: Wild-type MinD localises to the cell periphery whilst MinD(K16Q) is distributed throughout the cell (Hu *et al.*, 2002). MinD(K16Q) is however still able to bind ATP but can not bind phospholipids (Hu *et al.*, 2002) or interact with MinC (Hu and Lutkenhaus, 2003). Experiments have not been performed to test if MinD(K16Q) can interact with MinE. In agreement with the mis-localisation of MinD(K16Q) we show that the active site AtMinD1(K72A) mutant exhibits aberrant localisation patterns, AtMinD1(K72A) is distributed throughout plastids (Fig. 3.5). This mis-localisation is not due to loss of AtMinD1 dimerisation (Fig. 3.6) as observed for ARC11 (Fujiwara *et al.*, 2004) but may be due to lack of interaction with AtMinE1. Several studies in *E. coli* have shown that the formation of MinD polar zones is MinE-dependant (Raskin and de Boer, 1999; Hu and Lutkenhaus, 2001) and MinE mutations that cannot interact with MinD exhibit aberrant MinD localisation patterns (Ma *et al.*, 2003). Since AtMinD1(K72A) cannot interact with AtMinE1 it is likely that loss of interaction with AtMinE1 is the cause of the mis-localisation of AtMinD1(K72A) (Fig. 3.6A). The loss of interaction between AtMinD1(K72A) and AtMinE1 may either be because lysine 72 of AtMinD1 is directly involved in interaction with AtMinE1 or because AtMinD1(K72A) is unable to adopt the correct conformation upon binding ATP necessary for AtMinE1 interaction. In *E. coli*, two domains of MinE have been recognised; an N-terminal Anti-MinCD domain (AMD) and a C-terminal Topological Specificity Domain (TSD) (Pichoff *et al.*, 1995; Zhao *et al.*, 1995). The α -helical region of the MinE AMD interacts with MinD α -helix 7 forming a coiled-coil structure (Ma *et al.*, 2003; Ma *et al.*, 2004) and Lysine 11 within the Walker A region (P-loop) competes with MinE for residues within α -helix 7 (Ma *et al.*, 2004). MinE-mediated disruption of the non-covalent interaction between lysine 11 and α -helix 7 changes the lysine 11 side-chain orientation and the P-loop conformation and this transmits an activation signal to the neighbouring catalytic domain or to the bound ATP bringing about ATP hydrolysis (Ma *et al.*, 2004). This model suggests MinE stimulation is through conformational change in the Walker A motif rather than through direct interaction between MinE and Walker A residues. Based on this model it is unlikely that AtMinE1 interacts directly with the Walker A motif and we

favour that a Walker A mutation in AtMinD1 changes the overall conformation ultimately disabling its interaction with AtMinE1. The mis-localisation of AtMinD1(K72A) could also be due to an inability to bind the membrane, however further experimentation needs to be performed to confirm AtMinD1 does bind the chloroplast envelope and to investigate membrane binding of AtMinD1(K72A).

3.3.4. Conclusion

This study has revealed the importance of the biochemical activity of AtMinD1 and demonstrates that the topological specificity factor AtMinE1 modulates both AtMinD1 activity and AtMinD1 localisation dynamics. This study demonstrates that AtMinD1, in contrast to its bacterial counterpart, is a Ca²⁺-dependent ATPase and that the Walker A motif is important for both ATPase activity and correct intraplastidic localisation. Although an active site AtMinD1 mutant can still dimerise, loss of ATPase activity abolishes its interaction with AtMinE1. Together with the fact that AtMinE1 can stimulate the ATPase activity of AtMinD1 this data suggests that AtMinE1 not only modulates ATP hydrolysis but ensures correct AtMinD1 localisation within plastids during division.

Based on this data a working model for AtMinD1 mode of action during plastid division in *Arabidopsis* is proposed (Fig 3.7). In this model, AtMinD1 undergoes dimerisation and binds ATP; this AtMinD1 dimer complex exhibits low basal Ca²⁺-dependent ATPase activity. AtMinD1 then interacts with AtMinE1 stimulating ATP hydrolysis. How does this impinge on the function of AtMinD1 in ensuring the correct placement of the Z-ring? In line with the prokaryotic model, dimerised ATP-bound AtMinD1 may bind to the chloroplast envelope before AtMinE1 interaction, which stimulates ATP hydrolysis, membrane release followed by protein relocation. However, in contrast to *E. coli*, AtMinE1 can stimulate ATP hydrolysis in the absence of envelope lipids therefore AtMinE1 can enhance AtMinD1 activity prior to envelope binding. In addition, plants do not harbour MinC. A recent study has suggested that ARC3 may carry out a role similar to MinC (Maple *et al.*, In Press) however the ARC3 mode of action is different from MinC, also suggesting that AtMinD1 and AtMinE1 mode of actions differs from that in prokaryotes. Through this data together with the fact that AtMinD1 is dependent on Ca²⁺ and not Mg²⁺ it is clear that AtMinD1 has evolved at the biochemical and cell biological level presumably to adapt from being part of a cell division machinery in free-living prokaryotes to becoming an integral component of the plastid division machinery in higher plants.

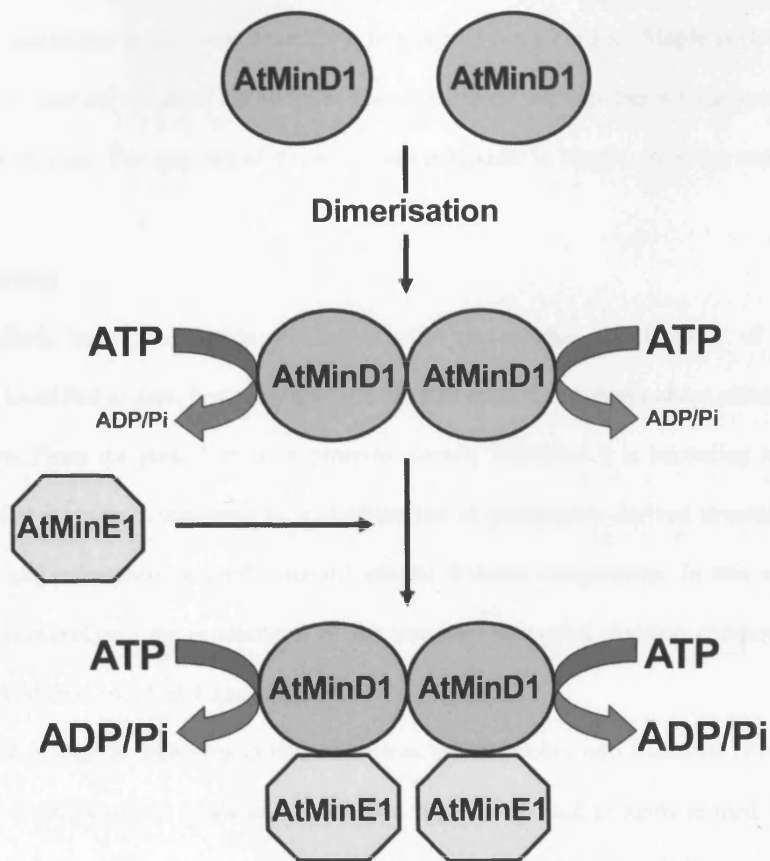


Fig. 3. 7. A working model for AtMinD1 mode of action during plastid division. AtMinD1 dimerises and binds ATP followed by recruitment of AtMinE1 which stimulates AtMinD1-mediated ATP hydrolysis. ATP hydrolysis by AtMinD1 is dependent on Ca^{2+} .

4. Interaction analysis of stromal plastid division proteins

The work performed in this chapter was carried out in collaboration with Jodi Maple, a PhD student/postdoctoral researcher in the same laboratory. In this collaboration Jodi Maple performed the cloning of the vectors, I carried out all of the biolistic transformations and together we analysed the localisation of the fusion proteins. The majority of this work was published in Maple, Aldridge and Møller, 2005.

4.1. Introduction

Although efforts have been made to individually characterise the handful of plastid division components identified to date, how they cooperate with each other to bring about chloroplast division is still unknown. From the plastid division proteins already identified it is becoming increasingly clear that chloroplast division is mediated by a combination of prokaryotic-derived stromal plastid division components and eukaryotic-derived cytosolic plastid division components. In this study it has been undertaken to investigate the interactions of the stromal chloroplast division components AtFtsZ1-1, AtFtsZ2-1, AtMinD1, AtMinE1 and ARC6.

FtsZ is a tubulin-like protein that undergoes self assembly into filaments (Rivas *et al.*, 2000). *Arabidopsis* and other plant genomes contain two families of FtsZ proteins termed FtsZ1 and FtsZ2 (Osteryoung *et al.*, 1998; Osteryoung and McAndrew, 2001; Stokes and Osteryoung, 2003). FtsZ proteins share high homology to each other although there are some conserved differences in amino acid sequences between the two families. Most notable of these differences is the presence or absence of a short peptide at the C-terminus called the core domain that is required in *E. coli* FtsZ for direct interactions with ZipA and FtsA (Wang *et al.*, 1997; Din *et al.*, 1998; Liu *et al.*, 1999; Hale *et al.*, 2000; Mosyak *et al.*, 2000; Yan *et al.*, 2000), proteins believed to be involved in anchoring and stabilising the FtsZ ring. The core domain is present in proteins belonging to the FtsZ2 family but absent in proteins from the FtsZ1 family (Stokes and Osteryoung, 2003). FtsZ is a critical player in chloroplast division; polymerisation of FtsZ proteins into the Z-ring is probably the initial step in chloroplast division (Miyagishima *et al.*, 2001c) and perturbations in the level of FtsZ protein from either family leads to inhibition of chloroplast division (Osteryoung *et al.*, 1998).

AtMinD1 and AtMinE1 are involved in the correct placement of the Z-ring to ensure symmetrical division of the chloroplast. AtMinD1 is a Ca²⁺-dependent ATPase stimulated by the topological specificity factor AtMinE1 (see Chapter 3; Aldridge and Møller, 2005). Studies have

shown that over-expression of AtMinD1 leads to chloroplast division inhibition and deficiency of AtMinD1 leads to asymmetric plastid division and subsequent heterogeneity in chloroplast size (Colletti *et al.*, 2000; Dinkins *et al.*, 2001; Fujiwara *et al.*, 2004). The *arc11* mutant contains a single missense mutation in *AtMinD1* (Fujiwara *et al.*, 2004). The chloroplasts of *arc11* are enlarged, irregularly shaped and have multiple constrictions placed randomly along the axis of the chloroplast, strong evidence that AtMinD1 is involved in the correct placement of the chloroplast division apparatus (Fujiwara *et al.*, 2004). AtMinE1 has also been shown to be involved division site selection; overexpression of AtMinE1 causes asymmetric division events and chloroplast size heterogeneity (Itoh *et al.*, 2001; Maple *et al.*, 2002; Reddy *et al.*, 2002). In *E. coli*, overexpression of MinD or deficiency of MinE leads to inhibition of cell division and subsequent filamentation whereas a deficiency of MinD or overexpression of MinE leads to asymmetric cell division and minicelling (de Boer *et al.*, 1989). The similarity between the phenotypes of the *E. coli* Min mutants and the *Arabidopsis* Min mutants suggests that the *Arabidopsis* Min proteins are functional homologues of the *E. coli* Min proteins. Indeed it has been demonstrated that *Arabidopsis* Min proteins and *E. coli* Min proteins act as functional substitutes for each other (Maple *et al.*, 2002; Tavva *et al.*, 2005). Due to the similarity of the *E. coli* and *Arabidopsis* Min proteins, the more well characterised behaviour of the *E. coli* Min proteins has been used as a paradigm for the functioning of the *Arabidopsis* Min proteins. In *E. coli*, the *minB* operon encodes MinC, MinD and MinE which function together to ensure Z-ring placement at midcell (de Boer *et al.*, 1989; Bi and Lutkenhaus, 1993; Pichoff and Lutkenhaus, 2001). MinC is an antagonist of FtsZ polymerisation (Bi and Lutkenhaus, 1993; Pichoff and Lutkenhaus, 2001), MinD activates and directs MinC to the membrane (Szeto *et al.*, 2002; Hu and Lutkenhaus, 2003; Zhou and Lutkenhaus, 2004) and MinE confers topological specificity on the MinC/MinD inhibitor through interaction with MinD (Hu and Lutkenhaus, 2001; Hale *et al.*, 2001; Hu *et al.*, 2002). Most of the analysis of the *Arabidopsis* Min proteins lends support to the use of the bacteria paradigm however despite extensive homology searches a MinC homologue has not been identified. A recent study has suggested that ARC3 may fill the role of a MinC protein in *Arabidopsis* (Maple *et al.*, In Press). ARC3 has been shown to interact with AtMinD1, AtMinD1 and AtFtsZ1-1 (Maple *et al.*, In Press) and therefore it is likely that ARC3 provides the bridge between the Min proteins and the Z-ring that is fulfilled by MinC in *E. coli*.

ARC6 plants contain two greatly enlarged chloroplasts per mesophyll cell (Pyke *et al.*, 1994; Robertson *et al.*, 1995; Vitha *et al.*, 2003). *arc6* is a homologue of the cyanobacterial *Ftn2* gene and homologues of *ARC6* are found only in plants and cyanobacteria (Vitha *et al.*, 2003). *ARC6* contains a putative J domain (Vitha *et al.*, 2003) characteristic of DnaJ cochaperones. DnaJ proteins deliver polypeptide substrates to Hsp70 chaperones and also regulate chaperone activity via interaction of the J domain with a Hsp70 partner (reviewed in Walter and Buchner, 2002). Studies suggest a function for *ARC6* in the stabilization of the Z-ring as *arc6* chloroplasts contain numerous short FtsZ filaments and lack Z-rings (Vitha *et al.*, 2003). Conversely, transgenic *Arabidopsis* overexpressing *ARC6* have enlarged chloroplasts and excessive FtsZ filament formation (Vitha *et al.*, 2003).

To investigate how AtFtsZ1-1, AtFtsZ2-1, AtMinD1, AtMinE1 and *ARC6* cooperate, interaction analysis was undertaken to see how these proteins function together during plastid division. Initially co-localisation experiments were performed to investigate which proteins shared the same localisation pattern and are therefore likely to interact. Interactions were then confirmed by Bi-molecular Fluorescence Complementation (BiFC) assays.

4.2. Results

4.2.1. Co-localisation of *Arabidopsis* Min proteins

Although the localisation patterns of AtMinD1 and AtMinE1 has previously been described (Maple *et al.*, 2002; Fujiwara *et al.*, 2004) the patterns described have been slightly different; AtMinD1 localises to a single spot or two spots at opposite ends of the chloroplast (Maple *et al.*, 2002; Fujiwara *et al.*, 2004) and AtMinE1 is observed as a single spot or as two spots in close proximity towards one pole of the chloroplast (Maple *et al.*, 2002). To investigate the localisation of both AtMinE1 and AtMinD1 simultaneously, combinations of plasmids containing fusions of AtMinD1/AtMinE1 to YFP/CFP (pWEN18 for YFP and pWEN15 for CFP) were created. *AtMinD1* cDNA was amplified using a proof-reading polymerase and the primers MIND/1 (5'-TACTCGAGATGGCGTCTCTGAGATTGTTC-3' *Xho*1 is underlined) and MIND/6 (5'-ATGGTACCGCCGCCAAAGAAAGAGAAGAAGCC-3' *Kpn*1 is underlined) removing the termination codon and cloned into pPCR-Script creating pPCR-Script/AtMinD1. *AtMinE1* cDNA was also amplified using a proof-reading polymerase and the primers MinE/1 (5'-TACTCGAGATGGCGATG TCTTCTGGAAC-3' *Xho*1 is underlined) and MinE/3 (5'-ATGGTACCCTCTGGAACATAAAAAATCG-3' *Kpn*1 is underlined) also removing the termination codon and the amplified fragment was cloned into pPCR-Script creating pPCR-Script/AtMinE1. *AtMinD1* and *AtMinE1* were subsequently subcloned into the *Xho*1 and *Kpn*1 sites of pWEN18 and pWEN15 (Kost *et al.*, 1998) as N-terminal fusions to YFP or CFP to generate pWEN18/AtMinE1, pWEN18/AtMinD1, pWEN15/AtMinE1 and pWEN15/AtMinD1 (Maple *et al.*, 2005). These constructs were introduced into tobacco leaf cells by particle bombardment as described in Section 2.5.1. Tobacco leaves were used instead of *Arabidopsis* since experimentation had shown that tobacco leaves were more agreeable to particle bombardment. Studies in which tobacco has been used as a substitute for *Arabidopsis* to investigate plastid division components have demonstrated that *Arabidopsis* plastid division components behave identically in both tobacco and *Arabidopsis* (Dinkins *et al.*, 2001; Reddy *et al.*, 2002; Maple *et al.*, 2002; Fujiwara *et al.*, 2004). In cells expressing both AtMinD1-YFP and AtMinD1-CFP, fluorescence was detected as one or two co-localised spot(s) inside the chloroplast (Fig. 1). AtMinE1-YFP and AtMinE1-CFP fluorescence was detected as either a single spot at one end of chloroplasts or as two spots in close proximity at one pole of the chloroplast (Fig. 1), for either pattern co-localisation of both AtMinE1-YFP and AtMinE1-CFP was always observed. Cells expressing both AtMinD1-YFP and AtMinE1-CFP also exhibited tight co-localisation. In 65% of

chloroplasts expressing both fusion proteins a single spot in close proximity to the membrane was observed (Fig. 1). The remaining 35% of the chloroplasts analysed had two spots, of these, 60% had spots at opposite poles of the chloroplast and 40% had two spots in close proximity at one pole of the chloroplast. The co-localisation of the Min proteins implies that AtMinD1 and AtMinE1 not only form homodimers or homo-oligomers but are also capable of interacting with each other.

4.2.2. *AtMinD1 and AtMinE1 interact*

To confirm the interaction between AtMinD1 and AtMinE1, Bi-molecular Fluorescence Complementation (BiFC) (Hu *et al.*, 2002) assays were used. *AtMinD1* and *AtMinE1* from pPCR-Script/*AtMinD1* and pPCR-Script/*AtMinE1* were subcloned into the *XhoI* and *KpnI* sites of the pWEN-NY and pWEN-CY vectors (see Chapter 3) creating fusions to the N-terminus of the N-terminal half and the C-terminal half of YFP fragments generating pWEN-NY/*AtMinE1*, pWEN-NY/*AtMinD1*, pWEN-CY/*AtMinE1* and pWEN-CY/*AtMinD1* (Maple *et al.*, 2005). These constructs were expressed in tobacco leaf cells through particle bombardment and reconstitution of YFP was analysed by epifluorescence microscopy.

In cell expressing both *AtMinD1*-NY and *AtMinD1*-CY a fluorescent signal was observed with a localisation pattern indistinguishable to the localisation of *AtMinD1* fused to full-length YFP signifying *AtMinD1* can form homodimers (Fig. 4.1). Similarly, a fluorescent signal is observed in cells expressing *AtMinE1*-NY and *AtMinE1*-CY demonstrating *AtMinE1* forms homodimers (Fig.4.1). In cells expressing *AtMinD1*-NY and *AtMinE1*-CY or *AtMinE1*-NY and *AtMinD1*-CY a fluorescent signal is also observed confirming that *AtMinE1* and *AtMinD1* also interact with each other (Fig. 4.1).

4.2.3. *Interaction of Arabidopsis FtsZ proteins*

To investigate the localisation of FtsZ proteins a protein from each family (FtsZ1 or FtsZ2) was chosen. This study used *AtFtsZ1*-1 and *AtFtsZ2*-1 in co-localisation analysis. As with the Min proteins, the FtsZ proteins were fused to both YFP and CFP. *FtsZ1*-1 cDNA was amplified using the primers *FtsZ/4* (5'-ATCTCGAGATGGCGATAATTCCGTTAGC-3' *XhoI* is underlined) and *FtsZ/6* (5'-ATGGTACCGAAGAAAAGTCTACGGGGAGAAGACG-3' *KpnI* is underlined) removing the termination codon and the amplified fragment was cloned into pPCR-Script creating pPCR-Script/*AtFtsZ1*-1.

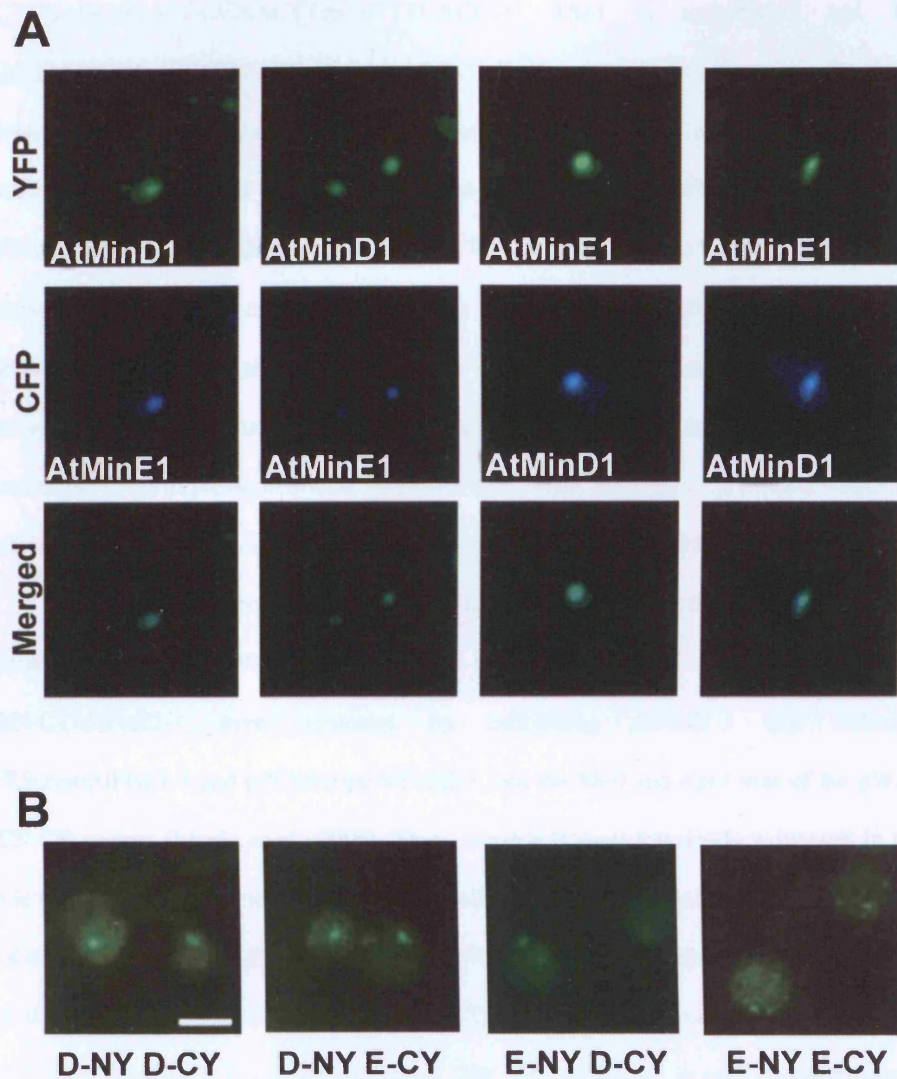


Fig. 4. 1. *Arabidopsis* Min proteins interact. (A) Co-localisation analysis of AtMinD1 and AtMinE1. Fusions of AtMinE1 and AtMinD1 to YFP or CFP were transiently expressed in tobacco leaf epidermal cells by particle bombardment. YFP and CFP were detected by epifluorescence microscopy. The green colour of the merged image indicates co-localisation. (B) BiFC assays were performed to confirm interactions. D-NY= AtMinD1 fused to the N-terminal fragment of YFP, D-CY= AtMinD1 fused to the C-terminal fragment of YFP, E-NY= AtMinE1 fused to YFP N-terminal and E-CY = AtMinE1 fused to YFP C-terminal. Fusions to YFP fragments were co-expressed in all possible combinations. Fluorescence of the reconstituted YFP signifies interaction. Scale bar = 5 μ m. This work was carried out in collaboration with Jodi Maple (Maple, Aldridge and Møller, 2005).

AtFtsZ1-1 cDNA was amplified using the primers FtsZ/14 (5'-ATCTCGAGCATATGGCAACTTACGTTTCACC-3' *Xho*I is underlined) and FtsZ/3 (5'-ATGGTACCGACTCGGGGATAACGAGAGC-3' *Kpn*I is underlined) also removing the termination codon and was subsequently cloned into pPCR-Script creating pPCR-Script/AtFtsZ2-1. AtFtsZ1-1 and AtFtsZ2-1 were subcloned into the *Xho*I and *Kpn*I sites of pWEN18 and pWEN15 creating pWEN18/AtFtsZ1-1, pWEN18/AtFtsZ2-1, pWEN15/AtFtsZ1-1 and pWEN15/AtFtsZ2-1. These constructs were transiently expressed in tobacco leaf cells using particle bombardment. All possible combinations of plasmids were used. For each combination of plasmids, tight co-localisation was observed inferring that AtFtsZ1-1 and AtFtsZ2-1 form both homodimers and heterodimers (Fig. 4.2). These results confirm previous double immunofluorescence labelling experiments which reported co-localisation of the FtsZ proteins (McAndrew *et al.*, 2001; Vitha *et al.*, 2001).

As with the Min proteins, BiFC assays were used to confirm the interactions indicated by co-localisation. Constructs pWEN-NY/AtFtsZ1-1, pWEN-NY/AtFtsZ2-1, pWEN-CY/AtFtsZ1-1, and pWEN-CY/AtFtsZ2-1 were generated by subcloning *AtFtsZ1-1* and *AtFtsZ2-1* from pPCRScript/AtFtsZ1-1 and pPCRScript/AtFtsZ2-1 into the *Xho*I and *Kpn*I sites of the pWEN-NY and pWEN-CY vectors (Maple *et al.*, 2005). These constructs were transiently expressed in tobacco leaf cells in all combinations. In tobacco mesophyll cells expressing both AtFtsZ1-1-NY and AtFtsZ1-1-CY or AtFtsZ2-1-NY and AtFtsZ2-1-CY, rings of YFP fluorescence, indistinguishable from those observed when the FtsZ proteins are fused to full-length YFP protein were observed, confirming FtsZ1-1 and FtsZ2-1 form homodimers or homo-oligomers (Fig. 4.2). Similarly, in cells co-expressing AtFtsZ1-1-NY and AtFtsZ2-1-CY or AtFtsZ2-1-NY and AtFtsZ1-1-CY rings of YFP fluorescence were observed (Fig. 4.2) demonstrating that AtFtsZ1-1 and AtFtsZ2-1 can form heterodimers as well as homodimers.

4.2.4. FtsZ proteins co-localise outside of a normal ring structure

In FtsZ co-localisation studies, FtsZ proteins formed clear Z-ring structures in 60-70% of the chloroplasts analysed. In the remaining 30-40% of chloroplasts, several different structures were observed, including long filaments, wheel-like structures and spots as well as rings. Similar structures have been previously observed and are believed to represent an artefact of FtsZ overexpression (Kießling *et al.*, 2000). Although in these structures the normal Z-ring assembly of the FtsZ proteins is perturbed, for each combination of FtsZ proteins analysed, tight co-localisation was always observed

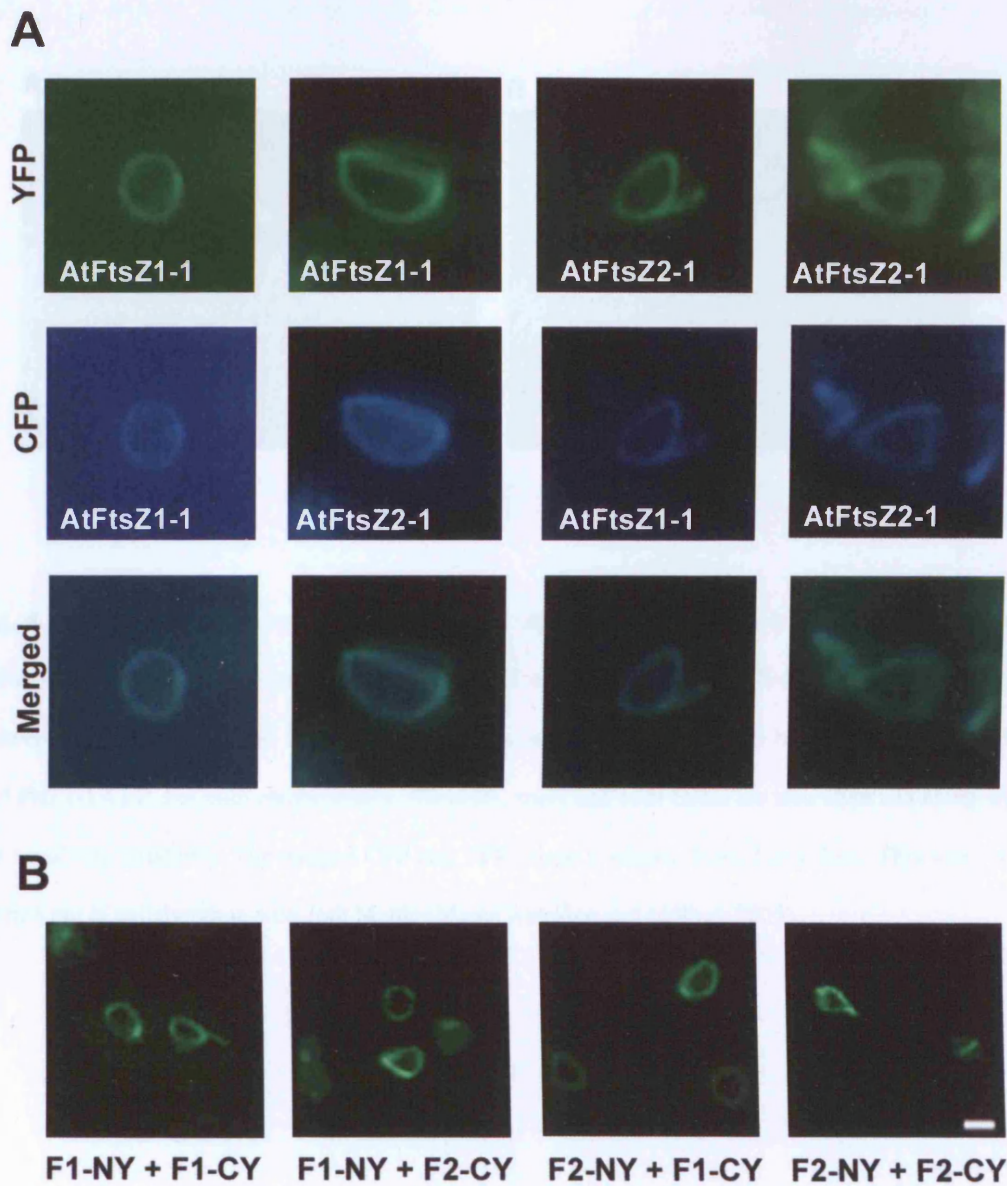


Fig. 4. 2. *Arabidopsis* FtsZ proteins can form both homodimers and heterodimers. (A) Fusions of FtsZ1-1 and FtsZ2-1 to YFP or CFP were co-expressed in tobacco leaf epidermal cells in all combinations. YFP and CFP were detected by epifluorescence microscopy. The green colour in the merged image indicates co-localisation. (B) BiFC assays were performed to confirm interactions. Fusions of AtFtsZ1-1 (F1) or AtFtsZ2-1 (F2) fused to the N-terminal (NY) or C-terminal (CY) fragment of YFP were co-expressed in leaf epidermal cells. Fluorescence of the reconstituted YFP indicates interaction. Scale bar = 5µm. This work was carried out in collaboration with Jodi Maple (Maple, Aldridge and Møller, 2005)

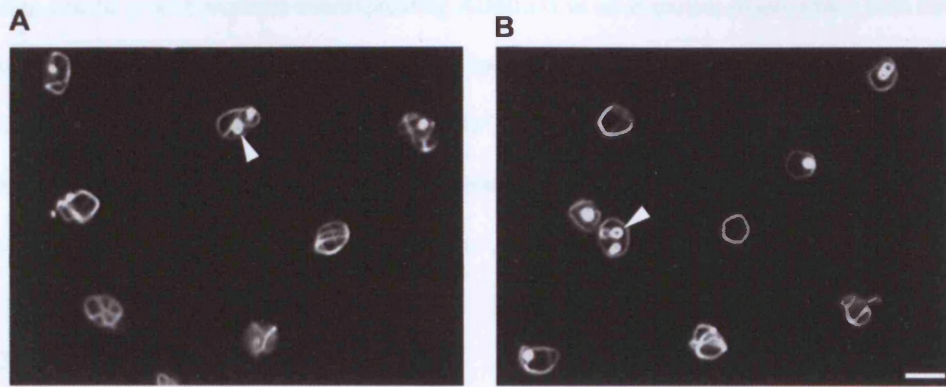


Fig. 4. 3. FtsZ proteins co-localise even when the structure of the Z-ring is perturbed. FtsZ fusion proteins to YFP and CFP were co-expressed in leaf epidermal cells. (A) Co-localisation is exhibited between AtFtsZ1-1-YFP and FtsZ2-1-CFP. (B) Co-localisation is observed between AtFtsZ2-1-YFP and FtsZ1-1-CFP. For both combinations, filaments, spots and mini circles are also observed along with the usual ring structures. The merged CFP and YFP image is shown. Scale bar = 5 μ m. This work was carried out in collaboration with Jodi Maple (Maple Aldridge and Møller., 2005).

(Fig. 4.3). This data agrees with previous observations of FtsZ co-localisation in plants with perturbed Z-ring structure, such as plants overexpressing AtMinD1 or *arc6* mutant plants which both have highly fragmented FtsZ filaments (Vitha *et al.*, 2003). Interestingly small 'mini circles' of FtsZ are observed in cells highly expressing FtsZ proteins (Fig. 4.3). These mini circles appear to have no contact with the chloroplast envelope suggesting that polymerisation of FtsZ into ring structures does not require anchorage to the envelope membranes.

4.2.5. ARC6 co-localises with the Z-ring

It has been previously reported that ARC6 localises to a ring structure at the chloroplast division site, similar to the localisation of FtsZ1 and FtsZ2 (Vitha *et al.*, 2003). Because *arc6* mutants only have numerous short FtsZ filaments and lack Z-rings, a role for ARC6 in the stabilisation of the Z-ring was suggested (Vitha *et al.*, 2003). In order to investigate whether ARC6 and FtsZ co-localise, ARC6 fused to YFP (pWEN18/ARC6 (Maple *et al.*, 2005)) was co-expressed with either AtFtsZ1-1-CFP or AtFtsZ2-1-CFP. ARC6 cDNA was amplified using the primers ARC6/4 (5'-ATGTCGACATGGAAGCTCTGAGTCACGTCGG-3' *Sall* is underlined) and ARC6/5 (5'-ATGGTACCTGSTGCAAGAAGAGGCC-3' *KpnI* is underlined) and cloned into pPCR-Script creating pPCR-Script/ARC6. ARC6 was subcloned into the *XhoI* and *KpnI* sites of pWEN18.

In cells expressing ARC6-YFP and FtsZ2-1-CFP, tight co-localisation of ARC6 with AtFtsZ2-1 was observed (Fig. 4.4). In 70% of chloroplasts expressing both ARC6-YFP and AtFtsZ2-CFP, clear ring structures were observed. The remaining chloroplasts analysed contained only short filaments of FtsZ2-1 and ARC6, in these filaments AtFtsZ2-1 and ARC6 still exhibited tight co-localisation. In cells co-expressing AtFtsZ1-1-CFP and ARC6-YFP only short filaments were observed. The lack of ring-like structures was probably due to disequilibrium between the levels of FtsZ proteins and ARC6 as altered levels of ARC6 is known to disrupt Z-ring structure (Vitha *et al.*, 2003). Despite the lack of Z-rings co-localisation was always observed between AtFtsZ1-1 and ARC6 (Fig. 4.4).

4.2.6. ARC6 interacts specifically with AtFtsZ2

To confirm the interactions between ARC6 and the FtsZ proteins BiFC assays were again employed. ARC6 was fused to the N-terminal of the YFP fragments to generate constructs pWEN-NY/ARC6 and pWEN-CY/ARC6 (Maple *et al.*, 2005). ARC6-CY and ARC6-NY were transiently expressed in

tobacco cells by particle bombardment. A discontinuous ring of YFP fluorescence was observed indicating that ARC6 can interact with itself (Fig. 4.5). In tobacco cells co-expressing ARC6-CY and FtsZ2-1-NY or ARC6-NY and FtsZ2-1-CY again a discontinuous ring of YFP fluorescence was observed indicating that ARC6 interacts with AtFtsZ2-1 (Fig. 4.5). Surprisingly in cells co-expressing ARC6-NY and AtFtsZ1-1-CY no fluorescence signal is observed suggesting that there is no interaction between ARC6 and AtFtsZ1-1 (Fig. 4.5). It therefore appears that ARC6 interacts specifically with FtsZ2.

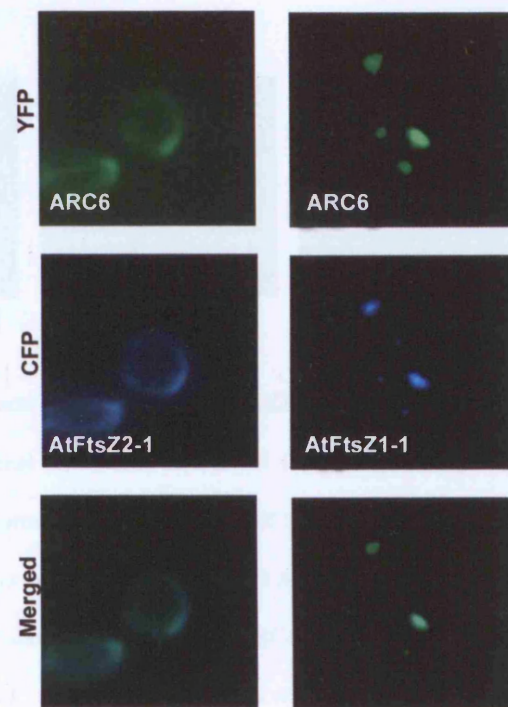


Fig. 4. 4. Co-localisation of ARC6 with the FtsZ proteins. ARC6-YFP was transiently expressed in tobacco leaf cells together with either FtsZ1-1-CFP or FtsZ2-1-YFP. The green colour of the merged images signifies co-localisation of the fusion proteins. Scale bar = 5 μ m. This work was carried out in collaboration with Jodi Maple (Maple, Aldridge and Møller, 2005).

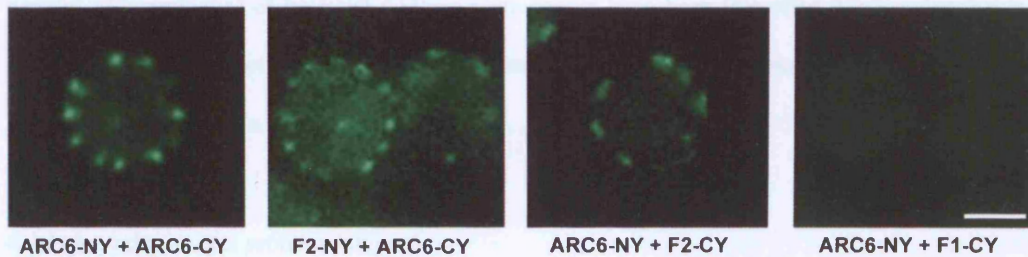


Fig. 4. 5. ARC6 interacts specifically with FtsZ2-1. BiFC assays were performed by co-expressing fusions to the N-terminal (NY) and C-terminal (CY) fragments of YFP. Reconstitution of YFP is observed in cells co-expressing ARC6-NY + ARC6-CY, FtsZ2-1 (F2)-NY + ARC6-CY and ARC6-NY + F2-CY, indicating that ARC6 self interacts and also interacts with FtsZ2-1. No reconstitution of YFP is observed in tobacco cells transformed with ARC6-NY + FtsZ1-1 (F1)-CY indicating that ARC6 does not interact with FtsZ1-1. Scale bar = 5µm. This work was carried out in collaboration with Jodi Maple (Maple, Aldridge and Møller, 2005).

4.3. Discussion

Although co-localisation is not proof of interaction it can act as a very strong indicator of which proteins may interact with each other. Because of the cyanobacterial origins of chloroplasts, bacterial cell division is often used as a paradigm for chloroplast division. Bacterial division has been studied much more extensively than chloroplast division and is known to involve at least 15 different components many of which make up a divisome complex that mediates cell division. Although only a handful of homologues of bacterial division components have been identified it is very probable that chloroplast division involves at least as many proteins as bacterial cell division and that many of these proteins work as part of a larger complex.

4.3.1. *Arabidopsis* Min proteins interact

Co-localisation analysis using YFP and CFP fusions to AtMinD1 and AtMinE1 suggests that AtMinD1 and AtMinE1 form both homodimers and heterodimers as co-localisation of proteins is observed between AtMinD1-YFP/AtMinD1-CFP, AtMinD1-YFP/AtMinE1-CFP, AtMinD1-CFP/AtMinE1-YFP and AtMinE1-YFP/AtMinE1-CFP (Fig. 4.1). Subsequent BiFC assays have established that AtMinD1 and AtMinE1 can form both homodimers and heterodimers (Fig. 4.1). Studies of interactions between AtMinE1 and AtMinD1 using yeast two-hybrid and FRET assays have further confirmed these interactions (Maple *et al.*, 2005).

Although a MinC homologue has not been identified in *Arabidopsis*, interestingly in a recent study expressing *E. coli* MinC within tobacco cells, MinC-GFP fluorescence appeared concentrated in one or two spots within the chloroplast in a similar localisation pattern to AtMinD1 and AtMinE1 (Tavva *et al.*, 2005). High expression of MinC in tobacco cells results in abnormally large chloroplasts indicating that *E. coli* MinC is functional in *Arabidopsis* (Tavva *et al.*, 2005). Together this data implies that a MinC-like protein is involved in the Min system in *Arabidopsis*.

Since this study MscS-like proteins have been implicated in the control of plastid size and shape. Two MscS-like (MSL) proteins in *Arabidopsis*; MSL2 and MSL3 function as mechanosensitive ion channels (Haswell and Meyerowitz, 2006). An *msl2-1* and *msl3-1* double mutant has variegated leaves and enlarged chloroplasts. MSL2-GFP and MSL3-GFP are associated with the plastid envelope where they localise as one or two distinct foci (Haswell and Meyerowitz, 2006), a similar pattern to AtMinD1 and AtMinE1. Co-bombardment of tobacco cells with AtMinE1-CFP and MSL2-GFP or

MSL3-GFP revealed overlapping AtMinE1-CFP and MSL2-GFP or MSL3-GFP signals demonstrating that MSL2 and MSL3 co-localise with AtMinE1. Although MSL2 and MSL3 co-localise with the AtMinE1/AtMinD1 complex it is not clear what the relationship is between these proteins. To clarify this relationship further analysis is required, perhaps it is simply that both the Min and MSL proteins are localising to the poles of the chloroplast as defined by some unidentified mechanism.

4.3.2. *Arabidopsis FtsZ proteins co-localise*

As with the Min proteins, AtFtsZ1-1 and AtFtsZ2-1 co-localisation analysis suggests that AtFtsZ1-1 and AtFtsZ2-1 can form both homodimers and heterodimers. YFP and CFP fusions to AtFtsZ1-1 and AtFtsZ2-1 co-expressed in tobacco cells always exhibit co-localisation (Fig. 4.2). The ability of AtFtsZ1-1 and AtFtsZ2-1 to form both homodimers and heterodimers is confirmed through BiFC assays (Fig. 4.2) and has also been confirmed using yeast two-hybrid and FRET assays (Maple *et al.*, 2005). Because the FtsZ proteins can form both homodimers and heterodimers the structure of the Z-ring is still unclear. Three possible models have been proposed to explain how the FtsZ proteins relate to each other within the Z-ring. (1) AtFtsZ1-1 and AtFtsZ2-1 form separate homopolymeric filaments that associate laterally. (2) AtFtsZ1-1 and AtFtsZ2-1 assemble as heteropolymers analogous to the relationship of α - and β -tubulin. (3) AtFtsZ1-1 and AtFtsZ2-1 form homodimers and heterodimers within any given Z-ring. The data presented in this study does not eliminate any of these models and further experimentation will have to be performed in order to elucidate the Z-ring structure.

Tight co-localisation of the FtsZ proteins is even maintained when the structure of the Z-ring is perturbed (Fig. 4.3). The data presented here agrees with the tight co-localisation observed between FtsZ proteins in plants overexpressing AtMinD1 or *arc6* mutant plants that both have highly fragmented FtsZ filaments (McAndrew *et al.*, 2001). The small mini circles observed within the chloroplasts of cells overexpressing FtsZ proteins have no contact with the chloroplast envelope, suggesting that membrane association is not a prerequisite for FtsZ to form ring-like structures. However, in tobacco, it has been reported that a small sub-section of FtsZ2 is associated with the both the inner and outer envelope membranes (El-Kafafi *et al.*, 2005) therefore is likely that a functional Z-ring requires some association with the envelope membranes.

4.3.3. *ARC6 co-localises with FtsZ proteins*

Studies had previously shown that ARC6 localises to a ring structure at the chloroplast division site (Vitha *et al.*, 2003). In order to analyse whether ARC6 is at the same location as the Z-ring, localisation analysis was carried out by co-expressing ARC6 with either AtFtsZ1-1 or AtFtsZ2-1. As expected ARC6-YFP could form a ring structure at the mid-point of the chloroplast, this ring structure was found to co-localise with the ring formed by AtFtsZ2-1-CFP (Fig 4.4) signifying that ARC6 interacts with AtFtsZ2-1. Frequently only short filaments of tightly co-localising AtFtsZ2-1-CFP and ARC6-YFP were observed. This filamentation and lack of Z-ring structure is probably due to disequilibrium between FtsZ proteins and ARC6 as altered levels of ARC6 is known to disrupt the Z-ring structure (Vitha *et al.*, 2003). In cells co-expressing AtFtsZ1-1-CFP and ARC6-YFP only short filaments of FtsZ1-1 and ARC6 were observed, however AtFtsZ1-1-CFP and ARC6-YFP are tightly co-localised suggesting AtFtsZ1-1 and ARC6 interact with each other. Interestingly BiFC analysis revealed that ARC6 interacts specifically with AtFtsZ2-1 and not AtFtsZ1-1 as no reconstitution of YFP was observed in cells expressing both ARC6-NY and AtFtsZ1-1-CY (Fig.4.6). Yeast two-hybrid analysis has confirmed that ARC6 interacts specifically with FtsZ2-1 (Maple *et al.*, 2005). Subsequent deletion analysis revealed that interaction between ARC6 and FtsZ2-1 is mediated through the C-terminal core domain which is present in FtsZ2 family proteins but is absent in FtsZ1 proteins (Maple *et al.*, 2005). In *E. coli*, the core domain is involved in direct interactions with ZipA and FtsA (Wang *et al.*, 1997; Din *et al.*, 1998; Liu *et al.*, 1999; Hale *et al.*, 2000; Mosyak *et al.*, 2000; Yan *et al.*, 2000). ZipA and FtsA are believed to be involved in anchoring and stabilising the Z-ring. This finding lends further credence to the suggestion that ARC6 is involved in stabilisation of the Z-ring and also establishes a functional difference between FtsZ1 and FtsZ2 proteins.

In BiFC assays in which ARC6-CY and ARC6-NY were transiently expressed in tobacco cells, a discontinuous ring of YFP fluorescence was observed indicating that ARC6 can interact with itself (Fig. 5). In *E. coli* the cellular ratio of FtsA to FtsZ is 1:100 and studies have shown that the appropriate stoichiometric ratio is critical for correct division (Dai and Lutkenhaus, 1992). It appears there is insufficient FtsA to form a complete ring and presumably FtsA makes only widely interspersed contacts with FtsZ filaments (Dai and Lutkenhaus, 1992). This proposed pattern of FtsA contact with FtsZ matches the punctuate ring pattern observed in tobacco expressing ARC6-CY and ARC6-NY and lends support to the theory that ARC6 may function in a role similar to FtsA.

Recently using the yeast two-hybrid system, interaction has been detected between ARC6 and AtCDT1a (Raynaud *et al.*, 2005). This interaction was also detected using BiFC assays in tobacco BY-2 protoplasts co-transformed with ARC6 fused to the N-terminal half of YFP and AtCDT1a fused to the C-terminal half of YFP (Raynaud *et al.*, 2005). AtCDT1a is a prereplication factor crucial for cell proliferation and genome stability (Castellano *et al.*, 2004). Simultaneous down-regulation of AtCDT1a and AtCDT1b results in severe developmental defects for the plant as a whole and also results in severe plastid division defects; ~50% of leaf cells contain only 3-4 enlarged chloroplasts (Raynaud *et al.*, 2005). AtCDT1a-GFP accumulates in both the nuclei and plastids and it has been suggested that AtCDT1a could coordinate plastid and cell division (Raynaud *et al.*, 2005).

4.3.4. Conclusion

It is clear from the data presented in this study that chloroplast division components do not act in isolation but as parts of complexes to bring about plastid division. Since the completion of this study more components of the plastid division machinery have been identified. They are proteins as diverse as mechanosensitive ion channel proteins (MSL2 and MSL3 (Haswell and Meyerowitz, 2006)) and prereplication factors (AtCDT1a and AtCDT1b (Raynaud *et al.*, 2005)). These proteins will also have to be fitted into the model of the chloroplast division machinery in order to understand how they function. In addition to the stromal proteins analysed in this study, many other proteins act on the cytosolic surface of the plastid division site, these include dynamin-like proteins; ARC5 (Gao *et al.*, 2003) and CmDnm2 (Miyagishima *et al.*, 2003) which are likely to be eukaryote derived. How the apparently prokaryotic-derived stromal plastid division proteins and eukaryotic-derived cytosolic plastid division proteins coordinate the process of plastid division remains to be investigated. Fig. 4.6 is a model of our current understanding of the stromal proteins involved in plastid division.

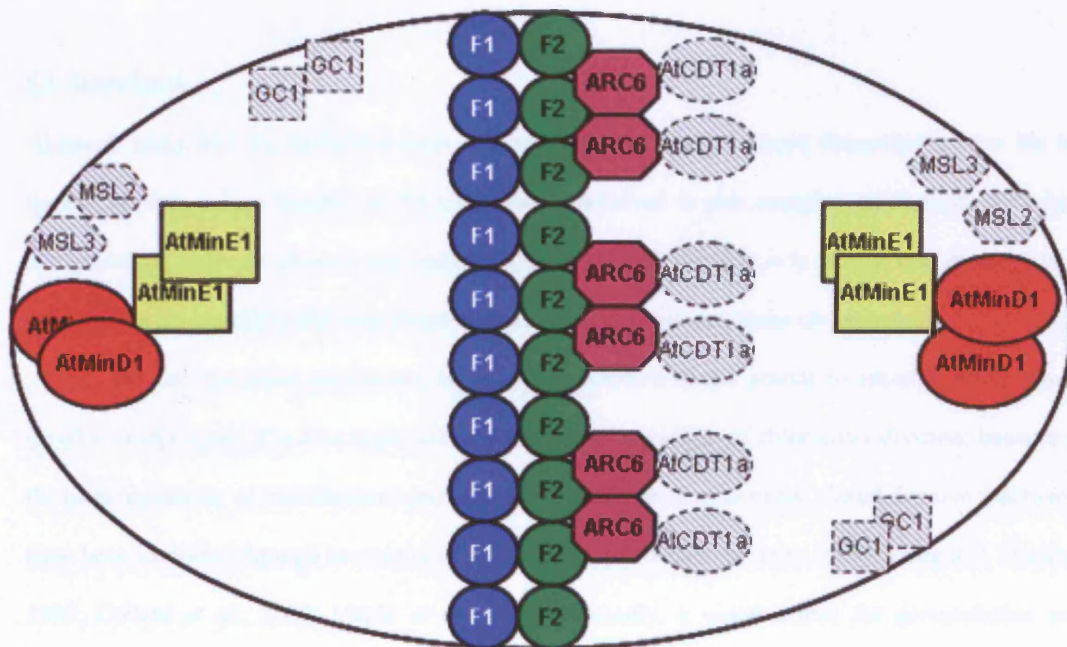


Fig. 4. 6. Model of interaction of stromal plastid division components. Those proteins not analysed in this study are thatched. Only one possible model of the Z-ring is presented. AtMinD1 undergoes dimerisation or polymerisation and localises to the poles of the chloroplast. AtMinE1 self interacts and interacts with AtMinD1 simulating the ATPase activity of AtMinD1. FtsZ1-1 and FtsZ2-1 form a ring or rings at the future chloroplast division site directed here by the coordinated action of AtMinD1 and AtMinE1. ARC6 interacts specifically with FtsZ2-1 possibly stabilising the Z-ring. Adapted from Maple, Aldridge and Møller, 2005

5. Searching for novel chloroplast division components using protein-protein interaction approaches.

5.1. Introduction

Although study into the molecular basis of plastid division has advanced dramatically over the last decade, to date only a handful of the components involved in this complex mechanism have been recognised. In order to advance our understanding of plastid division it is critical that more of these components are identified and their function in the plastid division process characterised.

So far two main approaches have been employed in the search to identify novel plastid division components. The first is the use of the bacterial paradigm of chloroplast division; because of the bacterial origins of plastids many prokaryotic-derived components of the plastid division machinery have been identified through homology to known bacterial division proteins (Osteryoung and Vierling, 1995; Colletti *et al.*, 2000; Maple *et al.*, 2002). Secondly, a visual screen for *accumulation and replication of chloroplast (arc)* mutants of ethyl methane sulfonate-mutagenised *Arabidopsis* seeds (Pyke and Leech, 1991) recognised twelve mutations with abnormal numbers of chloroplasts. Although use of the bacterial paradigm to identify chloroplast division proteins has been successful, cloning of the *arc* mutants (Gao *et al.*, 2003; Vitha *et al.*, 2003) and evidence of dynamin-like proteins involved in chloroplast division such as ARC5 (Gao *et al.*, 2003) and CmDnm2 (Miyagishima *et al.*, 2003) have shown that the process of chloroplast division is mediated by a combination of prokaryotic- and eukaryotic-derived factors. Therefore to identify all of the components involved in plastid division using homology to known bacterial division components is limited and can only reveal part of the plastid division machinery. In order to search for novel plastid division components other strategies need to be employed.

Since it has been demonstrated that most plastid division proteins do not act in isolation but operate as part of complexes (Maple *et al.*, 2005) it would appear logical to use protein-protein interaction approaches using known plastid division components as baits to identify novel components. This chapter describes how yeast two-hybrid screening has been used to hunt for novel interacting partners of AtFtsZ1-1 and AtFtsZ2-1.

Yeast two-hybrid screening is an *in vivo* technique to identify interacting partners of a known bait protein. The biological basis of the yeast two-hybrid system originates from observations that many eukaryotic transcription factors are modular with structurally and functionally distinct transcription activation domains (AD) and DNA binding domains (BD) (Hope and Struhl, 1986; Keegan *et al.*, 1986). The yeast two-hybrid system exploits the modular properties of eukaryotic transcription factors in construction of gene fusions to the AD and BD which when expressed as chimeric proteins simultaneously bind to a target DNA sequence and activate transcription of a downstream reporter. Typically a bait protein is fused to the GAL4 DNA-BD and a library of cDNA clones are fused to the GAL4 AD. If protein-protein interactions occur between the bait and the prey proteins then effective reconstitution of the GAL4 transcriptional activator is achieved. Reporter genes contain the 17-mer consensus sequence of the GAL4 upstream activation sequence (UAS) within their promoters. If reconstitution of the GAL4 transcriptional activator is achieved, transcription of the reporter genes is activated. The cDNA clones within the library that encode proteins capable of forming protein-protein interactions with the bait are identified by virtue of their ability to cause activation of the reporter gene.

In this study FtsZ2-1 and FtsZ1-1 proteins are used as baits in yeast two-hybrid screens to hunt for novel plastid division components. The use of co-immunoprecipitation as an alternative to yeast two-hybrid screening is also investigated.

5.2. Results

5.2.1. Selection of baits for yeast two-hybrid screening

AtFtsZ1-1 and AtFtsZ2-1 were selected as baits for use in yeast two-hybrid screens to search for novel plastid division components. There are numerous reasons for using FtsZ proteins as bait: In *E. coli* cell division, formation of the Z-ring initiates cell division (Bi and Lutkenhaus, 1991; Lutkenhaus and Addinall, 1997) and is also the target of many cell division inhibitors such as SulA and MinCD (Lutkenhaus and Addinall, 1997). FtsZ is universal among prokaryotes indicating its pivotal role in bacterial cell division. In agreement with the *E. coli* model, the FtsZ ring in *C. merolae* forms before visible constriction of the chloroplasts and before the formation of the plastid dividing (PD) rings (Miyagishima *et al.*, 2001c) suggesting Z-ring formation is the initial step in chloroplast division, making FtsZ a critical player in chloroplast division. It is also likely that inhibitors of chloroplast division act on FtsZ, a prime example of this would be a MinC-like protein or proteins acting in the role of MinC. From the bacterial paradigm it is probable that the *Arabidopsis* Z-ring forms a framework to which other stromal factors of the plastid division machinery assemble thus making FtsZ the ideal bait for yeast two-hybrid screening.

Why use proteins from both FtsZ families? It has been demonstrated that although the FtsZ proteins from both families are very similar, they are non redundant in their function as inhibiting the expression of either FtsZ protein reduces chloroplast division (Osteryoung *et al.*, 1998). Recent research has shown functional differences between tobacco FtsZ1 and FtsZ2 proteins. *In vitro* studies have shown that in conditions permissible for bacterial FtsZ polymerisation, FtsZ1 proteins polymerise efficiently whereas FtsZ2 proteins do not (El-Kafafi *et al.*, 2005). Tobacco FtsZ proteins have also been shown to have different sub-plastidal localisation; FtsZ1 is localised exclusively in the stroma whereas FtsZ2 although mainly located in the stroma is also found associated with both the inner and outer envelope membranes (El-Kafafi *et al.*, 2005). Finally it has been demonstrated that ARC6 interacts specifically with AtFtsZ2-1 and ARC3 interacts specifically with AtFtsZ1-1 (Maple *et al.*, 2005; Maple *et al.*, In press) indicating that each of the FtsZ proteins interact with a different subset of proteins. AtFtsZ2-1 interacts with ARC6 through a short peptide found at the extreme C-terminus of the FtsZ2 proteins termed the core domain. The core domain is highly conserved between plant FtsZ2 proteins and bacterial FtsZ proteins but is not found in plant FtsZ1 proteins. In *E. coli* this core domain is responsible for the direct interaction with ZipA and FtsA which are required for the stabilisation and

anchoring of the Z ring. It is possible that in plastid division ARC6 plays an analogous role. Given the predicted pivotal role that FtsZ proteins play in plastid division it is clear that FtsZ proteins are an integral part in the division machinery making FtsZ proteins excellent candidates for use as baits in yeast two-hybrid screens. Because of the functional differences, particularly the presence or absence of the core domain, between the two different families of FtsZ proteins one representative from each FtsZ family was selected to be used in yeast two-hybrid screens.

5.2.2. Generation of baits for yeast two-hybrid screen

Because they are imported into chloroplasts, FtsZ proteins contain an N-terminal transit peptide which is cleaved off upon import. To ensure that the transit peptide does not interfere with FtsZ interactions, either by changing the tertiary structure of the protein or by otherwise blocking potential interacting partners from interacting with FtsZ, the transit peptide was removed prior to cloning into the yeast two-hybrid vectors. To select the cleavage site to remove the transit peptide, alignments were performed between AtFtsZ2-1, AtFtsZ1-1 and bacterial FtsZ sequences from *E. coli* (EcFtsZ) and *Neisseria gonorrhoeae* (NgFtsZ). FtsZ amino acid sequences were obtained from the National Centre for Biotechnology Information database (<http://www.ncbi.nlm.nih.gov/entrez/>). Sequences were aligned using ClustalW (Higgins *et al.*, 1994; <http://www.ebi.ac.uk/clustalw/>) and viewed using BioEdit. All four FtsZ proteins exhibit a very high degree of similarity apart from the *Arabidopsis* FtsZ transit peptides. Therefore it was decided to amplify the *Arabidopsis* FtsZ sequences from where they begin to align with the *E. coli* sequence (Fig. 5.1). Cleavage site prediction was also performed using ChloroP (Emanuelsson *et al.*, 1999; <http://www.cbs.dtu.dk/services/ChloroP/>). However, ChloroP gave a prediction of a transit peptide length of 90 amino acids for FtsZ1-1 which would cleave off several residues shown to be involved in contacting GTP in the crystal structure of *Methanococcus jannaschii* FtsZ (Lowe and Amos, 1998; Erickson, 1998). These residues are highly conserved among all FtsZ proteins (Erickson, 1998) and are vital for FtsZ function. For FtsZ2-1, ChloroP predicted a transit peptide length of just 48 amino acids which appears to underestimate the length of the transit peptide as residues after this point show no homology to the bacterial FtsZ amino acid sequences (Fig. 5.1). These residues also exhibit features typical of transit peptide regions such as a high percentage of hydroxylated residues and a low percentage of acidic residues.

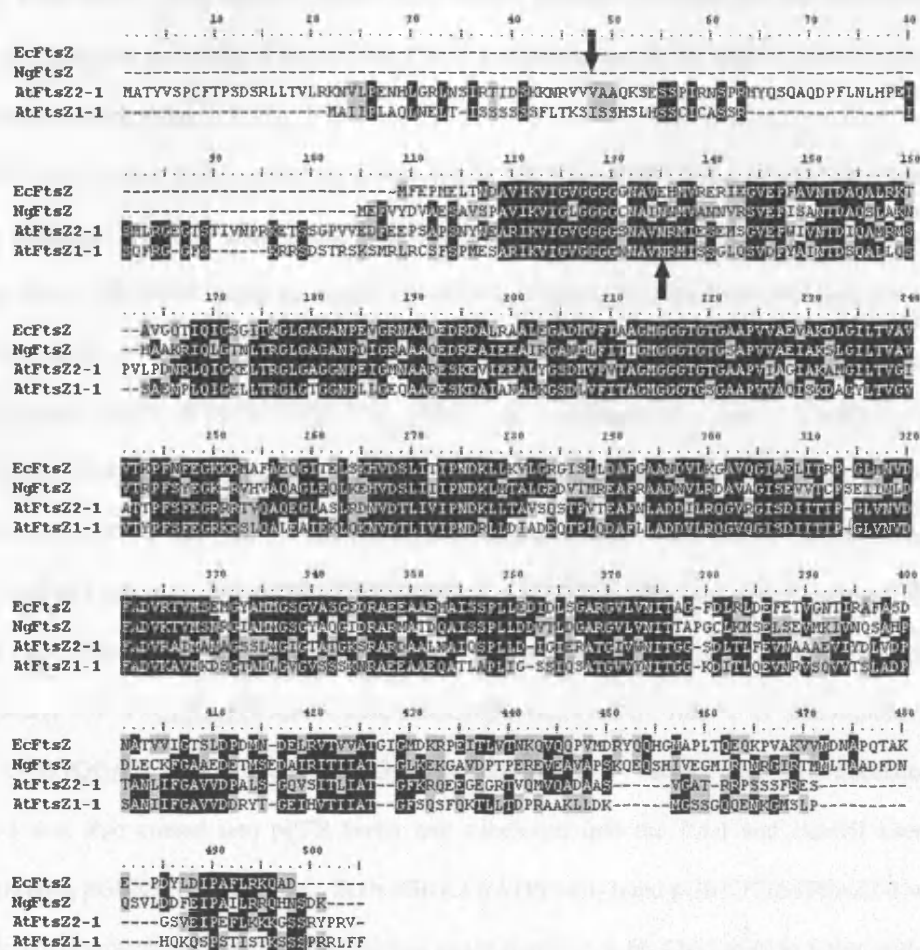


Fig. 5. 1. Alignment of FtsZ proteins. To determine the cleavage site for removal of the transit peptide, AtFtsZ1-1 and AtFtsZ2-1 protein sequences were aligned with FtsZ sequences from *Neisseria gonorrhoeae* (Ng) (accession number AAB18965) and *E. coli* (Ec) (accession number BAB33522). Sequences were aligned using ClustalW (Higgins *et al.*, 1994; <http://www.ebi.ac.uk/clustalw/>) and viewed using BioEdit. Cleavage site was determined to be the amino acid residue corresponding to where the *Arabidopsis* FtsZ sequences begin to align with the *E. coli* sequence. Black arrows indicate the ChloroP predicted transit peptide cleavage site.

In order to clone FtsZ1-1 and FtsZ2-1 without their transit peptides (Δ TPFtsZ1-1 and Δ TPFtsZ2-1), primers were designed to amplify FtsZ1-1 and FtsZ2-1 downstream of the transit peptide and also incorporate a new start codon.

To carry out the yeast two-hybrid screen the MATCHMAKER GAL4 two-hybrid system 3 (Clontech) was used. This system utilises the modular GAL4 transcriptional activator. Bait proteins are fused to the GAL4 DNA-BD within the pGBKT7 vector and library cDNAs (prey proteins) are fused to the GAL4 AD. Δ TPAtFtsZ1-1 was amplified from cDNA using the primers FtsZ/19 (5'-TGCATATGAGGTGTTCTTCTCTCCG-3' *NdeI* is underlined) and FtsZ/18 (5'-ATGGATCCCTAGAAGAAAAGTCTACGGGGAGAAACG-3' *BamHI* is underlined) and was cloned into pPCR-Script. Δ TPFtsZ1-1 was subsequently subcloned into the *NdeI* and *BamHI* sites of pGBKT7 creating a fusion to GAL4 DNA-BD generating pGBKT7/ Δ TPFtsZ1-1 which was used as the bait vector. To create the Δ TPFtsZ2-1 bait vector, Δ TPFtsZ2-1 was amplified from cDNA using primers FtsZ/20 (5'-TTCATATGCCATCTGCTCCGAGTAACTAC-3' *Nde I* is underlined) and FtsZ/15 (5'-ATGGATCCCTTAGACTCGGGGATAACGAGAGC-3' *Bam HI* is underlined). Δ TPFtsZ2-1 was also cloned into pPCR-Script and subcloned into the *NdeI* and *BamHI* sites of pGBKT7 creating pGBKT7/ Δ TPFtsZ2-1. Both pGBKT7/ Δ TPFtsZ1-1 and pGBKT7/ Δ TPFtsZ2-1 were subjected to DNA sequencing to ensure that the bait genes (FtsZ1-1 or FtsZ2-1) were in frame with the GAL4 DNA-BD.

5.2.3. Testing baits for autoactivation

Yeast two-hybrid screening was carried out by yeast mating whereby the cDNA library fused to the GAL4 AD is expressed in the AH109 (MAT α) *S. cerevisiae* strain and the bait expressed in Y187 (MAT α) *S. cerevisiae* strain. The yeast is mated and yeast diploids containing interacting bait and prey partners are selected. Before screening pGBKT7/ Δ TPFtsZ1-1 and pGBKT7/ Δ TPFtsZ2-1 were tested for autoactivation of the reporter genes in the AH109 strain. Auto-activation occurs if the bait protein has intrinsic transcription activation properties that activate the reporter genes in AH109. There are four different reporter genes; *HIS3*, *ADE2*, *MEL1* and *LacZ* which all contain the 17-mer consensus sequence which makes up the GAL4 upstream activation sequence (UAS) within their promoters. If the bait protein causes autoactivation of these reporter genes this leads to the occurrence of false positives. The initial screen was carried out using the *HIS3* reporter gene therefore the baits were tested for auto-

activation of *HIS3*. To test for auto-activation bait vectors (pGBKT7/ Δ TPFtsZ1-1 or pGBKT7/ Δ TPFtsZ2-1) were co-transformed into AH109 along with empty pGADT7 vector using the LiAc procedure outlined in Section 2.4.2. Colonies containing both plasmids were selected for on synthetic drop-out media –Leucine (L) –Tryptophan (T) (SD-TL). Since the pGBKT7 contains the *TRP1* gene, for tryptophan synthesis, and pGAD contains the *LEU2* gene for leucine synthesis. Positive colonies were then streaked onto plates containing SD-LTH (H=Histidine) and increasing quantities (0, 5, 10, 20, 30, 50 mM) of 3-amino-1,2,3 triazole (3-AT), a competitive inhibitor of the yeast *HIS3* protein which suppresses background growth. Plates were incubated at 30°C for 7 days and the appearance of colonies analysed. Plates containing only SD-TLH did not show any yeast growth after 7 days incubation establishing that the bait proteins do not autoactivate the *HIS3* reporter gene and therefore no 3-AT is required in the media for the screen.

5.2.4. Screening the cDNA library

The cDNA library used in this study was generated from *Arabidopsis* ecotype Columbia seedlings by Makoto Fujiwara, a postdoctoral associate in the laboratory, using the MATCHMAKER GAL4 two-hybrid system 3 library construction kit. The library cDNAs are expressed as fusion proteins to the GAL4 AD in AH109 cells. The library was created using recombination-mediated cloning and AH109 transformants pooled and frozen at -80°C in aliquots. The cDNA library was calculated to contain 1.7×10^6 independent clones (Makoto Fujiwara, personal communication). To screen the library, Y187 transformants containing either pGBKT7/ Δ TPFtsZ1-1 or pGBKT7/ Δ TPFtsZ2-1 were mated with the AH109 cells pre-transformed with the cDNA library as described in Section 2.4.3. Expression of the *HIS3* reporter gene was used to screen for interacting bait/prey partners and therefore the mating mixture was spread onto 30 X 150 mm plates containing SD-LTH, 300 μ l of mating mixture per plate. Plates were incubated at 30°C for 6 days. Any colonies that appeared were replica plated and numbered. When performing yeast two-hybrid screening by yeast mating occasionally a positive colony will contain more than one library-AD plasmid therefore the colonies were replica plated twice more onto SD-HTL plates to dilute out extra library-AD plasmids which would complicate subsequent analysis. Positive colonies were finally streaked onto a master plate and numbered for subsequent analysis (Fig. 2). The mating efficiency was calculated and found to be 55% and 58% for FtsZ1-1 and

Fig. 5.2. Example of a master plate from the yeast two-hybrid screens. After six days His⁺ colonies were streaked onto SD-LTH plates and assigned a number with which to identify them in subsequent analysis. The plate shown here is from the FtsZ1-1 screen.

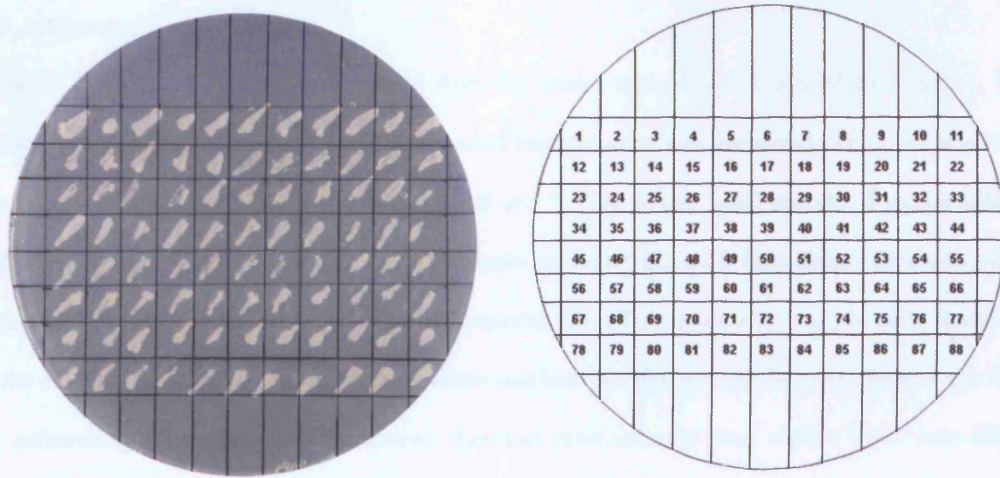


Fig. 5. 2. Example of a master plate from the yeast two-hybrid screens. After six days His⁺ colonies were streaked onto SD-LTH plates and assigned a number with which to identify them in subsequent analysis. The plate shown here is from the FtsZ1-1 screen.

FtsZ2-1 respectively (Section 2.4.3) and the number of clones screened was 4.5×10^5 for FtsZ1-1 and 1.1×10^6 for FtsZ2-1.

5.2.5. Selection of positive clones

A total of 203 His⁺ colonies were retrieved from the screen using FtsZ1-1 and 63 for FtsZ2-1. To narrow down this pool of candidate clones a second reporter gene was employed. The *LacZ* reporter gene is also under the control of the GAL4 UAS and TATA boxes. *LacZ* encodes β -galactosidase which cleaves X-gal into galactose and a blue insoluble product. Colony lift filter assays (Breedon and Nasmyth, 1985) were undertaken using the *LacZ* reporter gene. This qualitative assay is quite sensitive and the colour is indicative of the strength of interaction between the bait and the prey (the stronger the blue colouration the stronger the interaction). Streaked yeast colonies were replica lifted onto filter paper and the cells lysed by repeated freeze thaw cycles before been exposed to a solution containing X-gal (Section 2.4.7). Candidate colonies were graded for the strength of interaction based on the colour of the filter lift assays. Those colonies demonstrating the strongest interaction were selected as likely real FtsZ interacting proteins (Fig. 5.3 and 5.4). In total 21 colonies were selected for FtsZ1-1 and 20 colonies were selected for FtsZ2-1.

To identify the candidate clones, the library plasmids from the selected colonies were extracted from yeast following the protocol outline in Section 2.4.5 and the plasmids introduced into *E. coli* DH5 α using standard transformation protocols (Section 2.2.2). To ensure that only unique clones were further analysed, the plasmids were tested by restriction endonuclease digestion to investigate whether more than one of the colonies selected contained the same library clone. Candidate plasmids were extracted from *E. coli* and subjected to digestion by *Hind*III in the appropriate buffer at 37°C for 30 minutes (Fig. 5.5 and 5.6). *Hind*III cuts the pGADT7 library vector either side of the cloning/insertion site therefore the length of the library cDNA insert can be estimated and unique clones can be ascertained based on the size of the restricted fragment. The digested fragments were separated from the vector background by electrophoresis on a 1% agarose gel. Based on the restriction digest profile, 8 unique clones were isolated from the FtsZ1-1 screen (Fig. 5.5) and 6 unique clones were isolated from the FtsZ2-1 screen (Fig. 5.6).

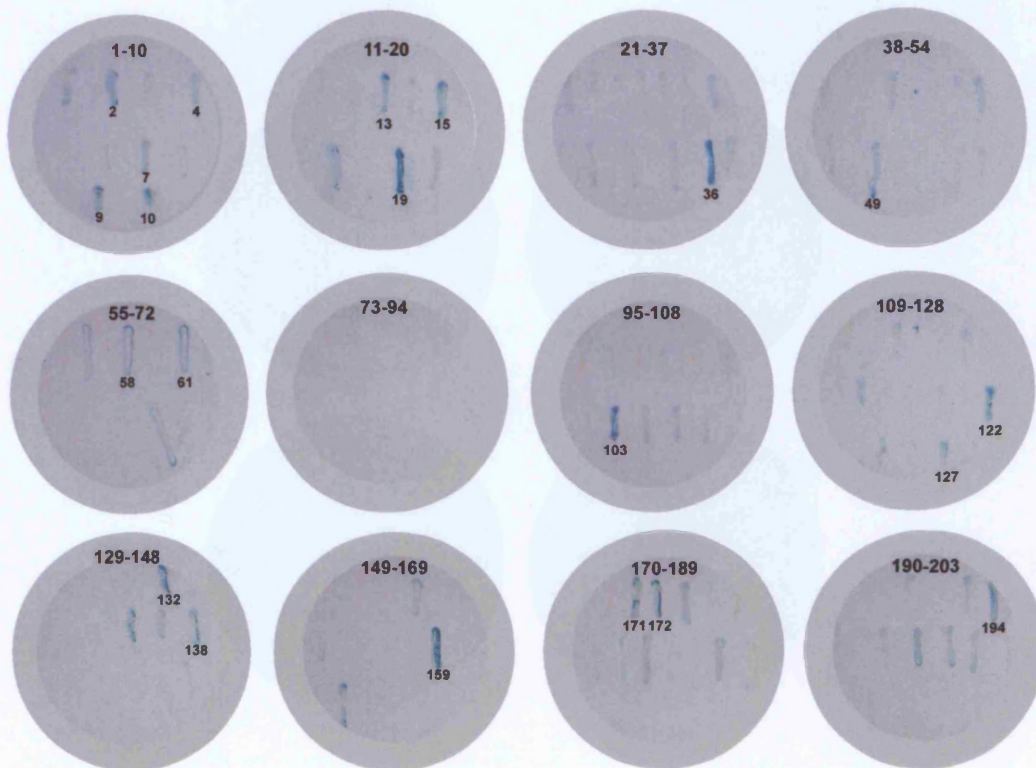


Fig. 5. 3. Colony lift filter assays of candidate colonies from the FtsZ1-1 screen. His⁺ colonies isolated from the FtsZ1-1 screen were further analysed for expression of the *LacZ* reporter gene. Colony lift filter assays were performed as outlined in Section 2.4.7 and candidate colonies were graded for the strength of interaction based on the colour of the filter lift assays. The candidate colonies exhibiting the strongest interaction were selected for further analysis (those colonies that are numbered).

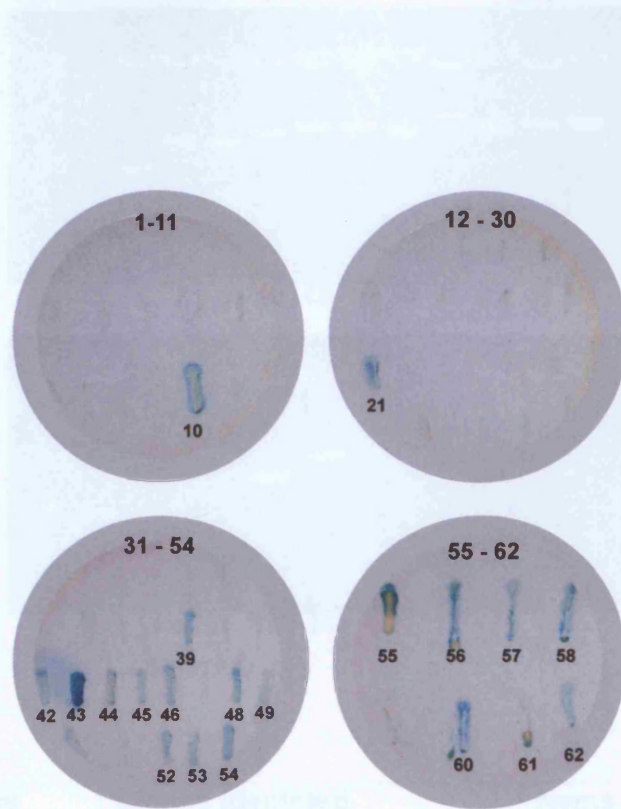
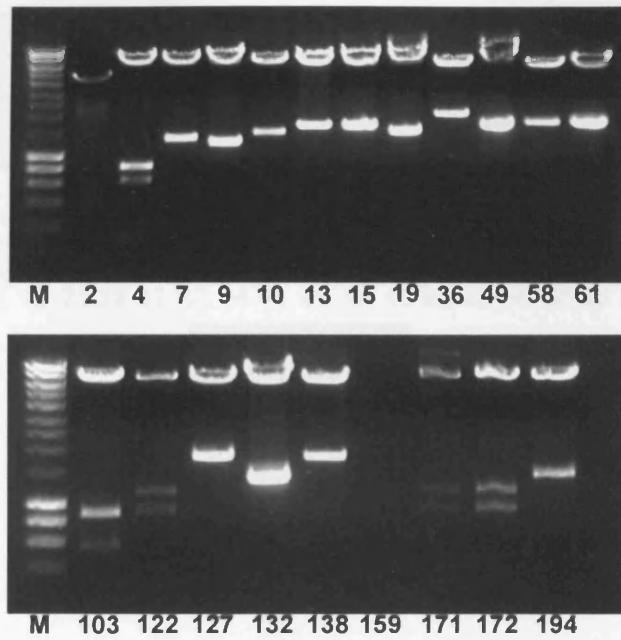
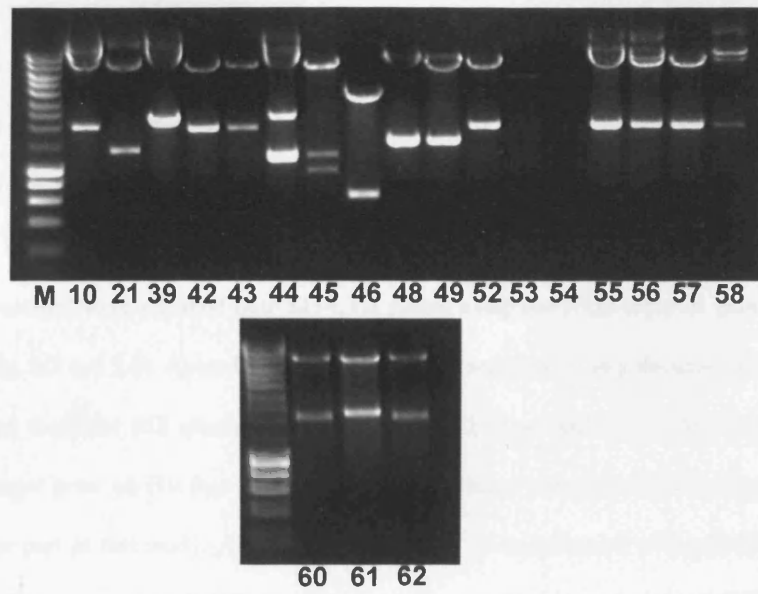


Fig. 5. 4. Colony lift filter assays of candidate colonies from the FtsZ2-1 screen. His⁺ colonies isolated from the FtsZ2-1 screen were further analysed for expression of the *LacZ* reporter gene. Colony lift filter assays were performed as outlined in Section 2.4.7 and candidate colonies were graded for the strength of interaction based on the colour of the filter lift assays. The candidate colonies exhibiting the strongest interaction were selected for further analysis (those colonies that are numbered).



Class	Clones identified	Name
1	4	F1-4
2	7, 10, 132, 194	F1-10
3	9	F1-9
4	13, 15	F1-13
5	36	F1-36
6	49, 58, 61, 127	F1-58
7	103	F1-103
8	122, 171, 172	F1-122

Fig. 5. 5. Restriction endonuclease digestion analysis of the library clones from the FtsZ1-1 screen. AD-Library plasmids were treated with *HinDIII* which cuts the pGADT7 library vector either side of the cDNA insertion site. Restricted fragments were separated on a 1% agarose gel. AD-library plasmids with the same digestion pattern were assigned to the same class.



Class	Clones identified	Name
1	10, 42, 43, 45, 52	F2-10
2	21	F2-21
3	39, 48, 49	F2-39
4	44	F2-44
5	46	F2-46
6	55, 56, 57, 58, 60, 61, 62	F2-62

Fig. 5. 6. Restriction endonuclease digestion analysis of the library clones from the FtsZ2-1 screen. AD-library plasmids were treated with *HinDIII* and restricted fragments were separated on a 1% agarose gel. AD-library plasmids with the same digestion pattern were assigned to the same class.

5.2.6. Testing unique clones for re-interaction

To verify that the unique clones still interacted with FtsZ1-1 or FtsZ2-1, the extracted plasmids were retransformed into AH109 along with the corresponding bait plasmid that was used to isolate the clone in the original screen. Transformations were plated on SD-LT plates to select for yeast containing both the candidate clone and the bait plasmid and incubated at 30°C. After the appearance of colonies (3 days) single colonies were streaked onto SD-LTH plates using the *HIS3* reporter gene as a marker for interaction (Fig. 5.7 and 5.8). Apart from F2-46, all other candidate clones demonstrated growth on His free media and therefore still interacted with either FtsZ1-1 or FtsZ2-1. F2-46 co-transformed with FtsZ2-1 no longer grew on His free media and therefore failed to re-interact with FtsZ2-1 and so will play no further part in this study. AH109 cells were also co-transformed with pGADT7-Rec + SV40 Large-T PCR fragment and pGBKT7-53 (Clontech) as a positive control and pGADT7 and pGBKT7 empty vectors as a negative control (Fig. 5.7 and 5.8).

5.2.7. DNA sequencing and analysis of unique clones.

Unique clones were sequenced using the T7 sequencing primer, apart from F1-58 which was found to be out of frame, all of the sequenced clones contained in-frame open reading frame fusions to the GAL4-AD. The sequences were identified by comparison to the annotated *Arabidopsis* genome within the NCBI database using the blastp and blastn algorithms to compare protein and nucleotide sequences respectively (<http://www.ncbi.nlm.nih.gov/BLAST/>; Altschul *et al.*, 1990). Yeast two-hybrid screening can often generate false positives, therefore a secondary criteria was implemented to distinguish false positives from true-interacting partners of FtsZ proteins. Firstly, the predicted function of each of the candidates was analysed. If the function of candidate genes had already been characterised and no role in chloroplast division established the candidate was eliminated. Similarly if a predicted function assigned through domain analysis of the candidate was found to be incompatible with a role in chloroplast division the candidate was also eliminated. The predicted localisation of the candidate proteins was used as a second criterion. A true interacting partner of FtsZ must reside in the same cellular component as FtsZ i.e. be localised to the chloroplast. The TargetP prediction server (<http://www.cbs.dtu.dk/services/TargetP/>; Emanuelsson *et al.*, 2000) was used to ascertain the presence of a chloroplast transit peptide. However, a negative TargetP prediction did not automatically eliminate a candidate as a recent study of chloroplast proteins demonstrated that 48% of proteins identified as

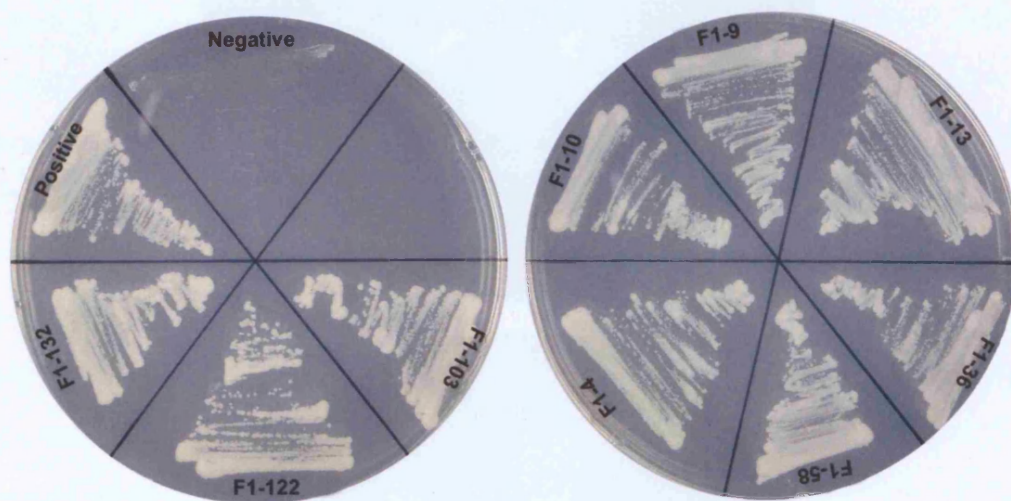


Fig. 5. 7. Retesting the interactions of FtsZ1-1 candidate clones. Yeast AH109 cells transformed with the library vector (pGADT7/F1-#) and the original bait (pGBKT7/ Δ TPFtsZ1-1) were selected for by plating on SD-LT media. Positive colonies were subsequently streaked onto SD-LTH. After three days incubation at 30°C plates were analysed for growth on His-free media. All candidate clones interact with BD- Δ TPFtsZ1-1. Sequence analysis revealed that candidate clone F1-132 is the same as clone F1-10 and will be referred to as F1-10. AH109 cells were co-transformed with pGADT7-Rec + SV40 Large-T PCR fragment and pGBKT7-53 as a positive control and pGADT7 and pGBKT7 empty vectors as a negative control.

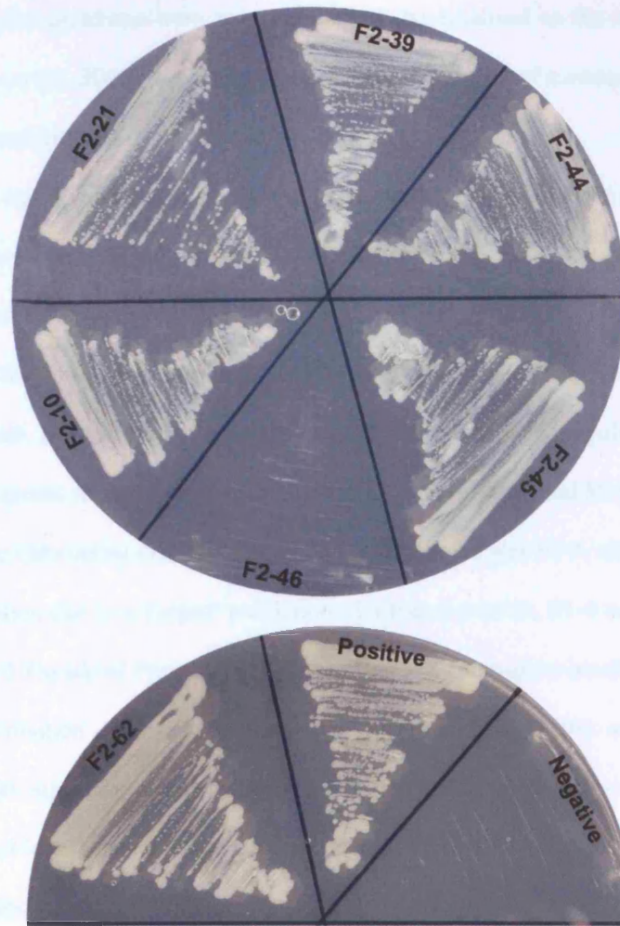


Fig. 5. 8. Retesting the interactions of FtsZ2-1 candidate clones. Yeast AH109 cells transformed with the library vector (pGADT7/F2-#) and the original bait (pGBKT7/ Δ TPFtsZ2-1) were selected for by plating on SD-LT media. Positive colonies were subsequently streaked onto SD-LTH. After three days incubation at 30°C plates were analysed for growth on His-free media. F2-46 did not re-interact with BD- Δ TPFtsZ1-1 and was eliminated from further analysis. All other candidates interacted with BD- Δ TPFtsZ1-1. Sequence analysis revealed that candidate clone F2-45 is the same as clone F2-10 and will be referred to as F2-10. AH109 cells were co-transformed with pGADT7-Rec + SV40 Large-T PCR fragment and pGBKT7-53 as a positive control and pGADT7 and pGBKT7 empty vectors as a negative control.

part of the chloroplast proteome were not predicted to be localised to the chloroplast when using TargetP (Kleffmann *et al.*, 2004) therefore it appears that the ability of a computer program to predict the presence of a transit peptide is not reliable.

Sequences identified through blastp and blastn were compared to the annotated sequences on the TAIR website (www.arabidopsis.org) and those that were already characterised to have a function separate from chloroplast division were eliminated. Those eliminated included F1-13 which is characterised as ATHM2, a chloroplast-targeted m-type thioredoxin involved in the redox regulation of malate dehydrogenase. M-type thioredoxins are probably involved in the regulation of enzymes of the Calvin cycle and enzymes related to sugar metabolism (Mestres-Ortega and Meyer, 1999) thus unlikely to be involved in the chloroplast division process. Also eliminated was F1-4, although initially selected for further investigation due to a TargetP prediction of a transit peptide, F1-4 was characterized during this study and named Thylakoid Formation 1 (Thf1). Thf1 is a chloroplast-localised protein involved in vesicle-mediated formation of thylakoid membranes (Wang *et al.*, 2004) and also thought to be involved in a sugar signalling pathway (Huang *et al.*, 2006). Although chloroplasts within the variegated regions of leaves of a T-DNA insertion mutant of *Thf1* lacked thylakoid membranes, grana or starch granules, the envelope membrane structure, size and shape of the chloroplast appears normal (Wang *et al.*, 2004) and therefore F1-4 was also discarded. F1-36 and F2-39 are both Toc159, an integral part of the protein import machinery located on the chloroplast outer membrane. Within the Toc complex Toc159 functions as a transit-sequence receptor (Kubris *et al.*, 2004; Smith *et al.*, 2004). Toc159 is well characterised and is not reported to be involved in plastid division. Further analysis showed that other candidates had predicted functions distinct from chloroplast division and these were also disregarded including F1-103, a MYB3 family transcription factor (Yanhui *et al.*, 2006) and F1-9 a glycosyl hydrolase family 38 protein involved in carbohydrate metabolism. F1-122 and F2-62 are proteins of unknown function. Analysis using the Pfam database (www.sanger.ac.uk/software/Pfam/; Bateman *et al.*, 2004) revealed no conserved protein domains for either F1-122 or F2-62. F1-122 and F2-62 were eliminated from further analysis as it is unlikely that they are localised to the chloroplast. Not only was the TargetP prediction negative for a chloroplast targeted transit peptide but also the N-terminal portion of the predicted protein contained non of the features characteristic of a transit peptide such as a high percentage of hydroxylated residues and a low percentage of acidic residues.

No proteins were selected from the FtsZ1 screen for further analysis as the candidates did not pass the secondary criteria, however three candidates from the FtsZ2-1 screen were selected for further experimentation. A protein of unknown function; F2-44 was selected as although TargetP predicted F2-44 to be targeted to mitochondria, this prediction was made with a low reliability class. Studies have demonstrated that many proteins exhibit dual targeting to the mitochondria and the chloroplast (reviewed in Peeters and Small, 2001) therefore F2-44 was not eliminated because of a negative TargetP prediction. F2-44 is an expressed protein whose biological processes and molecular function are unknown. Because this protein has yet to be characterised and because it showed strong interaction with FtsZ2-1 as indicated by LacZ levels (Fig. 5.4) F2-44 was chosen for further analysis. F2-10 was also selected for further analysis as F2-10 has homology to another C2-domain containing protein which was isolated in screens using both Δ TPFtsZ1-1 and AtMinE1 (Maple, 2005) as baits. From domain computational analysis F2-21 is a UDP-glucose glucosyltransferase family protein. Possibly F2-21 is involved in the GC1 pathway as GC1 has high secondary structural similarity to nucleotide-sugar epimerases (Maple *et al.*, 2004). UDP-glucosyl transferases catalyse the transfer of a glycosyl group from a UDP-sugar to a small hydrophobic molecule. Epimerases interconvert epimers often modifying protein activity or surface recognition. Nucleotide sugar epimerases use nucleotide-sugar substrates for a variety of chemical reactions, the conjugation of UDP to sugars and subsequent epimerase interconversion is important in prokaryotes for sugar activation to form polymers for a variety of functions (Baker *et al.*, 1998).

Table 1. Candidate genes from yeast two-hybrid screen using Δ TPFtsZ1-1 as bait.

Class	Repeated	Identity	Gene	Annotation	Source	*TP
1	1	F1-4	At2g20890	Thf1 Chloroplast-localized Thylakoid formation1 gene product involved in vesicle-mediated formation of thylakoid membranes.	Wang <i>et al.</i> , 2004; Huang <i>et al.</i> , 2006	yes
2	4	F1-10	At1g70800	C2 domain containing protein Isolated in screen with AtMinE1	PF00168 2.2×10^{-24}	no
3	1	F1-9	At5g13980	glycosyl hydrolase family 38 protein. Involved in carbohydrate metabolism	PF01074 3×10^{-166}	no
4	2	F1-13	At4g03520	ATHM2 thioredoxin	Mestres-Ortega and Meyer, 1999	yes
5	1	F1-36	At4g02510	Toc159 An integral membrane GTPase that functions as a transit-sequence receptor required for the import of proteins necessary for chloroplast biogenesis. Located in the outer chloroplast membrane	Kubris <i>et al.</i> , 2004; Smith <i>et al.</i> , 2004	no
6	4	F1-58	At2g43130	Out of frame with GAL4-AD		
7	1	F1-103	At1g22640	MYB3 family transcription factor	Yanhui <i>et al.</i> , 2006	no
8	3	F1-122	At3g07280	Unknown function		no

* Protein is predicted to contain a chloroplast targeted transit peptide

Table 2. Candidate genes from yeast two-hybrid screen using Δ TPFtsZ1-1 as bait.

Class	Repeated	Identity	Gene	Annotation	Source	*TP
1	5	F2-10	At2g20990	C2 domain containing protein	PF00168 5×10^{-20}	no
2	1	F2-21	At1g07240	UDP-glucuronosyl/UDP-glucosyl transferase family protein	PF00201 1×10^{-19}	no
3	3	F2-39	At4g02510	Toc159 An integral membrane GTPase that functions as a transit-sequence receptor required for the import of proteins necessary for chloroplast biogenesis. Located in the outer chloroplast membrane	Kubris <i>et al.</i> , 2004; Smith <i>et al.</i> , 2006	no
4	1	F2-44	At4g36980	Unknown function		Mitochondria
6	7	F2-62	At5g48610	Unknown function		no

* Protein is predicted to contain a chloroplast targeted transit peptide

5.2.8. Analysis of candidate clones

In order to investigate whether the candidate clones F2-44, F2-21 and F2-10 are real chloroplast division components T-DNA insertion mutants for each of the clones were obtained to examine possible plastid division phenotypes. *Arabidopsis* lines with potential T-DNA insertions in each of the candidate genes (F2-44, SALK_128572; F2-21, SALK_106222; F2-10, SALK_088781) were acquired after a search of the Salk Institute Genomic Analysis Laboratory *Arabidopsis* gene-mapping database (<http://signal.salk.edu/cgi-bin/tdnaexpress>). Primers were designed to verify the T-DNA insertion in the candidate gene in each of the SALK lines: F2-44 (SALK_128572): (128572lp 5'-ACGGAATACTCGGTAGCGGGA-3', 128572rp 5'-TGACCTCAAATCAAGTGGTCCAA-3') F2-21 (SALK_106222): (106222lp 5'-CGCCGGCTTGATTCTTGATTT-3', 106222rp 5'-ATCGGACGGCTGTGGCTATTT-3'), F2-10 (SALK_088781): (088781lp 5'-CGGTTTTACCGTTCGTGAGA-3', 088781rp 5'-CCCAATGAAATCCCAACTCCA-3'). PCRs using *Taq* DNA polymerase were performed using genomic DNA extracted from each of the T-DNA insertion lines as template (see Section 2.3.1.1 for DNA extraction from *Arabidopsis*) and primer pairs; lp+rp (left primer and right primer), rp+LBb1 and lp+rp+LBb1. LBb1 is the left border primer of the T-DNA insertion (LBb1 5'-GCGTGGACCGCTTGCTGCAACT-3). The lp and rp are designed so that if all three primers are used in the same PCR then for wild-type plants (no insertion) there will be a PCR product of ~900bp, for homozygous insertion plants there will be a PCR product of ~700bp and heterozygotes will have both 900 and 700bp PCR products. For the PCRs using primer pairs lp+rp and rp+LBb1 a PCR product is produced in the lp+rp reaction for wild-type plants or heterozygous plants but no product produced for homozygous insertion plants. A PCR product is achieved in PCRs using rp+LBb1 for heterozygous or homozygous insertion plants but no product is produced for wild-type plants (Fig. 9). Amplification of only the homozygous PCR product in each of the PCRs confirmed incorporation of the T-DNA insertion into each of candidate genes in the SALK insertion lines (Fig. 5.10, 5.11 and 5.12). All individual plants from each of the insertion lines were indistinguishable from wild-type *Arabidopsis* Columbia plants grown under the same conditions. Light microscopy was used to analyse the phenotype of each of the homozygous insertion lines. Leaves from 20 day old seedlings which had 8-10 rosette leaves were prepared following the procedure outlined in Section 2.6.1. Using light microscopy it was impossible to differentiate between the chloroplasts in each of the insertion lines and the chloroplasts in a wild-type control, thus signifying that none of the candidate clones has a

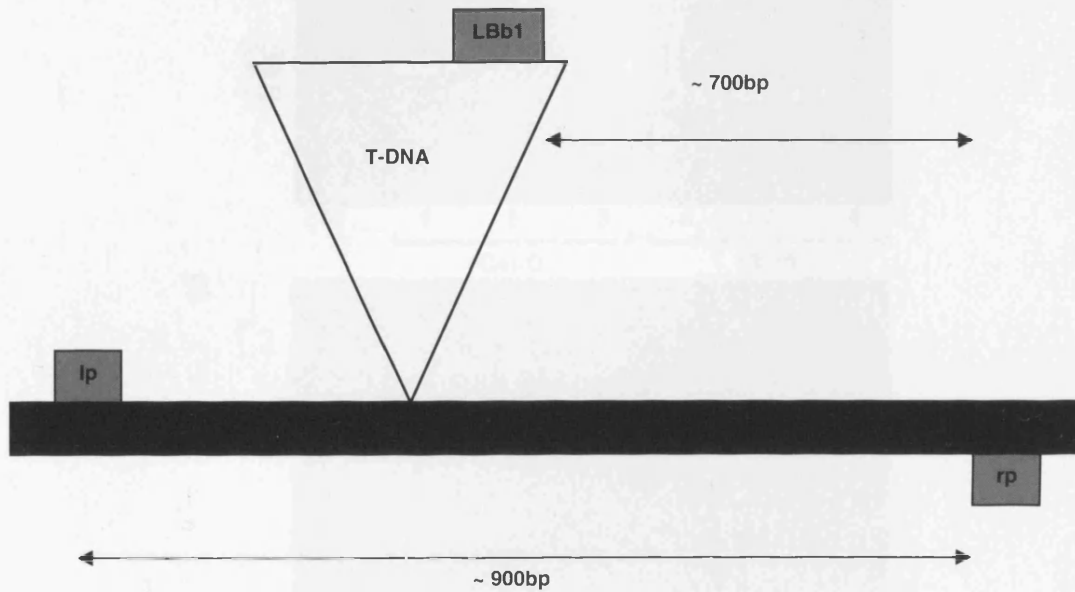


Fig. 5. 9. Schematic diagram illustrating the PCR products for SALK T-DNA insertion verification. For the PCRs using the primer pair lp+rp a PCR product of ~900bp is produced for wild-type plants and heterozygous plants but no PCR product for homozygous insertion plants. A PCR product is achieved in reactions using primers rp+LBb1 for heterozygous or homozygous plants but no product is produced for wild-type plants. If all three primers are used in the same reaction (lp + rp + LBb1), wild-type plants (no insertion) will have a PCR product of 900bp, homozygous insertion plants will have a PCR product of ~700bp and heterozygotes will have both 900 and 700 bp PCR products.

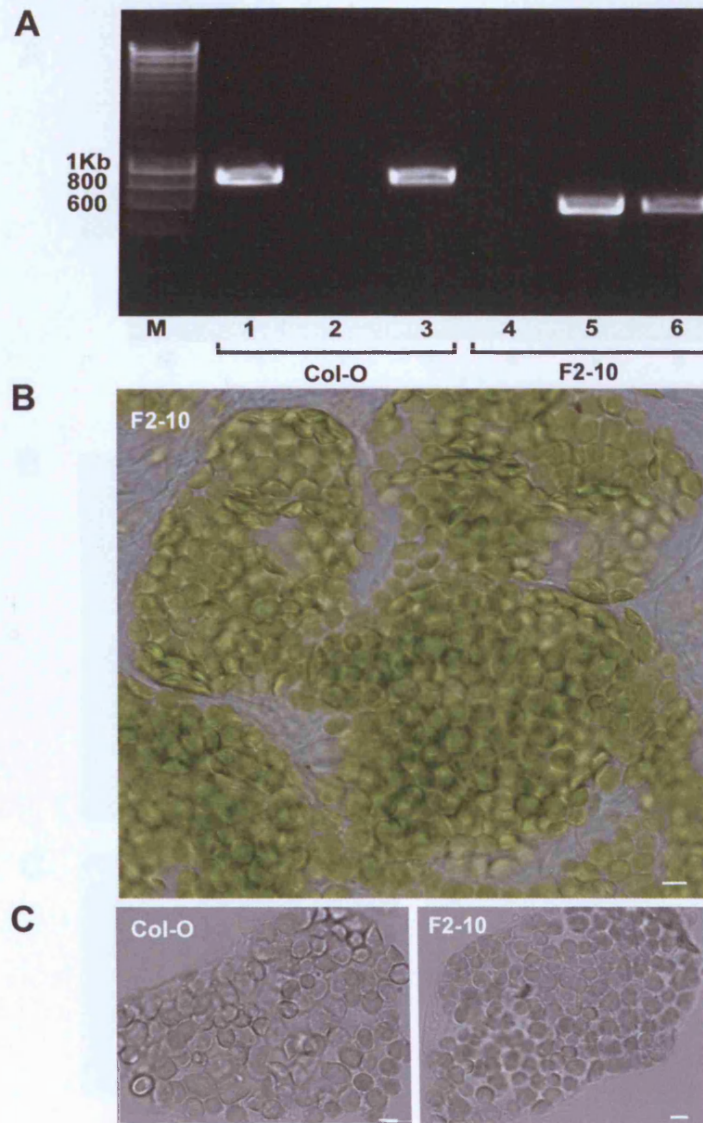


Fig. 5. 10. Analysis of T-DNA insertion mutants of F2-10. (A) T-DNA insertion verification PCR. In lanes 1-3 wild-type Col-O DNA was used as a template, for lanes 4-6 DNA from SALK_088781, a T-DNA insertion mutant of F2-10, was used as a template. For the PCRs in lanes 1 + 4 the primer pair lp + rp was used. For the PCRs in lanes 2 + 5 the primer pair LBb1 + rp was used. PCRs in lanes 3 + 6 used lp + rp + LBb1. The PCRs verified that the *Arabidopsis* plant analysed was homozygous for the T-DNA insertion in F2-10. (B) + (C) Microscopic analysis of the chloroplasts of SALK_088781 a T-DNA insertion in F2-10. Two week old seedlings were prepared as outlined in Section 2.6.1. Images were captured using a Nikon D100 digital camera (B) and Hamamatsu Orca ER 1394 cooled CCD camera (C). Non-fixed samples were also analyzed. Scale bars = 5 μ m.

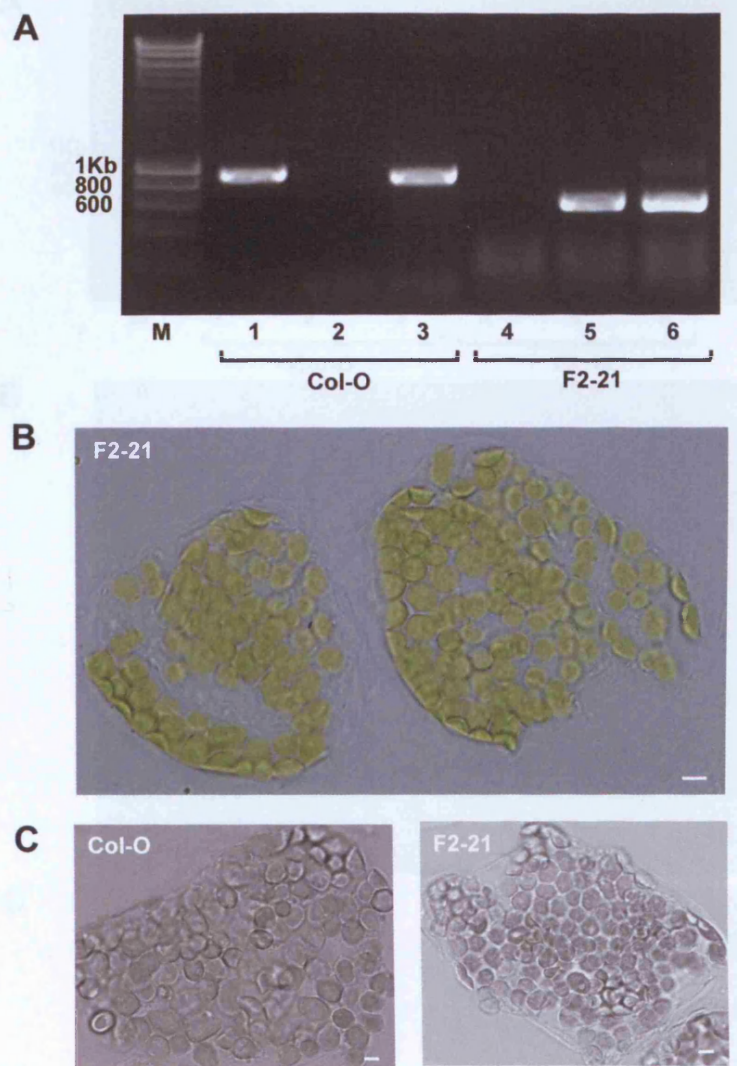


Fig. 5. 11. Analysis of T-DNA insertion mutants of F2-21. (A) T-DNA insertion verification PCR. In lanes 1-3 wild-type Col-O DNA was used as a template, for lanes 4-6 DNA from SALK_106222, a T-DNA insertion mutant of F2-21, was used as a template. For the PCRs in lanes 1 + 4 the primer pair lp + rp was used. For the PCRs in lanes 2 + 5 the primer pair Lbb1 + rp was used. PCRs in lanes 3 + 6 used lp + rp + Lbb1. The PCRs verified that the *Arabidopsis* plant analysed was homozygous for the T-DNA insertion in F2-21. (B) + (C) Microscopic analysis of the chloroplasts of SALK_106222. Two week old seedlings were prepared as outlined in Section 2.6.1. Images were captured using a Nikon D100 digital camera (B) and Hamamatsu Orca ER 1394 cooled CCD camera (C). Non-fixed samples were also analyzed. Scale bars = 5 μ m.

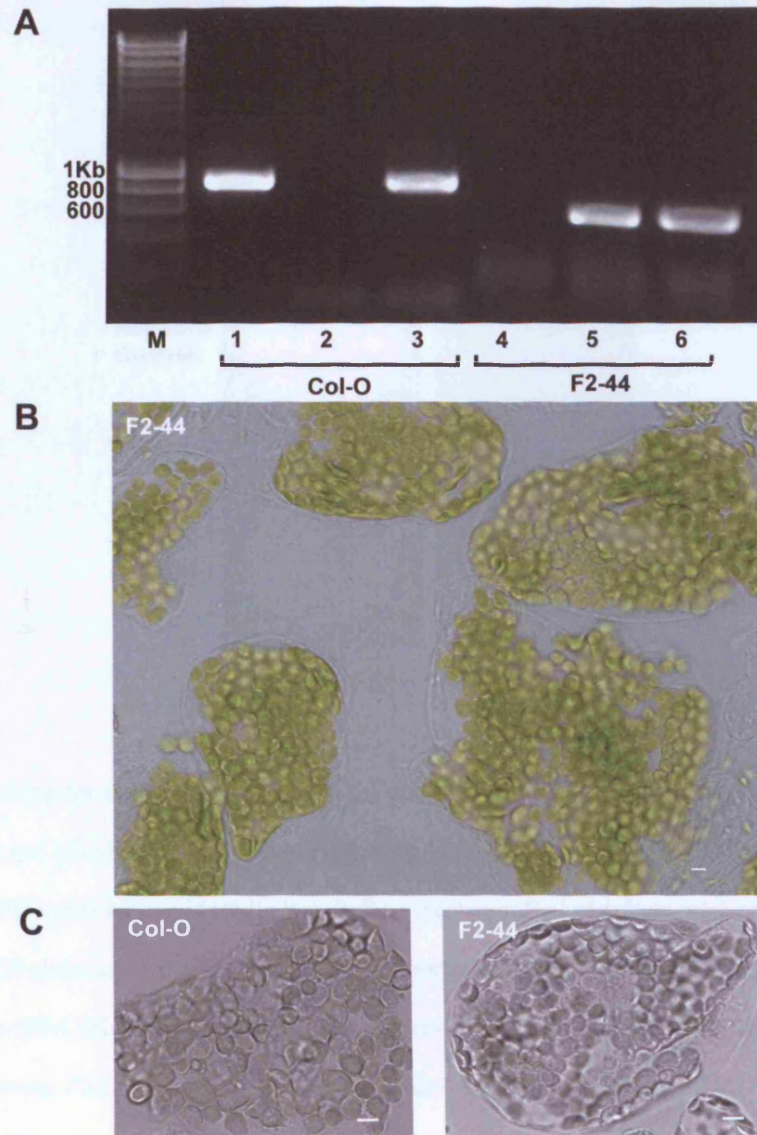


Fig. 5. 12. Analysis of T-DNA insertion mutants of F2-44. (A) T-DNA insertion verification PCR. In lanes 1-3 wild-type Col-O DNA was used as a template, for lanes 4-6 DNA from SALK_128572, a T-DNA insertion mutant of F2-44, was used as a template. For the PCRs in lanes 1 + 4 the primer pair lp + rp was used. For the PCRs in lanes 2 + 5 the primer pair LBB1 + rp was used. PCRs in lanes 3 + 6 used lp + rp + LBB1. The PCRs verified that the *Arabidopsis* plant analysed was homozygous for the T-DNA insertion in F2-44. (B) + (C) Microscopic analysis of the chloroplasts of SALK_128572. Two week old seedlings were prepared as outlined in Section 2.6.1. Images were captured using a Nikon D100 digital camera (B) and Hamamatsu Orca ER 1394 cooled CCD camera (C). Non-fixed samples were also analyzed. Scale bars = 5 μ m.

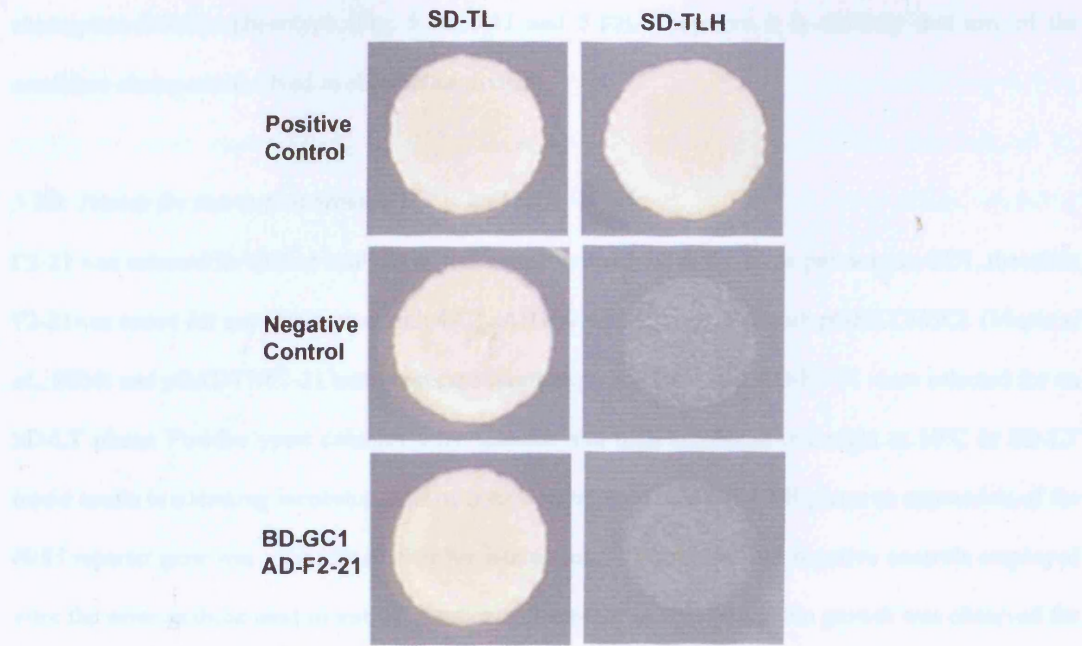


Fig. 5. 13. Testing for interaction between F2-21 and GC1. AH109 cells were co-transformed with pGBKT7/GC1 and pGADT7/F2-21. Yeast expressing both BD-GC1 and AD-F2-21 were incubated overnight at 30°C in SD-LT liquid media in a shaking incubator. 5 µl of culture were spotted onto SD-LT and SD-LTH plates and expression of the *HIS3* reporter gene was used as a marker for interaction. No growth on SD-LTH was observed in cells expressing BD-GC1 and AD-F2-21 signifying no interaction between F2-21 and GC1. AH109 cells were co-transformed with pGADT7-Rec + SV40 Large-T PCR fragment and pGBKT7-53 as a positive control and pGADT7 and pGBKT7 empty vectors as a negative control.

chloroplast division phenotype (Fig. 5.10, 5.11 and 5.12). Therefore it is unlikely that any of the candidate clones are involved in chloroplast division.

5.2.9. Testing for interaction between F2-21 and GC1

F2-21 was selected for further analysis as it is possibly involved in the same pathway as GC1, therefore F2-21 was tested for any interaction with GC1. AH109 was transformed with pGBKT7/GC1 (Maple *et al.*, 2004) and pGADT7/F2-21 and yeast expressing both BD-GC1 and AD-F2-21 were selected for on SD-LT plates. Positive yeast colonies were selected and cells incubated overnight at 30°C in SD-LT liquid media in a shaking incubator. 5 µl of cells were spotted onto SD-LTH plates as expression of the *HIS3* reporter gene was used as a marker for interaction. The positive and negative controls employed were the same as those used to test the candidate clones for re-interaction. No growth was observed for yeast co-expressing GC1 and F2-21 signifying that GC1 and F2-21 do not interact (Fig. 5.13).

5.2.10. Using Co-immunoprecipitation to hunt for novel chloroplast division components

As the yeast two-hybrid screening has proved to be unsuccessful in identifying novel chloroplast division components an alternative strategy of co-immunoprecipitation was investigated. The principal behind co-immunoprecipitation is simple; an antibody specific to the bait protein is added to a cell lysis. The antibody-protein complex is pelleted usually using protein-G sepharose which binds most antibodies. If there are any protein/molecules bound to the bait protein, they will also be pelleted. Identification of proteins in the pellet can be determined by sequencing purified protein bands. Often instead of using an antibody specific to the bait protein, tagged bait proteins are used. Antibodies to the tag are used to precipitate the bait protein and any interacting partners. This approach means that the time consuming process of raising antibodies is avoided.

FtsZ2-1 was chosen as bait to be used in co-immunoprecipitation. FtsZ2-1 was selected over FtsZ1-1 because of the presence of the core domain conserved from the bacterial FtsZ homologues, which is absent in FtsZ1 family proteins. It has already been demonstrated that this core domain is involved in interactions of FtsZ2-1 with other proteins; ARC6 interacts specifically with FtsZ2-1 and this interaction is mediated through the core domain (Chapter 4; Maple *et al.*, 2005).

Originally a haemagglutinin (HA) tag to FtsZ2-1 was used (FtsZ2-1-HA). FtsZ was fused to the N-terminus of a three consecutive copies of HA (MYPYDVPDYASL) within the vector PER-10

which contains the chemically induced transcription activator XVE (Zuo *et al.*, 2000). This construct was introduced to *Arabidopsis* through floral dipping (Section 2.1.4) and transgenic plants selected by plating on media containing 40 $\mu\text{g ml}^{-1}$ kanamycin. Expression of FtsZ2-1-HA was induced by spraying plants every 24 hours with 5 μM 17- β -estradiol. Microscopic analysis of seedlings expressing FtsZ2-1-HA revealed cells with few but enlarged chloroplasts indicating that overexpression of FtsZ2-1 had occurred. However, expression of FtsZ2-1-HA was patchy and many cells had a wild-type complement of chloroplasts. Co-immunoprecipitation assays were performed as described in Section 2.3.3.5 but failed to precipitate FtsZ2-1-HA. Possibly the HA tag was unstable and cleaved off within the chloroplasts or the expression of FtsZ2-1-HA was insufficient for successful co-immunoprecipitation.

After unsuccessful experimentation with HA tags, YFP was used to tag FtsZ2-1. FtsZ2-1 was amplified from cDNA using the primers FtsZ/24 (5'-ATCTCGAGATGGCAACTTACGTTTCACC-3' *XhoI* is underlined) and FtsZ/25 (5'-TATTAATTAAGACTCGGGGATAACGAGAGC-3' *PacI* is underlined) removing the termination codon and was cloned into pPCR-Script. FtsZ2-1 was subcloned into the *XhoI* and *KpnI* sites of pWEN18 fused to the N-terminal of YFP. FtsZ2-1-YFP was subsequently subcloned into the *XhoI* and *PacI* sites of the multiple cloning site of the pTA-211 vector. pTA-211/ FtsZ2-1-YFP was introduced into *Arabidopsis* using the floral dip method (Section 2.1.4).

pTA-211 has an inducible promoter controlled by the chimeric transcription factor GVG (Aoyama and Chua, 1997). GVG consists of the DNA-binding domain of GAL4, the activation domain of the herpes viral protein VP16 and the receptor domain of the rat glucocorticoid receptor (GR). Six copies of the GAL4 UAS are fused to the CaMV 35S promoter upstream of the pTA-211 multiple cloning site. GVG binds the GAL4 UAS sequences through the GAL4 DNA-binding domain and activates transcription through the VP16 activation domain. The GR domain controls the GVG transcription factor as it represses the VP16 activation domain unless glucocorticoids are bound to the GR. When glucocorticoids are bound to the GR de-repression of the VP16 activation domain occurs and transcription is activated. To induce expression of FtsZ2-1-YFP dexamethasone, a strong synthetic glucocorticoid, was used. The use of an inducible promoter meant that the expression of FtsZ2-1-YFP could be controlled; therefore co-immunoprecipitation could be performed in plants that have wild-type chloroplasts but are temporally overexpressing FtsZ2-1-YFP. If a constitutive promoter was used

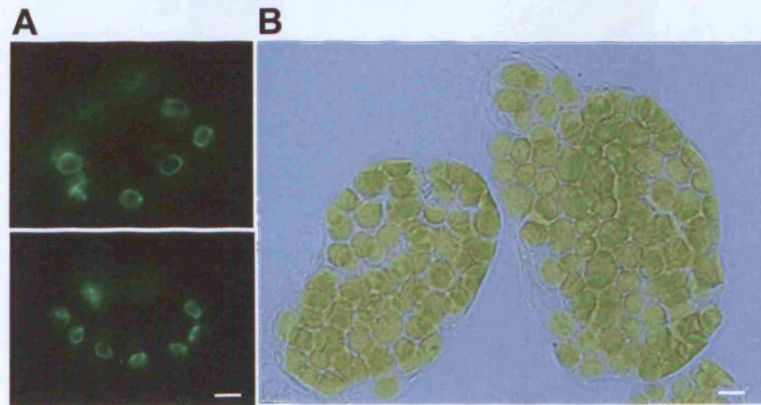


Fig. 5. 14. Transgenic *Arabidopsis* expressing FtsZ2-1-YFP. (A) Rings of FtsZ2-1-YFP were detected by epifluorescence microscopy after expression of FtsZ2-1-YFP was induced by spraying with dexamethasone. (B) Microscopic analysis of mesophyll cells from *Arabidopsis* transformed with pTA-211/FtsZ2-1-YFP. Chloroplasts appeared to be of wild-type size and number without induction of expression of FtsZ2-1-YFP demonstrating that expression of FtsZ2-1-YFP is tightly controlled. Scale bars = 5 μ m.

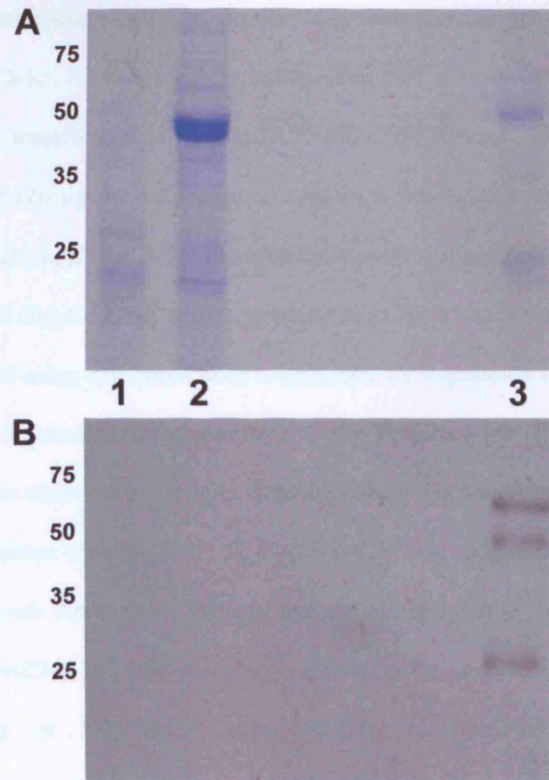


Fig. 5. 15. Co-immunoprecipitation using FtsZ2-1-YFP as bait. (A) Coomassie stained SDS-PAGE. (B) Western blot of SDS-PAGE. The primary antibody used on the western blot was the Living Colours Antibody also used for co-immunoprecipitation. Anti-rabbit antibody conjugated to horseradish peroxidase was used as a secondary antibody and was detected using BM Chemiluminescence Western Blotting Substrate (POD) (Roche). Lane 1 = cell lysate from Col-O seedlings, lane 2 = cell lysate from seedlings expressing FtsZ2-1-YFP, lane 3 = co-immunoprecipitation sample.

transgenic plants would contain only one or two large chloroplasts per cell due to the continuous overexpression of FtsZ2-1.

Arabidopsis seedlings transformed with pTA211/FtsZ2-1-YFP were selected for on Lehle plates containing hygromycin ($20 \mu\text{g ml}^{-1}$). Transgenic seedlings were grown and allowed to self pollinate and the T₂ progeny were used for co-immunoprecipitation experiments. The expression of FtsZ2-1-YFP was induced in 20 day-old seedlings by spraying with $30\mu\text{M}$ dexamethasone. After 16 hours the seedlings were analysed using epifluorescence microscopy for expression of FtsZ2-1-YFP. Feint rings of FtsZ2-1-YFP were detected in one of the lines of the T₂ generation (Fig. 5.14) however FtsZ2-1-YFP expression was not observed in all cells. Seedlings from this line were harvested and used in co-immunoprecipitation assays (Section 2.3.3.5). FtsZ2-1-YFP was precipitated using Full-Length A.v. Polyclonal Living Colours Antibody (Clontech) and the antibody/protein complex precipitated using protein-G sepharose. FtsZ2-1-YFP and any co-precipitated proteins were removed from the protein-G sepharose by boiling in SDS-PAGE sample buffer (Section 2.3.5.2). The resultant co-immunoprecipitation sample was analysed by SDS-PAGE, one gel was subsequently stained with coomassie staining and a replica gel was used for Western blotting to detect the presence of FtsZ2-1-YFP (Fig. 5.15). In the Western blot FtsZ2-1-YFP was not detected in a sample of the cell lysate taken before the co-immunoprecipitation procedure but FtsZ2-1-YFP was detected in the co-immunoprecipitation sample as a band of approximately 67kDa (Fig. 5.15). This is most probably due to an enrichment of FtsZ2-1-YFP during the co-immunoprecipitation procedure. On the coomassie stained gel apart from the bands corresponding to the heavy and light chains of the Living Colours antibody (50kDa and 25kDa respectively) only feint bands of protein were observed making identification of the proteins in the bands difficult. Because of the absence of a band corresponding to FtsZ2-1-YFP in the cell lysate sample on the Western blot and because only feint FtsZ2-1-YFP rings were detected by epifluorescence microscopy, it is likely that there was not enough FtsZ2-1-YFP in the cell lysate at the start of the co-immunoprecipitation assay for the experiment to be successful. Various parameters of the experiment were altered in order to increase the level of FtsZ2-1-YFP. This included increasing the concentration of dexamethasone up to 50 and 100 μM and spraying continually with dexamethasone every 24 hours for up to 14 days to try and increase the concentration of FtsZ2-1-YFP within the cell lysate. A larger cell lysate volume was also used at the beginning of the co-

immunoprecipitation procedure to increase the amount of FtsZ2-1.YFP present but FtsZ2-1.YFP was still not detectable by Western blotting within the cell lysate sample.

5. 3. Discussion

Yeast two-hybrid screens were performed using two different bait proteins, AtFtsZ1-1 and AtFtsZ2-1 to identify novel plastid division proteins. AtFtsZ1-1 and AtFtsZ2-1 were chosen as baits because the Z-ring formed by the polymerisation of FtsZ proteins is integral to the plastid division machinery. Screens were performed using both AtFtsZ1-1 and AtFtsZ2-1 because although FtsZ proteins from the FtsZ1 and FtsZ2 families share high homology at the amino acid level, they are functionally distinct (Osteryoung *et al.*, 1998; El-Kafafi *et al.*, 2005) and crucially for this study it has been demonstrated that other plastid division components interact specifically with FtsZ1 or FtsZ2 proteins (Maple *et al.*, 2005; Maple *et al.*, In Press). To complement the yeast two-hybrid studies, co-immunoprecipitation using AtFtsZ2-1 as bait was also performed.

5.3.1. Selection of candidate clones

After screening the cDNA library a total of 203 His⁺ colonies were retrieved for FtsZ1-1 and 63 colonies for FtsZ2-1. The strength of the interaction between the library and the bait proteins was estimated by the level of *LacZ* activation in colony lift filter assays and the strongest interacting candidates picked from each screen. Unique candidate clones were subjected to DNA sequencing and compared to the annotated *Arabidopsis* genome database for identification. Those candidates identified that are already characterised and assigned functions separate from plastid division and also those candidates that contain domains predicted by the Pfam database to have functions distinct from chloroplast division were discarded. Although many proteins were discarded due to their function being distinct from plastid division, several proteins recently identified to have a role in plastid division are also not typical plastid division candidates. These include MSL2 and MSL3 which function as mechanosensitive ion channels. In an *msl2-1* and *msl3-1* double mutant, cells are observed with large chloroplasts (Haswell and Meyerowitz, 2006). Additionally AtCDT1a, a pre-replication factor and substrate of the CDKA-cyclinD complex (Castellano *et al.*, 2004), has been shown through yeast two-hybrid and BiFC analysis to interact with ARC6 (Raynaud *et al.*, 2005). Simultaneous down regulation of AtCDT1a and AtCDT1b results in 50% of leaf cells containing 3-4 enlarged chloroplasts (Raynaud *et al.*, 2005). In light of these recent studies, the candidates dismissed through these yeast two-hybrid screens should not be eliminated because their predicted function appears distinct from plastid division. To decisively eliminate F1-10 (a MYB3 family transcription factor (Yanhui *et al.*, 2006)), and F1-9, (a

glycosyl hydrolase family 38 protein involved in carbohydrate metabolism), further analysis should be performed. F1-122 and F2-62, two proteins of unknown function were discarded due to the absence of a transit peptide. To further eliminate them as chloroplast division proteins localisation analysis and over-expression analysis can be performed.

Three proteins were selected for further analysis F2-44, a protein of unknown function, F2-10 a C2-domain containing protein and F2-21 a UDP-glucuronosyl/UDP-glucosyl transferase family protein.

5.3.2. Analysis of F2-44

F2-44 (At4g36980) encodes a protein of 560 amino acids. Searches using BlastN and BlastP algorithms revealed no homology to other *Arabidopsis* proteins although a homologue of this protein was found in rice *Oryza sativa*, accession number ABF96420, that had 68% amino acid identity. The *O. sativa* homologue is also a protein of unknown function, thus *F2-44* represents a unique gene within the *Arabidopsis* genome but a gene that is conserved across at least two higher plant species. Alignment of F2-44 and the *O. sativa* homologue is shown in (Fig. 5.16). Searching the Pfam database did not identify any conserved domains within F2-44. Transit peptide prediction for F2-44 and the *O. sativa* homologue was carried out by using the TargetP server; both proteins were predicted to localise to the mitochondria, although in both cases the prediction was made with low reliability. Transit peptide prediction is not always accurate and studies have demonstrated that some proteins have dual localisation to both the mitochondria and chloroplasts (AtSufE (Xu *et al.*, 2006) AtZn-MP (Bhushan *et al.*, 2003), Pea glutathione reductase (GR) (Rudhe *et al.*, 2004)), therefore F2-44 was not eliminated from further study because of a negative transit peptide prediction.

To investigate whether F2-44 is a chloroplast division component a T-DNA insertion mutant; SALK_128572 was investigated to see if plants deficient in F2-44 exhibited a chloroplast division mutant phenotype. F2-44 seedlings and mature plants were indistinguishable from wild-type *Arabidopsis* Columbia plants grown under the same conditions. Microscopic analysis of F2-44 seedlings revealed no abnormal chloroplast phenotype (Fig. 5.12) suggesting that F2-44 is not involved in the chloroplast division machinery. Although the phenotype of the proplastids in the meristems of F2-44 was not investigated it seems unlikely that proplastid division is altered in F2-44 seedlings. In

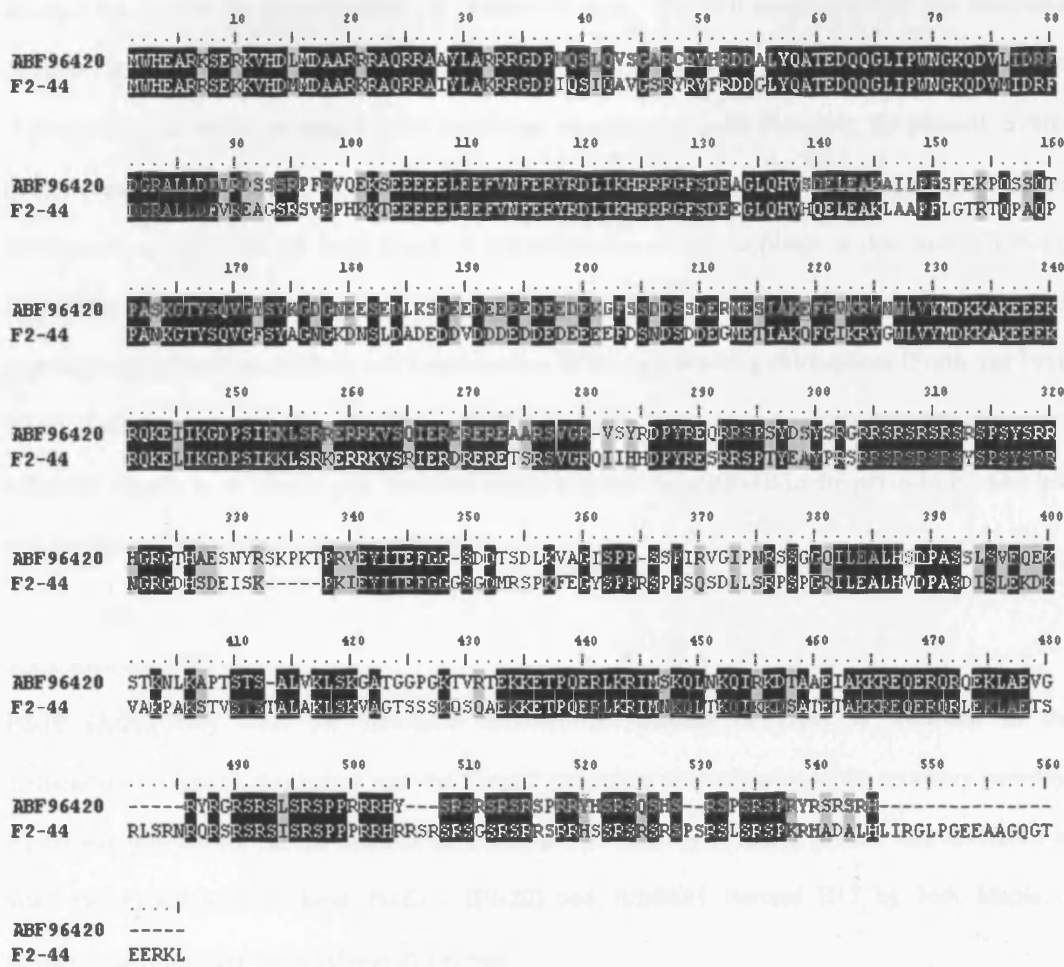


Fig.5. 16. Alignment of F2-44 and the *Oryza sativa* homologue (accession number ABF96420). Sequences were aligned using ClustalW (Higgins *et al.*, 1994; <http://www.ebi.ac.uk/clustalw/>) and viewed using BioEdit.

arc6 where the proplastid phenotype has been examined, both proplastid division and chloroplast division are affected by the *arc6* mutation (Roberson *et al.*, 1995). It seems doubtful that proplastid division can be altered without observing a chloroplast division phenotype due to the reduced number of proplastids that would be present in the progenitor of mesophyll cells. However, the plastids in other tissues could be examined. In mesophyll cells in *suffulta* mutants in tomato only a few greatly enlarged chloroplasts are observed but there is a wildtype population of chromoplasts in ripe fruit (Forth and Pyke, 2006). Analysis of the ripening tomatoes of the *suffulta* mutant reveals that the chromoplast population arises through budding and fragmentation of the degenerating chloroplasts (Forth and Pyke, 2006). This novel plastid division mechanism demonstrates that a plastid division mutation may not affect the plastids in all tissue types, therefore analysis of the chromoplasts in the petals of F2-44 could also be analysed for a plastid division phenotype.

5.3.3. Analysis of F2-10

F2-10 (At2g20990) from the annotated *Arabidopsis* database in TAIR is localised to the endomembrane system, this agrees with the TargetP prediction of localisation to the secretory pathway. F2-10 was selected for further analysis as a similar C2 domain-containing protein was identified in yeast two-hybrid screens using FtsZ1-1 (F1-10) and AtMinE1 (termed E17 by Jodi Maple, a postdoctoral researcher in the laboratory) as bait.

The Pfam database recognises two C2 domains within F2-10. The C2 domain is a Ca^{2+} -dependent membrane-targeting module found in many cellular proteins involved in signal transduction or membrane trafficking. C2 domains are thought to be involved in calcium-dependent phospholipid binding (Davletov and Sudhof, 1993) and are found in many eukaryotic proteins that interact with cellular membranes. One of the many proposed functions of C2 domain-containing proteins is the regulation of Ca^{2+} -triggered cellular events through Ca^{2+} -regulated membrane trafficking. Since the ATPase activity of AtMinD1 is Ca^{2+} -dependent (Chapter 3) F2-10 could be involved in the regulation of plastid division processes. Alignment of F2-10 and E17 together with rat synaptotagmin I (Syn1) and mouse syt13 shows both F2-10 and E17 contain the conserved asparagine residues implicated in Ca^{2+} binding (Sutton *et al.*, 1995) within the C2 domain. Despite similarities within the C2 domain of E17 and F2-10 the overall structure of the two proteins is different; E17 contains one N-terminal C2

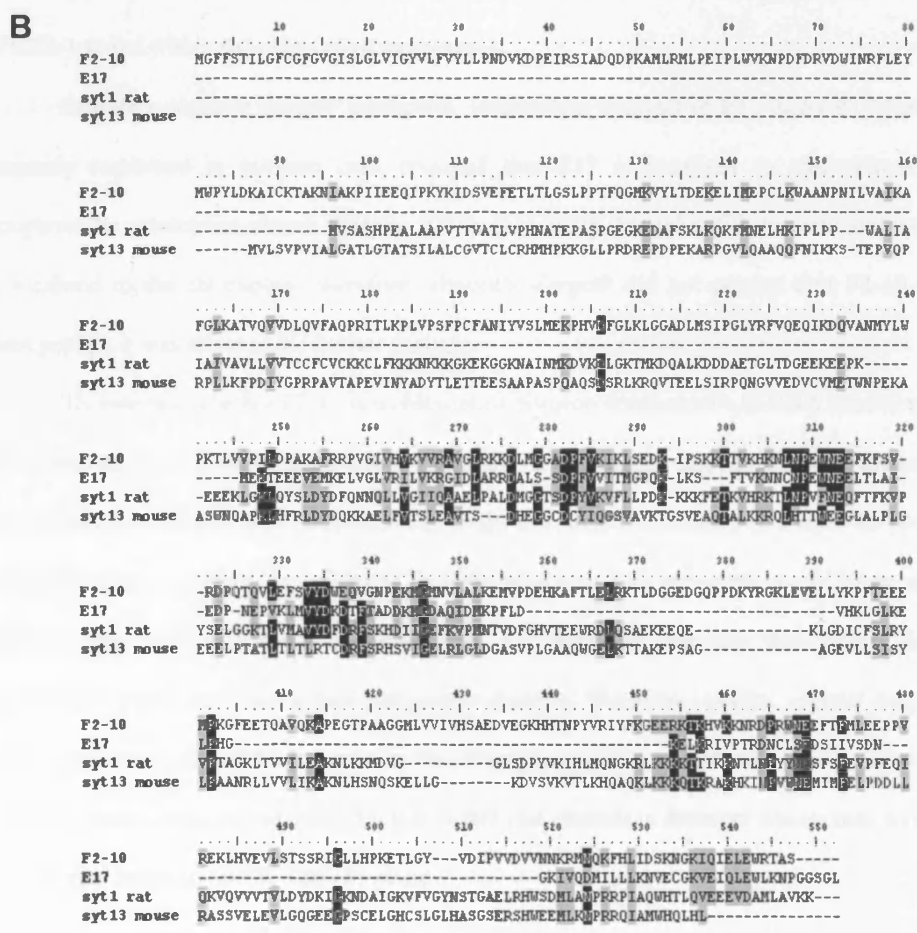
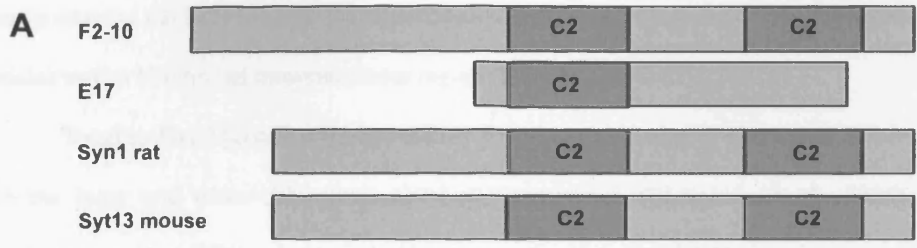


Fig. 5. 17. (A) Schematic of domain structure of F2-10 (Swiss-prot accession number Q9SKR2), E17 (accession number Q9S764), rat synaptotagmin I (Syn1) (accession number Q9EQT6) and mouse Syt13 (Q9EQT6). (B) Alignment of F2-10, E17, Syn1 and Syt13. Sequences were aligned using ClustalW (Higgins *et al.*, 1994; <http://www.ebi.ac.uk/clustalw/>) and viewed using BioEdit.

domain whereas F2-10 belongs to the C-terminal type (C-type) C2 protein family with two tandem C2 domains and an N-terminal transmembrane region (Fukuda, 2003) (Fig. 5.17).

Tobacco FtsZ2 protein although mainly found in the stroma is also found associated with the both the inner and outer chloroplast envelope membranes (El-Kafafi *et al.*, 2005). C2-domain containing proteins exhibit membrane binding properties therefore F2-10 may interact with the subset of FtsZ2-1 found within the chloroplast membranes.

Despite a negative TargetP prediction, localisation analysis of E17 using E17 fusions to YFP transiently expressed in tobacco cells revealed that E17 is localised to chloroplasts and found throughout the chloroplast stroma (Maple, 2005). It is likely that other C2-domain containing proteins are localised to the chloroplast, therefore, although TargetP did not predict that F2-10 contained a transit peptide it was selected for further analysis.

To ascertain whether F2-10 is a chloroplast division component a T-DNA insertion line SALK 088781 was analysed by light microscopy. Chloroplasts within the mesophyll cells of the rosette leaves of SALK 088781 exhibited no abnormal phenotype therefore a deficiency of the F2-10 protein has no discernable affect on chloroplast division. In agreement with this, transgenic *Arabidopsis* plants highly expressing E17-YFP contained chloroplasts of wild type-like numbers and sizes (Maple, 2005) suggesting that E17 does not affect chloroplast division. These two results suggest that C2-domain containing proteins do not have a role in the chloroplast division machinery. However as with F2-44 only green tissues were examined and it is possible that plastids in different tissues may have a division mutation phenotype in SALK_088781 plants.

5.3.4. Analysis of F2-21

F2-21 (At1g07240) was identified by the Pfam database as a UDP-glucose glucosyltransferase, a family of enzymes that catalyzes the transfer of glycosyl residues from a UDP-sugar to acceptor molecules thereby regulating the properties of the acceptor (reviewed in Ross *et al.*, 2001). F2-21 was selected for further analysis as is possibly involved in the GC1 pathway as GC1 has high secondary structural similarity to nucleotide-sugar epimerases (Maple *et al.*, 2004). An epimerase is an enzyme that interconverts epimers often modifying protein activity or surface recognition. Nucleotide sugar epimerases use nucleotide-sugar substrates for a variety of chemical reactions. The conjugation of UDP

to sugars and subsequent epimerase interconversion is important in prokaryotes for sugar activation to form polymers for a variety of functions (Baker *et al.*, 1998). It is possible that F2-21 could act in the same pathway as GC1 to regulate the UDP-sugar molecules.

BlastP and blastN searches revealed F2-10 has high homology to many other *Arabidopsis* UDP-glucose glucosyltransferases. This is no surprise as *Arabidopsis* UDP glucosyltransferases form a large multigene family with an estimated 120 members (Li *et al.*, 2001; Ross *et al.*, 2001). UDP glucosyltransferases are found throughout the plant and animal kingdoms and blastP searching of sequences of proteins from all organisms contained within the NCBI database revealed homologues of F2-21 in many different plant species.

To assess whether F2-10 was involved in chloroplast division a T-DNA insertion line of F2-10; SALK_106222 was analysed for a chloroplast division phenotype. The chloroplasts of SALK_106222 appeared wild-type for chloroplast size and number (Fig. 5.7). Because of the large number of UDP glucosyltransferase proteins within *Arabidopsis* it is possible that there is some redundancy exists between the functions of the different members of the UDP glucosyltransferase family, therefore if UDP glucosyltransferases are involved in chloroplast division it is unlikely that removal of a single gene will exhibit a chloroplast division phenotype. Interaction between GC1 and F2-10 was investigated using the yeast two-hybrid system. No interaction was detected between GC1 and F2-10. However lack of interaction with GC1 does not mean that F2-10 is not involved in the same pathway as GC1. F2-10 could act either upstream or down stream of GC1 in the same pathway.

5.3.5. Using co-immunoprecipitation to hunt for novel chloroplast division components

Co-immunoprecipitation can be used as an alternative to yeast two-hybrid screening. The main advantage of co-immunoprecipitation over the yeast two-hybrid system is that co-immunoprecipitation is carried out in the natural *in planta* environment rather than in a heterologous system. This means that every expressed protein that makes up the *Arabidopsis* proteome is definitely represented and is screened, this cannot be guaranteed when constructing a cDNA library for yeast two-hybrid screening. The conditions under which the proteins would normally interact are also maintained, the conditions in a heterologous system may not be favourable for some interactions.

FtsZ2-1 tagged with YFP was used as bait for co-immunoprecipitation. Although FtsZ2-1 was recovered from cell lysates of transgenic *Arabidopsis* expressing FtsZ2-1-YFP the quantities of FtsZ2-

1-YFP precipitated were not sufficient to successfully identify co-precipitated proteins as the amount of co-precipitated proteins was so little. It is likely that there was not enough FtsZ2-1-YFP expressed within the transgenic *Arabidopsis* to make co-immunoprecipitation successful. The evidence for this conclusion is that no FtsZ2-1-YFP was detectable by Western blotting in the cell lysate sample however enrichment of FtsZ2-1-YFP occurs during co-immunoprecipitation therefore FtsZ2-1-YFP must be present but in low amounts. When transgenic seedlings expressing FtsZ2-1-YFP were analysed by epifluorescence microscopy only faint rings of FtsZ2-1-YFP were observed compared to the network of FtsZ rings often observed when FtsZ proteins are overexpressed (Maple *et al.*, 2005; see Chapter 4). FtsZ2-1-YFP expression was not observed in all cells, suggesting that the level of expression of FtsZ2-1-YFP was probably insufficient for co-immunoprecipitation. Several of the parameters of the co-immunoprecipitation assay were adjusted to maximise the amount of FtsZ2-1-YFP within the cell lysate; Different concentrations of dexamethasone were used and seedlings were sprayed with dexamethasone over a prolonged period of time to try to increase *FtsZ2-1-YFP* expression. In addition to this, larger initial cell lysate volumes were used to try to increase the amount of FtsZ2-1-YFP. However, the level of FtsZ2-1-YFP remained inadequate to perform successful co-immunoprecipitation.

The reason for the low levels of FtsZ2-1-YFP is probably due to the transgenic *Arabidopsis* lines used. Patchy expression is often observed in transgenic plants even in those with inducible promoters (Zuo *et al.*, 2000). Transgenes can often be subject to gene silencing which may occur through both transcriptional and post-transcriptional mechanisms and usually involves either methylation of the transgene itself or methylation of promoter sequences (Vaucheret *et al.*, 1998). Although more research is required to understand the processes of gene silencing, several mechanisms of gene silencing have been investigated. Position effects are caused by the genomic context in which the transgene is located and may be affected by several factors such as abrupt changes in GC content, the repetitiveness of the flanking sequence, location within centromeric or intercalary heterochromatin and the methylation status of the flanking sequence (reviewed in Matzke and Matzke, 1998). However recent studies have dismissed position effects as a major contributing cause of transgene silencing (Schubert *et al.*, 2004) and post transcription mechanisms are believed to be the main factor in gene silencing. Integration of multiple copies of the transgene can silence transgene expression beyond a

gene specific threshold (Muskens *et al.*, 2000; Schubert *et al.*, 2004). This is thought to occur through the generation of siRNAs which target the transgene RNA and cause degradation of the RNA.

To improve the level of FtsZ2-1-YFP other transgenic *Arabidopsis* lines transformed with pTA-211/FtsZ2-1-YFP should be investigated, perhaps the line that was used in this study was subject to gene silencing and other lines could be used successfully.

Co-immunoprecipitation remains a good strategy to identify novel chloroplast division components. To improve the assay other tags could be tried, for example Histidine tags, or other inducible promoters may be used to generate a higher level of expression. As an alternative to using transgenic lines specific antibodies could be raised against the bait protein; if there is sufficient endogenous FtsZ2-1 within the chloroplasts antibodies raised against FtsZ2-1 can be used to precipitate FtsZ2-1 and any interacting proteins. Using specific antibodies also has the advantage of eliminating sometimes bulky tags which may affect the folding of the protein or block binding sites, this may be a concern when using FtsZ2-1 as a bait since the C-terminal core domain which mediates some interactions (Maple *et al.*, 2005) could be affected by bulky C-terminal tags. Because of the N-terminal transit peptide of FtsZ2-1 tags must be fused to the C-terminus potentially disrupting the core domain and therefore blocking interaction with other proteins.

5.3.6. Conclusion

Yeast two-hybrid screening using AtFtsZ2-1 and AtFtsZ1-1 as bait was used to try and identify novel chloroplast division components. Although altogether 13 unique candidate clones were identified as possible interacting proteins, through *in silico* analysis and microscopy of T-DNA insertion lines it seems unlikely that any of the candidates are involved in chloroplast division. However, investigation of each of the candidates was not exhaustive. Only three of the candidates were predicted to localise to the chloroplast but these are well characterised proteins and are not reported to be involved in chloroplast division. Experiments using YFP fusions to candidate clones could be performed to establish the localisation of each of the candidate clones to decisively eliminate some of the other candidates such as F1-122 and F2-62 which are expressed proteins of unknown function.

Yeast two-hybrid screening is a powerful tool to search for novel interacting proteins; it is a rapid and sensitive assay, however false positives often occur. Although in this study co-immunoprecipitation was unsuccessful, because co-immunoprecipitation is performed in the *in planta*

environment, it is likely to be a much more effective way of hunting for novel proteins through protein-protein interactions.

6. Regulation of gene expression and plastid division

6.1 Introduction

Although much research has been conducted into the molecular machinery of plastid division, to date, very little is known about the regulation of plastid division.

Chloroplast number per cell and cell size are closely correlated. Exposure to high light leads to elongation of the palisade cells and the chloroplasts proliferate to occupy this space (Pyke, 1999). Therefore chloroplast division initiation appears to respond to cell size. This response in chloroplast proliferation may be guided through monitoring of chloroplast envelope tension meaning that chloroplast division may exhibit density-dependent control (Pyke, 2006). However density-dependent control would only apply to chloroplast proliferation in mesophyll and palisade cells as plastids in other tissues are not as tightly packed. A mutually compensating mechanism between chloroplast number and chloroplast size exists, resulting in a consistent relationship between chloroplast compartment size and the size of a cell. Even when mutations inhibit chloroplast division the chloroplasts are larger thus compensating for the reduction in number maintaining the chloroplast compartment size within the cell (Pyke, 1997). One exception to this rule is the high pigment-1 (*hp-1*) mutant in tomato. In fully expanded leaves of *hp-1* there is increased chloroplast density and increased chloroplast size (Cookson *et al.*, 2003). The *HP-1* gene has been identified as the UV-damaged DNA binding protein 1 (DDB1) (Lieberman *et al.*, 2004; Liu *et al.*, 2004). The DDB1 *Arabidopsis* homologue (DDB1A; Schroeder *et al.*, 2002) has been shown to interact with DET1. The DET1/DDB1 complex is proposed to interact with chromatin via an association with the nonacetylated tail of histone H2B to negatively regulate the transcription of hundreds of genes (Schroeder *et al.*, 2002). The molecular reasons for the increased chloroplast density and chloroplast size in the tomato *hp-1* mutant remains to be resolved.

Two of the *arc* mutants, *arc3* and *arc5*, appear to specifically affect chloroplast division as the number of chloroplasts per cell is the same as the number of proplastids in the progenitor of mesophyll cells suggesting that proplastid division in these *arc* mutants is unaffected (Pyke and Leech, 1994; Marrison *et al.*, 1999). In *arc6* there are only 1-2 chloroplasts per cell (Pyke *et al.*, 1994). Analysis of the meristematic cells of *arc6* plants reveals that proplastid division is also affected by the *ARC6* mutation (Robertson *et al.*, 1995). Taken together these observations suggest that regulation of division of different plastid types in

various plant tissues is different.

In unicellular photosynthetic alga containing a single chloroplast coordination between cell division and chloroplast division is essential. In *C. merolae*, *ftsZ* transcripts accumulate specifically before cell and organelle division in cells synchronized by light/dark cycles (Takahara *et al.*, 2000). In synchronized *Chlamydomonas reinhardtii* cultures, *CrMinD*, *CrMinE* and *CrFtsZ* transcripts accumulate to high levels before the majority of cells undergo division and the lowest levels of transcripts are observed after the majority of cells have divided (Adams *et al.*, In Press). This is the first study to demonstrate that expression of many different chloroplast division components is coordinated. Nevertheless even in *C. merolae* which contains only a single chloroplast, chloroplast division and cell division can still be separated. In the event of cell division arrest the chloroplast is still able to divide resulting in aberrant cells with four chloroplasts (Nishida *et al.*, 2005). The necessity for intimate association between cell division and chloroplast division in unicellular species containing only a single chloroplast may mean that these species use different signaling controls to initiate chloroplast division than in higher plants.

In higher plants containing more than one chloroplast per cell, coordination between chloroplast division and the cell cycle can still be observed. In synchronized cultures of tobacco BY2 cells both families of *ftsZ* genes demonstrate an increase in expression immediately prior to and during cell division (El-Shami *et al.*, 2002). The first molecular component linking the cell and plastid division cycles in higher plants is AtCDT1, a cyclin-dependent kinase which forms part of the prereplication complex (Raynaud *et al.*, 2005). AtCDT1 is targeted to both plastids and the nucleus and down regulation of *AtCDT1* increases endoreduplication in rosette leaves coupled with a severe reduction in chloroplast number. Interestingly AtCDT1 interacts with the plastid division component ARC6 (Raynaud *et al.*, 2005). The role of AtCDT1 in the regulation of plastid division remains unclear, however the developmental defects observed when *AtCDT1* is down regulated underlines the importance of coordinated cell and organelle division for plant growth and morphogenesis.

Research into the regulation of plastid division in higher plants is hindered because a high level of plastid division occurs in only a sub-set of cells. In pea, *ftsZ* transcripts were shown to be present in young leaves of pea but *ftsZ* expression is barely detectable in roots, stems and older leaves (Gaikwad *et al.*, 2000). The high expression of *ftsZ* in young leaves is presumably because of the high cell division events

and chloroplast division occurring in these young leaves and indicates that expression of *ftsZ* is tissue regulated. Pea *ftsZ* transcripts accumulate rapidly after exposure of etiolated seedlings to light (Gaikwad *et al.*, 2000) suggesting that *ftsZ* expression is activated by light.

All of the chloroplast division components identified to date are nuclear encoded. Although the chloroplast contains its own genome the genome is reduced as genes have been relocated to the nuclear genome during integration of plastids. The chloroplast genome encodes genes necessary for the components of the four thylakoid photosynthetic complexes, proteins involved in their assembly and part of the genetic machinery necessary for transcription of these genes. However functional chloroplasts require the import of nuclear encoded proteins vital for the survival and replication of the chloroplast. Chloroplasts demonstrate retrograde signalling to the nucleus in order to control nuclear gene expression and many nuclear genes are regulated by chloroplast state (reviewed in Surpin *et al.*, 2002). How the division of chloroplasts is coordinated with cellular division or how proliferation of chloroplasts occurs during differentiation of mesophyll cells is unknown.

In order to investigate the regulation of plastid division several complementary methodologies were employed. Initially Quantitative PCR (QPCR) was used to investigate whether *ftsZ* and *min* gene expression in fully differentiated mesophyll cells was light regulated. DNA microarray technology was used then to analyse the effect on nuclear gene expression of chloroplast division inhibition. Finally, yeast one-hybrid assays were used to search for transcriptional activators or enhancers of *AtMinD1* and *AtMinE1*.

QPCR is a rapid and sensitive assay to quantify the initial amount of starting template (the amount of RNA transcript) in a sample. cDNA is synthesised from mRNA using reverse transcriptase. The amount of a particular species of cDNA is indicative of the starting amount of mRNA transcripts for that gene. QPCR amplifies the cDNA and quantifies the PCR product after each PCR cycle. In analysis of the QPCR data the number of PCR cycles required to generate enough PCR products to pass an assigned threshold gives the relative amount of starting transcript present in the sample.

For DNA microarray analysis oligonucleotide microarrays (or single-channel microarrays) were used. Probes of 25-mer oligonucleotides are designed to match part of the sequence of known or predicted mRNAs from the complete genome of *Arabidopsis*. These probes are synthesised directly onto

GeneChips® (Affymetrix Inc) and then probed by the target RNA. The target RNA is made by isolating RNA from control tissues and sample tissues. The RNA is amplified and labelled with biotin. Biotin labelled RNA is hybridised to the GeneChips through base pairing with the corresponding probe, the GeneChips are subsequently washed over with a fluorescent stain that sticks to the biotin. The GeneChips are finally scanned for emitted light from the fluorescent dye attached to the target RNA hybridised to the probe. The level of fluorescence recorded is indicative of the level of gene expression in the sample. Single-channel microarrays give estimations of the absolute value of gene expression therefore to compare gene expression of more than one treatment several GeneChips have to be used.

Yeast one-hybrid screening enables the user to identify proteins that bind to a target *cis*-acting DNA sequences. One or more tandem copies of the target DNA sequence is cloned upstream of *HIS3* gene in the reporter vector p*HIS2*. A cDNA library is cloned into the pGADT7-Rec2 vector as fusions to GAL4 activation domain (AD). The reporter vector containing the target DNA sequence, the cDNA library and the pGADT7-Rec2 vector are all transformed into yeast. Homologous recombination in yeast mediates the cloning of the cDNA library into the pGADT7-Rec2 vector. Interaction between a library protein fused to the GAL4-AD and the target DNA sequence stimulates transcription of *HIS3* enabling the yeast to grow on histidine free media. By plating the yeast screen on plates without histidine (H) in the media, library proteins that interact with the target DNA can be identified.

6.2. Results.

6.2.1. Light regulation of *FtsZ1-1*, *FtsZ2-1*, *AtMinD1* and *AtMinE1*.

Studies had suggested that *ftsZ* expression in plants may be regulated by light (Gaikwad *et al.*, 2000) as dark-grown 7-8 day old pea seedlings exposed to light show a sharp increase in expression of *ftsZ*. It is possible however that this sharp increase in *ftsZ* expression may be more related to the differentiation of chloroplasts and the development of the plants as the seedlings used in this experiment were etiolated. Studies have shown that upon light sensing a significant percentage of genes of dark-grown seedlings are up-regulated (Ma *et al.*, 2001). Therefore the observed up-regulation in *ftsZ* expression may be in response to developmental cues rather than to light. To establish whether light regulation of *ftsZ* expression occurs in fully differentiated leaf tissue Quantitative PCR (QPCR) analysis was used to analyse *ftsZ* expression of 20 day old *Arabidopsis* plants subjected to 24 hours of dark treatment followed by 24 hours of light treatment.

Arabidopsis Columbia seedlings were grown in continuous light until seedlings were 20 days old, at this age seedlings were at the rosette stage with 8-10 leaves. Seedlings were then treated to 24 hours dark followed by 24 hours light. Tissue samples were taken at regular intervals throughout the treatment (Fig. 6.1). Total RNA was extracted from the collected samples and contaminating DNA removed by treatment with DNase I (Sigma). RNA samples were quantified and 2 µg of RNA from each sample was used for first strand cDNA synthesis using oligo dT as a primer for cDNA synthesis. For QPCR analysis, reactions were set up using a robot (Corbett Research CAS1200). For each sample a 20 µl reaction was set up: 10 µl Sigma SYBR® Green JumpStart™ Taq ReadyMix™, 1µl of each 5 mM primers, 2 µl of cDNA was used in each reaction and the reaction was made up to 20 µl with water. To analyse the expression of *FtsZ1-1* the primers used were: *FtsZ1/QPCRr*: (5'-TAGAAGAAAAGTCTACGGGGAG-3') and *FtsZ1/QPCRl*: (5'-AGGTCAACAAGAGAACAAGGA-3'), to analyse the expression of *FtsZ2-1* the primers used were: *FtsZ2/QPCRl*: (5'-GTGGAAGTGA CTTAACACTGTTCG-3') and *FtsZ2/QPCRr*: (5'-CACCAAATATAAGATTTCGCTGTTG-3'). Two replicates of each reaction were set up and the whole experiment was performed twice for a biological replicate. As a control, QPCR for actin was performed in tandem with the *FtsZ1-1* and *FtsZ2-1* QPCR experiments. To check the expression of actin the primers *ACTINf*: (5'-TCAGATGCCAGAAAGTGTGTTCC-3') and *ACTINr*: (5'-

CCGTACAGATCCTTCCTGATATCC-3') were used. QPCR was performed using a MJ Research Chromo 4™ QPCR machine using the programme outlined in Section 2.3.2.6 and analysed using Opticon Monitor software. The log of the data points was used and the fixed fluorescence threshold was set at 0.02. All data points were standardised to the expression of actin. For each time point R was calculated; R is the relative value as compared to the starting level of *ftsZ* transcript. R was calculated using the method outlined in Pfaffl, 2001.

QPCR analysis revealed that *FtsZ2-1* and *FtsZ1-1* demonstrate clear light regulation. Expression of *FtsZ1-1* and *FtsZ2-1* is reduced in the dark and a sharp increase in *ftsZ* expression is observed when the seedlings are exposed to light after 24 hours of dark treatment (Fig. 6.1). Approximately 6 hours after exposure to light, the level of *ftsZ* expression plateaus and returns to the level observed at the start of the time-course when the plants had been growing in continuous light. *FtsZ1-1* and *FtsZ2-1* have an almost identical expression pattern (Fig. 6.1) indicating that they are probably regulated by the same pathway/proteins.

To establish whether other chloroplast division components were light regulated, the expression of *AtMinD1* and *AtMinE1* was also analysed by QPCR. The cDNA used to analyse expression of *ftsZ* was also used to analyse the expression of *AtMinD1* and *AtMinE1*. Reactions were set up in the same way as for *ftsZ* expression. Primers *AtMinD1/L* (5'-TCGTTGAGCAAGATAGTATGAAGG-3') and *AtMinD1/R* (5'-AAGAGAAGAAGCCACGTTTCTTAG-3') were used for *AtMinD1* QPCR and primers *AtMinE1/L* (5'-TTAGAAGGGTGAAACCAGAGTACC-3') and *AtMinE1/R* (5'-TTAGAAGGGTGAAACCAGAGTACC-3') for *AtMinE1* QPCR. The log of the data points was used and the fluorescence threshold was set at 0.02. All data points were standardised to the expression of actin. R was calculated as the relative expression compared to the starting level of *AtMinD1* or *AtMinE1* transcripts.

Like *ftsZ* expression the expression of the *min* genes also appears to be light regulated (Fig. 6.1). However, the reduction of *min* gene expression observed in the dark is not as pronounced as the reduction in *ftsZ* expression in the dark; *min* gene expression is reduced ~5-fold after 20 hours dark whereas *ftsZ* expression is reduced over 10-fold. Also the increase in *min* expression upon exposure to light appears to be more gradual compared to the sharp increase in *ftsZ* expression upon light exposure. Although the expression profile of *AtMinD1* and *AtMinE1* is slightly different from the expression profile of the *ftsZ*

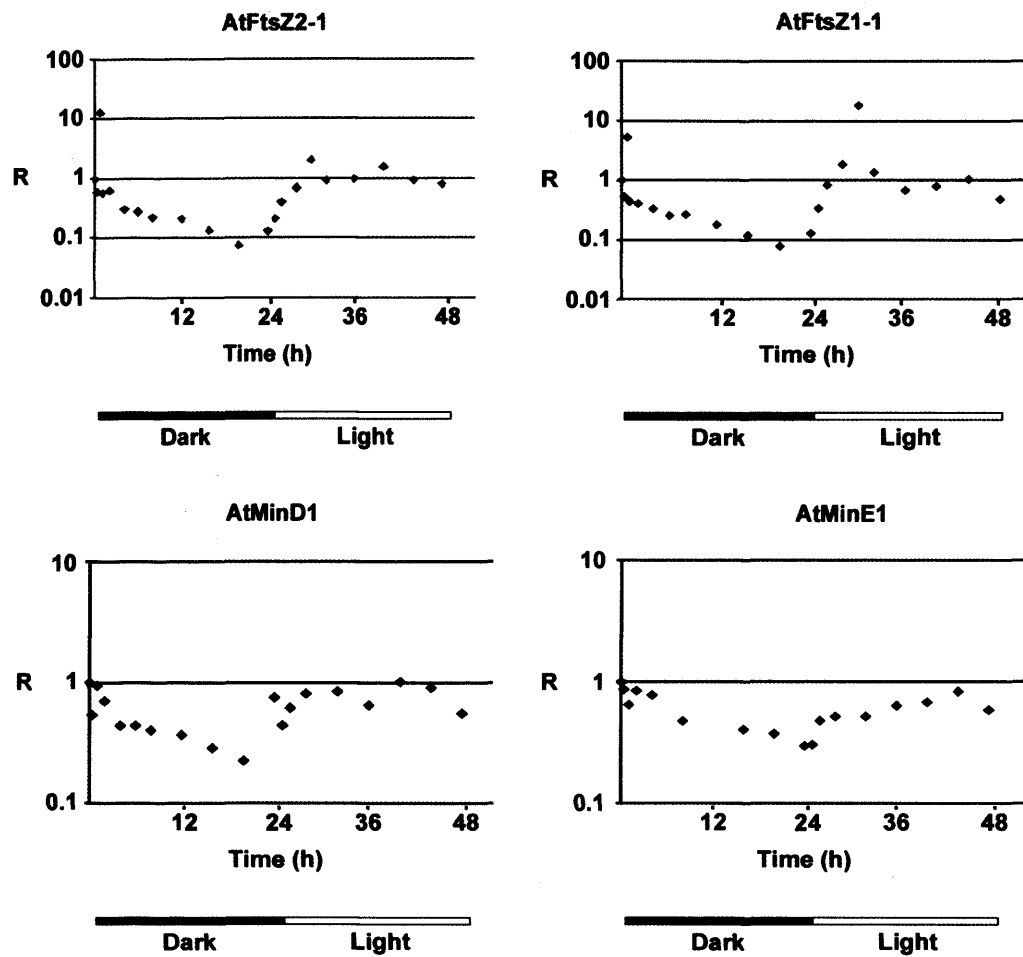


Fig. 6. 1. Light regulation of *ftsZ* and *min* genes. 20 day old Columbia seedlings grown in continuous light were subjected to 24 hours dark followed by 24 hours light. RNA was extracted from the seedlings and used to make cDNA which was subsequently used in QPCR. R = relative expression compared to expression at time 0 hours.

genes, the expression profiles of *AtMinD1* and *AtMinE1* are very similar suggesting that both of the *min* genes are regulated by the same proteins/pathways.

6.2.2. DNA Microarray analysis

All of the chloroplast division components identified to date are nuclear encoded and require import into chloroplasts after protein synthesis in the cell cytosol. The strict maintenance of plastid populations in dividing plant cells and the regulation of plastid number in different cell types is indicative of cellular regulation of plastid division. The discovery of a role for AtCDT1 prereplication factor in chloroplast division is the first link between cell and plastid division cycles (Raynaud *et al.*, 2005). However, how cellular and chloroplast division is co-ordinated remains unknown. In many of the *arc* mutants chloroplast division appears to be blocked (Pyke and Leech, 1992; Pyke *et al.*, 1994; Marrison *et al.*, 1999). What affects does a block in chloroplast division have on the expression profile of the cell? To try to answer these questions DNA microarray analysis was performed using RNA extracted from transgenic *Arabidopsis* in which chloroplast division has been inhibited.

Overexpression of *AtMinD1* has been shown to inhibit chloroplast division (Colletti *et al.*, 2000; Kanamaru *et al.*, 2000; Fujiwara *et al.*, 2004) therefore to inhibit chloroplast division overexpression of *AtMinD1* was used. Transgenic *Arabidopsis* containing *AtMinD1* downstream of the β -estradiol-inducible promoter were generated. Full length *AtMinD1* was amplified from cDNA using primers MIN/1 (5'-ATCTCGAGATGGCGTCTCTGAGATTGTTTC-3' *XhoI* is underlined) and MIN/2 (5'-ATACTAGTTTAGCCGCCAAAGAAAGAGAAGAAGCC-3' *SpeI* is underlined) and cloned into pPCRScripT. *AtMinD1* was then sub-cloned into the *XhoI* and *SpeI* of PER-10 a vector containing an inducible promoter activated by the chimeric transcription factor XVE. XVE is a fusion of the DNA-binding domain of the bacterial repressor LexA (X), the acidic transactivating domain of VP16 (V) and the regulatory region of the human estrogen receptor (E) (Zou *et al.*, 2000) A strong constitutive promoter G10-90 controls the expression of XVE. Eight copies of the LexA operator sequence are fused to the 35S minimal promoter upstream of the multiple cloning site. Dimerisation and subsequent binding of LexA DNA-binding domain to the LexA operator is controlled by the estrogen receptor which in turn is regulated by binding of 17- β -estradiol. Upon binding to the LexA operator XVE activates transcription of the target

gene cloned into the multiple cloning site (Zou *et al.*, 2000). *Agrobacteria* strain ABI was transformed with PER-10/AtMinD1 using the method described in Section 2.2.3. *Arabidopsis* ecotype Landsberg were transformed using the floral dip method (Section 2.1.4.). As a control, transgenic *Arabidopsis* transformed with the empty PER-10 vector were generated to ensure that expression of XVE would not interfere with the microarray analysis. Transformants were selected by plating seed on media containing $40 \mu\text{g ml}^{-1}$ kanamycin and subsequently transferred to fresh media. Transformed *Arabidopsis* plants were allowed to mature and self-fertilise and T2 plants were used for analysis. T2 seeds were surface sterilised and plated onto Lehle media containing kanamycin ~25 seeds per 9cm plate. Seeds were placed at 4°C for two days for stratification before being grown in constant light at a light intensity of $78 \mu\text{mol s}^{-1} \text{m}^{-2}$ at 21°C . Constant light was used to reduce circadian influences on the expression profile.

Three treatments were performed to investigate the expression profile in plants with normal chloroplast division, plants in which chloroplast division has been temporally inhibited or plants with prolonged chloroplast division inhibition. Treatment 1; Empty vector control seedlings (transformed with PER-10 only) were sprayed at 13 days old with $5 \mu\text{M}$ 17- β -estradiol and tissue harvested 24 hours later. Treatment 2 (prolonged induction (PI)); T2 seeds transformed with PER-10/AtMinD1 were sown on Lehle media containing $5 \mu\text{M}$ 17- β -estradiol and sprayed with $5 \mu\text{M}$ 17- β -estradiol every 24 hours to induce prolonged overexpression of AtMinD1. Seedlings were harvested at 14 days old. Treatment 3 (temporal induction (TI)) T2 seeds transformed with PER-10/AtMinD1 were sown on Lehle plates and sprayed at 13 days old with $5 \mu\text{M}$ 17- β -estradiol and harvested 24 hours later.

For all three treatments the chloroplasts were analysed for a chloroplast division phenotype indicating overexpression of AtMinD1. For treatment 1 the chloroplasts were of wild-type like size and number (Fig. 2(A)). For treatment 2 only 1-2 enlarged chloroplasts were observed per cell (Fig. 2(B)) indicating the chloroplast division had been inhibited in the seedlings. For treatment 3 the chloroplasts were wild-type like in size and number. This was to be expected as chloroplast division had only recently been inhibited by AtMinD1 overexpression. The wild-type size and number of the chloroplasts of treatment 3 indicated that expression of AtMinD1 from the inducible promoter was not leaky (Fig. 6.2(C)). All seedlings for microarray analysis were harvested at 14 days old at the 4-6 rosette leaves stage. Once harvested the tissue was snap frozen in liquid nitrogen. All three treatments were performed in replica.

RNA was extracted from the harvested seedlings using the protocol outlined in Section 2.3.1.2. The quantity of the RNA was analysed using a spectrophotometer at 260nm. RT-PCR was performed to check the expression of *AtMinD1* (Fig. 6.2(D)). 2 µg of RNA was used as template for first-strand cDNA synthesis followed by PCR using *AtMinD1*-specific primers MIN/1 and MIN/2. RT-PCR revealed that without induction (no induction; NI) the level of *AtMinD1* transcript in *Arabidopsis* seedlings transformed with PER-10/*AtMinD1* correlated to the amount of endogenous *AtMinD1* as compared to the empty vector control (Fig. 6.2(D)). This indicates that no leaky expression of *AtMinD1* occurred and expression of the *AtMinD1* transgene was under tight regulation. For seedlings in treatments 2 and 3 (Temporal Induction; TI and Prolonged Induction; PI) expression of the *AtMinD1* transgene was up-regulated and *AtMinD1* was overexpressed in these tissues (Fig. 6.2(D)). RNA was concentrated by ethanol precipitation to a final concentration of 1µg/µl. DNA microarray analysis was carried out using the Affymetrix service at NASC (www.affymetrix.arabidopsis.info/). This service amplifies, labels and hybridises the RNA to GeneChips® (Affymetrix Inc.) which contain the *Arabidopsis* genome represented as probes consisting of 25-mer oligos. For each spot on the GeneChip® a signal intensity corresponding to the number of molecules of mRNA hybridised to the particular spot is measured to give an estimation of absolute gene expression. The average signal intensity of the two replicates from each treatment was calculated and gene expression was compared between each of the three treatments (See CD/ROM). The fold change for each gene between different treatments was calculated. The significance of the fold change for each gene was analysed using T-test. The T-test null hypothesis was that there was no difference between treatments; any difference between samples was due to chance variation. A probability score of <0.05 was sufficient to reject the null hypothesis and indicated a significant difference in gene expression between two treatments.

Before analysing the microarray data, the expression of *AtMinD1* was checked to ensure that overexpression of *AtMinD1* had occurred in treatments 2 and 3. Compared to the empty vector control (treatment 1) the level of *AtMinD1* had increased ~7-fold upon temporal induction (treatment 3) and had increased ~21-fold over prolonged induction (treatment 2) (Table 1). A 7-fold increase in *AtMinD1* is sufficient to inhibit chloroplast division (Colletti *et al.*, 2000; Kanamaru *et al.*, 2000; Fujiwara *et al.*, 2004). Therefore chloroplast division was inhibited in seedlings following treatments 2 and 3. The expression of all of the known chloroplast division genes in each of the treatments was analysed (Table 1).

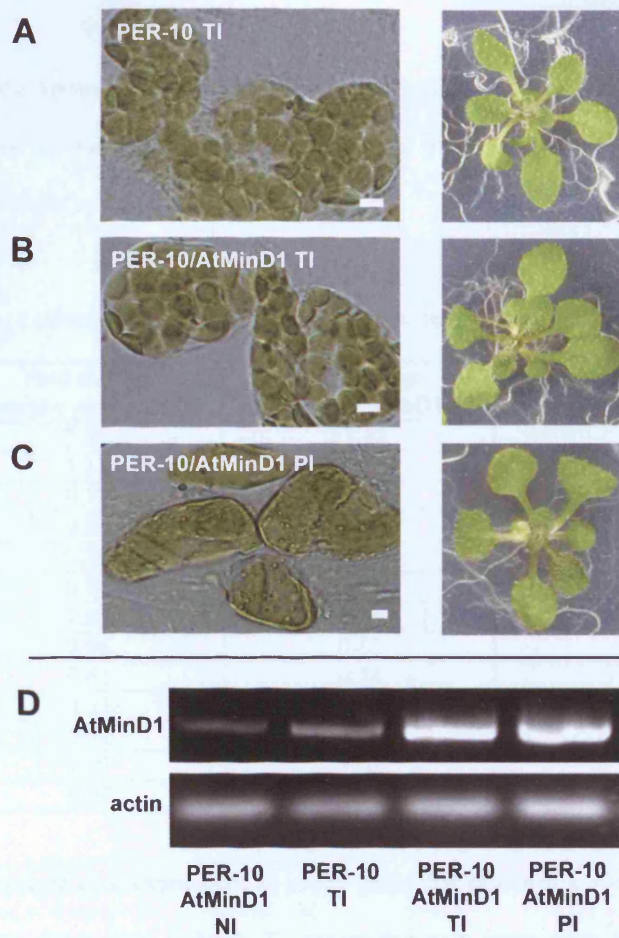


Fig. 6.2. Seedlings used for DNA microarrays. (A) Seedlings transformed with PER-10 empty vector control. Seedlings were grown on lehle plates and sprayed at 13 days old with 17- β -estradiol and harvested at 14 days. (B) Seedlings transformed with PER-10/AtMinD1. Seedlings were grown on lehle plates and sprayed at 13 days old with 17- β -estradiol and harvested at 14 days. (C) Seedlings transformed with PER-10/AtMinD1. Seedlings were grown on lehle plates containing 17- β -estradiol and sprayed every 24 hours with 17- β -estradiol. Tissue was harvested at 14 days. (D) RT-PCR of RNA extracted from seedling tissue to check expression of AtMinD1. Actin expression was used as a control. NI = no induction of overexpression of AtMinD1. TI = temporal induction of overexpression of AtMinD1. PI = prolonged induction of overexpression of AtMinD1. Scale bars = 5 μ m

Surprisingly none of the known chloroplast division genes exhibited altered expression in response to inhibition of chloroplast division (Table 6.1). Fold changes in gene expression between each of the treatments was not significant as determined by the T-test.

Table 6.1. Fold change of chloroplast division components between treatments

Gene	Fold change Control v AtMinD1 TI	Fold change Control v AtMinD1 PI	Fold change AtMinD1 TI v AtMinD1 PI
AtMinD1	7.38	21.42	2.90
AtMinE1	1.15	1.11	0.97
AtFtsZ1-1	0.77	0.79	1.03
AtFtsZ2-1	0.96	1.01	1.06
AtFtsZ2-2	0.39	0.53	1.38
GC1	0.71	0.68	0.95
ARC6	1.03	0.88	0.85
ARC5	0.86	0.67	0.77
ARC3	0.61	0.54	0.90
AtCDT1a	0.91	0.61	0.79
MSL2	0.72	1.02	1.41
MSL3	1.07	1.02	0.96
FZL	0.77	0.82	1.07

To begin to analyse gene expression, all of the genes that exhibited a >3-fold difference in gene expression between treatments were isolated. To ensure that only genes were selected in which gene expression was significantly different, only those genes with a signal intensity of over 30 were analysed. Below this signal intensity large fold changes can be observed with relatively small variation in signal intensity. To generate a gene expression profile, genes which exhibited a >3-fold change in expression were functionally characterised using the gene ontology database at TAIR (www.arabidopsis.org/tools/bulk/go/index.jsp). This program categorizes the genes based on molecular function, biological process and cellular component. Genes are assigned attributes based upon the gene ontology terms outlined by the gene ontology consortium (www.geneontology.org) (Fig. 6.3, 6.4 and 6.5). Analysis of the expression data reveals that generally the same genes have increased expression for both temporal and prolonged inhibition of chloroplast division. From the gene ontology data the same proportion of genes for both the temporal induced treatment and also the prolonged induced treatment have the same cellular component, molecular function and biological process (Fig. 6.3, 6.4 and 6.5).

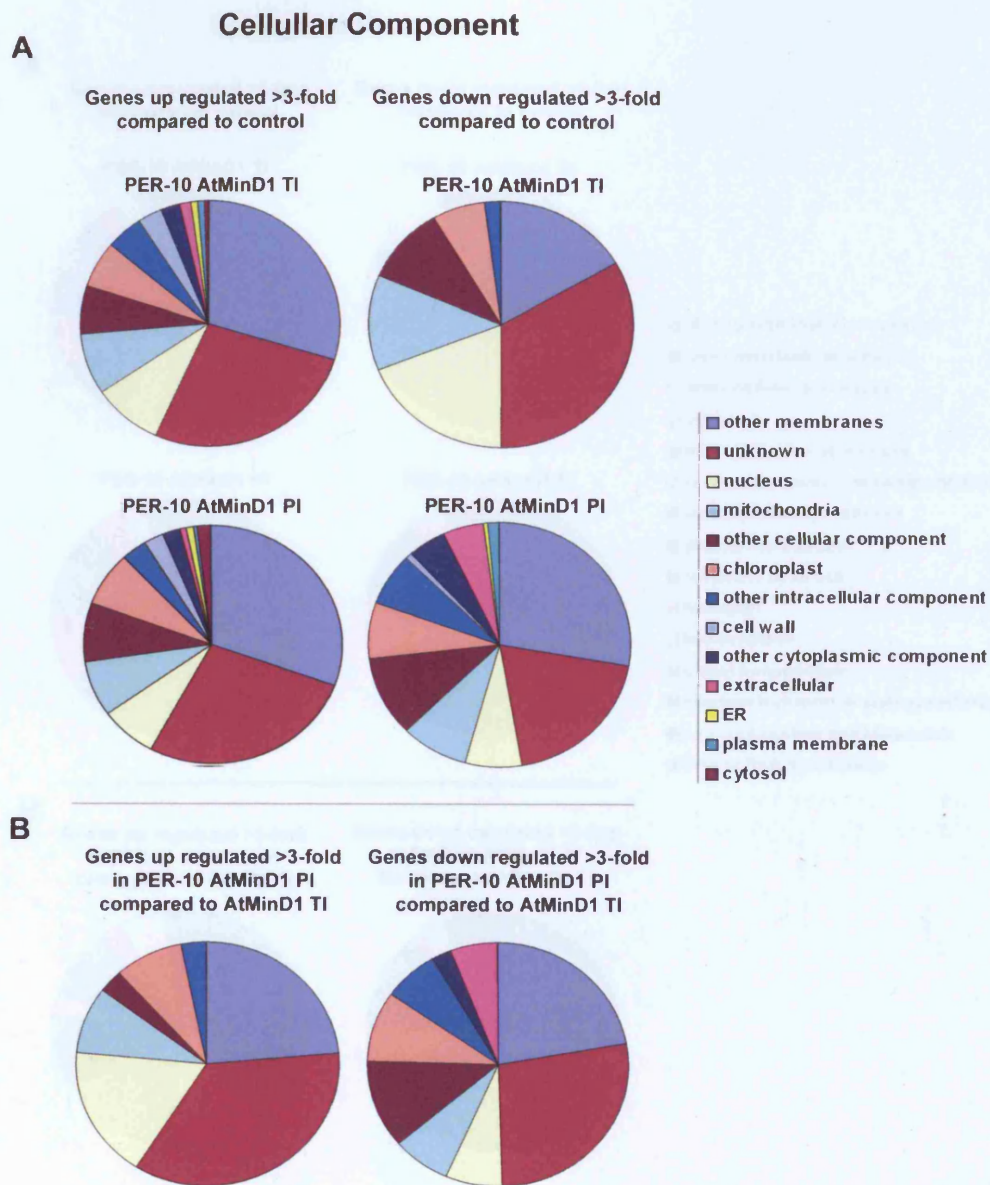


Fig. 6. 3. Predicted cellular localisation of proteins of genes that exhibit >3 fold change in gene expression. Performed using the gene ontology database at TAIR (www.arabidopsis.org/tools/bulk/go/index.jsp). The control was gene expression in Landsberg seedlings transformed with empty vector control. Categorization was based upon the gene ontology terms outlined by the gene ontology consortium (www.geneontology.org)
 TI = temporal induction of overexpression of AtMinD1. PI = prolonged induction of overexpression of AtMinD1.

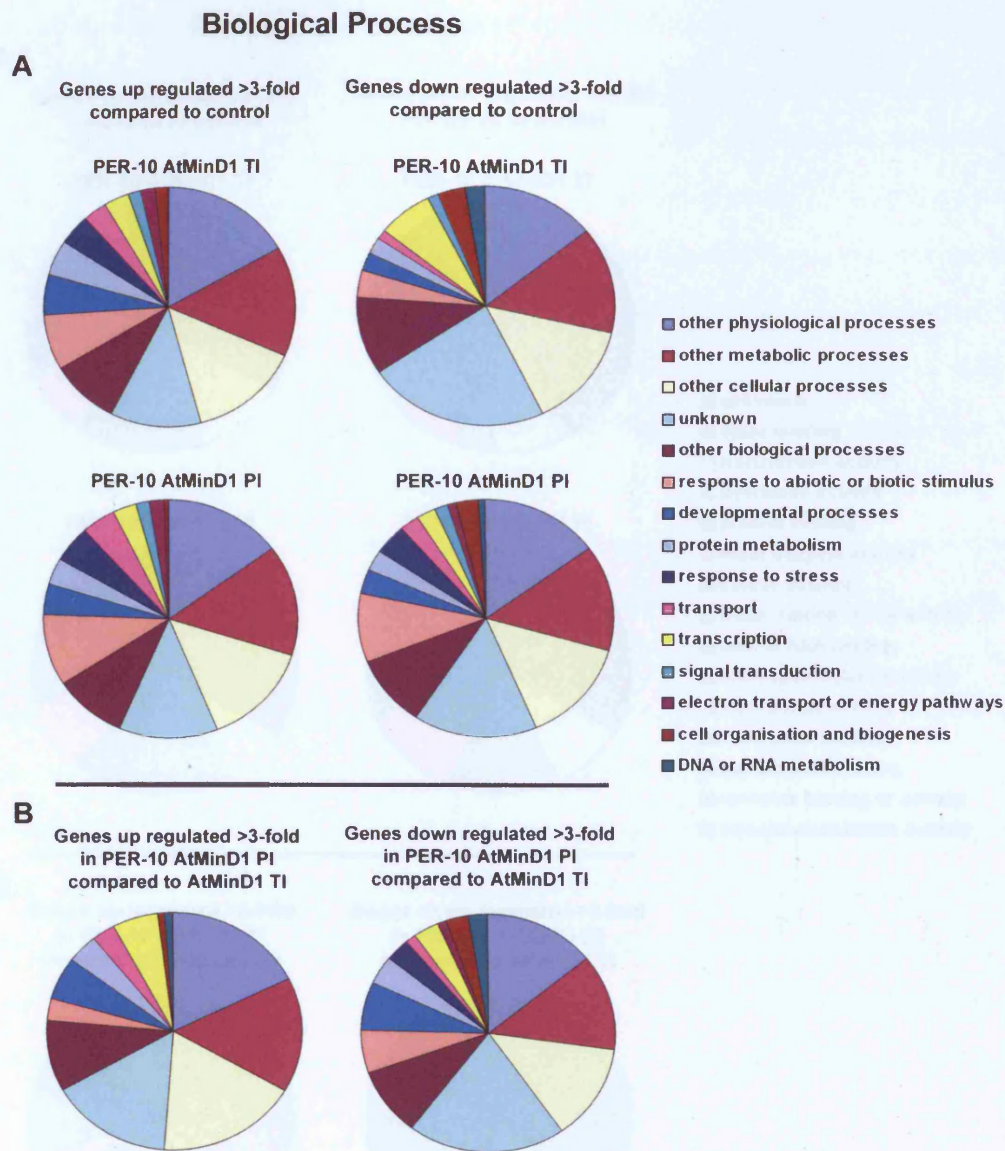


Fig. 6. 4. Predicted biological process of proteins of genes that exhibit >3 fold change in gene expression. Performed using the gene ontology database at TAIR. The control was gene expression in Landsberg seedlings transformed with empty vector control. Categorization was based upon the gene ontology terms outlined by the gene ontology consortium. TI = temporal induction of overexpression of AtMinD1. PI = prolonged induction of overexpression of AtMinD1.

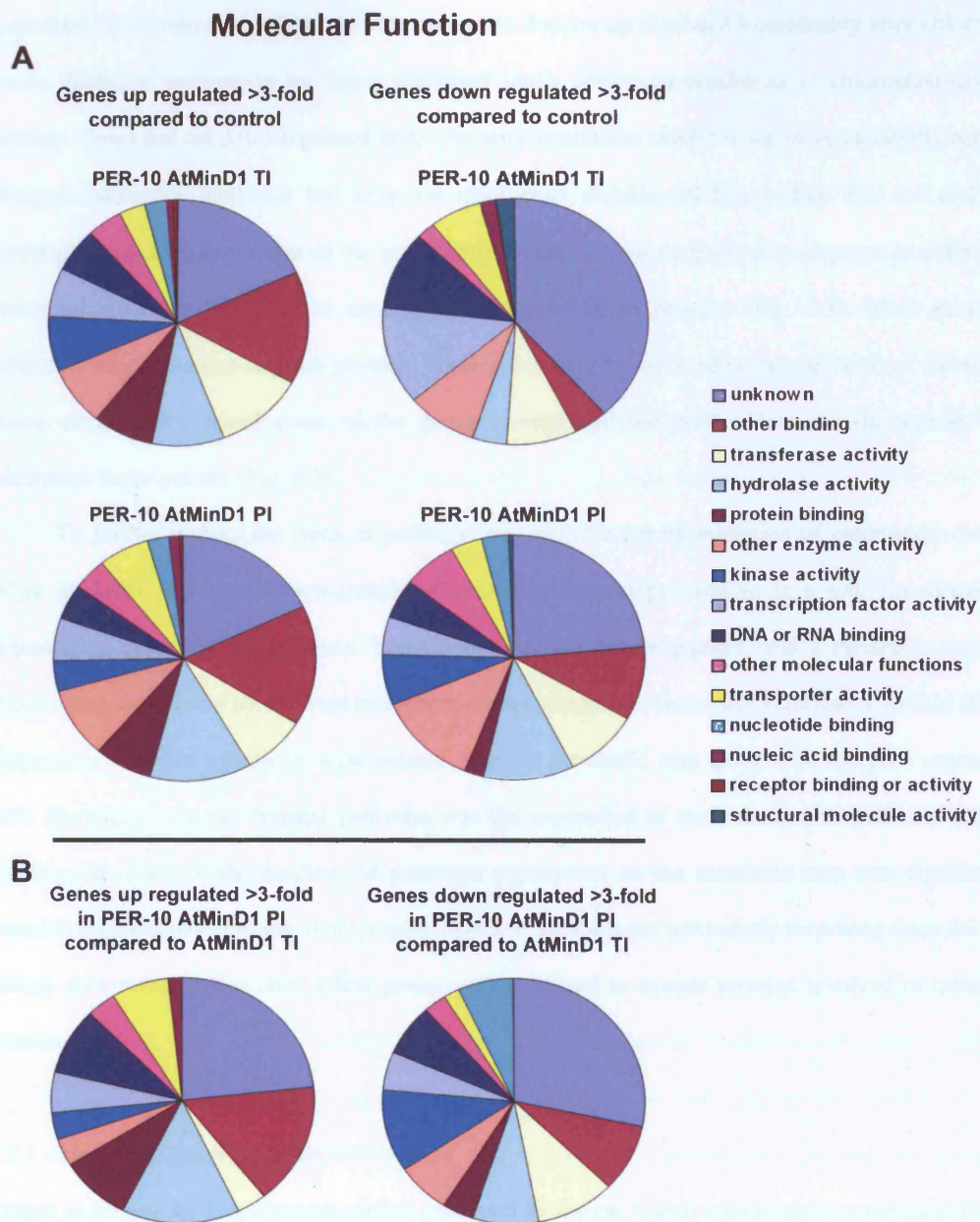


Fig. 6. 5. Predicted molecular function of proteins of genes that exhibit >3 fold change in gene expression. Performed using the gene ontology database at TAIR. The control was gene expression in Landsberg seedlings transformed with empty vector control. Categorization was based upon the gene ontology terms outlined by the gene ontology consortium. TI = temporal induction of overexpression of AtMinD1. PI = prolonged induction of overexpression of AtMinD1.

Comparison of the microarray data confirms that genes that are up regulated immediately after chloroplast division inhibition continue to be highly expressed under prolonged conditions of chloroplast division inhibition. Genes that are down-regulated under the same conditions exhibit much more variability between prolonged chloroplast inhibition and temporal chloroplast division inhibition (Fig. 6.3, 6.4 and 6.5). Surprisingly only a small fraction of the genes up-regulated or down-regulated in response to chloroplast division inhibition are predicted to encode chloroplast-localised proteins (Fig. 6.3). More genes are predicted to encode nuclear-targeted proteins. These genes may be involved in the regulation of chloroplast division components; indeed some of the genes up-regulated are predicted to encode proteins with transcription factor activity (Fig. 6.5).

To further analyse the types of pathways that are affected by inhibition of chloroplast division AraCyc at TAIR was used (www.arabidopsis.org/biocyc/index.jsp). AraCyc is a tool for visualising biochemical pathways in *Arabidopsis*. Transcriptomics data can be painted onto a metabolic map and pathways that are affected by different treatments can be recognised. Genes that exhibited a >3-fold change in expression between treatments were painted onto the metabolic map along with the gene expression values. In none of the biochemical pathways was the expression of more than one metabolite affected indicating that none of the biochemical pathways represented on the metabolic map was significantly affected in response to inhibition of chloroplast division. This was not particularly surprising since the gene ontology data revealed that only a few genes were predicted to encode proteins involved in metabolic processes.

6.2.2.1. Selection of genes for further analysis

To begin to analyse the huge amount of data generated by the microarray experiments a selection of genes were chosen for further investigation. Due to time restrictions it was not possible to analyse all genes whose expression was altered due to inhibition of chloroplast division. Therefore it was initially decided to restrict analysis to those genes that were up-regulated in response to prolonged chloroplast division inhibition and to concentrate on genes that encode proteins predicted to be chloroplast targeted. In total 17 genes had up-regulated expression in response to prolonged chloroplast division inhibition and were predicted to encode chloroplast-targeted proteins. Of these a handful of genes were selected for analysis.

At1g80920 and At4g36040 encode proteins that contain a J-domain motif characteristic of DNA-J chaperones. ARC6 also contains a J-domain (Vitha *et al.*, 2003). DnaJ proteins are believed to deliver polypeptide substrates to Hsp70 chaperones for processing. The J-domain stimulates Hsp70 ATPase activity necessary for stable binding of Hsp70 to its protein substrates (reviewed in Walter and Buchner, 2002). TargetP predicts that the protein products of At1g80920 and At4g36040 are chloroplast-localised.

At5g64510, At5g22270 and At1g68875 encode expressed proteins of unknown function and are predicted to be targeted to the chloroplast. A search of the Pfam database (www.sanger.ac.uk/software/pfam) for putative conserved protein domains detected no putative protein domains. At5g47420 also encodes an expressed protein of unknown function predicted to be targeted to the chloroplast. The Pfam database predicts a domain DUF124, a protein domain of unknown molecular function found in many prokaryotic proteins. Many prokaryotic derived proteins are involved in chloroplast division because of the cyanobacterial origins of chloroplasts (Osteryoung *et al.*, 1998; Colletti *et al.*, 2000; Maple *et al.*, 2002). At5g47420 may be a derived form a prokaryotic gene involved in bacterial cell division.

In addition to the chloroplast localised proteins At4g24540 was also selected for investigation. At4g24540 is a MADS-box family protein AGL24. Analysis of the microarray data revealed that many MADS-box family proteins are up-regulated upon chloroplast division inhibition. MADS-box domain containing transcription factors are a large family of regulators involved in plant development particularly regulation of flower development. Analysis of the promoter of *AtMinD1* reveals a binding site for MADS box transcription factors, this binding site contains the consensus sequence for the binding of AGL (AGAMOUS-like) MADS transcription factors. AGL24 promotes inflorescence identity and flowering (Gregis *et al.*, 2006). AGL24 is expressed in vegetative tissue before floral transition (Gregis *et al.*, 2006).

6.2.2.2. Analysis of selected genes

To analyse the selected genes, T-DNA insertion lines were acquired from NASC after searching the Salk Institute Genomic Analysis Laboratory Arabidopsis gene-mapping database (<http://signal.salk.edu/cgi-bin/tdnaexpress>). Each of the T-DNA insertion lines contains a T-DNA insertion within the exon of the selected gene. Plants that were homozygous for the T-DNA insertion were verified by PCR. Primers were

designed so that PCRs using three primers; the left primer, right primer and LBb1 would give a PCR product of ~900bp for wild-type plants, a PCR product of ~700bp for plants homozygous for the T-DNA insertion and both PCR products if the plants are heterozygous for the T-DNA insertion. The left-primers and right-primers designed for each T-DNA insertion line are in Table 6.2.

Table 6.2. Primers for T-DNA insertion verification PCRs

Gene	SALK	Primer name	Primer sequence
At5g22270	043410	043410lp	5'-CCAAACCTATTTATTGTTTGACG-3'
		043410rp	5'-AAACCATGGATCTCCATCTAAAG-3'
At1g80920	024617	024617lp	5'-CGAAGCAAGAGAAAGACATGG-3'
		024617rp	5'-TGTAGAGGAAGCAATTGTGGG-3'
At4g36040	052270	052270lp	5'-TCTTGCTTGGAACAAAATTG-3'
		052270rp	5'-TTCTTCTCCGCCTCTATCTCC-3'
At5g47420	111654	111654lp	5'-CAAAGGAATGCATCTGGCTAC-3'
		111654rp	5'-CTGTCGCGAATTTGTTAAAGC-3'
At1g68875	020620	020620lp	5'-ACGGGATCAATATGTGGTGTGTC-3'
		020620rp	5'-TGCATGACCAATTCAGAGTG-3'
At5g64510	006509	006509lp	5'-TTACATGCAAAGGTTTCGTGG-3'
		006509rp	5'-CGGTTACATCTTCAAGAAGC-3'
At4g24540	095007	095007lp	5'-TGGCATATAATCATTAAATCTTGAAGC-3'
		095007rp	5'-TATTCTCATCCACCAATCCG-3'
		LBb1	5'-GCGTGGACCGCTTGCTGCAACT-3'

Fluorescence microscopy using a chlorophyll autofluorescence filter was used to analyse the chloroplasts of the homozygous insertion lines. Unprepared whole leaf samples were analysed for a chloroplast division phenotype. For each of the insertion lines analysed the chloroplasts within the mesophyll cells and petioles appeared to be wild-type in size and number indicating that the gene being analysed does not affect chloroplast division (Fig. 6-12.). At the macroscopic level the plants were indistinguishable from wild-type Columbia plants grown under the same conditions however SALK 24540, a T-DNA insertion in At4g24540 which encodes AGL24 was late flowering.

6.2.3. Analysis of the promoter regions of the min genes

QPCR analysis revealed that expression of *AtMinD1* and *AtMinE1* was light regulated (Fig. 6.1). *AtMinD1* and *AtMinE1* appeared to follow the same expression profile (Fig.6.1) suggesting that they are regulated by

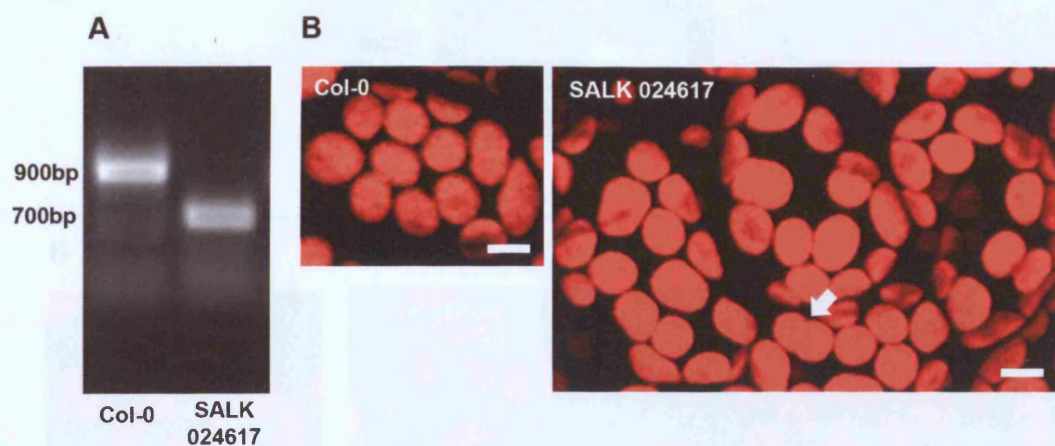


Fig. 6. 6. Analysis of SALK 024617. (A) PCR using primers 024617lp, 024617rp and LBb1 were used to verify a homozygous T-DNA insertion in At1g80920. (B) Fluorescence microscopy using chlorophyll autofluorescence filters (exciter HQ630/30, emitter HQ680/40) (Chroma Technologies, USA) was used to analyse the chloroplasts of SALK 024617. Images were captured using a Hamamatsu Orca ER 1394 cooled CCD camera. Velocity II (Improvision) was used to capture 0.5 μm Z-sections through the sample and to generate the extended focus image. White arrows indicate chloroplasts undergoing division. Scale bars = 5 μm .

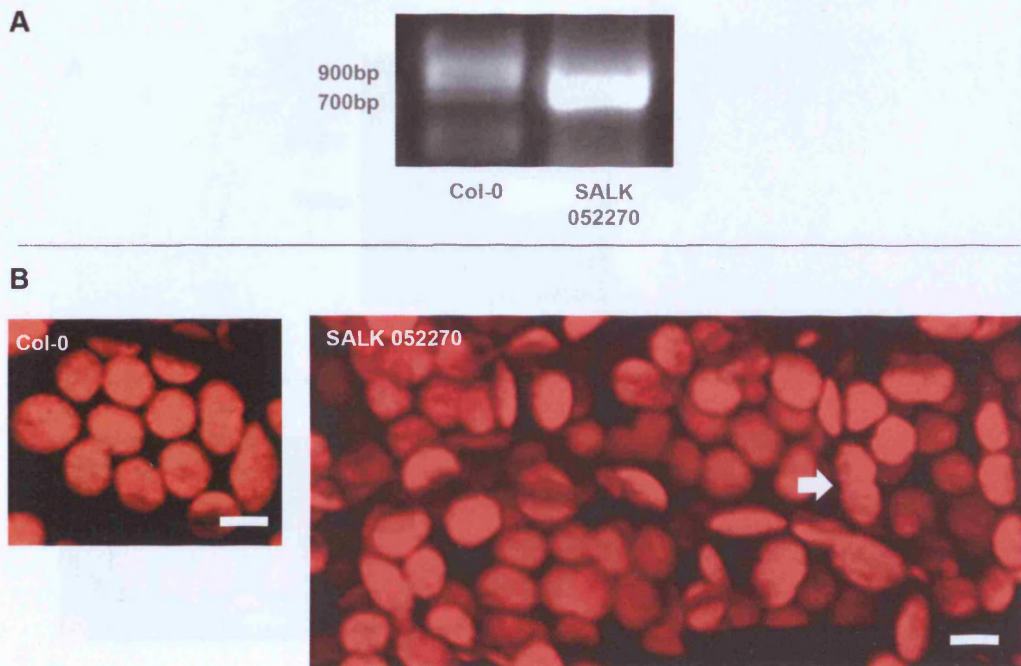


Fig. 6. 7. Analysis of SALK 052270. (A) PCR using primers 052270lp, 052270rp and LBb1 were used to verify a homozygous T-DNA insertion in At4g36040. (B) Fluorescence microscopy using chlorophyll autofluorescence filters (exciter HQ630/30, emitter HQ680/40) (Chroma Technologies, USA) was used to analyse the chloroplasts of SALK 052270. Images were captured using a Hamamatsu Orca ER 1394 cooled CCD camera. Volocity II (Improvision) was used to capture 0.5 μm Z-sections through the sample and to generate the extended focus image. White arrows indicate chloroplasts undergoing division. Scale bars = 5 μm .

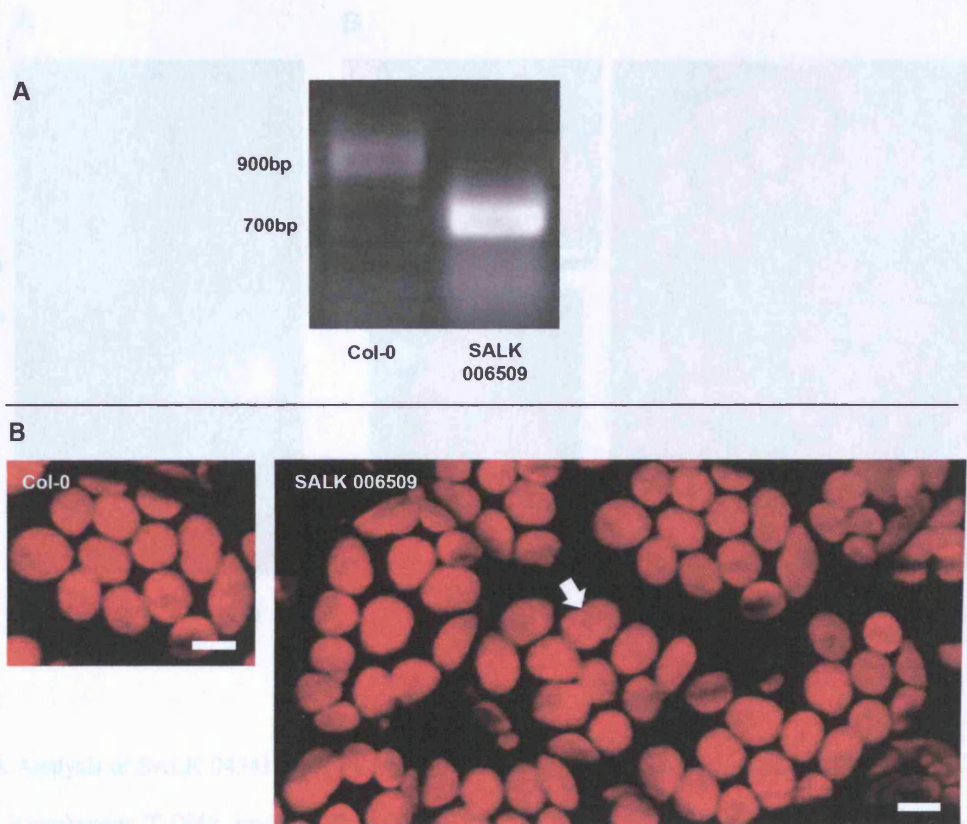


Fig. 8. Analysis of SALK 006509. (A) PCR using primers 006509lp, 006509rp and LBb1 were used to verify a homozygous T-DNA insertion in At5g64510. (B) Fluorescence microscopy using chlorophyll autofluorescence filters (exciter HQ630/30, emitter HQ680/40) (Chroma Technologies, USA) was used to analyse the chloroplasts of SALK 006509. Images were captured using a Hamamatsu Orca ER 1394 cooled CCD camera. Volocity II (Improvision) was used to capture 0.5 μm Z-sections through the sample and to generate the extended focus image. White arrows indicate chloroplasts undergoing division. Scale bars = 5 μm .

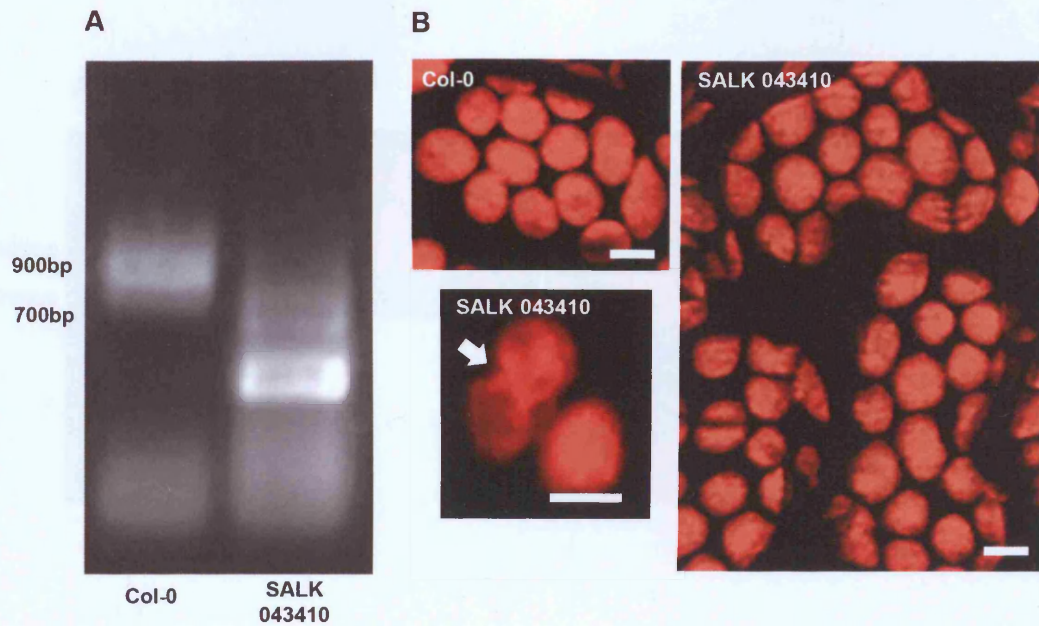


Fig. 6. 9. Analysis of SALK 043410. (A) PCR using primers 043410lp, 043410rp and LBb1 were used to verify a homozygous T-DNA insertion in At5g22270. (B) Fluorescence microscopy using chlorophyll autofluorescence filters (exciter HQ630/30, emitter HQ680/40) (Chroma Technologies, USA) was used to analyse the chloroplasts of SALK 043410. Images were captured using a Hamamatsu Orca ER 1394 cooled CCD camera. Volocity II (Improvision) was used to capture 0.5 μm Z-sections through the sample and to generate the extended focus image. White arrows indicate chloroplasts undergoing division. Scale bars = 5 μm .

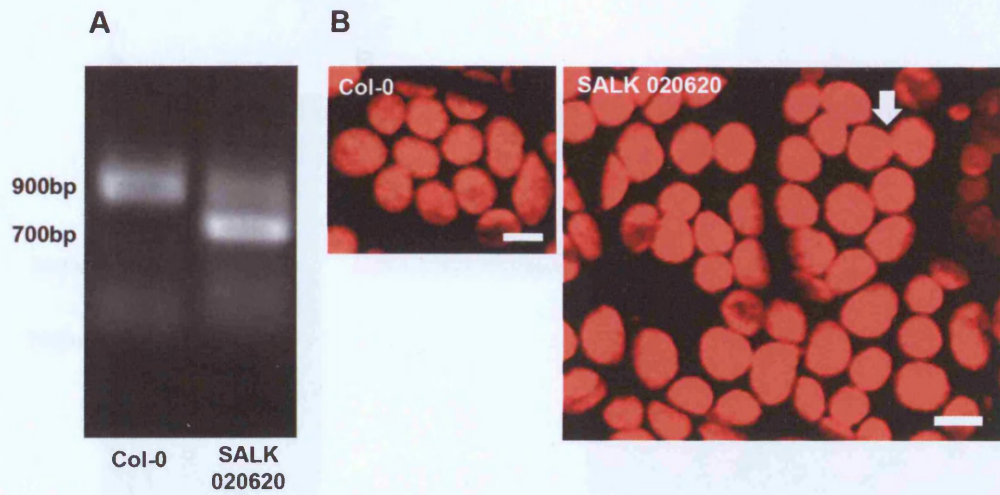


Fig. 6. 10. Analysis of SALK 020620. (A) PCR using primers 020620lp, 020620rp and LBb1 were used to verify a homozygous T-DNA insertion in At1g68875. (B) Fluorescence microscopy using chlorophyll autofluorescence filters (exciter HQ630/30, emitter HQ680/40) (Chroma Technologies, USA) was used to analyse the chloroplasts of SALK 020620. Images were captured using a Hamamatsu Orca ER 1394 cooled CCD camera. Volocity II (Improvision) was used to capture 0.5 μm Z-sections through the sample and to generate the extended focus image. White arrows indicate chloroplasts undergoing division. Scale bars = 5 μm .

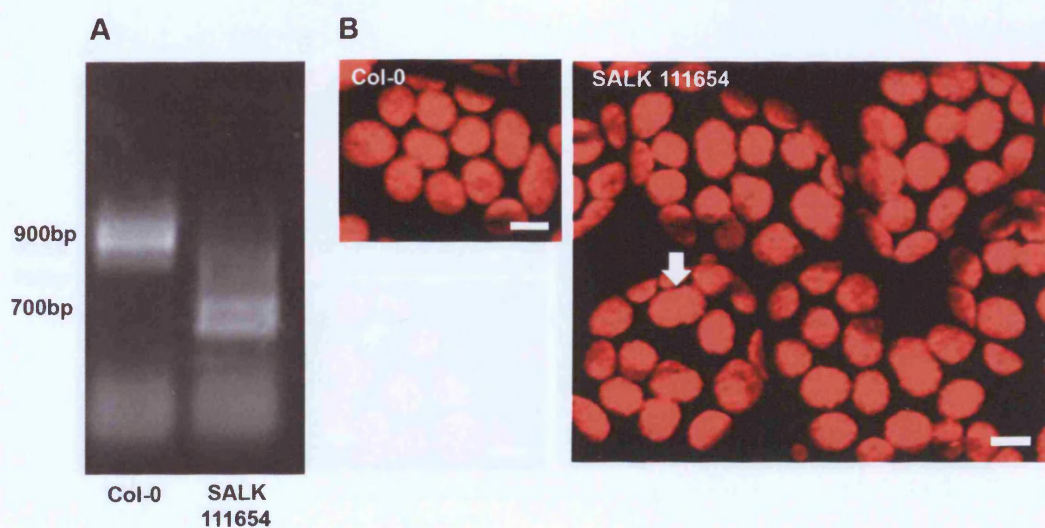


Fig. 6. 11. Analysis of SALK 111654. (A) PCR using primers 111654lp, 111654rp and LBb1 were used to verify a homozygous T-DNA insertion in At5g47420. (B) Fluorescence microscopy using chlorophyll autofluorescence filters (exciter HQ630/30, emitter HQ680/40) (Chroma Technologies, USA) was used to analyse the chloroplasts of SALK 111654. Images were captured using a Hamamatsu Orca ER 1394 cooled CCD camera. Volocity II (Improvision) was used to capture 0.5 μm Z-sections through the sample and to generate the extended focus image. White arrows indicate chloroplasts undergoing division. Scale bars = 5 μm .

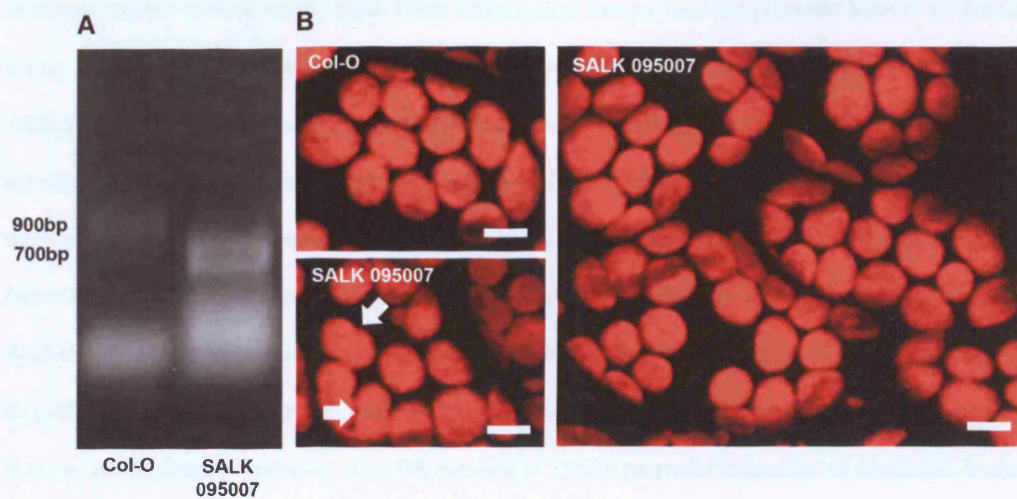


Fig. 6. 12. Analysis of SALK 095007. (A) PCR using primers 095007lp, 095007rp and LBb1 were used to verify a homozygous T-DNA insertion in At4g24540. (B) Fluorescence microscopy using chlorophyll autofluorescence filters (exciter HQ630/30, emitter HQ680/40) (Chroma Technologies, USA) was used to analyse the chloroplasts of SALK 095007. Images were captured using a Hamamatsu Orca ER 1394 cooled CCD camera. Volocity II (Improvision) was used to capture 0.5 μm Z-sections through the sample and to generate the extended focus image. White arrows indicate chloroplasts undergoing division. Scale bars = 5 μm .

the same proteins or pathways. The expression of eukaryotic genes is usually tightly regulated by a whole host of factors that either up-regulate or down-regulate the expression of genes depending on developmental or environmental cues. These *trans*-acting factors bind the promoter regions of genes at *cis*-acting sites regulating the transcription of these genes. Alignment of the region immediately upstream of *AtMinD1* and *AtMinE1* revealed no significant homology suggesting that the promoters of the two genes do not contain the same *cis*-acting elements. *In silico* analysis of the *AtMinD1* and *AtMinE1* promoter regions was performed. To identify *cis*-acting elements AthaMap and AGRIS were used. AthaMap (www.athamap.de/; Steffens *et al.*, 2004; Steffens *et al.*, 2005) uses the binding specificities of 103 *Arabidopsis* transcription factors to identify transcription factor binding sites. AGRIS (*Arabidopsis* Gene Regulatory Information Server; <http://arabidopsis.med.ohio-state.edu/>) contains AtcisDB (*Arabidopsis thaliana cis*-regulatory database). AtcisDB consists of 25,516 promoter sequences of annotated *Arabidopsis* genes with a description of putative *cis*-regulatory elements (Davuluri *et al.*, 2003; Palaniswamy *et al.*, 2006).

Analysis of the promoter region of *AtMinD1* using AthaMap and AtcisDB revealed some putative transcription factor binding sites (Fig. 6.13 and Table 6.3). AthaMap recognised binding sites for ARR1 and ARR2 (*Arabidopsis* Response Regulator). These transcription factors are similar to bacterial response regulators found in prokaryotes plants, slime-moulds, fungi and yeast. ARR1 and ARR2 bind DNA through the ARRM domain which has a consensus sequence of 5'-(G/A)GAT(T/C)-3' (Sakai *et al.*, 2000). AthaMap also recognised the binding site for MADS-box transcription factors. The MADS box is a highly conserved sequence motif found in a family of transcription factors. Most MADS-box domain containing transcription factors are involved in the regulation and control of developmental processes, particularly flower morphogenesis. There are 107 genes within the *Arabidopsis* genome that encode MADS-box domain containing proteins (Parenicova *et al.*, 2003). Searching the AtcisDB recognized MYB family transcription factor binding sites, there are over 100 MYB family transcription factors in *Arabidopsis* involved in a diverse range of functions. The MYB-family of transcription factors are predominantly transcriptional activators (Stracke *et al.*, 2001).

Analysis of the promoter region of *AtMinE1* using AthaMap and AtcisDB also revealed some putative transcription factor binding sites (Fig. 6.14 and Table 6.4). AthaMap revealed the binding

sequence for GATA-1 transcription factor. Many light responsive promoters contain GATA motifs (Teakle *et al.*, 2002; Reyes *et al.*, 2004) Transcripts of GATA-1 can be detected in all tissues suggesting that GATA-1 is not developmentally regulated at the level of transcription (Teakle *et al.*, 2002). In the promoter region of *AtMinE1* a bZIP family transcription factor is also recognised. In plants basic region/leucine zipper motif (bZIP) transcription factors regulate processes including pathogen defense, light and stress signaling, seed maturation and flower development. The *Arabidopsis* genome contains 75 distinct members of the bZIP family. RAV-1 binding site was also recognized by AtcisDB. RAV1 in *Arabidopsis* consists of two domains. The N-terminal region of RAV1 is homologous to the AP2 (APETALA2) DNA-binding domain. The C-terminal region exhibits homology to the highly conserved C-terminal domain, designated B3, of VP1/ABI3 transcription factors (Kagaya *et al.*, 1999) RAV1 binds specifically to bipartite recognition sequences composed of two unrelated motifs, 5'-CAACA-3' and 5'-CACCTG-3', separated by various spacing in two different relative orientations. RAV1 is up-regulated in response to low temperature. It has circadian regulation and may function as a negative growth regulator (Fowler *et al.*, 2005). In the promoter region of *AtMinE1* only the binding site of the B3 DNA-binding domain of RAV1 could be detected therefore it is unlikely that RAV1 will bind to the promoter of *AtMinE1* however other transcription factors containing the B3 DNA-binding domain may bind.

Table 6.3. Binding sites for transcription factors in the promoter of *AtMinD1*.

Binding site name	Binding site sequence	Binding site family	Refs
ARR1	TANGATTGT	GARP/ARR-B	Sakai <i>et al.</i> , 2000
ARR2	TANGATTGT	GARP/ARR-B	Sakai <i>et al.</i> , 2000
AGL3/AGL15		MADS	Parenicova <i>et al.</i> , 2003
MYB binding site motif	ACCAAAC	MYB	Stracke <i>et al.</i> , 2001

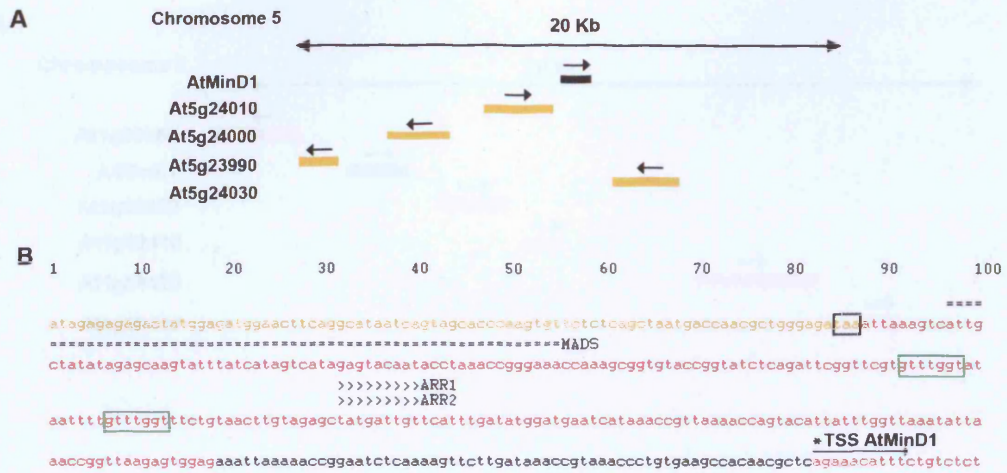


Fig. 6. 13. Analysis of the promoter region of *AtMinD1*. (A) Schematic of the region of chromosome 5 around *AtMinD1*. Arrows indicate the direction of transcription. (B) Promoter region of *AtMinD1*. Nucleotides highlighted in red indicate potential transcription binding sites (AthaMap). Nucleotides highlighted in orange indicate the reading frame of the previous gene (*At5g24010*). Black box indicates the stop codon of *At5g24010*. Green boxes indicate MYB transcription factor binding sites. ===== indicates combinatorial elements. TSS = Transcriptional Start Site.

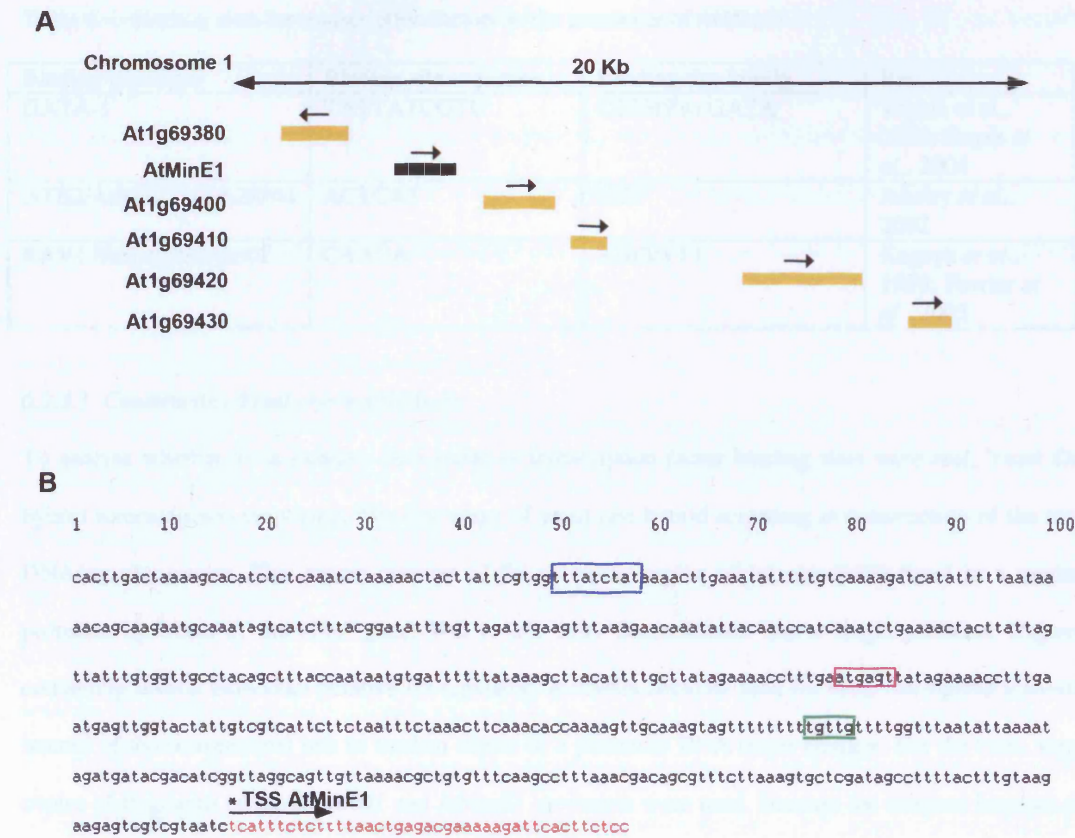


Fig. 6. 14. Analysis of the promoter region of *AtMinE1*. (A) Schematic of the region of chromosome 1 around *AtMinE1*. Arrows indicate the direction of transcription. (B) Promoter region of *AtMinE1*. Blue box indicates GATA1 binding site. Pink box indicates bZIP transcription factor binding site. Green box indicates RAVI-A binding site. TSS = Transcriptional Start Site.

Table 6.4. Binding sites for transcription factors in the promoter of *AtMinE1*.

Binding site name	Binding site sequence	Binding site family	Refs
GATA-1	TATTATCGTC	C2C2(Zn) GATA	Teakle <i>et al.</i> , 2002; Reyes <i>et al.</i> , 2004
ATB2/AtbZIP53/AtbZIP44	ACTCAT	bZIP	Jakoby <i>et al.</i> , 2002
RAV1 binding site motif	CAACA	ABI3/VP1	Kagaya <i>et al.</i> , 1999; Fowler <i>et al.</i> , 2005

6.2.3.1. Constructing Yeast one-hybrid baits

To analyse whether these putative *cis*-regulatory transcription factor binding sites were real, Yeast One-hybrid screening was employed. The first stage of yeast one-hybrid screening is construction of the target DNA/reporter vector. This vector consists of the promoter region of interest (bait) fused to a minimal promoter upstream of the *HIS3* gene. Wei *et al.*, 1999 demonstrated that a single promoter fragment containing several individual putative *cis*-regulatory elements could be used for yeast one-hybrid screening instead of the conventional bait of tandem copies of a particular DNA target element. For the baits, single copies of fragments of the *AtMinD1* and *AtMinE1* promoters were used. Because the distance between the stop codon of the previous gene and the transcription start site of *AtMinD1* is only 295bp (Fig. 6.13) the entire region was cloned into the reporter vector pHIS2 (Clontech). Primers were designed to amplify this region; PMIND/1 (5'-ATGAATTCATTAAGTCATTGCTATATAGAGC-3' *EcoRI* is underlined) and PMIND/2 (5'-ATGAGCTCGAGCGTTGTGGCTTCACAGG-3' *SacI* is underlined). Genomic DNA was extracted from *Arabidopsis* Columbia ecotype following the protocol outlined in Section 2.3.1.1. The promoter region was amplified using ACCUZYME, a proof-reading polymerase, and cloned into pPCRScripT. The promoter of *AtMinD1* was subsequently sub-cloned into the *EcoRI* and *SacI* sites of the multiple cloning site of pHIS2.

The distance between *AtMinE1* and the open reading frame of the previous gene is much larger than between *AtMinD1* and the gene upstream of *AtMinD1* (Fig. 14), therefore it was decided to isolate a similar ~300bp fragment of the *AtMinE1* promoter. Primers were designed to amplify this fragment; promE1: (5'-ATGAATTC AAGCTTACATTTTGC-3' *EcoRI* is underlined) and promE2; (5'-ATGAGCTCGATTACGACGAC-3'. *SacI* is underlined) however this fragment could not be amplified from the genomic DNA. The promoter fragment was split into two halves, E1 and E2, to make

amplification easier. E1 refers to -1 to -116 of *AtMinE1* and E2 refers to -101 to -270. E1 was amplified from genomic DNA using the primers; promE2 and promE3 (promE3: 5'-ATGAATTCAGATGATACGAC-3' *EcoRI* is underlined) and E2 was amplified from genomic DNA using primers promE1 and promE4 (promE4 5'-ATGAGCTCCGATGTCGTATCAT-3' *SacI* is underlined). E1 and E2 were cloned into pPCRScript and subsequently subcloned into the *EcoRI* and *SacI* sites of pHIS2.

6.2.3.2. Testing baits for leaky *HIS3* expression

Yeast one-hybrid screening requires the ability of a DNA-binding protein to bind the bait DNA and activate transcription of the downstream *HIS3* gene. As inserting the target element into pHIS2 may alter the level of background *HIS3* expression the constructs were tested for leaky *HIS3* expression before yeast one-hybrid screening. 3-amino-1,2,4-triazole (3-AT) is a competitive inhibitor of *HIS3* and can suppress background growth of yeast. To test for leaky *HIS3* expression *S. cerevisiae* strain Y187 was transformed with the constructs and positive colonies selected for on synthetic drop-out media (SD) without Tryptophan (T), SD-T, since the pHIS2 vector contains the *TRP1* gene. Positive colonies were streaked onto plates containing SD-TH (H= Histidine) and 0, 5, 10, 20, 30, 40, 50 or 60 mM 3-AT. Plates were incubated at 30°C for 7 days and the appearance of colonies analysed. The promoter region of *AtMinD1* required 50 mM 3-AT to suppress background growth, E1 required 40 mM 3-AT and E2 required 60 mM 3-AT (Fig. 6.15).

6.2.3.3. Library construction

To perform yeast one-hybrid screening the BD Matchmaker One-hybrid Library Construction and Screening Kit (Clontech) was used. In this kit, library construction and screening are performed simultaneously through co-transformation of the reporter/bait vector (pHIS2) with the cDNA library and the library vector (pGADT7-Rec2). The library vector is constructed through *in vivo* homologous recombination between pGADT7-Rec2 and the cDNA library. Library proteins fused to GAL4-AD within the pGADT7-Rec2 vector are screened for those that interact with the DNA target by plating the transformation onto His free media. Simultaneous library construction and screening means that unlike two-hybrid screening by yeast mating in which the same library can be used for many different screens, in one-hybrid screening the library created is only used once. The possibility of first constructing the library



Fig. 6. 15. Testing for autoactivation of the *HIS3* gene in the pHIS2/bait DNA reporter vectors. Y187 was transformed with pHIS2/bait DNA constructs and plated on SD-T. Colonies were subsequently streaked onto SD-TH plates containing 3-AT.

vectors and then using the same library for many different screens was investigated. Initially the possibility of one-hybrid screening through yeast mating was investigated. To perform yeast mating in *S. cerevisiae* a MAT α strain and a MAT α strain must be used. Y187 in which one-hybrid screening is performed is a MAT α strain. For a MAT α strain AH109 was used. AH109 contains the *HIS3* gene under the control of the GAL1_{UAS}. Both Y187 and AH109 strains are used in two-hybrid screening by yeast mating. To test the viability of using yeast mating for one-hybrid screening, leaky expression of *HIS3* was tested for in the AH109 strain. AH109 was transformed with the pHIS2/promoter AtMinD1 construct and positive colonies selected for on SD-T. Colonies were subsequently streaked onto SD-TH + 3-AT media. No amount of 3-AT could suppress the background growth of AH109 on His-free media. The leaky *HIS3* expression was probably due to the *HIS3* gene present in the genome of AH109 meaning that screening by yeast mating would be impossible without a MAT α strain that did not contain a *HIS3* gene.

Secondly the possibility of creating the library vectors and subsequently isolating them from yeast cells for later use in co-transformation with the pHIS2 constructs was investigated. Y187 was transformed with the library cDNA and the pGADT7-Rec2 vector and *in vivo* library construction occurred. The transformation was plated on media without leucine (L) since pGADT7-Rec2 contains the *LEU2* gene for leucine synthesis. The resulting yeast library was pooled together and the library plasmids isolated and replicated by extraction from the yeast cells and transformation into *E. coli*. The idea was that the library plasmids could be extracted from *E. coli* and used in one-hybrid screening by co-transformation with the pHIS2/bait DNA construct. The library contained within the *E. coli* could easily be amplified and used again by simply growing the *E. coli* and extracting the plasmids. However it proved to be too difficult to extract the library plasmids from the yeast and transform them into *E. coli* on a large scale, the process was too inefficient to be plausible.

Finally yeast one-hybrid screening was performed in accordance with the manufacturer's instructions. RNA for cDNA library construction was isolated from 20 day-old *Arabidopsis* ecotype Columbia seedlings. cDNA library construction was performed as instructed by the manufacturer (Fig. 16). Library plasmid construction and library screening were performed simultaneously by co-transformation of the pHIS2 construct, the cDNA library and the pGADT7-Rec2 vector. Each transformation was plated out

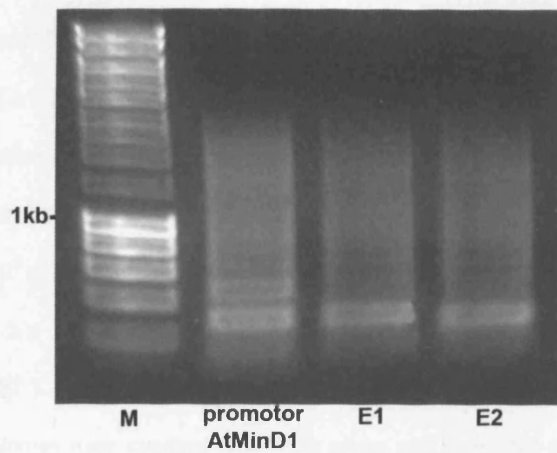
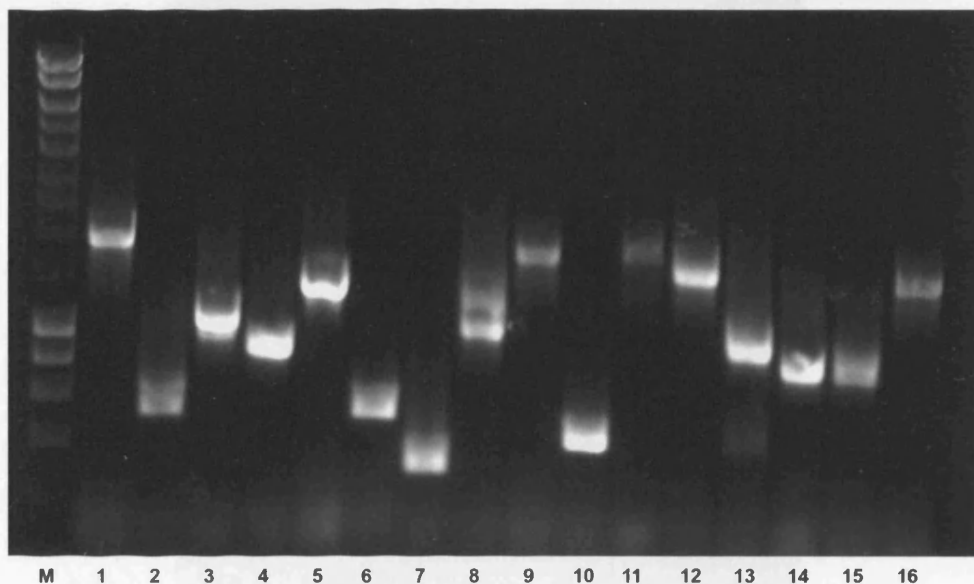


Fig. 6. 16. cDNA libraries used in yeast one-hybrid screens.

onto 20 X 15 cm round Petri dishes, 300 μ l of transformation per plate. Plates contained SD-TLH media with 50, 40 and 60 mM 3-AT for *AtMinD1* promoter, E1 and E2 screens respectively. For each transformation 100 μ l of a 1:10, 1:100 and 1:1000 dilution was spread onto SD-L, SD-T and SD-LT plates to determine transformation efficiency and to calculate the number of clones screened (Section 2.4.4.). Plates were incubated at 30°C for 5 days and the appearance of colonies analysed. For the *AtMinD1* promoter screen, 1.2×10^5 clones were screened and there were 4.3×10^5 transformants per 3 μ g pGADT7-Rec2. For E1 screen, 1.3×10^5 clones were screened and there were 4.9×10^5 transformants per 3 μ g pGADT7-Rec2 and for E2 1.1×10^5 clones were screened and there were 5.0×10^5 transformants per 3 μ g pGADT7-Rec2. His⁺ colonies were streaked onto fresh plates and incubated at 30°C for 3 days. Because His⁺ transformants may contain more than one library plasmid, which can complicate the analysis of putative positive clones, the colonies were replica plated twice more onto SD/-HTL plates to dilute out extra library plasmids. His⁺ colonies were finally streaked onto a master plate and assigned a number for subsequent analysis. 16 positive colonies were isolated from the screen using the *AtMinD1* promoter as bait, 6 positive colonies were isolated from the E1 screen and 4 colonies were isolated from the screen using E2. Library plasmids were extracted from the yeast using the method in Section 2.4.5. A PCR test was employed to analyse whether each of the colonies contained a unique library clone or if a library clone was represented more than once. Vector specific T7 sequencing primer (5'-TAATACGACTCACTATAGGGCG -3') and 3'AD sequencing primer (5'-AGATGGTGCACGATGCACGTT -3') which span the cDNA insertion site were used to amplify the cDNA insert. PCR products were separated on a 1% agarose gel and the number of unique cDNA clones recorded (Fig. 17, 18 and 19). For *AtMinD1* there were 12 unique library clones and 6 and 4 unique library clones for E1 and E3 respectively. Unique library plasmids were rescued by extraction from yeast cells and transformation into *E. coli*. Transformations were plated on LB containing 50 μ g.ml⁻¹ ampicillin. A single colony from each of the transformations was used to inoculate 5 mls of liquid LB containing 50 μ g.ml⁻¹ ampicillin and cell were incubated over night at 37°C with shaking. Library plasmids were extracted from *E. coli* using standard protocol (Section 2.3.1.3.). To ensure that these library plasmids could interact with the respective DNA bait the isolated library plasmids were tested for re-interaction with the respective bait plasmid. Unique library clones from each of the screens were co-transformed into Y187 yeast cells along



Class	Clones Identified	Name
1	1	D-1
2	2, 6	D-2
3	3	D-3
4	4, 13	D-4
5	5	D-5
6	7	D-6
7	8	D-7
8	9, 11	D-8
9	10	D-9
10	12	D-10
11	14, 15	D-11
12	16	D-12

Fig. 6. 17. PCR analysis of the AD-Library clones from the AtMinD1 promoter yeast one-hybrid screen. DNA was extracted from 16 yeast colonies isolated in the yeast one-hybrid screen. The cDNA insert in the AD-Library vector was amplified by PCR and the products separated on a 1% agarose gel to identify unique library plasmids.

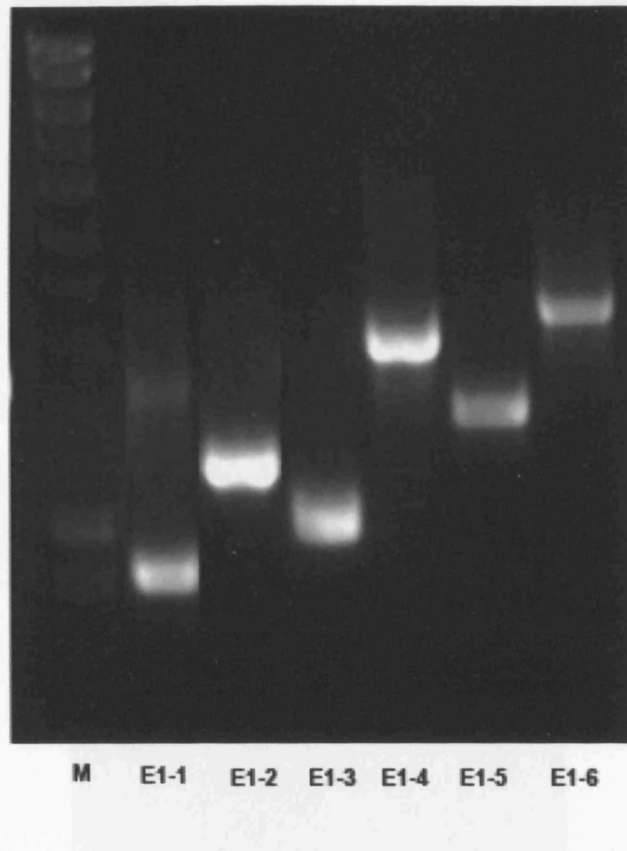


Fig. 6. 18. PCR analysis of the AD-Library clones from the E1 yeast one-hybrid screen. DNA was extracted from 6 yeast colonies isolated in the yeast one-hybrid screen. The cDNA insert in the AD-Library vector was amplified by PCR and the products separated on a 1% agarose gel to identify unique library plasmids.

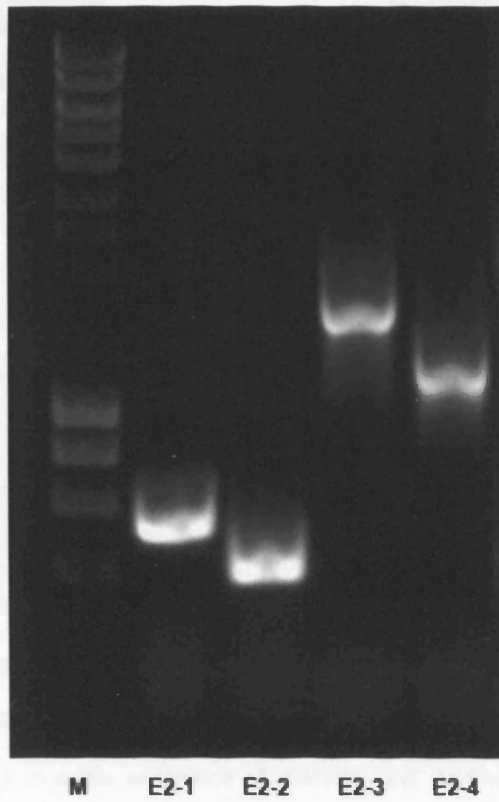


Fig. 6. 19. PCR analysis of the AD-Library clones from the E2 yeast one-hybrid screen. DNA was extracted from 4 yeast colonies isolated in the yeast one-hybrid screen. The cDNA insert in the AD-Library vector was amplified by PCR and the products separated on a 1% agarose gel to identify unique library plasmids.

with pHIS2/*AtMinD1* promoter, pHIS2/E1 or pHIS2/E2. Y187 cells containing both plasmids were selected for on SD-LT plates. To test for interaction a single colony from each of the transformations was streaked on SD-LTH media containing either 50mM 3-AT for pHIS2/*AtMinD1* promoter, 40 mM 3-AT for pHIS2/E1 and 60mM 3-AT for pHIS2/E2. Plates were incubated for 3 days at 30°C and the appearance of growth analysed. All of the library plasmids demonstrated re-interaction with the respective bait plasmid therefore all of the library plasmids were selected for further analysis (Fig. 6.20, 6.21 and 6.22).

6.2.3.4. Analysis of Library Clones

To identify the library clones the library plasmids were sequenced with the T7 sequencing primer. E1-5, E1-6 and E2-4 were found to be out of frame with the GAL4-AD. Due to restriction on time only *in silico* analysis was performed for each of the candidate clones to assess whether they might regulate expression of *AtMinD1* or *AtMinE1*. Initially the Blastn algorithm was used to identify the candidates based upon sequence homology to the *Arabidopsis* genome contained in the NCBI database (<http://www.ncbi.nlm.nih.gov/blast/>). Once the candidate genes were identified, several aspects of the encoded protein could be analysed. Initially the predicted sub-cellular localization of the candidate protein was analysed. Proteins that regulate expression of *AtMinD1* and *AtMinE1* should be localized to the nucleus. Although TargetP (www.cbs.dtu.dk/services/TargetP/) does not give nuclear localization predictions it can be used to eliminate those candidates predicted to be targeted to the chloroplast or mitochondria. Secondly positive transcription activators must contain a DNA-binding domain to bind the target *cis*-regulatory elements within the *AtMinD1* or *AtMinE1* promoter. To search for putative DNA-binding domains the Pfam database was used (www.sanger.ac.uk/Software/Pfam/).

D-7 was discovered to contain only a small fragment (<50bp) of an *Arabidopsis* gene and therefore to be mostly just the empty pGADT7-Rec2 cloning vector. D-1 was identified as At1g20340 which encodes a plastocyanin family protein annotated by TAIR (www.arabidopsis.org) to be involved in electron transport and located in the thylakoid lumen. In agreement with this TargetP predicts a chloroplast targeted transit peptide. Analysis of the Pfam database detected a putative copper binding domain (PF00127) of the plastocyanin family. D6 is At5g66190 which encodes a ferredoxin NADP(H) oxidoreductase involved in electron transport within the chloroplast (Hanke *et al.*, 2005). D-3 was also

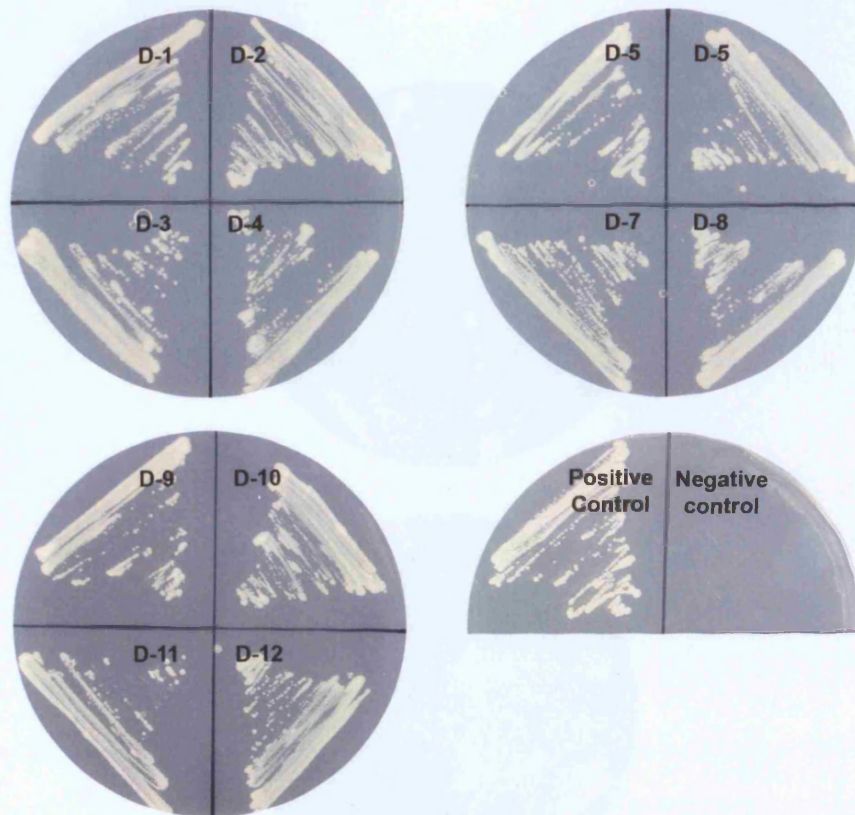


Fig. 6. 20. Re-interaction of candidate library plasmids from the yeast on-hybrid screen using the promoter region of *AtMinD1* as bait. Library-AD plasmids along with the p_{HIS2}/promoter *AtMinD1* bait vector were used to transform Y187 cells. Colonies containing both vectors were streaked on SD-TLH + 50mM 3-AT and the appearance of growth analysed. All candidates grew on His-free media signifying interaction between the library-AD protein and the bait. Y187 cells were co-transformed with pGADT7-Rec2-53 + p_{53HIS2} as a positive control and pGADT7-Rec2-53 + p_{HIS2} empty vector as a negative control.

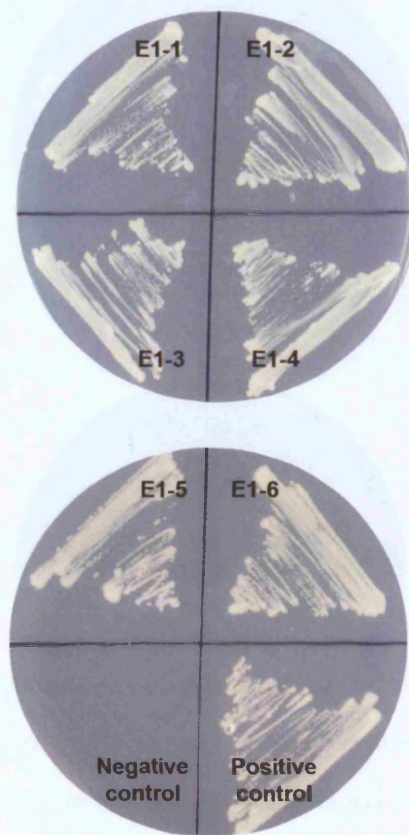


Fig. 6. 21. Re-interaction of candidate library plasmids from the yeast on-hybrid screen using E1 as bait. Library-AD plasmids along with the pHIS2/E1 bait vector were used to transform Y187 cells. Colonies containing both vectors were streaked on SD-TLH + 50mM 3-AT and the appearance of growth analysed. All candidates grew on His-free media signifying interaction between the library-AD protein and the bait. Y187 cells were co-transformed with pGADT7-Rec2-53 + p53HIS2 as a positive control and pGADT7-Rec2-53 + pHIS2 empty vector as a negative control.



Fig. 6. 22. Re-interaction of candidate library plasmids from the yeast on-hybrid screen using E2 as bait. Library-AD plasmids along with the pHIS2/E2 bait vector were used to transform Y187 cells. Colonies containing both vectors were streaked on SD-TLH + 50mM 3-AT and the appearance of growth analysed. All candidates grew on His-free media signifying interaction between the library-AD protein and the bait. Y187 cells were co-transformed with pGADT7-Rec2-53 + p53HIS2 as a positive control and pGADT7-Rec2-53 + pHIS2 empty vector as a negative control.

identified as a chloroplast-targeted protein. D-3 is At1g79040 annotated by TAIR to encode the 10 kDa PsbR subunit of photosystem II (PSII). In agreement with the TAIR annotation, blastp of At1g79040 predicted protein sequence reveals homology to PSII 10 kDa proteins from many different plant species. D-9 was identified as At1g30380. A search of the Pfam database detected the photosystem I (PS I) – PsaK protein domain. In barley PsaK is a subunit of PS I and is a small hydrophobic protein containing two transmembrane regions (Kjaerulff *et al.*, 1993) As part of PS I PsaK is localized to the thylakoid membranes in agreement with the TargetP prediction of a chloroplast targeted transit peptide for the protein product of At1g30380. D-12 is At1g67090 which encodes the ribulose biphosphate carboxylase (RuBisCO) small chain subunit 1A. RuBisCo is involved in fixation of carbon dioxide and is present on the thylakoid membranes. D-1, D-3, D-6, D-9 and D-12 from *in silico* analysis are all involved in aspects of photosynthesis. D-1, D-3, D-6, D-9 and D-12 have no putative DNA binding domains and the predicted chloroplast localization means that D-1, D-3, D-6, D-9 and D12 do not regulate the expression of *AtMinD1*.

D-4 was identified as At1g52870. At1g52870 is annotated by the TAIR database to encode a protein related to peroxisomal membrane proteins. Searching of the Pfam database detected the Mpv17/PMP22 family domain. PMP22 is a major component of peroxisomal membranes and is thought to be involved in pore-forming activities. Mpv17 in *S. cerevisiae* is an integral membrane protein of the inner mitochondrial membrane. TargetP predicts chloroplast localization and it is therefore likely that D4 is involved in pore formation in the chloroplast envelope.

All of the candidates identified above are localized to the chloroplast and do not harbor putative DNA-binding domains necessary to interact with the promoter region of *AtMinD1*. It appears that these candidates are false positives of the yeast one-hybrid screening process.

D-8 was identified as At4g21810 which encodes a protein of unknown function. TargetP does not predict the presence of a transit or signal peptide and gives an unknown localisation. Pfam detects a DER1 protein domain PF04511. In *S. cerevisiae*, Der1 (Degradation in the endoplasmic reticulum 1) is able to selectively degrade mis-folded luminal secretory proteins (Knop *et al.*, 1996). D-8 is not predicted to contain a DNA-binding motif and the putative function of degradation of unfolded proteins means that D-8 is not a transcriptional activator of *AtMinD1*.

D-10 is At3g06650 which encodes ACLB1, one of the two genes encoding subunit B of the trimeric enzyme ATP Citrate lyase. The ATP citrate lyase complex catalyzes the reaction; citrate = acetate + oxaloacetate (Fatland *et al.*, 2002). TargetP predicts a mitochondria targeted transit peptide. Pfam detects the CoA-ligase domain PF00549.

D-11 is At4g14230. TargetP predicts a signal peptide and a localization of the secretory pathway. Pfam recognizes two domains within the protein product of At4g14230; the CBS domain and DUF21 domain. CBS domains can act as binding domains for adenosine derivatives and may regulate the activity of attached enzymatic or other domains. DUF21 is a domain of unknown function; this domain is found in the N-terminus of the proteins adjacent to two CBS domains.

Only two candidates from the one-hybrid screen using the AtMinD1 promoter as bait would be selected for future analysis: D-5 is At5g51110 which encodes a protein of unknown function. TargetP predicts the protein product of At5g51110 to contain a chloroplast-targeted transit peptide. Pfam detects a putative domain: Pterin 4a (PF01329). Pterin 4 alpha carbinolamine dehydratase is also known as DCoH (dimerisation cofactor of hepatocyte nuclear factor 1-alpha). DCoH functions as both a transcriptional coactivator and a pterin dehydratase (Cronk *et al.*, 1996). Although D-5 is predicted to be chloroplast localized instead of nuclear localization, the role of DCoH as a transcriptional co-factor means that it is worth further investigation. The second candidate that would be selected for future analysis is D-2. D-2 was identified as At1g64370. At1g64370 encodes an expressed protein of unknown function. TargetP detects no putative transit or signal peptides and gives no localization for the protein product of At1g64370. Searching of the Pfam database revealed no conserved protein domains. Blastp of the predicted protein sequence of At1g64370 detected no homology to any other proteins contained within the NCBI database. D-2 would be selected for further investigation because it is a protein of unknown function therefore it is possible that it might be a regulator of transcription.

6.2.3.5. Analysis of candidates using E1 as bait.

E1-1 was discovered to contain only a small fragment (<50bp) of an *Arabidopsis* gene and therefore to be mostly just the empty pGADT7-Rec2 cloning vector.

E1-3 is At1g62980 which encodes an expansin-like protein termed AtEXPA18. 38 different expansins are present in the nuclear genome of *Arabidopsis*. Expansins are a group of extracellular proteins that directly modify the mechanical properties of plant cell walls (Li *et al.*, 2002). TargetP predicts a localization of the secretory pathway. Because of the functional prediction of expansin-like protein, it is very unlikely that E1-3 plays a role in the regulation of *AtMinE1*. Interestingly, from examination of the microarray data AtEXP18 although not significantly altered upon induction of chloroplast division inhibition it is reduced 3-fold upon prolonged chloroplast division inhibition (See CD-ROM)

Two proteins would be selected for further analysis from the one-hybrid screen using E1 as bait: E1-2 was identified as At1g09750 which as annotated by TAIR to encode a pepsinA family protein. TAIR also annotates the At1g09750 protein product to be related to DNA-binding proteins. Pfam predicts an aspartyl protease domain PF00026 involved in the catalysis of hydrolysis of peptide bonds. Blastp reveals homology to other DNA-binding proteins and PepsinA proteins from other plant species. TargetP gives a prediction of the secretory pathway. This candidate would be selected for further analysis because of the relation to other DNA-binding proteins. Analysis of the microarray data reveals that expression of At1g09750 exhibits a 0.61-fold change upon induction of chloroplast division inhibition. During a prolonged period of chloroplast division inhibition a 0.4-fold change is observed, this is a two-fold reduction in expression of At1g09750. The t-test score indicates that this fold change is significant.

E1-4 is At4g35890. Pfam recognizes the La domain PF05383. The La domain is of uncertain function. In humans, La acts as a RNA polymerase III (RNAP III) transcription factor in the nucleus, while in the cytoplasm, La acts as a translation factor (Intine *et al.*, 2003). In the nucleus, La binds to the 3'UTR of nascent RNAP III transcripts to assist in folding and maturation (Alfano *et al.*, 2003). In the cytoplasm, La recognizes specific classes of mRNAs that contain a 5'-terminal oligopyrimidine (5'TOP) motif known to control protein synthesis (Keene, 2003). TargetP predicts chloroplast localization for the protein product of At4g35890.

6.2.3.6. Analysis of candidates using E2 as bait.

E2-1 was identified as Chlorophyll A/B Binding Protein 1 (CAB1). CAB1 is chloroplast-localised and is a subunit of light-harvesting complex II (LHCII), which absorbs light and transfers energy to the

photosynthetic reaction center. Due to the role of CAB1 in LHCII, CAB1 is not a transcriptional regulator of *AtMinE1* and should be eliminated from further investigation.

E2-2 was identified as At4g23400. At4g23400 features a conserved protein domain the MIP domain (Major Intrinsic Protein). MIP family proteins are transmembrane channel proteins. The protein product of At4g23400 is annotated by TAIR to have water channel activity. TargetP did not predict the presence of a transit or signal peptide and gives an unknown localisation for the protein product of At4g23400.

Blastn searching revealed that E2-3 is At3g05880 which encodes RCI2A (Rare Cold-Inducible 2A). RCI2A expression is induced in response to low temperature, dehydration, salt stress, and abscisic acid (Medina *et al.*, 2001). Like E2-2, E2-3 is also likely to be a membrane protein; searching of the Pfam database for putative domains detected UPF0057 domain PF01679. Proteins that contain UPF0057 domain are small proteins of from 52 to 140 amino-acids that contain two transmembrane domains. TargetP predicts the presence of a signal peptide and RCI2A is localized to the secretory pathway. E2-2 and E2-3 are both membrane proteins and no putative DNA-binding domains were detected therefore E2-2 and E2-3 are unlikely to be transcriptional activators of *AtMinE1*.

Table 6.5. Library clones identified in yeast one-hybrid screen using the promoter of *AtMinD1* as bait

Class	Repeated	Identity	Gene	Annotation	Source	*TP
1	1	D-1	At1g20340	Plastocyanin family protein	Peltier <i>et al.</i> , 2002	Yes
2	2	D-2	At1g64370	Expressed protein	-	-
3	1	D-3	At1g79040	PsbR subunit of PSII	Suorsa <i>et al.</i> , 2006	Yes
4	2	D-4	At1g52870	Peroxisomal membrane protein	Pfam PF01329	Yes
5	1	D-5	At5g51110	Expressed protein. Pterin 4a domain	Cronk <i>et al.</i> , 1996	Yes
6	1	D-6	At5g66190	Ferredoxin NADP(H) oxidoreductase	Okutani <i>et al.</i> , 2005	Yes
7	1	D-7	-	Fragment <50bp	-	-
8	2	D-8	At4g21810	Expressed protein. Der1 protein domain detected	Knop <i>et al.</i> , 1996	-
9	1	D-9	At1g30380	PsaK PSI subunit	Kjaerulff <i>et al.</i> , 1993	Yes
10	1	D-10	At3g06650	ACLB1 subunit B of ATP Citrate lyase	Fatland <i>et al.</i> , 2002	Mitochondria
11	2	D-11	At4g14230	CBS domain-containing protein	Pfam PF01595 and PF00571	Secretory pathway
12	1	D-12	At1g67090	RuBisCo small chain subunit 1A	Kawamura and Uemura, 2003	Yes

* Protein is predicted to contain a chloroplast targeted transit peptide

Table 6.6. Library clones identified in yeast one-hybrid screen using E1 as bait

Identity	Gene	Annotation	Source	*TP
E1-1	-	Fragment <50bp	-	-
E1-2	At1g09750	Homology to PepsinA/DNA-binding proteins	PF00026	Secretory pathway
E1-3	At1g62980	Expansin-like protein AtEXPA18	Li <i>et al.</i> , 2002	Secretory pathway
E1-4	At4g35890	La domain containing protein	Intine <i>et al.</i> , 2003; Alfano <i>et al.</i> , 2003	Yes
E1-5	-	Out of frame	-	-
E1-6	-	Out of frame	-	-

* Protein is predicted to contain a chloroplast targeted transit peptide

Table 6.7. Library clones identified in yeast one-hybrid screen using E2 as bait

Identity	Gene	Annotation	Source	*TP
E2-1	At1g29930	Chlorophyll A/B Binding Protein 1 (CAB1).	Gao and Kaufman, 1994	Yes
E2-2	At4g23400	MIP family protein transmembrane channel protein	Johanson <i>et al.</i> , 2001	-
E2-3	At3g05880	RCI2A (Rare Cold-Inducible 2A). Membrane protein	Medina <i>et al.</i> , 2001	Secretory pathway
E2-4	-	Out of frame	-	-

* Protein is predicted to contain a chloroplast targeted transit peptide

6.3. Discussion

Although much research has been dedicated to the molecular machinery involved in chloroplast division very little research has been performed into the regulation of plastid division. In this study QPCR, DNA microarrays and yeast one-hybrid assays were used to investigate the light regulation of expression of chloroplast division components, the affect on nuclear gene expression of chloroplast division inhibition and transcriptional activators of *AtMinD1* and *AtMinE1*.

6.3.1. Expression of *Arabidopsis ftsZ* and *min* genes is light regulated

QPCR analysis revealed that *FtsZ1-1* and *FtsZ2-1* gene expression in *Arabidopsis* is light regulated (Fig. 1). 20 day old light-grown seedlings were treated to 24 hour dark followed by 24 hours light. After 24 hours dark the expression of *ftsZ* was 10-fold lower than in continuous light. A 10-fold reduction in *ftsZ* gene expression is significant decrease and would be enough to inhibit chloroplast division. This result suggests that chloroplast division does not occur in the dark and is a light-regulated process. *AtMinD1* and *AtMinE1* also show a reduction of gene expression in the dark demonstrating that other chloroplast division components are co-regulated with *FtsZ* genes (Fig. 6.1).

After the 24 hour light treatment the level of *ftsZ* and *min* gene expression returned approximately to the level of expression when grown in continuous light. It is possible that this level of *ftsZ* and *min* gene expression is the optimum level of expression for correct division of chloroplasts. Experiments altering the level of FtsZ proteins and Min proteins in *Arabidopsis* demonstrate that strict stoeochemistry is required for correct chloroplast division (Osteryoung *et al.*, 1998; Colletti *et al.*, 2000; Stokes *et al.*, 2000; Maple *et al.*, 2002).

Although gene expression is an excellent indicator of protein expression the absolute amount of protein within the cell cannot be measured by using the amount of RNA transcripts due to post-transcriptional regulation of protein expression. Also the life span of the proteins in the cell cannot be estimated; proteins may be short-lived and so levels of protein within the cell may fluctuate with gene expression or proteins may be long-lived and accumulate to high levels in the cell even following a reduction in gene expression. Therefore it would be interesting to map the protein level onto the expression

data to see if protein levels are also differentially affected by light. This could be accomplished by raising antibodies against AtFtsZ1-1, AtFtsZ2-1, AtMinD1 and AtMinE1 and using them to probe western blots.

It would also be interesting to investigate whether *ftsZ* and *min* gene expression is altered with regard to the intensity of light; is expression reduced in dim light or is the total absence of light required for reduced gene expression? Plastids can respond to different intensities of light. Exposure to high intensity light causes redistribution of thylakoid antenna complexes and chloroplast movement is observed towards weak light or away from strong light (reviewed in Lopez-Juez and Pyke, 2005). Perhaps it is possible that chloroplast division is also controlled by the intensity of light with higher level of chloroplast division observed in plants exposed to high light intensity and lower levels of chloroplast division at lower light intensities or shaded leaves.

Analysis of the promoter region of *AtMinD1* using AtCisDB revealed the binding sites of MYB family transcription factors. The expression of some MYB transcription factors is induced by light (Jin *et al.*, 2000) and it is possible that the light regulation of *AtMinD1* expression is mediated by MYB-family transcription factors. The promoter region of *AtMinE1* was not predicted to contain the binding site for MYB transcription factors however analysis of *AtMinE1* promoter region using AthaMap did reveal the binding sequence for GATA-1 transcription factors. Many light responsive promoters contain GATA motifs (Reyes *et al.*, 2004) and it is possible that GATA-1 transcription factors are involved in the light regulation of expression of *AtMinE1*. Yeast-one hybrid analysis of the *AtMinE1* promoter region failed to identify any GATA-1 transcription factors. However yeast one-hybrid analysis was not very successful at identifying *AtMinE1* transcription factors and only two candidates identified in the yeast one-hybrid screen are worth further investigation.

Why would chloroplast division be a light regulated process? QPCR analysis revealed fluctuations in expression of four chloroplast division components in response to exposure to light or dark with reduced expression in the dark and up-regulated expression upon exposure to light. Perhaps the observed fluctuations are to control the cycle of division and expansion of the chloroplasts. Morphological analysis of dividing chloroplasts reveals that the process of chloroplast division can be separated into four distinct stages (Possingham and Lawrence, 1983, Leech *et al.*, 1981): (i) Slight chloroplast expansion, (ii) chloroplast constriction and dumbbell formation, (iii) Further constriction, isthmus formation and thylakoid

membrane separation, and (iv) Isthmus breakage, chloroplast separation and envelope resealing. Perhaps the reduction in gene expression of chloroplast division genes prevents the chloroplasts dividing in the dark at night allowing time for chloroplast expansion before the next round of chloroplast division. However when grown in constant light chloroplasts do not appear smaller than the chloroplasts of plants grown in light/dark cycle suggesting that adequate chloroplast expansion has occurred before chloroplast division.

6.3.2. *Affect of chloroplast division inhibition on nuclear gene expression*

DNA microarrays were used to analyse the affect of chloroplast division inhibition on nuclear gene expression. Overexpression of AtMinD1 was used to inhibit chloroplast division. Surprisingly none of the characterised chloroplast division components exhibited a significant change in gene expression upon inhibition of chloroplast division (Table 1). The assembly of FtsZ proteins into the Z-ring is believed to be the initial step in chloroplast division. Therefore it would be expected that *ftsZ* expression would be up-regulated in response to lack of chloroplast division.

It is possible that the plant cannot sense the division state of the chloroplasts. Studies indicate that the expression of a set of nuclear genes that encode chloroplast-localised proteins is dependant on the functional state of the plastid via a process known as retrograde signalling. At least two independent retrograde signalling pathways have been identified. Several reports suggest that one of the plastid signals is a tetrapyrrole (Reviewed in Surpin *et al.*, 2002). Tetrapyrroles are the intermediates and end products of heme, chlorophyll and phytochromobilin biosynthetic pathways. Three GUN mutants (Genome UNcoupled) are part of the plastid tetrapyrrole biosynthetic pathway (GUN2/HY1; At2g26670, GUN3/HY2; At3g09150 and GUN5/ChlH; At5g13630) and are believed to be involved in retrograde signalling (Reviewed in Surpin *et al.*, 2002). The expression of these three genes in each of the treatments of the microarray was investigated. No significant change in gene expression for any of these genes was detected upon chloroplast division inhibition. The second retrograde signalling pathway identified is mediated by redox signalling. The redox status of the plastoquinone pool in the photosynthetic electron transport chain exerts control over nuclear gene expression of some chloroplast-encoded genes (Reviewed in Surpin *et al.*, 2002). The expression of two nuclear genes, PsaD (At1g03130) and PsaF (At1g31330),

known to be regulated by redox signalling was examined in each of the treatments. No significant change in gene expression was detected for either of these genes upon chloroplast division inhibition. Research into retrograde signalling is still in its infancy and it is possible that other signalling pathways will be discovered, however these results suggest a lack of retrograde signalling in response to chloroplast division inhibition.

The plants do not appear to be altering gene expression in response to the difference between reduced numbers of large chloroplasts and wild-type like chloroplast size and number. In plants experiencing prolonged chloroplast division inhibition mesophyll cells have few but large chloroplasts (Fig. 6.2). In plants experiencing temporal chloroplast division inhibition mesophyll cells have wild-type like chloroplast size and number (Fig. 6.2). However, the same genes are up-regulated in temporal and prolonged induction of chloroplast division inhibition (See CD/ROM) indicating that the size and number of the chloroplasts is not the factor altering nuclear gene expression.

Gene ontology predictions revealed that of the many genes up-regulated or down-regulated in response to inhibition of chloroplast division, not many of these genes are predicted to encode chloroplast localised proteins. However it has been demonstrated that chloroplast division involves both cytosolic and stromal proteins. ARC5 is an example of a cytosolic plastid division protein (Gao *et al.*, 2003). TargetP is unable to assign a localisation prediction for ARC5. Therefore many of the proteins not assigned to the chloroplast may still make up part of the chloroplast division machinery.

None of the candidates selected from the microarray data for further analysis exhibited a chloroplast division phenotype when a T-DNA insertion line of the candidate gene was analysed. However more exhaustive analysis of these candidates including localisation analysis and overexpression data would have to be undertaken to completely eliminate these candidates as not being involved in chloroplast division. At1g80920 and At4g36040, like ARC6, encode proteins that contain a J-domain motif characteristic of DNA-J chaperones (Vitha *et al.*, 2003). It is possible that these two genes exhibit functional redundancy and perhaps a double mutant would exhibit a chloroplast division phenotype. AGL24 was also chosen for further investigation. AGL24 is a MADS-box containing transcription factor involved in promoting inflorescence identity (Gregis *et al.*, 2006). AGL24 is expressed in vegetative tissue before floral transition (Gregis *et al.*, 2006). Although the seedlings used in the microarray analysis were

too young to be undergoing floral transition, many of the MADS-box transcription factors involved in flower development were up-regulated in response to chloroplast division inhibition such as APETALA1, APETALA3, AGL24, AGL9 and ANR1 (See CD/ROM). Genes encoding MADS-box transcription factors may have been up-regulated because the seedlings used for the microarray were stressed, as early onset flowering often occurs when plants are stressed. However the control plants were subjected to the same conditions and this did not induce up-regulation of these genes.

Only a handful of genes from a small portion of the microarray data were chosen for further analysis. The criterion for selecting genes for further analysis was that they should be up-regulated upon inhibition of chloroplast division and be chloroplast-localised. Comprehensive analysis of the microarray data is likely to yield new chloroplast division components, in particular those genes involved in the regulation of plastid division.

6.3.3. Analysis of the promoter regions of *AtMinD1* and *AtMinE1*

Alignment of the promoter regions of *AtMinD1* and *AtMinE1* and analysis using AthaMap and AtCisDB revealed no similarity between the two promoter regions suggesting that *AtMinD1* and *AtMinE1* are regulated by different proteins/pathways. However, the similar expression pattern of *AtMinD1* and *AtMinE1* in the light-regulation experiment indicated that they are regulated by the same pathway/proteins. The expression of *AtMinD1* and *AtMinE1* may be regulated by uncharacterised transcription factors whose DNA-binding sites are not recognised by AthaMap and AtCisDB.

Analysis of the promoter region of *AtMinD1* using AthaMap detected the binding site of MADS-family transcription factors. In the microarray project many MADS-box transcription factors had significantly altered expression in response to inhibition of chloroplast division (See CD/ROM). APETALA1, APETALA3, AGL24, AGL9 and ANR1 are all up-regulated following chloroplast division inhibition. The MADS box binding site identified in the promoter of *AtMinD1* is for the AGL-type MADS-box transcription factors. However, a T-DNA insertion line of AGL24 did not exhibit a chloroplast division phenotype that would have been expected if AGL24 was involved in the transcriptional activation of *AtMinD1* (Fig. 12). Although T-DNA insertion of AGL24 did not affect chloroplast division this may be due to functional redundancy between transcription factors; there are predicted to be >100 MADS-box

transcription factors in *Arabidopsis*. Surprisingly ARR2, a transcription factor predicted by AthaMap to bind to the promoter region of *AtMinD1* is predominately expressed in pollen (Lohmann *et al.*, 2001). Studies suggest that ARR2 forms part of a multi-step two-component signalling mechanism which includes proteins like AHP1 or AHP2 (Lohmann *et al.*, 2001). Two-component systems, consisting of a histidine protein kinase that senses the input (such as AHP proteins) and a response regulator that mediates the output (such as ARR proteins), control signal transduction pathways in many prokaryotes and in some eukaryotes.

AthaMap revealed the binding sequence for GATA-1 transcription factors in the promoter of *AtMinE1*. Many light responsive promoters contain GATA motifs (Teakle *et al.*, 2002; Reyes *et al.*, 2004;) and it is possible that the light regulation exhibited by *AtMinE1* may be regulated by GATA family transcription factors.

6.3.4. Yeast one-hybrid screening

Yeast-one hybrid assays produced many of what appear to be false positives; proteins that induce *HIS3* expression but from *in silico* analysis do not encode DNA-binding proteins. Surprisingly, the majority of the false positives identified were chloroplast-localised proteins. Many of these proteins are involved in aspects of photosynthesis from carbon-fixation to components of the photosystem complexes and proteins involved in electron transport. Perhaps the reason for the high proportion of photosynthesis proteins is because the RNA used to construct the cDNA library was extracted from 20 day-old seedlings which have a high rate of photosynthesis. Therefore the most abundant transcripts in the RNA could have been from photosynthetic genes and so would be highly represented in the cDNA library and more likely to generate a false positive.

Only four candidates from the yeast one hybrid screens would be selected for further analysis; two candidates from the screen using *AtMinD1* promoter as bait and two candidates using *AtMinE1* promoter as bait. D-5 is a protein of unknown function. TargetP predicts that D-5 contains a chloroplast-targeted transit peptide. Pfam detects a putative domain: Pterin 4a (PF01329). Pterin 4 alpha carbinolamine dehydratase is also known as DCoH (dimerisation cofactor of hepatocyte nuclear factor 1-alpha). DCoH functions as both a transcriptional coactivator and a pterin dehydratase (Cronk *et al.*, 1996). Although D-5 is predicted to be

chloroplast localized instead of nuclear localization, the role of DCoH as a transcriptional co-factor means that D-5 is worthy of further investigation. D-2 encodes an expressed protein of unknown function. TargetP detects no putative transit or signal peptides and gives no localization for D-2. No putative protein domains or homology to any other proteins contained within the NCBI database were detected. D-2 would be selected for further investigation because it is a protein of unknown function therefore it is possible that it might be a regulator of transcription. E1-2 encodes a pepsinA family protein. TAIR also annotates E1-2 to be related to DNA-binding proteins and blastp reveals homology to other DNA-binding proteins and PepsinA proteins from other plant species. This candidate would be selected for further analysis because of the relation to other DNA-binding proteins. Analysis of the microarray data reveals that expression of E1-2 exhibits a 0.4-fold change in gene expression in response to prolonged chloroplast division inhibition this is a two-fold reduction in expression of E1-2. The t-test score indicates that this fold change is significant. E1-4 contains an La domain. The La domain is of uncertain function. In humans, La acts as a RNA polymerase III (RNAP III) transcription factor in the nucleus, while in the cytoplasm, La acts as a translation factor (Intine *et al.*, 2003). In the nucleus, La binds to the 3'UTR of nascent RNAP III transcripts to assist in folding and maturation (Alfano *et al.*, 2003). In the cytoplasm, La recognizes specific classes of mRNAs that contain a 5'-terminal oligopyrimidine (5'TOP) motif known to control protein synthesis (Keene, 2003).

Further investigation of these candidates could involve analysis of T-DNA insertion lines, overexpression analysis or localization studies.

Analysis of the data in this study reveals that expression of several chloroplast division components is light regulated. Analysis of the promoter regions of *AtMinE1* suggests that light regulation may be mediated by GATA family transcription factors. Examination of the microarray data suggests that retrograde signaling is not involved in the communication of the division state of chloroplasts and reveals that the expression of all of the known chloroplast division components remains unaltered following chloroplast division inhibition. More exhaustive analysis of the microarray data will undoubtedly identify new chloroplast division components and regulators of chloroplast division.

7. Discussion

This study aims to further our knowledge of plastid division. This study hoped to achieve this through the characterisation of known plastid division components, particularly AtMinD1 and through the construction of an interaction map of the stromal plastid division proteins to enable the assembly of a model of plastid division. In addition this study also set out to try to identify novel plastid division components and attempt to shed light upon the regulation of the plastid division process.

7.1 Characterisation of AtMinD1 and the Min system.

AtMinD1 was among one of the first plastid division components to be identified in *Arabidopsis* (Colletti *et al.*, 2000). Like many stromal plastid division proteins AtMinD1 was identified through homology to bacterial cell division proteins (Colletti *et al.*, 2000). *E. coli* MinD (EcMinD) is a well characterised protein and the *min* system in *E. coli* and other bacteria has been well researched. Research into bacterial MinD proteins had previously enabled us to make many assumptions about the properties of AtMinD1 and how the Min system in *Arabidopsis* functions. This study has revealed that many of the properties of EcMinD are conserved in AtMinD1; EcMinD and AtMinD1 are both ATPases and the ATPase activity of both proteins is stimulated through interaction with respective MinE partners (de Boer *et al.*, 1991; Hu and Lutkenhaus, 2001; Aldridge and Møller, 2005; Chapter 3). Use of a AtMinD1 mutant AtMinD1(K72A) that is incapable of interaction with AtMinE1 demonstrates that AtMinE1 is also involved in mediating the localisation of AtMinD1, a situation analogous to the *E. coli* system (Raskin and de Boer, 1999; Rowland *et al.*, 2000; Chapter 3).

Although many of the properties of EcMinD are conserved in AtMinD1, small but significant differences exist between the two proteins. One of these is the requirement of different cations for ATPase activity. EcMinD requires Mg^{2+} for ATPase activity (de Boer *et al.*, 1991) and AtMinD1 requires Ca^{2+} for ATPase activity. Also EcMinD is only activated by EcMinE when bound to phospholipid membranes (Hu and Lutkenhaus, 2001) however; stimulation of AtMinD1 ATPase activity by AtMinE1 is independent of membrane binding. Finally, EcMinE is unable to stimulate the ATPase activity of AtMinD1 suggesting that functional differences exist in the modes of interaction between EcMinD and EcMinE and AtMinD1 and AtMinE1. Why EcMinD and AtMinD1 require different metal ions for ATPase activity is unclear. Perhaps

the requirement of AtMinD1 for Ca^{2+} is an evolutionary adaptation to existence within the plant cell. Many plant processes are regulated by calcium. Indeed studies have suggested a regulatory role for plastidic Ca^{2+} fluxes (Sai and Johnson, 2002) therefore it is possible plastidic Ca^{2+} levels regulate AtMinD1 activity during plastid division. However, the level of Ca^{2+} used in this study is far above the physiological Ca^{2+} levels present in the chloroplasts (Sai and Johnson, 2002). Therefore it would be interesting to investigate whether physiological levels of Ca^{2+} , particularly during Ca^{2+} fluxes, would differentially affect the ATPase activity of AtMinD1.

AtMinE1 can stimulate the ATPase activity of AtMinD1 independently of membrane binding (Chapter 3; Aldridge and Møller, 2005). Although it has not been proved experimentally that AtMinD1 is a membrane binding protein, AtMinD1 is always observed in close proximity to the chloroplast envelope (Maple *et al.*, 2002; Fujiwara *et al.*, 2004; Chapters 3 and 4) and AtMinD1 also contains the conserved C-terminal membrane targeting sequence (MTS) involved in membrane association in EcMinD (Szeto *et al.*, 2002). In *E. coli*, stimulation of EcMinD by EcMinE causes disassociation of EcMinD from the membrane and subsequent oscillation to the opposite pole of the cell thereby controlling the localisation of EcMinD (Hu and Lutkenhaus, 2001; Suefuji *et al.*, 2002; Lackner *et al.*, 2003). The membrane-independent stimulation of AtMinD1 suggests that AtMinE1-mediated stimulation of AtMinD1 ATPase does not underlie the topological specificity of AtMinD1. However, only a 3-fold increase in ATPase activity is observed upon membrane-independent stimulation of AtMinD1. It is unlikely that the observed 3-fold increase is the maximal ATPase activity that can be achieved by AtMinD1 since in *E. coli*, EcMinD activity is increased 10-fold when incubated with phospholipids and EcMinE (Hu and Lutkenhaus, 2001). Therefore it seems likely that increased ATPase stimulation would be observed if AtMinD1 were bound to chloroplast membranes. Investigation into the ATPase activity of AtMinD1 when incubated with envelope membranes and AtMinE1 should shed light on this. It is possible that the function of the ATPase activity of AtMinD1 is not to release AtMinD1 from the membrane as it is in *E. coli* but perhaps fulfills some other function. AtMinD1 ATPase activity may provide the energy for some novel process yet to be identified.

Most strikingly different between the *E. coli* Min system and the *Arabidopsis* Min system is the lack of a MinC homologue in higher plants. ARC3 is believed to fill the role of MinC in *Arabidopsis* (Maple *et al.*, In Press). ARC3 is a chimera of part of FtsZ and part of the eukaryotic PIP5K (Shimada *et*

al., 2004). ARC3 has been shown to interact with both FtsZ1-1 and AtMinD1 which would be expected from a MinC-like protein, but unexpectedly ARC3 has also been shown to interact with AtMinE1 (Maple *et al.*, In Press). In *E. coli*, MinC does not interact with MinE (Rothfield *et al.*, 2005). The dual localisation of ARC3, localising as both a ring with the Z-ring and also as discrete foci with the Min proteins, differs from that of bacterial MinC which localises exclusively in the same localisation pattern as MinD (Raskin and de Boer, 1999; Maple *et al.*, In Press). Not all bacteria contain the classical *min* system consisting of MinC, MinD and MinE (Errington *et al.*, 2003). MinD proteins are present across a broad range of bacterial species, MinC is less highly conserved and MinE is even more restricted in its distribution (Margolin, 2000). In systems that do not contain all three Min proteins one or more of the proteins is substituted in order to adapt the Min system to the particular needs of different organisms. An example of this is *Bacillus subtilis*. In *B. subtilis* the role of MinE is partially fulfilled by the non-homologous protein DivIVA, which is required for the polar localisation of MinCD (Edwards and Errington, 1997). The MinCD complex in *B. subtilis* does not undergo the characteristic oscillatory behaviour of MinCD in *E. coli*. It is believed that DivIVA tethers the MinCD inhibitor to the cell poles instead of inducing the oscillatory cycle (Marston *et al.*, 1998).

The differences that exist between the Min system in *Arabidopsis* and the Min system in *E. coli* require questioning of how well conserved the process of plastid division and bacterial cell division is. The validity of the bacterial paradigm as a guide to the mechanism of the Min system in plastid division requires critical evaluation. It has been presumed that AtMinD1 and AtMinE1 exhibit dynamic behaviour analogous to the *E. coli* proteins, however dynamic redistribution of AtMinD1 or AtMinE1 has not been observed and it is possible that it does not occur. In *E. coli* it has been reported that the Min proteins are redistributed within a coiled structure that extends between the cell poles (Shih *et al.*, 2003), such coiled structures have not been observed in chloroplasts suggesting that a different system may operate in *Arabidopsis*.

Apart from differences in the Min system, in many other respects plastid division and bacterial cell division appear different. Instead of the single FtsZ protein observed in bacterial cell division, higher plants contain two families of FtsZ proteins. Each of these families of FtsZ proteins have different characteristics and both families appear to interact with a different subset of proteins (Stokes and Osteryoung, 2003; El-

Kafafi *et al.*, 2005; Maple *et al.*, 2005; Maple *et al.*, In Press). Many reports indicate that the Z-ring provides the contractile force necessary for *E. coli* cell division (reviewed in Errington *et al.*, 2003). In *Arabidopsis* the principal function of the Z-ring appears to be a scaffold for the assembly of the other components of plastid division. A eukaryote-derived dynamin ring has been implicated in providing the contractile force necessary for plastid division (Yoshida *et al.*, 2006). Many of the essential *E. coli* cell division proteins do not have homologues in *Arabidopsis* or other higher plants. The roles of proteins like ZipA and FtsA in the stabilisation and anchorage of the Z-ring seem to have been filled by proteins that share no homology to the *E. coli* cell division proteins, for example ARC6 (Vitha *et al.*, 2003; Maple *et al.*, 2005).

In conclusion, chloroplast division components that appear to be homologous to characterised bacterial cell division proteins still require rigorous characterisation to prove their function. Presumed functions should not be applied based entirely on homology to bacterial cell division components.

7.2. Future directions in the characterisation of the *min* system

The identification of ARC3 as a potential MinC-like protein has begun to fill a void in efforts to understand how the *min* system in *Arabidopsis* functions. However it remains to be seen if ARC3 is an antagonist of FtsZ polymerisation as MinC is. It would be interesting to observe the structure of FtsZ filaments in ARC3 overexpressing plants. It would be expected that ARC3 overexpressing plants would contain only short filaments of FtsZ as observed in plants overexpressing AtMinD1 (Vitha *et al.*, 2003).

The *min* system in *E. coli* functions through the constant redistribution and oscillation of MinC between the two poles of the *E. coli* cell. This oscillation ensures that the lowest concentration of MinC occurs at midcell enabling the polymerisation of FtsZ at the correct mid-cell point (Raskin and de Boer, 1999). Dynamic behaviour of Min proteins in *Arabidopsis* or other higher plants has not been observed and it is possible that dynamic behaviour does not occur. In order to get a handle on the functioning of the Min system in *Arabidopsis* it is vital that the question of the localisation dynamics of the Min proteins is addressed. If the Min proteins in *Arabidopsis* do not share the dynamic behaviour exhibited by their bacterial counterparts this has a direct consequence on the role of AtMinE1 in the spatial placement of the chloroplast division site as EcMinE is responsible for the constant redistribution of MinCD in *E. coli* (Hu

and Lutkenhaus, 2001; Huang *et al.*, 2003). If AtMinD1 does not exhibit dynamic localisation then the function of AtMinE1 in the Min system in *Arabidopsis* is unclear. However, if oscillatory behaviour of AtMinD1 and AtMinE1 does occur, what form does it take? Several plausible models exist for the oscillation of the Min proteins (Fig. 1). (A) AtMinD1 and AtMinE1 may oscillate directly from pole to pole as observed in *E. coli*. (B) In *E. coli rodA* cells that have round rather than the normal rod-shaped cells MinD and MinE move to and from multiple sites on the cell surface (Corbin *et al.*, 2002). When the cells expand and exhibit a long axis MinD oscillates parallel to the long axis (Corbin *et al.*, 2002). Due to the ellipsoidal nature of chloroplast it is possible that if AtMinD1 and AtMinE1 exhibit dynamic behaviour it may oscillate in a pattern similar to that observed in *rodA* cells. (C) If the Min proteins in *Arabidopsis* do not exhibit oscillatory behaviour then it is possible that the Min proteins are tethered to the chloroplast poles in a situation analogous to *B. subtilis*. (D) Due to the presence of the densely packed thylakoid membranes the Min proteins may not be able to oscillate directly from pole to pole of the chloroplasts. Either the Min proteins do not exhibit oscillatory behaviour or they may move along the chloroplast envelope avoiding travel through the thylakoid membranes.

In *E. coli*, MinE and MinD travel along a spiral-like path, suggesting that polymerisation of these proteins into a helical filament underlies their dynamic behavior (Shih *et al.*, 2003). Although it has been demonstrated that AtMinD1 and AtMinE1 can self interact (Fujiwara *et al.*, 2004; Aldridge and Møller, 2005; Maple *et al.*, 2005) it is unclear whether only dimers are formed or whether they form longer polymeric filaments.

7.3. Assembly of the stromal plastid division machinery

In order to understand the mechanism behind plastid division it is important to assemble the components involved in plastid division into a division machinery. In this study a combination of co-localisation analysis and BiFC assays were used to investigate the interactions between stromal plastid division components. These experiments revealed that AtMinE1 and AtMinD1 assemble into a Min protein complex, AtFtsZ1-1 and AtFtsZ2-1 can form both homopolymeric and heteropolymeric Z-ring structures in living plastids and ARC6 specifically interacts with AtFtsZ2-1 but not with AtFtsZ1-1. This data reveals that chloroplast division components do not act in isolation but rather function as parts of complexes in

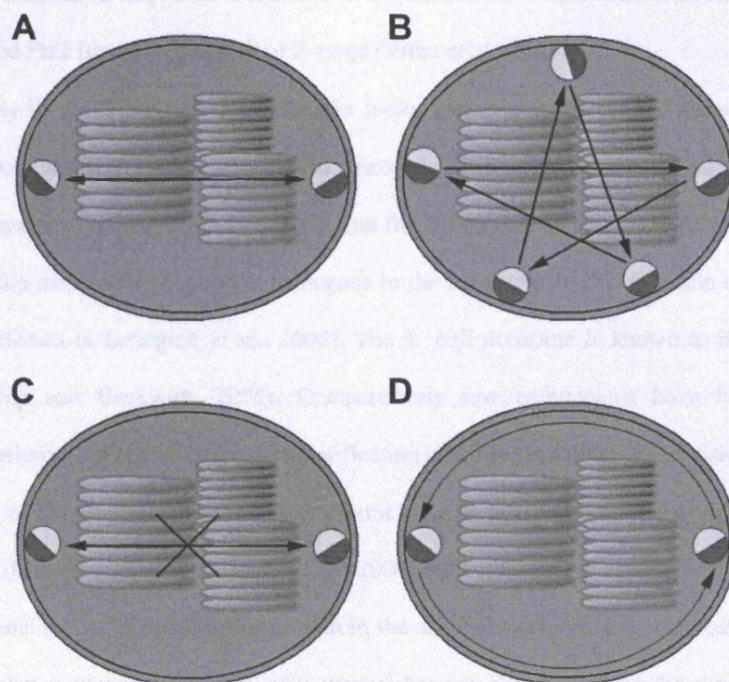


Fig. 1. Models for Min protein movement in *Arabidopsis*. AtMinD1 and AtMinE1 (red/yellow circle) may oscillate within chloroplasts analogous to the *E. coli* model in wild-type (arrow represents side to side oscillations along a spiral pathway) (A) or spherical *rodA* mutant cells (B). Equivalent to the *B. subtilis* model AtMinD1 and AtMinE1 may remain associated with each pole of the chloroplast (C). Alternatively, a plant-specific solution may involve AtMinD1 and AtMinE1 relocating along a different pathway to circumvent the thylakoid membranes (D).

order to bring about plastid division. The evidence points to ARC6 having a role in the stabilization of the Z-ring or in anchoring the Z-ring to the membrane as examination of FtsZ filaments in the *arc6* background reveals fragmented FtsZ filaments and lack of Z-rings (Vitha *et al.*, 2003).

Assembly of the Z-ring appears to be the initial phase of chloroplast division (Kuroiwa *et al.*, 2002). This is consistent with the observations in this study of Z-ring formation in chloroplasts which are not yet visibly constricted (Chapter 4). It is likely that the Z-ring acts as a scaffold for the assembly of the chloroplast division machinery, a situation analogous to the formation of the divisome complex in *E. coli* cell division (reviewed in Errington *et al.*, 2003). The *E. coli* divisome is known to involve at least 13 proteins (Goehring and Beckwith, 2005). Comparatively few components have been identified in *Arabidopsis* underlining the necessity for the identification of the remaining plastid division components.

Cloning of the *arc* mutants reveals that plastid division involves both prokaryotic and eukaryotic-derived proteins (Gao *et al.*, 2003; Shimada *et al.*, 2004) indicating that the process of plastid division is mediated by a combination of machineries present in the original symbiont and also host-derived proteins. Chloroplast division components are not only stromal but are also located on the cytosolic face of the chloroplast (Gao *et al.*, 2003) reflecting the integration of the two machineries. The formation of the Z-ring probably initiates the assembly of both the stromal and cytosolic division machineries and it will be interesting to investigate how these different components are coordinated to bring about plastid division. PDV1 and PVD2 were recently identified as integral outer envelope proteins that mediate the recruitment of the cytosolic protein ARC5 to the plastid division site (Miyagishima *et al.*, 2006). The membrane-spanning nature of this protein and the observation that in the *pdv1 pvd2* double mutant ARC5 cannot localise to the division site indicates that PDV1 and PVD2 may coordinate the formation of the stromal and cytosolic division machineries (Miyagishima *et al.*, 2006). Z-ring formation appears unaltered in the *pdv1 pvd2* double mutant, further verification of Z-ring formation being the initial step in plastid division. Yeast two-hybrid analysis failed to detect interaction between PDV1 and ARC5 suggesting that other proteins may act as a bridge between PDV1, PVD2 and ARC5. It is clear that further analysis of PDV1 and PVD2 function is required to investigate whether these two proteins act alone to coordinate the division machineries. Yeast two-hybrid screens and co-immunoprecipitation using PDV1 and PVD2 as baits may identify other proteins involved in the coordination of the stromal and cytosolic division machineries.

Investigation of the coordination of the stromal and cytosolic division machineries will also shed light on the evolutionary integration of chloroplast division within the eukaryotic host.

Co-localisation and BiFC assays revealed that AtMinD1 and AtMinE1 form a complex. It is not surprising that the *Arabidopsis* Min proteins interact as part of a complex and that this complex appears to be distinct from the other chloroplast division components as this is the situation observed within bacterial cells. ARC3 appears to be the vital bridge connecting the Min complex to the Z-ring complex and appears to complete the mechanism by which division site selection is mediated (Maple *et al.*, In Press).

Because FtsZ1-1 and FtsZ2-1 can interact with both themselves and each other the exact structure of the Z-ring remains unclear. Three possible models exist to explain how the FtsZ proteins relate to each other within the Z-ring. (1) AtFtsZ1-1 and AtFtsZ2-1 form separate homopolymeric filaments that associate laterally. (2) AtFtsZ1-1 and AtFtsZ2-1 assemble as heteropolymers analogous to the relationship of α - and β -tubulin. (3) AtFtsZ1-1 and AtFtsZ2-1 form homodimers and heterodimers within any given Z-ring. The assembly of the plastid division proteins into complexes allows the proposal of a model of the plastid division process. A portion of AtFtsZ2-1 has been shown to associate with the chloroplast envelope and studies show that only AtFtsZ1-1 can form GTP-dependent rod-shaped polymers but that AtFtsZ2-1 can promote GTP-independent AtFtsZ1-1 polymerisation (El-Kafafi *et al.*, 2005). The discovery that ARC6 interacts specifically with AtFtsZ2-1 suggests a model whereby inner membrane-bound AtFtsZ2-1 is stabilized through its interactions with ARC6, which is an inter-membrane protein, and that subsequently AtFtsZ1-1 polymerises and interacts with AtFtsZ2-1, allowing further protein recruitment to the site of division.

7.4. Future directions in assembly of chloroplast division components

During the course of this study many new potential chloroplast division components have been identified. Many of the chloroplast division components recently identified affect cellular processes and may only have a pleiotrophic effect on chloroplast division making the interpretation of plastid mutant phenotypes difficult. The *crumpled leaf* (*crl*) mutant was the first mutant to show defects in both plant morphology and plastid division (Asano *et al.*, 2004). *Arabidopsis* *crl* mutants have few but enlarged chloroplasts and

display abnormalities in cell division orientation, cell differentiation and overall plant development (Asano *et al.*, 2004).

The *fzl* mutant also exhibits altered chloroplast morphology. Depletion of FZL alters chloroplast and thylakoid morphology. FZL is believed to be a membrane-remodeling GTPase that regulates the organization of the thylakoid networks (Gao *et al.*, 2006). Overexpression of FZL does not cause chloroplast division defects and it is likely that the altered chloroplast morphology in *fzl* mutants is an indirect effect of FZL depletion caused by the perturbed thylakoid structure (Gao *et al.*, 2006).

AtCDT1a and AtCDT1b are members of the prereplication complex (Castellano *et al.*, 2004). Down-regulation of AtCDT1 leads to plants of reduced stature and leaves that are pale green, crumpled and smaller than wild-type (Raynaud *et al.*, 2005). Half of the leaf cells of AtCDT1-RNAi lines contain few but enlarged chloroplasts (Raynaud *et al.*, 2005). Surprisingly AtCDT1a interacts with ARC6 (Raynaud *et al.*, 2005) indicating that altered chloroplast phenotype is not just a pleiotrophic affect of perturbed plant development and implicates a real role for AtCDT1 in chloroplast division, perhaps involvement in chloroplast division regulation.

Potential chloroplast division components require critical evaluation to ascertain whether they are real plastid division components or whether altered chloroplast morphology is a pleiotrophic effect of perturbed plant development. As each new component of chloroplast division machinery is identified it is essential that they are incorporated into the current model of chloroplast division in order for us to understand the mechanisms underlying chloroplast division. Although each component requires careful individual characterisation it also needs to be examined in the wider context as part of the plastid division machinery.

7.5. Hunting for novel chloroplast division components

To date new chloroplast division components have been identified through either homology to bacterial division components in the case of AtMinD1, AtMinE1, FtsZ1-1, FtsZ2-1, and FtsZ2-2 or through visual screening of EMS mutagenised seeds in the case of the *arc* mutants. Although both of these methodologies have been successful in the identification of chloroplast division components the use of the bacterial homologues appears to have already been performed exhaustively and the visual screening of mutagenised

plants is a very laborious process and it is extremely difficult to identify mutants with subtle defects in chloroplast division. Due to these reasons, new methodologies were sought to identify novel plastid division proteins.

In the assembly of the chloroplast division machinery it is clear that chloroplast division components act in complexes and may even form a large divisome complex analogous to the bacterial system. Therefore this study aimed to identify novel plastid division components through protein-protein interactions. The yeast two-hybrid system was utilised to screen for novel protein interacting partners. FtsZ1-1 and FtsZ2-1 were selected for use as baits in yeast two-hybrid screens due to their potential role as a scaffold for the assembly of the plastid division machinery. Unfortunately no strong candidates for potential chloroplast division components were identified through yeast two-hybrid screening. Other yeast-two hybrid screens have been performed using GC1 and AtMinE1 as baits and have also failed to identify new plastid division components (Maple, 2005) suggesting that yeast two-hybrid screening cannot be relied upon to identify new chloroplast division components and should be used in conjunction with other approaches. However, it is likely that the yeast two-hybrid library used in this study has not been screened exhaustively and now that new chloroplast division components have been identified these could also be used as baits for yeast two-hybrid screening. This study has mainly focused on the stromal plastid division components. The outer plastid dividing ring and ARC5 assemble on the cytosolic face of the plastid division site. Yeast two-hybrid screening could also be performed using ARC5 as bait to identify new cytosolic components of plastid division.

7.6. Future directions in the hunt for novel plastid division components

Although yeast two-hybrid screening has proved to be ineffective at identifying novel chloroplast division components the principal of using protein-protein interactions to isolate new interacting partners can be applied in other techniques. In this study the use of co-immunoprecipitation to hunt for novel interacting partners of FtsZ2-1 was also attempted. Although in this study this co-immunoprecipitation was unsuccessful this was due to insufficient expression of FtsZ2-1.YFP in the material used for co-immunoprecipitation rather than the technique itself. Co-immunoprecipitation is the perfect technique to identify interacting partners as the assay uses *in planta* tissue in which native interactions are occurring. To

circumvent the possibility of tags interfering with interactions and to maintain the native condition of interactions, protein specific antibodies could be raised and used for co-immunoprecipitation. Provided the washing procedure is stringent enough, co-immunoprecipitation should also reduce the number of false positives which can be very high when using yeast two-hybrid screening. Co-immunoprecipitation screening has been used successfully in *Arabidopsis* before, the technique has been used to identify phytochrome interacting candidates using native holophytochromes as bait (Phee *et al.*, 2006). The work carried out by Phee *et al.* highlights the usefulness of co-immunoprecipitation in hunting for novel chloroplast division components.

Although use of homology to bacterial division proteins appears to have been exhausted in terms of *E. coli* cell division proteins, there is a diverse range of other division machineries that can be taken advantage of. Division proteins unique to cyanobacteria and higher plants have been identified (Ftn2, Koksharova and Wolk, 2002; ARC6 Vitha *et al.*, 2003), indicating that cyanobacteria could represent a rich resource for homologues of *Arabidopsis* chloroplast division proteins.

7.7. Regulation of chloroplast division

The observation that plants with severe plastid division defects can appear macroscopically normal illustrates that plastid division can be uncoupled from the cell cycle. However, the strict maintenance of plastid populations in dividing plant cells and the regulation of plastid number in different cell types is indicative of cellular regulation of plastid division. To date, very little is known about how chloroplast division is regulated. Studies into the regulation of chloroplast division have used synchronized cultures of unicellular organisms or tobacco BY2 cells, however this does not represent the multi-cellular environment in *Arabidopsis*. This study has demonstrated that the regulation of four chloroplast division components; FtsZ1-1, FtsZ2-1, AtMinD1 and AtMinE1 is controlled by light. The expression of these genes is reduced upon darkness and increases upon exposure to light (Chapter 6). Therefore chloroplast division at the transcript level appears to be regulated by light. Why chloroplast division may be regulated by light is not known but light regulation may help to control the expansion and division cycle of chloroplasts. In cultured leaf discs of spinach, minimum generation times of chloroplasts extended to 51.5 hours in the dark compared to just 19.4 hours in continuous light (Hashimoto and Possingham, 1989). In cultured leaf discs

kept in the dark chloroplast division is halted at the dumb-bell stage. Within an hour after being exposed to light most dumbbell-shaped chloroplasts are separated into daughter chloroplasts (Hashimoto and Possingham, 1989). This data appears to agree with the rapid increase in expression of *AtFtsZ1-1*, *AtFtsZ2-1*, *AtMinD1* and *AtMinE1* upon exposure to light and demonstrates that the plastid division process in slowed down or stops in the dark.

To investigate the regulation of plastid division, DNA microarrays were used to analyse gene expression in plants in which chloroplast division had been inhibited compared to plants with normal chloroplast division. Surprisingly, inhibition of chloroplast division did not cause a change in gene expression of any of the known chloroplast division components and also did not alter the gene expression of known retrograde signaling components (Chapter 6). It remains unclear what kind of signals may be perceived by the plant in the event of chloroplast division arrest or what kind of response is effected. This study has demonstrated that several proteins of the chloroplast division machinery are regulated by light (Chapter 6). The similar expression profile of these plastid division genes suggests that the expression of these genes is co-regulated by a common signal. Since the expression of none of the chloroplast division genes appeared to be altered upon chloroplast division inhibition it appears that signals governing the regulation of chloroplast division genes were not activated upon chloroplast division arrest. This suggests that the division state of the chloroplasts does not determine the expression of chloroplast division genes and other environmental or internal signals control chloroplast division. The components of many other pathways in plants are co-regulated, for example co-expression analysis has been used to identify Jasmonic Acid (JA) biosynthesis enzymes through genes that are coordinately regulated with known JA biosynthetic components (Koo *et al.*, 2006). Although light regulates the expression of many genes in *Arabidopsis* as new regulation pathways are identified in chloroplast division perhaps co-expression analysis can be used to identify new chloroplast division components.

Because DNA microarrays generate a huge amount of data, in this study only a small portion of the genes that exhibited altered gene expression were able to be further analysed. More exhaustive analysis of the DNA microarray data generated in Chapter 6 will undoubtedly throw light on the cellular response to chloroplast division arrest.

Yeast one-hybrid assays using fragments of *AtMinD1* and *AtMinE1* promoters as bait were used to

try to identify transcription factors controlling the expression of *AtMinD1* and *AtMinE1*. Yeast one-hybrid assays isolated only four potential DNA-binding transcription factors. Yeast one-hybrid screens have been used successfully to identify proteins that regulate transcription of *CpC2* in *Craterostigma plantagineum* (Ditzer and Bartels, 2006) and C4 phosphoenolpyruvate carboxylase in *Flaveria trinervia* (Windhoval *et al.*, 2001) in both of these cases the bait DNA element used was well-defined and present in more than one copy. More specific target/bait elements may achieve better results in yeast one-hybrid screens using promoter elements of *AtMinD1* and *AtMinE1* as bait. However, another yeast one-hybrid screen to look for transcriptional activators of *Bkn3* was successful using a 305bp single copy fragment of the *Bkn3* promoter (Santi *et al.*, 2003) which is a similar bait element used in the *AtMinD1*-promoter yeast one-hybrid screen. Perhaps more exhaustive yeast one-hybrid screening will identify transcription factors of *AtMinD1* and *AtMinE1* without the need for additional characterization of the promoter regions. More specific *cis*-acting elements may be defined by deletional analysis of the *AtMinD1* and *AtMinE1* promoters. The expression of a reporter gene could be put under control of the *AtMinD1* or *AtMinE1* promoter and various deletions of the promoters made and the expression of the reporter gene analysed. It will be interesting to include in yeast one-hybrid assays potential *cis*-acting elements of *FtsZ1-1* and *FtsZ2-1* to investigate common transcription factors in controlling the expression of proteins involved in different complexes during chloroplast division.

7.8. Future directions for investigation of the regulation of plastid division.

Analysis of several of the *arc* mutants suggests that the regulation of chloroplast proliferation is specifically affected by the *arc* mutation since the mesophyll cells of *arc5* and *arc3* contain a similar number of chloroplasts as proplastids contained within the progenitor of mesophyll cells (Roberson *et al.*, 1996; Marrison *et al.*, 1999). This data suggests that chloroplast proliferation and proplastid division are subject to different controls. It would be interesting to investigate the difference in plastid division control between proplastids and plastids in other tissues.

Different mechanisms of plastid division aside from the classical binary fission mechanism have been reported. In the *suffulta* mutation in tomato enlarged chloroplasts degenerate and give rise to a wild-type population of chromoplasts in ripe fruit by a process of plastid budding and fragmentation (Forth and

Pyke, 2006). *suffulta* plants have mesophyll cells containing only a single chloroplast greatly enlarged compared to wild-type but have a wild-type population of chloroplasts in ripe fruit (Forth and Pyke, 2006). The existence of different chloroplast division mechanisms is intriguing and may explain how mutant plants containing giant chloroplasts such as *arc6* segregate plastids during cell divisions in the shoot apical meristem. How the transition between binary fission of plastid division and a process of plastid budding is mediated remains to be investigated. It is likely that this transition is a tissue type specific process.

Many difficulties exist in trying to investigate the regulation of chloroplast division in *Arabidopsis*. The primary difficulty is that division of the chloroplasts is not synchronised and only occurs in a subset of tissues making analysis of gene expression during chloroplast division difficult. Studies in synchronised unicellular photosynthetic algae and tobacco BY2 cell have demonstrated that the expression of chloroplast division components is up-regulated immediately prior to and during cell division suggesting cell cycle regulation of chloroplast division. One way to look for regulators of chloroplast division may be an EMS screen looking for chloroplast division defects much like the screen that identified the *arc* mutants. However this may be difficult as it is likely that many components that regulate chloroplast division are also likely to affect cell division and therefore could be lethal mutations.

7.9. Numerous chloroplasts versus giant chloroplasts

Why have lots of small chloroplasts at all? As previously mentioned, plants with severe plastid division defects mostly appear macroscopically normal therefore why do higher plant chloroplasts need to divide rather than simply expand? Plastids perform many cellular functions vital for the correct functioning of the cell. Perhaps the reason for containing many chloroplasts is protection against damage to chloroplasts. If a plant cell harbored only a single chloroplast, damage to this chloroplast may be disastrous to the cell. Chloroplasts exhibit movement towards weak light and away from strong light as strong light damages the chloroplasts. A single greatly enlarged chloroplast would be unable to move effectively in response to changes in light intensity and therefore may sustain damage potentially crippling the cell. It has also been shown that reduced chloroplast number affects both the composition and structure of the photosynthetic apparatus (Austin and Webber, 2005). *arc3*, *arc5* and *arc6* plants all exhibit reduced numbers of

chloroplasts and have reduced photosynthetic capacity (Austin and Webber, 2005). This data shows that photosynthetic competence is dependent on proper chloroplast division and development (Austin and Webber, 2005).

The observation that plants with severe chloroplast division defects can appear macroscopically normal demonstrates that chloroplast proliferation is not essential for the survival of the plant however the observations of reduced photosynthetic capability of several of the *arc* mutants (Austin and Webber, 2005) and the potential for damage to the chloroplasts indicates that many small chloroplasts are preferable to a single large chloroplast and therefore chloroplast division represents an important cellular process.

7.10. Concluding remarks

The research that has been completed over the last few years has enabled us to begin to unravel the complex process of plastid division. The number of plastid division components identified has risen exponentially year by year. However, the identification of new plastid division components will clearly widen our knowledge of how plastid division is controlled in higher plants and needs to be of top priority.

As discussed throughout this chapter there are many challenges confronting researchers including the identification of novel chloroplast division components, elucidation of how the Min system functions now that ARC3 has been characterized, and the incorporation of newly identified plastid division components into the division machinery. Aside from this, one of the major challenges that researchers face is investigation of the regulation of plastid division. In order to elucidate how plastid division is regulated it seems that synchronized cultured cells may initially be the best path for investigation.

There are still many questions to be answered in order to elucidate the complex processes that underlie plastid division. However new plastid division components are being identified every year and existing knowledge combined with the use of new technology will undoubtedly enable us to answer these questions.

References

Abrahams JP, Leslie AG, Lutter R, Walker JE. (1994) Structure at 2.8 Å resolution of F₁-ATPase from bovine heart mitochondria. *Nature* **370**, 621-628.

Adams S, Maple J, Møller SG. *Chlamydomonas reinhardtii* as a new model system for the study of plastid division. In Press

Addinall SG, Lutkenhaus J. (1995) FtsA is localized to the septum in an FtsZ-dependent manner. *Journal of Bacteriology* **178**, 7167-7172.

Aldridge C, Møller SG. (2005) The plastid division protein AtMinD1 is a Ca²⁺-ATPase stimulated by AtMinE1. *Journal of Biological Chemistry* **280**, 31673-31678.

Aldridge C, Maple J, Møller SG. (2005) The Molecular Biology of Plastid Division in Higher Plants. *Journal of Experimental Botany* **56**, 1061-77.

Alfano C, Babon J, Kelly G, Curry S, Conte MR. (2003) Resonance assignment and secondary structure of an N-terminal fragment of the human La protein. *Journal of Biomolecular NMR* **27**, 93-94.

Altschul SF, Gish W, Miller W, Myers EW, Lipman DJ. (1990) "Basic local alignment search tool." *Journal of Molecular Biology* **215**, 403-410.

Aoyama T, Chua NH. (1997) A glucocorticoid-mediated transcriptional induction system in transgenic plants. *Plant Journal* **11**, 605-612.

Arimura S, Tsutsumi N. (2002) A dynamin-like protein (ADL2b), rather than FtsZ, is involved in *Arabidopsis* mitochondrial division. *Proceedings of the National Academy of Sciences, USA* **99**, 5727-5731.

Asano T, Yoshioka Y, Kurei S, Sakamoto W, Machida Y; Sodmergen. (2004) A mutation of the CRUMPLED LEAF gene that encodes a protein localized in the outer envelope membrane of plastids affects the pattern of cell division, cell differentiation, and plastid division in *Arabidopsis*. *Plant Journal* **38**, 448-459.

Austin J, Webber AN. (2005) Photosynthesis in *Arabidopsis thaliana* mutants with reduced chloroplast number. *Photosynthesis Research* **85**, 373-384.

Baker ME, Grundy WN, Elkan CP. (1998) Spinach CSP41, an mRNA-binding protein and ribonuclease, is homologous to nucleotide-sugar epimerases and hydroxysteroid dehydrogenases. *Biochemical and Biophysical Research Communications* **248**, 250-4.

Bateman A, Coin L, Durbin R, Finn RD, Hollich V, Griffiths-Jones S, Khanna A, Marshall M, Moxon S, Sonnhammer E, Studholme DJ, Yeats C, Eddy SR. (2004) The Pfam Protein Families Database. *Nucleic Acids Research* **32** (Database issue), D138-141.

Begg KJ, Dewar SJ, Donachie WD. (1995) A new *Escherichia coli* cell division gene, ftsK. *Journal of Bacteriology* **177**, 6211-6222.

Ben-Yehuda S, Losick R. (2002) Asymmetric cell division in *B. subtilis* involves a spiral-like intermediate of the cytokinetic protein FtsZ. *Cell* **109**, 257-266.

Berger G, Girault G. (2001) Comparison of different cations (Mn²⁺, Mg²⁺, Ca²⁺) on the hydrolytic activity of chloroplast ATPase. *Journal of bioenergetics and biomembranes* **33**, 93-98.

Bernhardt TG, de Boer PA. (2003) The *Escherichia coli* amidase AmiC is a periplasmic septal ring component exported via the twin-arginine transport pathway. *Molecular Microbiology* **48**, 1171-1182.

Bhushan S, Lefebvre B, Stahl A, Wright SJ, Bruce BD, Boutry M, Glaser E. (2003) Dual targeting and function of a protease in mitochondria and chloroplasts. *EMBO Reports* **4**, 1073-1078.

Bi E, Lutkenhaus J. (1991) FtsZ ring structure associated with division in *Escherichia coli*. *Nature* **354**, 161-164.

Bi E, Lutkenhaus J. (1993) Cell division inhibitors SulA and MinCD prevent formation of the FtsZ ring. *Journal of Bacteriology* **175**, 1118-1125.

Bleazard W, McCaffery JM, King EJ, Bale S, Mozdy A, Tieu Q, Nunnari J, Shaw JM. (1999) The dynamin-related GTPase Dnm1 regulates mitochondrial fission in yeast. *Nature Cell Biology* **1**, 298-304.

Boasson R, Laetsch WH, Price I. (1972) The etioplasts/chloroplast transformation in tobacco: Correlation of ultrastructure, replication and chlorophyll synthesis. *American Journal of Botany* **59**, 217-233.

Bouet JY, Funnell BE. (1999) P1 ParA interacts with the P1 partition complex at parS and an ATP-ADP switch controls ParA activities. *EMBO Journal* **18**: 1415-1424.

Buddelmeijer N, Judson N, Boyd D, Mekalanos JJ, Beckwith J. (2002) YgbQ, a cell division protein in *Escherichia coli* and *Vibrio cholerae*, localizes in codependent fashion with FtsL to the division site. *Proceedings of the National Academy of Sciences, USA* **99**, 6316-6321.

Castellano M, Boniotti MB, Caro E, Schnittger A, Gutierrez C. (2004) DNA replication licensing affects cell proliferation or endoreplication in a cell type-specific manner. *Plant Cell* **16**, 2380-93.

Chaly N, Possingham JV. (1981) Structure of constricted proplastids in meristematic plant tissue. *Biology of the Cell* **41**, 203-210.

Chen JC, Weiss DS, Ghigo J, Beckwith J. (1999) Septal localization of FtsQ, an essential cell division protein in *Escherichia coli*. *Journal of Bacteriology* **181**, 521-520.

Clough, SJ, Bent, AF. (1998) Floral dip: a simplified method for *Agrobacterium*-mediated transformation of *Arabidopsis thaliana*. *Plant Journal* **16**, 735-743.

Colletti KS, Tattersall EA, Pyke KA, Froelich JE, Stokes KD, Osteryoung KW. (2000) A homologue of the bacterial cell division site-determining factor MinD mediates placement of the chloroplast division apparatus. *Current Biology* **10**, 507-516.

Coleman DE, Berghuis AM, Lee E, Linder ME, Gilman AG, Sprang SR. (1994) Structures of active conformations of Gi alpha 1 and the mechanism of GTP hydrolysis. *Science* **265**, 1405-1412.

Cookson PJ, Kiano JW, Shipton CA, Fraser PD, Romer S, Schuch W, Bramley PM and Pyke KA. (2003) Increases in cell elongation, plastid compartment size and phytoene synthase activity underlie the phenotype of the high pigment-1 mutant of tomato. *Planta* **217**, 896-903.

Corbin BD, Yu XC, Margolin W. (2002) Exploring intracellular space: function of the Min system in round-shaped *Escherichia coli*. *EMBO Journal* **21**, 1998-2008.

Cran DG, Possingham JV. (1972) Variation of plastid types in spinach. *Protoplasma* **74**, 345-356.

Cronk JD, Endrizzi JA, Alber T. (1996) High-resolution structures of the bifunctional enzyme and transcriptional coactivator DCoH and its complex with a product analogue. *Protein Science* **5**, 1963-72.

Dai K, Lutkenhaus J. (1991) ftsZ is an essential cell division gene in *Escherichia coli*. *Journal of Bacteriology* **173**, 3500-3506.

Dai K, Lutkenhaus J. (1992) The proper ratio of FtsZ to FtsA is required for cell division to occur in *Escherichia coli*. *Journal of Bacteriology* **174**, 6145-51.

- Danino D, Hinshaw JE.** (2001) Dynamin family of mechanoenzymes. *Current Opinion in Cell Biology* **13**, 454-460.
- Datta P, Dasgupta A, Bhakta S, Basu J.** (2002) Interaction between FtsZ and FtsW of *Mycobacterium tuberculosis*. *Journal Biological Chemistry* **277**, 24983-7.
- Davletov BA, Sudhof TC.** (1993) A single C2 domain from synaptotagmin I is sufficient for high affinity Ca²⁺/phospholipid binding. *Journal of Biological Chemistry*. **268**, 26386-90.
- Davuluri RV, Sun H, Palaniswamy SK, Matthews N, Molina C, Kurtz M, Grotewold E.** (2003) AGRIS: *Arabidopsis* gene regulatory information server, an information resource of *Arabidopsis* cis-regulatory elements and transcription factors. *BMC Bioinformatics*. **4**, 25.
- de Boer PAJ, Crossley RE, Rothfield LI.** (1989) A division inhibitor and a topological specificity factor coded for by the minicell locus determine proper placement of the division septum in *E. coli*. *Cell* **56**, 641-649.
- de Boer PAJ, Crossley RE, Rothfield LI.** (1990) Central role for the *Escherichia coli* *minC* gene product in two different cell division-inhibition systems. *Proceedings of the National Academy of Sciences, USA* **87**, 1129-1133.
- de Boer PA, Crossley RE, Hand AR, Rothfield LI.** (1991) The MinD protein is a membrane ATPase required for the correct placement of the *Escherichia coli* division site. *EMBO Journal* **10**, 4371-4380.
- de Boer PAJ, Crossley RE, Rothfield LI.** (1992) Roles of MinC and MinD in the site-specific septation block mediated by the MinCDE system of *Escherichia coli*. *Journal of Bacteriology* **174**, 63-70.
- Din N, Quardokus EM, Sackett MJ, Brun YV.** (1998) Dominant C-terminal deletions of FtsZ that affect its ability to localize in *Caulobacter* and its interaction with FtsA. *Molecular Microbiology* **27**, 1051-1063.
- Dinkins R, Reddy MS, Leng M, Collins GB.** (2001) Overexpression of the *Arabidopsis thaliana* *MinD1* gene alters chloroplast size and number in transgenic tobacco plants. *Planta* **214**, 180-188.
- Ditzer A, Bartels D.** (2006) Identification of a dehydration and ABA-responsive promoter regulon and isolation of corresponding DNA binding proteins for the group 4 LEA gene CpC2 from *C. plantagineum*. *Plant Molecular Biology* **61**, 643-63.
- Edwards DH, Errington J.** (1997) The *Bacillus subtilis* DivIVA protein targets to the division septum and controls the site specificity of cell division. *Molecular Microbiology* **24**, 905-915.

El-Kafafi ES, Mukherjee S, El-Shami M, Putaux JL, Block MA, Pignot-Paintrand I, Lerbs-Mache S, Emanuelsson O, Nielsen H, von Heijne G. (1999) ChloroP, a neural network-based method for predicting chloroplast transit peptides and their cleavage sites. *Protein Science* **8**, 978-984.

Erickson HP. (1998) Atomic structures of tubulin and FtsZ. *Trends in cell biology* **8**, 133-7.

Errington J, Daniel RA, Scheffers DJ. (2003) Cytokinesis in bacteria. *Microbial and Molecular Biology Reviews* **67**, 52-65.

Falconet D. (2005) The plastid division proteins, FtsZ1 and FtsZ2, differ in their biochemical properties and sub-plastidial localisation. *Biochemical Journal* **387**, 669-676.

Fatland BL, Ke J, Anderson MD, Mentzen WI, Cui LW, Allred CC, Johnston JL, Nikolau BJ, Wurtele ES. (2002) Molecular characterization of a heteromeric ATP-citrate lyase that generates cytosolic acetyl-coenzyme A in *Arabidopsis*. *Plant Physiology* **130**, 740-56.

Forth D, Pyke KA. (2006) The suffulta mutation in tomato reveals a novel method of plastid replication during fruit ripening *Journal of Experimental Botany* **57**, 1971-1979.

Fowler SG, Cook D, Thomashow MF. (2005) Low temperature induction of *Arabidopsis* CBF1, 2, and 3 is gated by the circadian clock. *Plant Physiology* **137**, 961-968.

Fu X, Shih YL, Zhang Y, Rothfield LI. (2001) The MinE ring required for proper placement of the division site is a mobile structure that changes its cellular location during the *Escherichia coli* division cycle. *Proceedings of the National Academy of Sciences, USA* **98**, 980-985.

Fujiwara M, Yoshida S. (2001) Chloroplast targeting of chloroplast division FtsZ2 proteins in *Arabidopsis*. *Biochemical and Biophysical Research Communications* **287**, 462-467.

Fujiwara M, Nakamura A, Itoh R, Shimada Y, Yoshida S, Møller SG. (2004). Chloroplast division site placement requires dimerisation of the ARC11/AtMinD1 protein in *Arabidopsis*. *Journal of Cell Science* **117**, 2399-410.

Fukuda M. (2003) Molecular cloning and characterization of human, rat, and mouse synaptotagmin XV. *Biochemical and Biophysical Research Communications* **306**, 64-71.

Fulgosi H, Gerdes L, Westphal S, Glockmann C, Soll J. (2002) Cell and chloroplast division requires ARTEMIS. *Proceedings of the National Academy of Sciences, USA* **99**, 11501-11506.

Galili G. (1995) Regulation of lysine and threonine synthesis. *The Plant Cell* **7**, 899-906.

- Gaikwad A, Babbarwal V, Pant V, Mukherjee SK.** (2000) Pea chloroplast FtsZ can form multimers and correct the thermosensitive defect of an *Escherichia coli* ftsZ mutant. *Molecular & general genetics* **263**, 213-21.
- Gao H, Kadirjan-Kalbach D, Froehlich J E, Osteryoung KW.** (2003) ARC5, a cytosolic dynamin-like protein from plants, is part of the chloroplast division machinery. *Proceedings of the National Academy of Sciences, USA* **100**, 4328-4333.
- Gao H, Sage TL, Osteryoung KW.** (2006) FZL, an FZO-like protein in plants, is a determinant of thylakoid and chloroplast morphology. *Proceedings of the National Academy of Sciences, USA* **103**, 6759-6764.
- Gao J, Kaufman LS.** (1994) Blue-Light Regulation of the *Arabidopsis thaliana* Cab1 Gene. *Plant Physiology* **104**, 1251-1257.
- Gerdes L, Bals T, Klostermann E, Karl M, Philippar K, Hunken M, Soll J, Schunemann D.** (2006) A second thylakoid membrane-localized Alb3/OxaI/YidC homologue is involved in proper chloroplast biogenesis in *Arabidopsis thaliana*. *Journal of Biological Chemistry* **281**, 16632- 16642.
- Ghigo JM, Beckwith J.** (2000) Cell division in *Escherichia coli*: role of FtsL domains in septal localization, function, and oligomerization. *Journal of Bacteriology* **182**, 116-129.
- Goehring NW, Beckwith J.** (2005) Diverse paths to midcell: assembly of the bacterial cell division machinery. *Current Biology* **15**, R514-526.
- Gray MW.** (1999) Evolution of organellar genomes. *Current Opinion in Genetics and Development* **9**, 678-687.
- Gregis V, Sessa A, Colombo L, Kater MM.** (2006) AGL24, SHORT VEGETATIVE PHASE, and APETALA1 redundantly control AGAMOUS during early stages of flower development in *Arabidopsis*. *Plant Cell* **18**, 1373-1382.
- Gueiros-Filho FJ, Losick R.** (2002) A widely conserved bacterial cell division protein that promotes assembly of the tubulin-like protein FtsZ. *Genes and Development* **16**, 2544-2556.
- Hale CA, de Boer PA.** (1997) Direct binding of FtsZ to ZipA, an essential component of the septal ring structure that mediates cell division in *E. coli*. *Cell* **88**, 175-185.

- Hale CA, Rhee AC, de Boer PA.** (2000) ZipA-induced bundling of FtsZ polymers mediated by an interaction between C-terminal domains. *Journal of Bacteriology* **182**, 5153-5166.
- Hale C A, Meinhardt H, de Boer PAJ.** (2001) Dynamic localization cycle of the cell division regulator MinE in *Escherichia coli*. *The EMBO Journal* **20**, 1563-1572.
- Haney SA, Glasfeld E, Hale C, Keeney D, He Z, de Boer P.** (2001) Genetic analysis of the *Escherichia coli* FtsZ.ZipA interaction in the yeast two-hybrid system. Characterization of FtsZ residues essential for the interactions with ZipA and with FtsA. *Journal of Biological Chemistry* **276**, 11980–11987.
- Hashimoto H.** (1986) Double ring structure around the constricting neck of the dividing plastids of *Avena sativa*. *Protoplasma* **135**, 166-172.
- Hashimoto, H, and Possingham, JV.** (1989) Division and DNA distribution in ribosome-deficient plastids of the barley mutant “albostrians”. *Protoplasma* **149**, 20-23.
- Haswell ES, Meyerowitz EM.** (2006) MscS-like proteins control plastid size and shape in *Arabidopsis thaliana*. *Current Biology* **16**, 1-11.
- Hayashi I, Oyama T, Morikawa K.** (2001) Structural and functional studies of MinD ATPase: implications for the molecular recognition of the bacterial cell division apparatus. *EMBO Journal* **20**, 1819-1828
- Higgins D, Thompson J, Gibson T, Thompson JD, Higgins DG, Gibson TJ.** (1994) CLUSTAL W: improving the sensitivity of progressive multiple sequence alignment through sequence weighting, position-specific gap penalties and weight matrix choice. *Nucleic Acids Research* **22**, 4673-4680.
- Hinshaw JE.** (2000) Dynamin and its role in membrane fission. *Annual Review of Cell and Developmental Biology* **16**, 483-519.
- Hope IA, Struhl K.** (1986) Functional dissection of a eukaryotic transcriptional activator protein, GCN4 of yeast *Cell* **46**, 885-894.
- Hu Z, Lutkenhaus J.** (1999) Topological regulation of cell division in *Escherichia coli* involves rapid pole to pole oscillation of the division inhibitor MinC under the control of MinD and MinE. *Molecular Microbiology* **34**, 82-90.

Hu J, Mukherjee A, Pichoff S, Lutkenhaus J. (1999) The MinC component of the division site selection system in *Escherichia coli* interacts with FtsZ to prevent polymerization. *Proceedings of the National Academy of Sciences, USA* **96**, 14819-24.

Hu Z, Lutkenhaus J. (2001) Topological regulation of cell division in *E. coli*. spatiotemporal oscillation of MinD requires stimulation of its ATPase by MinE and phospholipid. *Molecular Cell* **7**, 1337-1343.

Hu Z, Gogol EP, Lutkenhaus J. (2002) Dynamic assembly of MinD on phospholipid vesicles regulated by ATP and MinE. *Proceedings of the National Academy of Sciences, USA* **99**, 6761–6766.

Hu Z, Lutkenhaus J. (2003) A conserved sequence at the C-terminus of MinD is required for binding to the membrane and targeting MinC to the septum. *Molecular Microbiology* **47**, 345-355.

Huang J, Lutkenhaus J. (1996) Interaction between FtsZ and inhibitors of cell division. *Journal of Bacteriology* **178**, 5080-5085.

Huang CK, Meir Y, Wingreen NS. (2003) Dynamic structures in *Escherichia coli*: Spontaneous formation of MinE rings and MinD polar zones. *Proceedings of the National Academy of Sciences, USA* **100**, 12724-12728.

Huisman O, D'Ari R, Gottesman S. (1984) Cell-division control in *Escherichia coli*: specific induction of the SOS function SfiA protein is sufficient to block septation. *Proceedings of the National Academy of Sciences, USA* **81**, 4490-4.

Huang J, Taylor JP, Chen JG, Uhrig JF, Schnell DJ, Nakagawa T, Korth KL, Jones AM. (2006) The plastid protein THYLAKOID FORMATION1 and the plasma membrane G-protein GPA1 interact in a novel sugar-signaling mechanism in *Arabidopsis*. *Plant Cell* **18**, 1226-1238.

Intine RV, Tenenbaum SA, Sakulich AL, Keene JD, Marais RJ. (2003) Differential phosphorylation and subcellular localization of La RNPs associated with precursor tRNAs and translation-related mRNAs. *Molecular Cell* **12**, 1301-7.

Itoh R, Fujiwara M, Nagata N, Yoshida S. (2001) A chloroplast protein homologous to the eubacterial topological specificity factor MinE plays a role in chloroplast division. *Plant Physiology* **27**, 1644-1655.

Jakoby M, Weisshaar B, Droge-Laser W, Vicente-Carbajosa J, Tiedemann J, Kroj T, Parey F; bZIP Research Group. (2002) bZIP transcription factors in *Arabidopsis*. *Trends in Plant Science* **7**, 106-11.

- Jin H, Cominelli E, Bailey P, Parr A, Mehrtens F, Jones J, Tonelli C, Weisshaar B, Martin C.** (2000) Transcriptional repression by AtMYB4 controls production of UV-protecting sunscreens in *Arabidopsis*. *EMBO Journal*. 19, 6150-61.
- Johanson U, Karlsson M, Johansson I, Gustavsson S, Sjovald S, Fraysse L, Weig AR, Kjellbom P.** (2001) The complete set of genes encoding major intrinsic proteins in arabidopsis provides a framework for a new nomenclature for major intrinsic proteins in plants. *Plant Physiology* 126, 1358-69.
- Juniper BE, Clowes FAL.** (1965) Cytoplasmic organelles and cell growth in root caps. *Nature* 208, 864-865.
- Justice SS, Garcia-Lara J, Rothfield LI.** (2000) Cell division inhibitors Sula and MinC/MinD block septum formation at different steps in the assembly of the Escherichia coli division machinery. *Molecular Microbiology* 37, 410-23.
- Kagaya Y, Ohmiya K, Hattori T.** (1999) RAV1, a novel DNA-binding protein, binds to bipartite recognition sequence through two distinct DNA-binding domains uniquely found in higher plants. *Nucleic Acids Research* 27, 470-8.
- Kanamaru K, Fujiwara M, Kim M, Nagashima A, Nakazato E, Tanaka K, Takahashi H.** (2000) Chloroplast targeting, distribution and transcriptional fluctuation of AtMinD1, a Eubacteria-type factor critical for chloroplast division. *Plant Cell Physiology* 41, 1119-28.
- Kawamura Y, Uemura M.** (2003) Mass spectrometric approach for identifying putative plasma membrane proteins of *Arabidopsis* leaves associated with cold acclimation. *Plant Journal* 36, 141-154.
- Keegan L, Gill G, Ptashne M.** (1986) Separation of DNA binding from the transcription-activating function of a eukaryotic regulatory protein. *Science* 231, 699-704.
- Keene JD.** (2003) Posttranscriptional generation of macromolecular complexes. *Molecular Cell* 12, 1347-9.
- Kleffmann T, Russenberger D, von Zychlinski A, Christopher W, Sjolander K, Gruissem W, Baginsky S.** (2004) The *Arabidopsis thaliana* chloroplast proteome reveals pathway abundance and novel protein functions. *Current Biology* 14, 354-362

Klockow B, Tichelaar W, Madden DR, Niemann HH, Akiba T, Hirose K, Manstein DJ. (2002) The dynamin A ring complex: molecular organization and nucleotide-dependant conformational changes. *EMBO journal* **21**, 240-250.

Kiessling J, Kruse S, Rensing SA, Harter K, Decker EL, Reski R. (2000) Visualization of a cytoskeleton-like FtsZ network in chloroplasts. *Journal of Cell Biology* **151**, 945-950.

Kjaerulff S, Andersen B, Nielsen VS, Moller BL, Okkels JS. (1993) The PSI-K subunit of photosystem I from barley (*Hordeum vulgare* L.). Evidence for a gene duplication of an ancestral PSI-G/K gene. *Journal of Biological Chemistry* **268**, 18912-18916.

Knop M, Finger A, Braun T, Hellmuth K, Wolf DH. (1996) Der1, a novel protein specifically required for endoplasmic reticulum degradation in yeast. *EMBO Journal* **15**, 753-763.

Koksharova OA, Wolk CP. (2002) A novel gene that bears a DnaJ motif influences cyanobacterial cell division. *Journal of Bacteriology* **184**, 5524-5528.

Koo AJ, Chung HS, Kobayashi Y, Howe GA. (2006) Identification of a peroxisomal acyl-activating enzyme involved in the biosynthesis of Jasmonic acid in *Arabidopsis*. *Journal of Biological Chemistry* Epub ahead of print.

Kost B, Spielhofer P, Chua NH. (1998) A GFP-mouse talin fusion protein labels plant actin filaments *in vivo* and visualises the actin cytoskeleton in growing pollen tubes. *Plant Journal* **16**, 393-401.

Kubis S, Patel R, Combe J, Bedard J, Kovacheva S, Lilley K, Biehl A, Leister D, Rios G, Koncz C, Jarvis P. (2004) Functional specialization amongst the *Arabidopsis* Toc159 family of chloroplast protein import receptors. *Plant Cell*. **16**, 2059-2077.

Kuroiwa, H, Mori, T, Takahara, M, Miyagishima, S, and Kuroiwa, T. (2002) Chloroplast division machinery as revealed by immunofluorescence and electron microscopy. *Planta* **215**, 185-190.

Labie C, Bouche S, Bouche JP. (1990) Minicell-forming mutants of *Escherichia coli*: suppression of both DicB- and MinD-dependent division inhibition by inactivation of the minC gene product. *Journal of Bacteriology* **172**, 5852-5855.

Lackner LL, Raskin DM, de Boer PA. (2003) ATP-dependent interactions between *Escherichia coli* Min proteins and the phospholipid membrane in vitro. *Journal of Bacteriology* **185**, 735-749.

- Levina N, Totemeyer S, Stokes NR, Louis P, Jones MA, Booth IR.** (1999) Protection of *Escherichia coli* cells against extreme turgor by activation of MscS and MscL mechanosensitive channels: identification of genes required for MscS activity. *EMBO Journal* **18**, 1730-1737.
- Leech RM, Thomson WW, Platt-Aloia, KA.** (1981) Observations on the mechanism of chloroplast division in higher plants. *New Phytologist* **87**, 1-9.
- Li Y, Baldauf S, Lim EK, Bowles DJ.** (2001) Phylogenetic analysis of the UDP-glycosyltransferase multigene family of *Arabidopsis thaliana*. *Journal of Biological Chemistry* **276**, 4338-4343.
- Li Y, Darley CP, Ongaro V, Fleming A, Schipper O, Baldauf SL, McQueen-Mason SJ.** (2002) Plant expansins are a complex multigene family with an ancient evolutionary origin. *Plant Physiology* **128**, 854-64.
- Lieberman M, Segev O, Gilboa N, Lalazar A and Levin I.** (2004) The tomato homolog of the gene encoding UV-damaged DNA binding protein 1 (DDB1) underlined as the gene that causes the high pigment-1 mutant phenotype. *Theoretical and Applied Genetics* **108**, 1574-1581.
- Liu Y, Roof S, Ye Z, Barry C, van Tuinen A, Vrebalov J, Bowler C and Giovannoni J.** (2004) Manipulation of light signal transduction as a means of modifying fruit nutritional quality in tomato. *Proceedings of the National Academy of Sciences, USA* **101**, 9897-9902.
- Liu Z, Mukherjee A, Lutkenhaus, J.** (1999) Recruitment of ZipA to the division site by interaction with FtsZ. *Molecular Microbiology* **31**, 1853-1861.
- Lohrmann J, Sweere U, Zabaleta E, Baurle I, Keitel C, Kozma-Bognar L, Brennicke A, Schafer E, Kudla J, Harter K.** (2001) The response regulator ARR2: a pollen-specific transcription factor involved in the expression of nuclear genes for components of mitochondrial complex I in *Arabidopsis*. *Molecular Genetics and Genomics*. **265**, 2-13.
- Lopez-Juez E, Pyke KA** (2005) Plastids unleashed: their development and their integration in plant development. *The International journal of developmental biology* **49**, 557-77.
- Löwe J, Amos LA.** (1998) Crystal structure of the bacterial cell-division protein FtsZ. *Nature* **391**, 203-206.
- Löwe J, Amos LA.** (1999) Tublin-like protofilaments in Ca²⁺-induced FtsZ sheets. *EMBO Journal* **18**, 2364-2371.

- Lu C, Stricker J, Erickson HP.** (1998) FtsZ from *Escherichia coli*, *Azotobacter vinelandii*, and *Thermotoga maritima*--quantitation, GTP hydrolysis, and assembly. *Cell Motility and Cytoskeleton* **40**, 71-86.
- Lutkenhaus J, Addinall SG.** (1997) Bacterial cell division and the Z ring. *Annual Review of Biochemistry* **66**, 93-116.
- Lydon RF, Roberson ES.** (1976) The quantitative ultrastructure of the pea shoot apex in relation to leaf initiation. *Protoplasma* **87**, 387-402.
- Ma LY, King G, Rothfield L.** (2003) Mapping the MinE site involved in interaction with the MinD division site selection protein of *Escherichia coli*. *Journal of Bacteriology* **185**, 4948-4955.
- Ma L, Li J, Qu L, Hager J, Chen Z, Zhao H, Deng XW.** (2001) Light Control of *Arabidopsis* Development Entails Coordinated Regulation of Genome Expression and Cellular Pathways *The Plant Cell* **13**, 2589-2607.
- Ma L, King GF, Rothfield L.** (2004) Positioning of the MinE binding site on the MinD surface suggests a plausible mechanism for activation of the *Escherichia coli* MinD ATPase during division site selection. *Molecular Microbiology* **54**, 99-108.
- Ma S, Margolin, W.** (1999) Genetic and functional analyses of the conserved C-terminal core domain of *Escherichia coli* FtsZ. *Journal of Bacteriology* **181**, 7531-7544.
- Ma, X, Ehrhardt, DW, Margolin, W.** (1996) Colocalization of cell division proteins FtsZ and FtsA to cytoskeletal structures in living *Escherichia coli* cells by using the green fluorescent protein. *Proceedings of the National Academy of Sciences, USA* **93**, 12998-13003.
- Maple J.** (2005) The Molecular Biology of Plastid Division. PhD Thesis, Department of Biology, University of Leicester, Leicester, UK.
- Maple J, Chua NH, Møller SG.** (2002) The topological specificity factor AtMinE1 is essential for correct plastid division site placement in *Arabidopsis*. *Plant Journal* **31**, 269-277.
- Maple J, Aldridge C, Møller SG.** (2005) Plastid division is mediated by a combinatorial assembly of plastid division proteins. *The Plant Journal* **43**, 811-823.
- Maple J, Fujiwara MT, Kitahata N, Lawson T, Baker NR, Yoshida S, Moller SG.** (2004) GIANT CHLOROPLAST 1 is essential for correct plastid division in *Arabidopsis*. *Current Biology* **14**, 776-81.

Maple J, Vojta L, Soll J, Møller SG. ARC3 is a Stromal Plastid Division Protein with MinC-like Properties. In Press.

Margolin J. (2000) Of Mice, men and the genome. *Genome Research* **10**, 1341-1342.

Margulis L. (1970) Recombination of non-chromosomal genes in *Chlamydomonas*: assortment of mitochondria and chloroplasts? *Journal of Theoretical Biology* **26**(2), 337-42.

Marrison JL, Rutherford SM, Robertson EJ, Lister C, Dean C, Leech RM. (1999) The distinctive roles of five different *ARC* genes in the chloroplast division process in *Arabidopsis*. *Plant Journal* **18**, 651-662.

Marston AL, Errington J. (1999) Selection of the midcell division site in *Bacillus subtilis* through MinD-dependent polar localization and activation of MinC. *Molecular Microbiology* **33**, 84-96.

Matzke AJ, Matzke MA. (1998) Position effects and epigenetic silencing of plant transgenes. *Current Opinion Plant Biology* **1**, 142-8.

McAndrew RS, Froehlich JE, Vitha S, Stokes KD, Osteryoung KW. (2001) Colocalization of plastid division proteins in the chloroplast stromal compartment establishes a new functional relationship between FtsZ1 and FtsZ2 in higher plants. *Plant Physiology* **127**, 1656-1666.

McFadden GI. (1999) Endosymbiosis and evolution of the plant cell. *Current Opinion in Plant Biology* **2**, 513-519.

McFadden GI. (2001) Chloroplast origin and integration. *Plant Physiology* **125**, 50-53.

Medina J, Catala R, Salinas J. (2001) Developmental and stress regulation of RCI2A and RCI2B, two cold-inducible genes of *Arabidopsis* encoding highly conserved hydrophobic proteins. *Plant Physiology* **125**, 1655-1666.

Meinhardt H, de Boer PA. (2001) Pattern formation in *Escherichia coli*: a model for the pole-to-pole oscillations of Min proteins and the localization of the division site. *Proceedings of the National Academy of Sciences, USA* **98**, 14202-14207.

Mestres-Ortega D, Meyer Y. (1999) The *Arabidopsis thaliana* genome encodes at least four thioredoxins m and a new prokaryotic-like thioredoxin *Gene* **240**, 307-316.

Mita T, Kanbe T, Tanaka K, Kuroiwa T. (1986) A ring structure around the dividing plane of the *Cyanidium caldarium* chloroplast. *Protoplasma* **130**, 211-213.

- Miyagishima S, Itoh R, Toda K, Takahashi H, Kuroiwa H, Kuroiwa T.** (1998a) Identification of a triple ring structure involved in plastid division in the primitive red alga *Cyanidioschyzon merolae*. *Journal of Electron Microscopy* **47**, 269-272.
- Miyagishima S, Itoh R, Toda K, Takahashi H, Kuroiwa H, Kuroiwa T.** (1998b) Orderly formation of the double ring structures for plastid and mitochondrial division in the unicellular red alga *Cyanidioschyzon merolae*. *Planta* **206**, 551-560.
- Miyagishima S, Itoh R, Toda K, Takahashi H, Kuroiwa H, Kuroiwa T.** (1999) Real-time analyses of chloroplast and mitochondrial division and differences in the behaviour of their dividing rings during contraction. *Planta* **207**, 343-353.
- Miyagishima S, Takahara M, Kuroiwa T.** (2001a) Novel filaments 5 nm in diameter constitute the cytosolic ring of the plastid division apparatus. *The Plant Cell* **13**, 707-721.
- Miyagishima S, Kuroiwa H, Kuroiwa T.** (2001b) The timing and manner of disassembly of the apparatuses for chloroplast and mitochondrial division in the red alga *Cyanidioschyzon merolae*. *Planta* **212**, 517-528.
- Miyagishima S, Takahara M, Mori T, Kuroiwa H, Higashiyama T, Kuroiwa T.** (2001c) Plastid division is driven by a complex mechanism that involves differential transition of the bacterial and eukaryotic division rings. *The Plant Cell* **13**, 2257-2268.
- Miyagishima S, Nishida K, Mori T, Matsuzaki M, Higashiyama T, Kuroiwa H, Kuroiwa T.** (2003) A plant-specific dynamin-related protein forms a ring at the chloroplast division site. *The Plant Cell* **15**, 655-665.
- Miyagishima SY, Froehlich JE, Osteryoung KW.** (2006) PDV1 and PDV2 Mediate Recruitment of the Dynamin-Related Protein ARC5 to the Plastid Division Site. *Plant Cell* Epub ahead of print.
- Moehs CP, Tian L, Osteryoung KW, Dellapenna D.** (2001) Analysis of carotenoid biosynthetic gene expression during marigold petal development. *Plant Molecular Biology* **45**, 281-293.
- Moore M, Harrison MS, Peterson EC, Henry R.** (2000) Chloroplast Oxa1p homolog albino3 is required for post-translational integration of the light harvesting chlorophyll-binding protein into thylakoid membranes. *Journal of Biological Chemistry* **275**, 1529-32.

- Mosyak L, Zhang Y, Glasfeld E, Haney S, Stahl M, Seehra J, Somers WS.** (2000) The bacterial cell division protein ZipA and its interaction with an FtsZ fragment revealed by X-ray crystallography. *EMBO Journal* **19**, 3179-3191.
- Mukherjee A, Lutkenhaus J.** (1999) Analysis of FtsZ assembly by light scattering and determination of the role of divalent metal cations. *Journal of Bacteriology* **181**, 823-832.
- Muskens MW, Vissers AP, Mol JN, Kooter JM.** (2000) Role of inverted DNA repeats in transcriptional and post-transcriptional gene silencing. *Plant Molecular Biology* **43**, 243-60.
- Nishitani H, Lygerou Z.** (2002) Control of DNA replication licensing in a cell cycle. *Genes to Cells* **7**, 523-34.
- Nishida K, Takahara M, Miyagishima SY, Kuroiwa H, Matsuzaki M, Kuroiwa T.** (2003) Dynamic recruitment of dynamin for final mitochondrial severance in a primitive red alga. *Proceedings of the National Academy of Sciences, USA* **100**, 2146-2151.
- Nishida K, Yagisawa F, Kuroiwa H, Nagata T, Kuroiwa T.** (2005) Cell cycle-regulated, microtubule-independent organelle division in *Cyanidioschyzon merolae*. *Molecular Biology of the Cell* **16**, 2493-2502.
- Nogales E, Wolf SG, Downing K H.** (1998a) Structure of the α tubulin dimer by electron crystallography. *Nature* **391**, 199–203.
- Ohlrogge J, Browse J.** (1995) Lipid biosynthesis. *The Plant Cell* **7**, 1-7.
- Okutani S, Hanke GT, Satomi Y, Takao T, Kurisu G, Suzuki A, Hase T.** (2005) Three maize leaf ferredoxin:NADPH oxidoreductases vary in subchloroplast location, expression, and interaction with ferredoxin. *Plant Physiology* **139**, 1451-1459.
- Osawa M, Erikson HP.** (2005) Probing the domain structure of FtsZ by random truncation and insertion of GFP. *Microbiology* **151**, 4033-43.
- Osteryoung KW, Vierling E.** (1995) Conserved cell and organelle division. *Nature* **376**, 473-474.
- Osteryoung KW, Stokes KD, Rutherford SM, Percival AL, Lee WY.** (1998) Chloroplast division in higher plants requires members of two functionally divergent gene families with homology to bacterial *ftsZ*. *The Plant Cell* **10**, 1991-2004.
- Osteryoung KW, McAndrew RS.** (2001) The plastid division machine. *Annual Review of Plant Physiology and Plant Molecular Biology* **52**, 315-333.

- Palaniswamy SK, James S, Sun H, Lamb RS, Davuluri RV, Grotewold E.** (2006) AGRIS and AtRegNet. a platform to link cis-regulatory elements and transcription factors into regulatory networks. *Plant Physiology* **140**, 818-29.
- Parenicova L, de Folter S, Kieffer M, Horner DS, Favalli C, Busscher J, Cook HE, Ingram RM, Kater MM, Davies B, Angenent GC, Colombo L.** (2003) Molecular and phylogenetic analyses of the complete MADS-box transcription factor family in *Arabidopsis*: new openings to the MADS world. *Plant Cell*. **15**, 1538-1551.
- Pastoret S, Fraipont C, den Blaauwen T, Wolf B, Aarsman ME, Piette A, Thomas A, Brasseur R, Nguyen-Disteche M.** (2004) Functional analysis of the cell division protein FtsW of *Escherichia coli*. *Journal of Bacteriology* **186**, 8370-8379.
- Peeters N, Small I.** (2001) Dual targeting to mitochondria and chloroplasts. *Biochimica et biophysica acta*. **154**, 154-63.
- Peltier JB, Emanuelsson O, Kalume DE, Ytterberg J, Friso G, Rudella A, Liberles DA, Soderberg L, Roepstorff P, von Heijne G, van Wijk KJ.** Central functions of the lumenal and peripheral thylakoid proteome of *Arabidopsis* determined by experimentation and genome-wide prediction. *Plant Cell* **14**, 211-236.
- Pichoff S, Vollrath B, Touriol C, Bouche JP.** (1995) Deletion analysis of gene minE which encodes the topological specificity factor of cell division in *Escherichia coli*. *Molecular Microbiology* **18**, 321-329.
- Pichoff S, Lutkenhaus J.** (2002) Unique and overlapping roles for ZipA and FtsA in septal ring assembly in *Escherichia coli*. *EMBO Journal* **21**, 685-693
- Pivetti CD, Yen MR, Miller S, Busch W, Tseng YH, Booth IR, Saier MH Jr.** (2003) Two families of mechanosensitive channel proteins. *Microbiology and Molecular Biology Reviews* **67**, 66-85.
- Platt-Aloia K, Thomson WW.** (1977) Chloroplast development in young sesame plants. *New Phytologist* **78**, 599-605.
- Possingham JV, Saurer W.** (1969) Changes in chloroplast number per cell during leaf development in spinach. *Planta* **86**, 186-194.
- Possingham JV, Lawrence ME.** (1983) Controls to plastid division. *International Review of Cytology* **84**, 1-56.

- Pyke KA.** (1999) Plastid division and development. *The Plant Cell* **11**, 549-556.
- Pyke K.** (2006) Plastid division: the squeezing gets tense. *Current Biology* **16**, R60-2.
- Pyke KA, Leech RM.** (1991) Rapid image analysis screening procedure for identifying chloroplast number mutants in mesophyll cells of *Arabidopsis thaliana* (L.) Heynh. *Plant Physiology* **96**, 1193-1195.
- Pyke KA, Leech RM.** (1992) Chloroplast division and expansion is radically altered by nuclear mutations in *Arabidopsis thaliana*. *Plant Physiology* **99**, 1005-1008.
- Pyke KA, Leech RM.** (1994) A genetic analysis of chloroplast division and expansion in *Arabidopsis thaliana*. *Plant Physiology* **104**, 201-207.
- Pyke KA, Rutherford SM, Robertson EJ, Leech RM.** (1994) *arc6*, a fertile *Arabidopsis* mutant with only two mesophyll cell chloroplasts. *Plant Physiology* **106**, 1169-1177.
- Pyke KA, Page AM.** (1998) Plastid ontogeny during petal development in *Arabidopsis*. *Plant Physiology* **116**, 797-803.
- Raskin DM, de Boer PA.** (1997) The MinE ring: an FtsZ-independent cell structure required for selection of the correct division site in *E. coli*. *Cell* **91**, 685-694.
- Raskin DM, De Boer PJA** (1999) MinDE-dependent pole-to-pole oscillation of division inhibitor MinC in *Escherichia coli*. *Journal of Bacteriology* **181**, 6419-6424.
- RayChaudhuri D, Park JT.** (1992) *Escherichia coli* cell-division gene *ftsZ* encodes a novel GTP-binding protein. *Nature* **359**, 251-254.
- Raynaud C, Cassier-Chauvat C, Perennes C, Bergounioux C.** (2004) An *Arabidopsis* homolog of the bacterial cell division inhibitor Sula is involved in plastid division. *The Plant Cell* **16**, 1801-1811.
- Raynaud C, Perennes C, Reuzeau C, Catrice O, Brown S, Bergounioux C.** (2005) Cell and plastid division are coordinated through the prereplication factor AtCDT1. *Proceedings of the National Academy of Sciences, USA*. **102**, 8216-8221.
- Reddy MS, Dinkins R, Collins GB.** (2002) Overexpression of the *Arabidopsis thaliana* MinE1 bacterial division inhibitor homologue gene alters chloroplast size and morphology in transgenic *Arabidopsis* and tobacco plants. *Planta* **215**, 167-176.
- Reyes JC, Muro-Pastor MI, Florencio FJ.** (2004) The GATA family of transcription factors in *Arabidopsis* and rice. *Plant Physiology* **134**, 1718-32.

- Rivas G, Lopez A, Mingorance J, Ferrandiz MJ, Zorrilla S, Minton AP, Vicente M, Andreu JM.** (2000) Magnesium-induced linear self-association of the FtsZ bacterial cell division protein monomer. The primary steps for FtsZ assembly. *Journal of Biological Chemistry* **275**, 11740-11749.
- Robertson EJ, Pyke KA, Leech RM.** (1995) *arc6*, an extreme chloroplast division mutant of *Arabidopsis* also alters proplastid proliferation and morphology in shoot and root apices. *Journal of Cell Science* **108**, 2937-44.
- Robertson EJ, Rutherford SM, Leech RM.** (1996) Characterization of chloroplast division using the *Arabidopsis* mutant *arc5*. *Plant Physiology* **112**, 149-159.
- Ross J, Li Y, Lim E, Bowles DJ** (2002) Higher plant glycosyltransferases. *Genome Biology* **2**, REVIEWS3004.
- Rothfield L, Taghbalout A, Shih YL.** (2005) Spatial control of bacterial division-site placement. *Nature Reviews Microbiology* **3**, 959-68.
- Rowland SL, Fu X, Sayed MA, Zhang Y, Cook WR, Rothfield LI.** (2000) Membrane redistribution of the *Escherichia coli* MinD protein induced by MinE. *Journal of Bacteriology* **182**, 613-619
- Rudhe C, Clifton R, Chew O, Zemam K, Richter S, Lamma G, Whelan J, Glaser E.** (2004) Processing of the dual targeted precursor protein of glutathione reductase in mitochondria and chloroplasts. *Journal of Molecular Biology* **343**, 639-647.
- Rutherford SM.** (1996) The Genetic and Physical Analysis of Mutants of Chloroplast Number and Size in *Arabidopsis thaliana*. PhD thesis Department of Biology. University of York, York, UK.
- Sai J, Johnson CH.** (2002) Dark-stimulated calcium ion fluxes in the chloroplast stroma and cytosol. *Plant Cell* **14**, 1279-1291.
- Sakai H, Aoyama T, Oka A.** (2000) *Arabidopsis* ARR1 and ARR2 response regulators operate as transcriptional activators. *Plant Journal* **24**, 703-11.
- Santi L, Wang Y, Stile MR, Berendzen K, Wanke D, Roig C, Pozzi C, Muller K, Muller J, Rohde W, Salamini F.** (2003) The GA octonucleotide repeat binding factor BBR participates in the transcriptional regulation of the homeobox gene *Bkn3*. *Plant Journal* **34**, 813-826.

Schmidt KL, Peterson ND, Kustus RJ, Wissel MC, Graham B, Phillips GJ, Weiss DS. (2004) A predicted ABC transporter, FtsEX, is needed for cell division in *Escherichia coli*. *Journal of Bacteriology* **186**, 785-793.

Schroeder DF, Gahrtz M, Maxwell BB, Cook RK, Kan JM, Alonso JM, Ecker JR and Chory J. (2002) De-etiolated 1 and damaged DNA binding protein 1 interact to regulate *Arabidopsis* photomorphogenesis. *Current Biology* **12**, 1462-1472.

Shih YL, Le T, Rothfield L. (2003) Division site selection in *Escherichia coli* involves dynamic redistribution of Min proteins within coiled structures that extend between the two cell poles. *Proceedings of the National Academy of Sciences, USA* **100**, 7865-7870.

Shimada H, Koizumi M, Kuroki K, Mochizuki M, Fujimoto H, Ohta H, Masuda T, Takamiya K. (2004). ARC3, a chloroplast division factor, is a chimera of prokaryotic FtsZ and part of eukaryotic phosphatidylinositol-4-phosphate 5-kinase. *Plant Cell Physiology* **45**, 960-967.

Schubert D, Lechtenberg B, Forsbach A, Gils M, Bahadur S, Schmidt R. (2004) Silencing in *Arabidopsis* T-DNA transformants: the predominant role of a gene-specific RNA sensing mechanism versus position effects. *Plant Cell* **16**, 2561-2572.

Smirnova E, Griparic L, Shurland DL, van der Blik AM. (2001) Dynamin-related protein Drp1 is required for mitochondrial division in mammalian cells. *Molecular Biology of the Cell* **12**, 2245-2256.

Smith MD, Rounds CM, Wang F, Chen K, Afithile M, Schnell DJ. (2004) atToc159 is a selective transit peptide receptor for the import of nucleus-encoded chloroplast proteins. *Journal of Cell Biology* **165**, 323-34.

Steffens NO, Galuschka C, Schindler M, Bulow L, Hehl R. (2005) AthaMap web tools for database-assisted identification of combinatorial cis-regulatory elements and the display of highly conserved transcription factor binding sites in *Arabidopsis thaliana*. *Nucleic Acids Research* **33**, (Web Server issue):W397-402.

Steffens NO, Galuschka C, Schindler M, Bulow L, Hehl R. (2004) AthaMap: an online resource for in silico transcription factor binding sites in the *Arabidopsis thaliana* genome. *Nucleic Acids Research*. **32**, (Database issue):D368-72.

- Stokes KD, McAndrew RS, Figueroa R, Vitha S, Osteryoung KW.** (2000) Chloroplast division and morphology are differentially affected by overexpression of *FtsZ1* and *FtsZ2* genes in *Arabidopsis*. *Plant Physiology* **124**, 1668-1677.
- Stokes KD, Osteryoung KW.** (2003) Early divergence of the *FtsZ1* and *FtsZ2* plastid division gene families in photosynthetic eukaryotes. *Gene* **320**, 97-108.
- Stracke R, Werber M, Weisshaar B.** (2001) The R2R3-MYB gene family in *Arabidopsis thaliana*. *Current Opinion Plant Biology* **4**, 447-456.
- Strepp R, Scholz S, Kruse S, Speth V, Reski R.** (1998) Plant nuclear gene knockout reveals a role in plastid division for the homolog of the bacterial cell division protein FtsZ, an ancestral tubulin. *Proceedings of the National Academy of Sciences, USA* **95**, 4368-4373.
- Stricker J, Maddox P, Salmon ED, Erickson HP.** (2002) Rapid assembly dynamics of the *Escherichia coli* FtsZ-ring demonstrated by fluorescence recovery after photobleaching. *Proceedings of the National Academy of Sciences, USA* **99**, 3171-3175.
- Suefuji K, Valluzzi R, RayChaudhuri D.** (2002) Dynamic assembly of MinD into filament bundles modulated by ATP, phospholipids, and MinE. *Proceedings of the National Academy of Sciences, USA* **99**, 16776-16781.
- Suorsa M, Sirpio S, Allahverdiyeva Y, Paakkarinen V, Mamedov F, Styring S, Aro EM.** (2006) PsbR, a missing link in the assembly of the oxygen-evolving complex of plant photosystem II. *Journal Biological Chemistry* **281**, 145-150.
- Suzuki K, Ehara T, Osafune T, Kuroiwa H, Kawano S and Kuroiwa T** (1994) Behavior of mitochondria, chloroplasts and their nuclei during the mitotic cycle in the ultramicroalga *Cyanidioschyzon merolae*. *European Journal of Cell Biology* **63**, 280-288
- Sundberg E, Slagter JG, Fridborg I, Cleary SP, Robinson C, Coupland G.** (1997) ALBINO3, an *Arabidopsis* nuclear gene essential for chloroplast differentiation, encodes a chloroplast protein that shows homology to proteins present in bacterial membranes and yeast mitochondria. *Plant Cell* **9**, 717-730.
- Surpin M, Larkin RM, Chory J.** (2002) Signal transduction between the chloroplast and the nucleus. *Plant Cell*. **14** Suppl:S327-38.

Sutton RB, Davletov BA, Berghuis AM, Sudhof TC, Sprang SR. (1995) Structure of the first C₂ domain of synaptotagmin I: A novel Ca²⁺/phospholipid-binding fold. *Cell* **80**, 929-938.

Sweitzer SM, Hinshaw JE. (1998) Dynamin undergoes a GTP-dependent conformational change causing vesiculation. *Cell* **93**, 1021-1029.

Szeto TH, Rowland SL, Rothfield LI, King GF. (2002) Membrane localization of MinD is mediated by a C-terminal motif that is conserved across eubacteria, archaea, and chloroplasts. *Proceedings of the National Academy of Sciences, USA* **99**, 15693-15698.

Taghbalout A, Ma L, Rothfield L. (2006) Role of MinD-membrane association in Min protein interactions. *Journal of Bacteriology* **188**, 2993-3001.

Takahara M, Takahashi H, Matsunaga S, Miyagishima S, Takano H, Sakai A, Kawano S, Kuroiwa T. (2000) A putative mitochondrial ftsZ gene is present in the unicellular primitive red alga *Cyanidioschyzon merolae*. *Molecular Genetics and Genomics* **264**, 452-460.

Takehima H, Komazaki S, Nishi M, Iino M, Kangawa K. (2000) Junctophilins: a novel family of junctional membrane complex proteins. *Molecular Cell* **6**, 11-22.

Tanaka S, Diffley JF. (2002) Deregulated G1-cyclin expression induces genomic instability by preventing efficient pre-RC formation. *Genes and Development* **16**, 2639-49.

Tavva VS, Collins GB, Dinkins RD (2006) Targeted overexpression of the Escherichia coli MinC protein in higher plants results in abnormal chloroplasts. *Plant Cell Reports* **25**, 341-348.

Teakle GR, Manfield IW, Graham JF, Gilmartin PM. (2002) *Arabidopsis thaliana* GATA factors: organisation, expression and DNA-binding characteristics. *Plant Molecular Biology* **50**, 43-57.

Thanedar S, Margolin W. (2004) FtsZ exhibits rapid movement and oscillation waves in helix-like patterns in *Escherichia coli*. *Current Biology*. **14**, 1167-1173.

Uehara T, Matsuzawa H, Nishimura A. (2001) HscA is involved in the dynamics of FtsZ-ring formation in *Escherichia coli* K12. *Genes Cells* **6**, 803-814.

Vaucheret H, Beclin C, Elmayan T, Feuerbach F, Godon C, Morel JB, Mourrain P, Palauqui JC, Vernhettes S. (1998) Transgene-induced gene silencing in plants. *Plant Journal* **16**, 651-659.

Vitha S, McAndrew RS, Osteryoung KW. (2001) FtsZ ring formation at the chloroplast division site in plants. *Journal of Cell Biology* **153**, 111-119.

Vitha S, Froehlich JE, Koksharova O, Pyke KA, van Erp H, Osteryoung KW. (2003) ARC6 is a J-domain plastid division protein and an evolutionary descendant of the cyanobacterial cell division protein Ftn2. *The Plant Cell* **15**, 1918–1933.

Wakasugi T, Nagai T, Kapoor M, Sugita, M, Ito M, Ito S, Tsudzuki J, Nakashima K, Tsudzuki T, Suzuki Y, Hamada A, Ohta T, Inamura A, Yoshinaga K, Sugiura M. (1997) Complete nucleotide sequence of the chloroplast genome from the green alga *Chlorella vulgaris*: the existence of genes possibly involved in chloroplast division. *Proceedings of the National Academy of Sciences, USA* **94**, 5967-5972.

Walter S, Buchner J. (2002) Molecular chaperones, cellular machines for protein folding. *Angewandte Chemie (International ed. in English)* **41**, 1098-113.

Wang Q, Sullivan RW, Kight A, Henry RL, Huang J, Jones AM, Korth KL. (2004) Deletion of the chloroplast-localized Thylakoid formation1 gene product in Arabidopsis leads to deficient thylakoid formation and variegated leaves. *Plant Physiology* **136**, 3594-3604.

Wang X, Huang J, Mukherjee A, Cao C, Lutkenhaus J. (1997) Analysis of the interaction of FtsZ with itself, GTP, and FtsA. *Journal of Bacteriology* **179**, 5551-5559.

Ward JE Jr, Lutkenhaus J. (1985) Overproduction of FtsZ induces minicell formation in *E. coli*. *Cell* **42**, 941-949.

Wei Z, Angerer RC, Angerer LM. (1999) Identification of a new sea urchin ets protein, SpEts4, by yeast one-hybrid screening with the hatching enzyme promoter. *Molecular Cell Biology* **19**, 1271-1278.

Weiss, DS, Chen, JC, Ghigo, J, Boyd, D, Beckwith, J. (1999) Localization of FtsI (PBP3) to the septal ring requires its membrane anchor, the Z ring, FtsA, FtsQ, and FtsL. *Journal of Bacteriology*. **181**, 508-520.

Whatley JM. (1983) The ultrastructure of plastids in roots. *International Review of Cytology* **85**, 175-220.

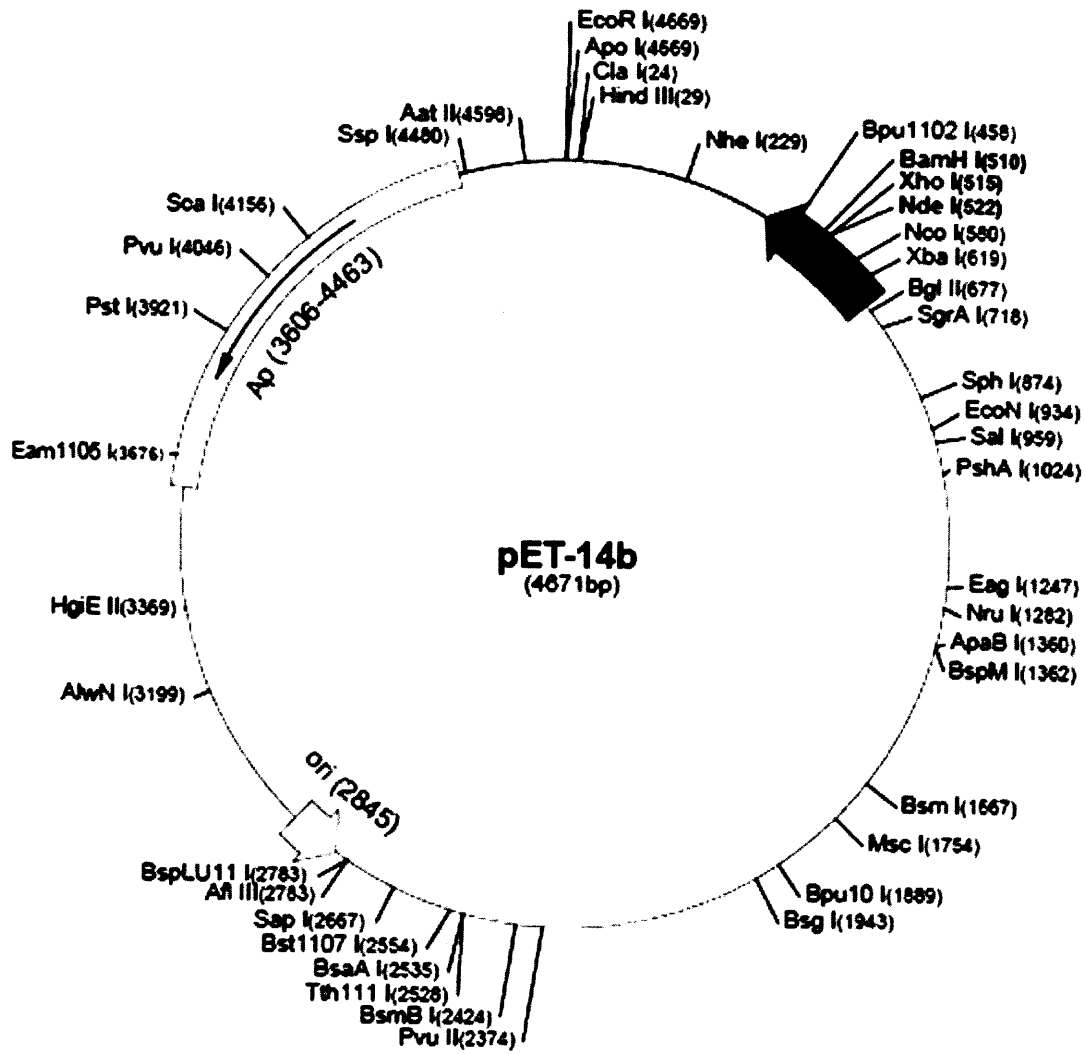
Windhovel A, Hein I, Dabrowa R, Stockhaus J. (2001) Characterization of a novel class of plant homeodomain proteins that bind to the C4 phosphoenolpyruvate carboxylase gene of *Flaveria trinervia*. *Plant Molecular Biology* **45**, 201-214.

Wu LJ, Errington J. (2004) Coordination of cell division and chromosome segregation by a nucleoid occlusion protein in *Bacillus subtilis*. *Cell* **117**, 915-925.

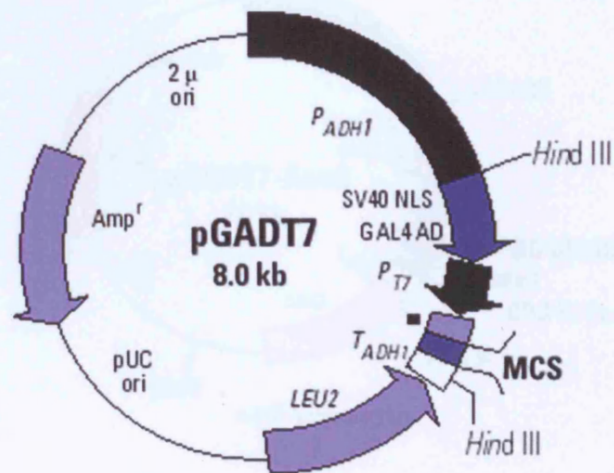
- Xu XM, Moller SG.** (2006) AtSufE is an essential activator of plastidic and mitochondrial desulfurases in *Arabidopsis*. *EMBO Journal* **25**, 900-909.
- Yamamoto K, Pyke KA, Kiss JZ.** (2002) Reduced gravitropism in inflorescence stems and hypocotyls, but not roots, of *Arabidopsis* mutants with large plastids. *Physiologia Plantarum* **114**, 627-636.
- Yan K, Pearce KH, Payne DJ.** (2000) A conserved residue at the extreme C-terminus of FtsZ is critical for the FtsA-FtsZ interaction in *Staphylococcus aureus*. *Biochemical and Biophysical Research Communications* **270**, 387-392.
- Yanhui C, Xiaoyuan Y, Kun H, Meihua L, Jigang L, Zhaofeng G, Zhiqiang L, Yunfei Z, Xiaoxiao W, Xiaoming Q, Yunping S, Li Z, Xiaohui D, Jingchu L, Xing-Wang D, Zhangliang C, Hongya G, Li-Jia Q.** (2006) The MYB transcription factor superfamily of *Arabidopsis*: expression analysis and phylogenetic comparison with the rice MYB family. *Plant Molecular Biology* **60**, 107-124.
- Yoshida Y, Kuroiwa H, Misumi O, Nishida K, Yagisawa F, Fujiwara T, Nanamiya H, Kawamura F, Kuroiwa T.** (2006) Isolated chloroplast division machinery can actively constrict after stretching. *Science* **313**, 1435-1438.
- Yu C, Margolin, W.** (1997) Ca²⁺-mediated GTP-dependent dynamic assembly of bacterial cell division protein FtsZ into asters and polymer networks in vitro. *EMBO Journal* **16**, 5455-5463.
- Zhao CR, de Boer PA, Rothfield LI.** (1995) Proper placement of the *Escherichia coli* division site requires two functions that are associated with different domains of the MinE protein. *Proceedings of the National Academy of Sciences, USA* **92**, 4313-4317.
- Zhou H, Lutkenhaus J.** (2004) The switch I and II regions of MinD are required for binding and activating MinC. *Journal of Bacteriology* **186**, 1546-1555.
- Zuo J, Niu QW, Chua NH.** (2000) Technical advance: An estrogen receptor-based transactivator XVE mediates highly inducible gene expression in transgenic plants. *Plant Journal* **24**, 265-73.

Appendix 1.

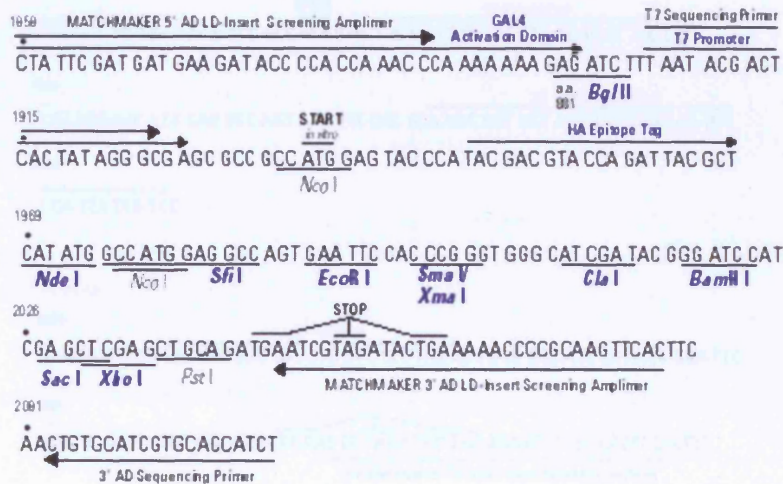
Vectors used in this study:



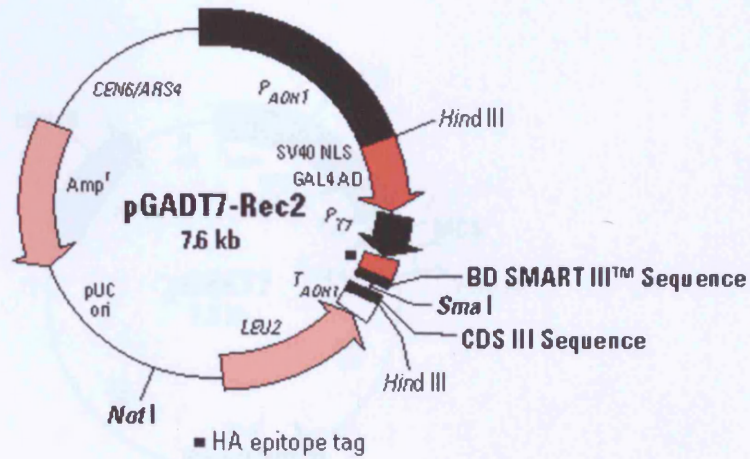
A1. pET-14 (Novagen)



■ HA epitope tag



A2. pGADT7 (Clontech Matchmaker™)



BD SMART IIITM terminus

```

1859
• BD Matchmaker™ 5' ADL D-Insert Screening Amplimer          GAL4 Act Intron Domain          T7 Promoter Sequencing Primer
CTA TTC GAT GAT GAA GAT ACC CCA CCA AAC CCA AAA AAA GAG ATC TTT AAT ACG ACT

1915
•                               START                               HA Epitope Tag
CAC TAT AGG GCG AGC GCC GCC ATG GAG TAC CCA TAC GAC GTA CCA GAT TAC GCT

1969
•                               BD SMART III Primer
CAT ATG GCC ATG GAG GCC AGT GAA TTC CAC CCA AGC AGT GGT ATC AAC GCA GAG TGG

2026
•
CCA TTA TGG CCC
  
```

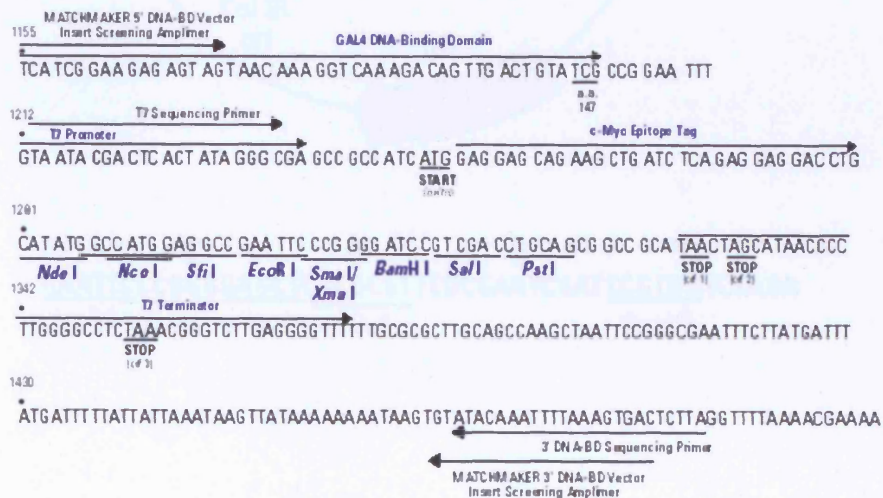
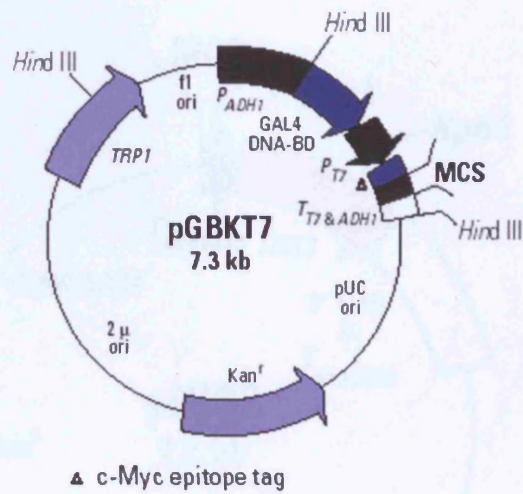
CDS III terminus

```

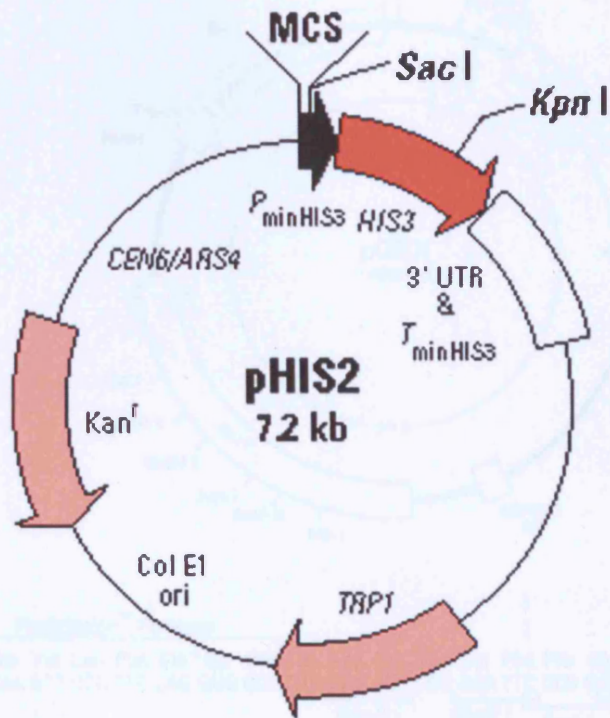
2039
•                               CDS III Primer
GGG AAA AAA CAT GTC GGC CGC CTC GGC CTC TAG AGG GTG GGC ATC GAT ACG GGA TCC

2095
•                               STOP
ATC GAG CTC GAG CTG CAG ATG AAT CGT AGA TAC TGA AAA ACC CGC AAG TTC ACT TC
•                               BD Matchmaker™ 5' ADL D-Insert Screening Amplimer
  
```

A3. pGADT7-Rec2 (Clontech Mathmaker™)

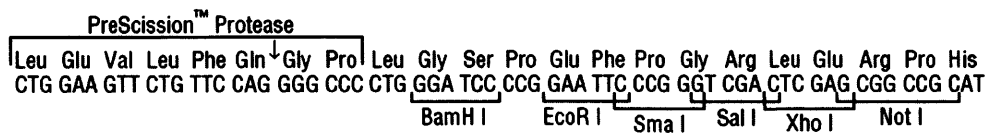
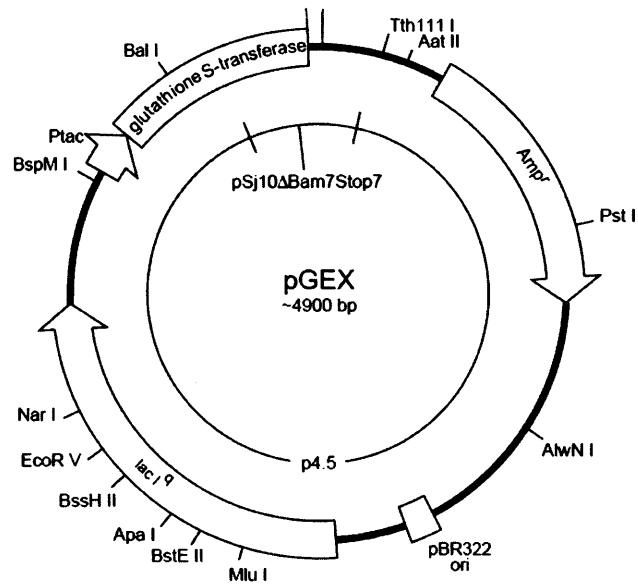


A4. pGBKT7 (Clontech Matchmaker™)

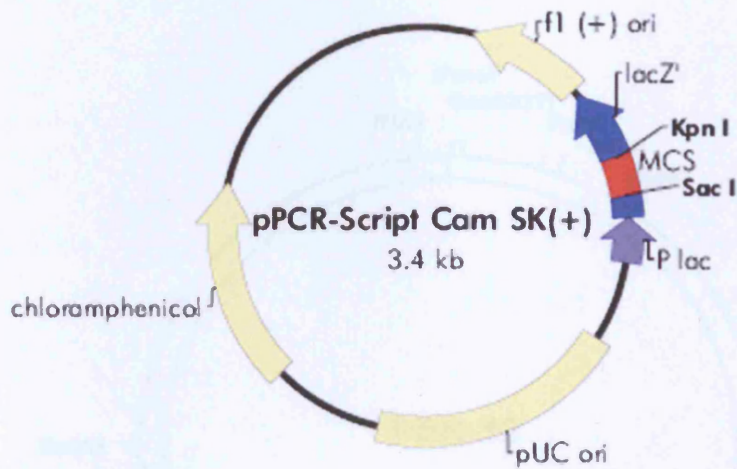


10 20 30 40
 GAATCCC66GGAGCTCACGCGTTCGCGAATCGATCCGCGGTCTAGA
 EcoRI SmaI SacI MluI SacII*

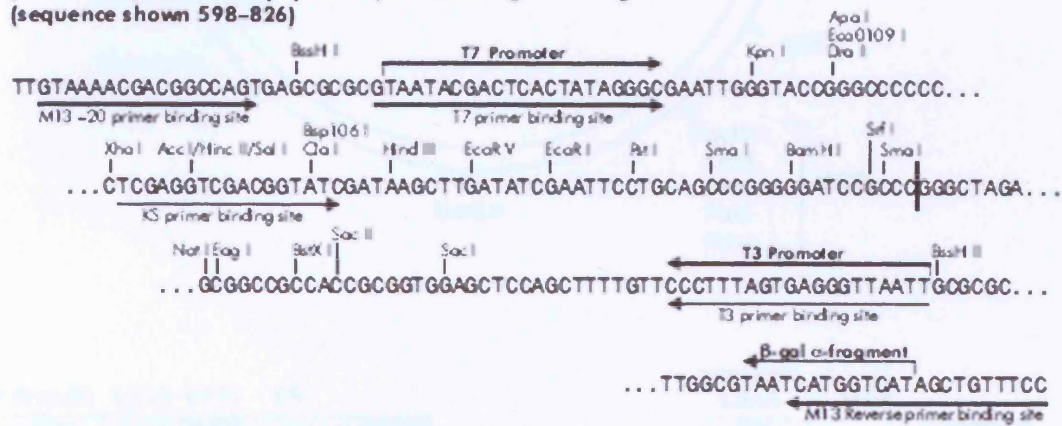
A5. pHIS2 (Clontech Matchmaker™)



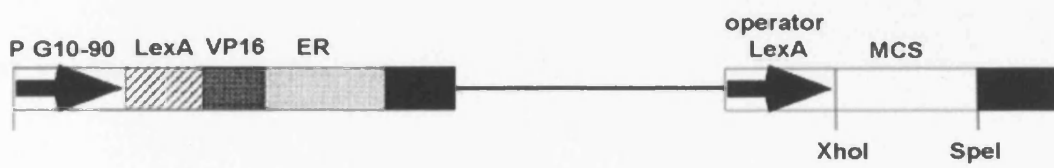
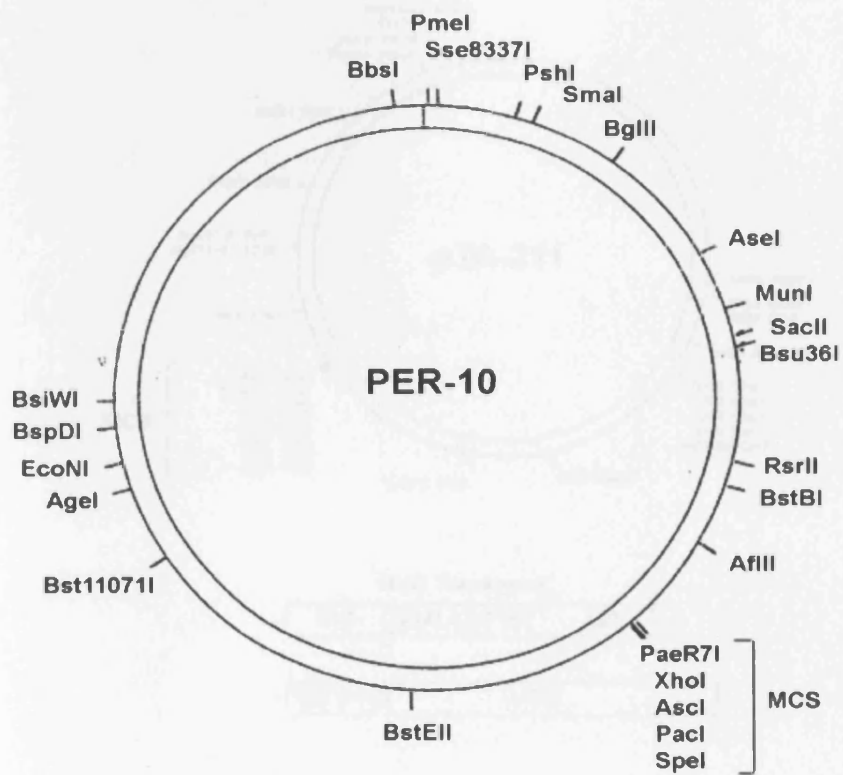
A6. pGEX-6P (GE Healthcare)



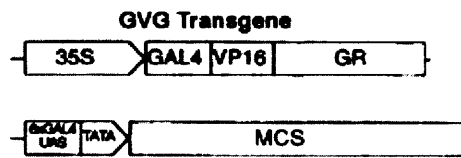
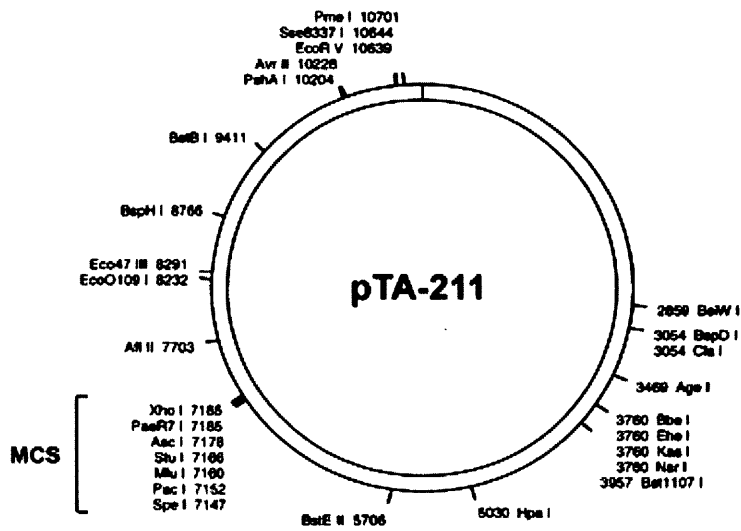
pPCR-Script Cam SK(+) Multiple Cloning Site Region
(sequence shown 598-826)



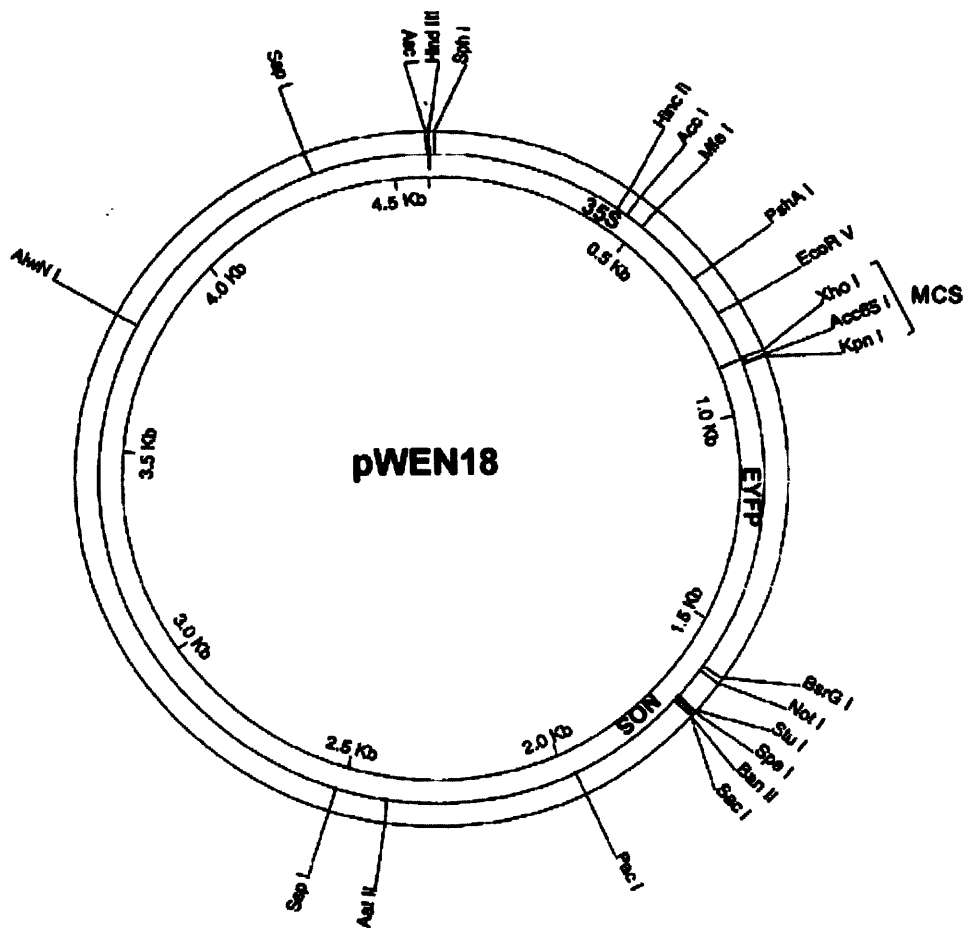
A7. pPCR-Script (Stratagene)



A8. PER-10 (Zuo *et al.*, 2000).



A9. pTA-211 (Aoyama and Chua, 1997).



A.11 pWEN18 (Kost *et al.*, 1998).

Appendix 2.

Publications resulting from this study:

Aldridge C, Maple J, Møller SG. (2005) The Molecular Biology of Plastid Division in Higher Plants.

Journal of Experimental Botany **56**, 1061-77.

Aldridge C, Møller SG. (2005) The plastid division protein AtMinD1 is a Ca²⁺-ATPase stimulated by

AtMinE1. *Journal of Biological Chemistry* **280**, 31673-8.

Maple J, Aldridge C, Møller SG. (2005). Plastid division is mediated by a combinatorial assembly of

plastid division proteins. *Plant Journal* **43**, 811-23.

A3. Plasmids used in this study

Construct	Relevant genotype ¹	Intermediate vector ²	Source or reference
pPCRScript			Stratagene
pPCRScript/AtMinD1	<i>AtMinD1</i>		this study
pPCRScript/AtMinE1	<i>AtMinE1</i>		Maple <i>et al.</i> , 2002
pPCRScript/AtFtsZ1-1	<i>AtFtsZ1-1</i>		this study
pPCRScript/AtFtsZ2-1	<i>AtFtsZ2-1</i>		this study
pPCRScript/(K72A)AtMinD1	(K72A) <i>AtMinD1</i>		this study
pPCRScript/EcMinD	<i>EcMinD</i>		this study
pPCRScript/ Δ TPAtFtsZ1-1	Δ TPAtFtsZ1-1		this study
pPCRScript/ Δ TPAtFtsZ2-1	Δ TPAtFtsZ2-1		this study
pPCRScript/prom AtMinD1	<i>AtMinD1</i> ₁₋₂₉₅		this study
pPCRScript/E1	<i>AtMinE1</i> ₁₋₁₁₆		this study
pPCRScript/E2	<i>AtMinE1</i> ₁₀₁₋₁₇₀		this study
U19395	ARC6		ABRC
pGBKT7	<i>P_{ADHI}-BD</i>		Clontech
pGBKT7/AtMinE1	<i>P_{ADHI}-BD::AtMinE1</i> ₁₋₆₉₀	pPCR-Script/AtMinE1 (<i>Nde</i> I/ <i>Bam</i> HI)	Maple <i>et al.</i> , 2005
pGBKT7/AtMinD1	<i>P_{ADHI}-BD::AtMinD1</i> ₁₋₉₈₁	pPCR-Script/AtMinD1 (<i>Nde</i> I/ <i>Bam</i> HI)	Maple <i>et al.</i> , 2005
pGBKT7/ Δ TPAtFtsZ1-1	<i>P_{ADHI}-BD::AtFtsZ1-1</i> ₁₋₁₃₀₂	pPCR-Script/ Δ TPAtFtsZ1-1 (<i>Nde</i> I/ <i>Bam</i> HI)	this study
pGBKT7/ Δ TPAtFtsZ2-1	<i>P_{ADHI}-BD::AtFtsZ2-1</i> ₁₋₁₄₃₇	pPCR-Script/ Δ TPAtFtsZ2-1 (<i>Nde</i> I/ <i>Bam</i> HI)	this study
pGBKT7/GC1	<i>P_{ADHI}-BD::GC1</i> ₁₋₁₀₄₄		Maple <i>et al.</i> , 2004
pGADT7	<i>P_{ADHI}-AD</i>		this study
pGADT7/AtMinE1	<i>P_{ADHI}-AD::AtMinE1</i> ₁₋₆₉₀	pPCR-Script/AtMinE1 (<i>Nde</i> I/ <i>Bam</i> HI)	this study
pGADT7/AtMinD1	<i>P_{ADHI}-AD::AtMinD1</i> ₁₋₉₈₁	pPCR-Script/AtMinD1 (<i>Nde</i> I/ <i>Bam</i> HI)	this study
pWEN18	<i>CaMV35S::YFP</i>		Kost <i>et al.</i> , 1998
pWEN18/AtMinE1	<i>P_{35S}-AtMinE1</i> _{1-687::YFP}	pPCR-Script/AtMinE1 (<i>Xho</i> I/ <i>Kpn</i> I)	Maple <i>et al.</i> , 2005
pWEN18/AtMinD1	<i>P_{35S}-AtMinD1</i> _{1-978::YFP}	pPCRScript/AtMinD1 (<i>Xho</i> I/ <i>Kpn</i> I)	Fujiwara <i>et al.</i> , 2004
pWEN18/(K72A)AtMinD1	<i>P_{35S}-(K72A)AtMinD1</i> _{1-978::YFP}	pPCRScript/(K72A)AtMinD1 (<i>Xho</i> I/ <i>Kpn</i> I)	this study
pWEN18/AtFtsZ1-1	<i>P_{35S}-AtFtsZ1-1</i> _{1-1299::YFP}	pPCR-Script/AtFtsZ1-1 (<i>Xho</i> I/ <i>Kpn</i> I)	Maple <i>et al.</i> , 2005
pWEN18/AtFtsZ2-1	<i>P_{35S}-AtFtsZ2-1</i> _{1-1434::YFP}	pPCR-Script/AtFtsZ2-1 (<i>Xho</i> I/ <i>Kpn</i> I)	Maple <i>et al.</i> , 2005
pWEN18/ARC6	<i>P_{35S}-ARC6</i> _{1-2403::YFP}	pPCR-Script/ARC6 (<i>Sal</i> I/ <i>Kpn</i> I)	Maple <i>et al.</i> , 2005
pWEN15	<i>CaMV35S::CFP</i>		Kost <i>et al.</i> , 2004
pWEN15/AtMinE1	<i>P_{35S}-AtMinE1</i> _{1-687::CFP}	pPCR-Script/AtMinE1 (<i>Xho</i> I/ <i>Kpn</i> I)	Maple <i>et al.</i> , 2005
pWEN15/AtMinD1	<i>P_{35S}-AtMinD1</i> _{1-978::CFP}	pPCR-Script/AtMinE1 (<i>Xho</i> I/ <i>Kpn</i> I)	Maple <i>et al.</i> , 2005
pWEN15/AtFtsZ1-1	<i>P_{35S}-AtFtsZ1-1</i> _{1-1299::CFP}	pPCR-Script/AtFtsZ1-1 (<i>Xho</i> I/ <i>Kpn</i> I)	Maple <i>et al.</i> , 2005
pWEN15/AtFtsZ2-1	<i>P_{35S}-AtFtsZ2-1</i> _{1-1434::CFP}	pPCR-Script/AtFtsZ2-1 (<i>Xho</i> I/ <i>Kpn</i> I)	Maple <i>et al.</i> , 2005

pWEN15/ARC6	<i>P</i> _{35S} - <i>ARC6</i> ₁₋₂₄₀₃ :: <i>CFP</i>	pPCR-Sript/ARC6 (<i>Sall/KpnI</i>)	Maple <i>et al.</i> , 2005
pWEN-NY	<i>CaMV35S</i> :: <i>YPF</i> ₁₋₄₆₂	pPCR-Sript/YPF ₁₋₁₅₄ (<i>KpnI/NotI</i>)	Maple <i>et al.</i> , 2005
pWEN-CY	<i>CaMV35S</i> :: <i>YPF</i> ₄₆₃₋₇₁₄	pPCR-Sript/YPF ₁₅₅₋₂₃₈ (<i>KpnI/NotI</i>)	Maple <i>et al.</i> , 2005
pWEN-NY/AtMinE1	<i>P</i> _{35S} - <i>AtMinE1</i> ₁₋₆₈₇ :: <i>YPF</i> ₁₋₄₆₂	pPCR-Sript/AtMinE1 (<i>XhoI/KpnI</i>)	Maple <i>et al.</i> , 2005
pWEN-NY/AtMinD1	<i>P</i> _{35S} - <i>AtMinD1</i> ₁₋₉₇₈ :: <i>YPF</i> ₁₋₄₆₂	pPCR-Sript/AtMinD1 (<i>XhoI/KpnI</i>)	Maple <i>et al.</i> , 2005
pWEN-NY/(K72A)AtMinD1	<i>P</i> _{35S} -(<i>K72A</i>) <i>AtMinD1</i> ₁₋₉₇₈ :: <i>YPF</i> ₁₋₄₆₂	pPCRScript/(<i>K72A</i>) <i>AtMinD1</i> (<i>XhoI/KpnI</i>)	this study
pWEN-NY/AtFtsZ1-1	<i>P</i> _{35S} - <i>AtFtsZ1-1</i> ₁₋₁₂₉₉ :: <i>YPF</i> ₁₋₄₆₂	pPCR-Sript/AtFtsZ1-1 (<i>XhoI/KpnI</i>)	Maple <i>et al.</i> , 2005
pWEN-NY/AtFtsZ2-1	<i>P</i> _{35S} - <i>AtFtsZ2-1</i> ₁₋₁₄₃₄ :: <i>YPF</i> ₁₋₄₆₂	pPCR-Sript/AtFtsZ2-1 (<i>XhoI/KpnI</i>)	Maple <i>et al.</i> , 2005
pWEN-NY/ARC6	<i>P</i> _{35S} - <i>ARC6</i> ₁₋₂₄₀₃ :: <i>YPF</i> ₁₋₄₆₂	pPCR-Sript/ARC6 (<i>Sall/KpnI</i>)	Maple <i>et al.</i> , 2005
pWEN-CY/AtMinE1	<i>P</i> _{35S} - <i>AtMinE1</i> ₁₋₆₈₇ :: <i>YPF</i> ₄₆₃₋₇₁₄	pPCR-Sript/AtMinE1 (<i>XhoI/KpnI</i>)	Maple <i>et al.</i> , 2005
pWEN-CY/AtMinD1	<i>P</i> _{35S} - <i>AtMinD1</i> ₁₋₉₇₈ :: <i>YPF</i> ₄₆₃₋₇₁₄	pPCR-Sript/AtMinD1 (<i>XhoI/KpnI</i>)	Maple <i>et al.</i> , 2005
pWEN-CY/AtFtsZ1-1	<i>P</i> _{35S} - <i>AtFtsZ1-1</i> ₁₋₁₂₉₉ :: <i>YPF</i> ₄₆₃₋₇₁₄	pPCR-Sript/AtFtsZ1-1 (<i>XhoI/KpnI</i>)	Maple <i>et al.</i> , 2005
pWEN-CY/AtFtsZ2-1	<i>P</i> _{35S} - <i>AtFtsZ2-1</i> ₁₋₁₄₃₄ :: <i>YPF</i> ₄₆₃₋₇₁₄	pPCR-Sript/AtFtsZ2-1 (<i>XhoI/KpnI</i>)	Maple <i>et al.</i> , 2005
pWEN-CY/ARC6	<i>P</i> _{35S} - <i>ARC6</i> ₁₋₂₄₀₃ :: <i>YPF</i> ₄₆₃₋₇₁₄	pPCR-Sript/ARC6 (<i>Sall/KpnI</i>)	Maple <i>et al.</i> , 2005
pET-14b	<i>T7</i> :: <i>His</i> ₍₆₎		Novagen
pET-14b/AtMinD1	<i>T7</i> - <i>His</i> ₍₆₎ :: <i>AtMinD1</i>	pPCRScript/AtMinD1(<i>NdeI/BamHI</i>)	This study
pET-14b/(K72A)AtMinD1	<i>T7</i> - <i>His</i> ₍₆₎ ::(<i>K72A</i>) <i>AtMinD1</i>	pPCRScript/(<i>K72A</i>) <i>AtMinD1</i> (<i>NdeI/BamHI</i>)	This study
pET-14b/EcMinD	<i>T7</i> - <i>His</i> ₍₆₎ :: <i>EcMinD</i>	pPCRScript/EcMinD(<i>NdeI/BamHI</i>)	This study
pGEX-6P	<i>P</i> _{tac} - <i>GST</i>		GE Healthcare
pGEX-6P/AtMinE1	<i>P</i> _{tac} - <i>GST</i> :: <i>AtMinE1</i>	pPCRScript/AtMinE1(<i>NdeI/BamHI</i>)	Maple <i>et al.</i> , 2002
PER-10	<i>CaMV35S</i> :: <i>XVE</i>		Zuo <i>et al.</i> , 2000).
PER-10/AtMinD1	<i>P</i> _{LexA 35S} - <i>AtMinD1</i>	pPCRScript/AtMinD1(<i>XhoI/SpeI</i>)	This study
pTA-211	<i>CaMV35S</i> :: <i>GVG</i>		Aoyama and Chua, 1997
pTA-211/FtsZ2-1	<i>P</i> _{GAL4} - <i>FtsZ2-1</i> ₁₋₁₄₃₄ :: <i>YFP</i>	pWEN18/AtFtsZ2-1(<i>XhoI/PacI</i>)	This study
pHIS2	<i>P</i> _{minHIS3} - <i>HIS3</i>		Clontech
pHIS2/promoter AtMinD1	<i>P</i> _{minHIS3} - <i>AtMinD1</i> _{.1 - .295}	pPCRScript/prom AtMinD1 (<i>EcoRI/SacI</i>)	This study
pHIS2/E1	<i>P</i> _{minHIS3} - <i>AtMinE1</i> _{.1 - .116}	pPCRScript/E1 (<i>EcoRI/SacI</i>)	This study
pHIS2/E2	<i>P</i> _{minHIS3} - <i>AtMinE1</i> _{.101 - .170}	pPCRScript/E2 (<i>EcoRI/SacI</i>)	This study

¹ The genotype refers to the nucleotide sequence. ²Where an intermediate vector is listed the cDNA was initially PCR amplified and cloned into pPCR-Script before subcloning into the destination vector with the restriction sites indicated.